IDENTIFYING COLD-AIR DAMMING

IN THE REGION OF THE OZARK PLATEAU

A Dissertation

presented to

the Faculty of the Graduate School

at the University of Missouri-Columbia

In Partial Fulfillment

Of the Requirements for the Degree

Doctor of Philosophy

---

by

JONATHON BONGARD

Dr. Patrick Market, Dissertation Supervisor

MAY 2024

The undersigned, appointed by the dean of the Graduate School, have examined the dissertation entitled

IDENTIFYING COLD-AIR DAMMING IN THE REGION OF THE OZARK PLATEAU

Presented by Jonathon Bongard,

A candidate for the degree of doctor of philosophy,

and hereby certify that, in their opinion, it is worthy of acceptance.

_____

Director Patrick Market

_____

Professor Anthony Lupo

_____

Professor Neil Fox

_____

Adjunct Professor Patrick Guinan

_____

Professor Tim Matisziw

ACKNOWLEDGEMENTS

The success of this dissertation defense would not be possible without the guidance of my advisor, Dr. Patrick Market, the Director of the School of Natural Resources. Dr. Market has had a profound impact on my life over the past 9 years ever since I enrolled in classes at the University of Missouri back in the spring of 2015. Jumping back into academia after an 8-year hiatus was not an easy task, but Dr. Market was instrumental in reigniting the fire in me that I needed to remind myself of why I had a lifelong dream of becoming a meteorologist. Our very healthy working relationship over the years culminated in this dissertation defense. Dr. Market's ability to keep me financially stable as I navigated grad school, his tutelage and guidance through the research and writing portions of this process, and his role as the most impactful professor I have ever had at any institution, all while fulfilling his role as the director of the School of Natural Resources, I am forever grateful for. The late Jim Moore, Dr. Market's mentor, would be proud of his protégé if he were with us today.

I thank my committee for their time and assessment of my performance through this dissertation process. My time in atmospheric science classes at the University of Missouri helped shape the meteorologist I am today. This is largely due to the important roles played by Anthony Lupo, Neil Fox, and Patrick Guinan. Their expertise and teaching styles impacted on me both as a student in their classes and as a graduate instructor in my own classrooms. A special thank you to my outside committee member, Dr. Tim Matisziw. His class on Transportation Geography resonated with me

and I could not think of a better professor outside of our atmospheric science department to aid in my assessment.

A very special thank you is owed to Dr. Chasity Wright for her guidance through the WRF modeling portion of this research. There is no possible way that this phase of the research would have been successful without her expertise. Working a full-time job as a meteorologist for the engineering company ENSCO, Inc. in Melbourne, FL, there is not much extra time in her schedule these days. That she used some of her time to help me with the script writing and troubleshooting that comes with research modeling was an incredible gift and something I am eternally thankful for. As a former graduate student and PhD graduate of the University of Missouri, Chasity is an example of what it is to be a great student, tedious researcher, and ultimately good friend. I am proud to have Dr. Chasity Wright in my circle.

Throughout my 9 years at the University of Missouri I can think of countless fellow students and friends that I had the privilege of interacting with and navigating both my undergraduate and graduate schools with. All of you will hold a special place in my memories of my time here. Mizzou will always be home no matter where my career takes me, and I am thankful to those of you that made this period of my life so incredibly special. My colleagues Paula Sumrall, Evan Travis, and my longtime office-mate Dr. Chris Steward deserve a special thank you. Graduate school is tough and getting the opportunity to vent, bounce ideas, and make each other laugh while we were studying, launching weather balloons, or hanging out at conferences in cities all over the country are experiences I will never forget. Thank you all for walking with me on this journey.

I have been blessed with an incredible support system that makes my success possible. My mother and father, Diane, and Tom, deserve a ton of credit for supporting what has truly been a lifelong dream of becoming a meteorologist. I have wanted to be a meteorologist ever since I was a little kid and watched Bob Richards on the TV in St. Louis. Mom and dad never discouraged me, always supported me, and guided me in the right directions to make this dream a reality. Moving from California to mid-Missouri in 2009, mom and dad reunited our family and helped strengthen my resolve to return to school and finish what I had started. This move allowed me to focus solely on my education and attaining this degree would have been incredibly difficult without their love and support these past few years. I share this achievement with them. My brother Shawn, who joined me in Columbia 4 months after my move to mid-Missouri from the St. Louis area, has been by my side for this journey the longest. I would not change one thing about the last 18 years we've spent together as I've enjoyed the greatest experience getting to watch you grow as a person. The family man and successful business owner you are today is a testament to your character and your work ethic. You are someone I look to as an example of how to achieve success, even as the "elder" brother. We share in each other's successes, and I certainly share this achievement with you. Even though my time in Columbia is ending I will continue to watch and enjoy your future success. My fiancée Whitney, and her daughter Greenlee, have been my inspiration and motivation throughout this doctoral process. Upon learning of my career as an atmospheric scientist, Whitney proclaimed me to be a "sky genius" and holds me accountable whenever there is significant weather in our area. Their love and support have made the last few years fun and therefore this process of doctoral research that much easier. I'm certainly proud of

my doctoral achievement, but there are many people with PhDs. Only one of them gets to come home to see you though, and that is what I am most proud of. We have built a relationship that will stand the test of time and I'm so anxious to see what the future holds for us.

Finally, my time in Columbia has left me with a collection of friends that I will enjoy for the rest of my life. The past 18 years have been filled with memories of softball, tailgates, float trips, weddings, sporting events, and even just hanging out and having some drinks. I'll never forget these experiences. You all know who you are, and you all will hold a very special place in my heart forever for all the time we had to experience life together. I am full of gratitude for all of you and look forward to growing older together.

TABLE OF CONTENTS

LIST OF FIGURES

LIST OF TABLES

ABSTRACT

Following the events of March 2014 in which icy, hazardous conditions stranded motorists along the roadways and interstate highways of eastern Arkansas, an investigation is launched to determine if the event was the result of cold-air damming occurring in the region. This investigation led to a larger three-phase study on cold-air damming events in the region of the Ozark Plateau. First, the initial phase studies the marquee event of March 2014 and what atmospheric conditions led to the event. Second, a 5-year study to find the frequency and intensity of cold-air damming events in the region. Finally, a numerical analysis using the WRF model to study the effects of terrain height on cold-air damming cases. The objective analysis, results, and conclusions will be showcased including chart analysis, numerical analysis utilizing the Froude number, and WRF output analysis.

CHAPTER 1. INTRODUCTION

Ice storms and hazardous road conditions are common occurrences during the winter months in the central portion of the United States. Crippling blizzards commonly impact the northern states of Nebraska, Kansas, and Iowa, while freezing rain and ice storms plague more southern locations such as Oklahoma and Arkansas, as numerous mid-latitude cyclones traverse the continent during the colder seasons (Changnon 2003). Lesser known is the frequency and intensity of cold-air damming events that occur in these ice storm prone regions.

Cold-air damming is a weather phenomenon that is commonly associated with mountain chains when specific synoptic meteorological conditions exist. Typically, when high-pressure builds upstream of a propagating mid-latitude cyclone (specifically to the north or northeast of the affected region; Baker 1971) cold-air damming can occur (Richwein 1980). When synoptic conditions are ideal, the western Carolinas (Bell and Bosart 1988) and portions of Colorado (Dunn 1987) are known to observe ice storm type conditions on the leeward side of their respective mountain chains even in the absence of a weather-creating cyclone, such as what occurred in the initial case study of this research.

Despite these two regions being the emphasis areas for cold-air damming in the continental United States, an occurrence of conditions commonly associated with the cold-air damming phenomenon occurred in the Mid-South region of the southern Plains in March 2014. After the passage of an early spring mid-latitude cyclone early on 03 March 2014, formation of freezing fog and drizzle, as well as icing roads, began to occur

later in the day and into 04 March 2014 long after precipitation associated with the cyclone had propagated to the east and south. Reports from cooperative observers within the region (www.cocorahs.org) observed “freezing fog/drizzle” in locations such as Poplar Bluff, Missouri and “freezing fog, ice and snow covered” to the south in Jonesboro and Sulphur Rock, Arkansas. Local newspaper reports (Day and Roberts 2014) from 05 March 2014 describe conditions in which “…thousands of motorists…” (Lesnick 2014) along Interstates 40 & 55 in eastern Arkansas became stranded for as long as 18 hours prompting state police and local authorities to call upon the Arkansas National Guard to assist in aiding stranded motorists across the affected region.

Figure 1.1 - Motorists on Interstate 55 in Blytheville, Arkansas trapped overnight on the highway as conditions become too hazardous for travel. Photo courtesy of: https://www.arkansasonline.com/news/2014/mar/05/idled-wheels-choke-icy-interstates-20140305/

Due to evidence such as placement of the parent anticyclone in a favorable position to the north-northeast and observations from local airport ASOS (Automated Surface Observing Systems) terminals and meteorograms from various locations within the region it is suggested that the post-system icing event was the possible result of cold-air damming associated with the Ozark Plateau. With cold-air damming commonly associated with higher elevations to the east (the Appalachians) and west (the Rocky Mountains) further investigation of this possible Ozark Plateau induced event is warranted.

1.1 Objectives

With the exact cause of this icing event in eastern Arkansas and southeastern Missouri in question, this study evaluates the role of the Ozark Plateau in contributing to cold-air damming events in the Mid-South region of the central United States. The research uses a 3-phase approach in which the first 2 phases involve observational approaches, and the final phase takes a modeling approach that focuses solely on elevation height to dictate the presence, frequency, and intensity of cold-air damming events in the Ozark region of the southern Plains. With that purpose in mind several objectives of this research are as follows:

1. Evaluate and determine both synoptic and mesoscale conditions that occurred during the event of March 2014 through the analysis of upper-air and surface maps, observed sounding profiles, and meteorograms from

locations within the affected region, and establish this as a cold-air damming event.

2. Use these observed conditions as a template of research to determine the frequency and intensity of other cold-air damming events taking place over a 5-year period from 01 January 2016 through 31 December 2020. Potential case studies are found using METAR reports from 6 ASOS terminals located within the region of interest that is defined primarily as southeastern Missouri and east-central Arkansas. These conditions are used to evaluate these potential case studies to determine if cold-air damming occurred and, if so, the intensity of the event based upon impact and time length of the event.

3. A modeling approach is used to evaluate in this case the impact of the elevation of the topography associated with the Ozark Plateau. Specifically, the Weather Research and Forecasting (WRF) model is utilized to modify and study the role of the Plateau in 3 case studies involving cold-air damming events. For each study the elevation is altered by multiplying elevation height by factors between 0.001 and 2.0. Changes to conditions are observed and conclusions are drawn about the role of Ozark Plateau topography in these cold-air damming events.

CHAPTER 2. MOTIVATION

2.1 Literature Review

Cold-air damming is defined in the American Meteorological Society (AMS) glossary as “the piling up, or complete blocking of cold air approaching the slopes of a mountain barrier. This produces high-pressure along the windward slopes and, when it persists for more than several hours, can also produce a barrier jet” (AMS; Rackley and Knox 2016). Earliest mention of the phenomenon occurred in a study outlining the passage of a “backdoor” cold front between 16-20 of May 1951 (Carr 1951). The study mentions the existence of these cold fronts associated with the Front Range of the Rocky Mountains and the eastern slopes of the Appalachian Mountains. The study states “In these regions the cold air banks up against the mountains and is forced southward, or southwestward, at a wide angle across the isobars in the area. Thus, the cold air advances farther south than it would ordinarily if the orographic effect were absent.” Additional studies two decades later, involving the phenomenon that is cold-air damming, focused on the creation and evolution of the leeward-side high-pressure ridge, specifically involving the Appalachian Mountains of the eastern United States (Baker 1971). This initial study treats the surface high-pressure ridges (both “corner ridges” and “wedge ridges” as defined by the study) that develop to the east of the Appalachians as products of a steady-state, surface, stable layer and the inversion immediately above the surface layer. Further investigation of East Coast backdoor cold fronts (Bosart et al. 1973) again referenced the strong influence of friction and topography on the speed and location of these backdoor cold fronts. Orographic influence on frontal boundaries resurfaced in a study conducted in Australia (Colquhoun and Sheperd 1985) concerning “southerly

bursters", an aggressive orographically forced cold front that impacts the southern coast of the continent in much the same way backdoor cold fronts influence the East Coast of the United States.

Concurrent research by Richwien, (1980) took lessons from the initial study on high-pressure ridges (Carr 1951; Baker 1971) and applied them in a more fundamental way to the operational "problem" of cold-air damming focusing more on the effect of the terrain itself (the southern extent of the Appalachian Mountains) and treated the high-pressure center and associated ridge as more of a "parent anticyclone". This study used the depth of the high-pressure center as an indicator for cold air available for damming up against the mountain slopes of the southern Appalachians.

Cold-air damming research expanded considerably in the late 1980's with a series of studies performed on the weather phenomenon. A synoptic and mesoscale investigation of a January 1980 ice storm (Forbes et al. 1987) concluded that the synoptic setup of the parent anticyclone and the influence of topography associated with the Appalachians helped to cultivate and maintain both the cold dome of surface air "dammed" against the eastern slopes as well as the wedging of the ridge along the spine of the mountains allowing for the easterly ageostrophic surface flow. A numerical approach was also used on the same January 1980 storm event in which a mesoscale model was utilized as a diagnostic tool to determine the mesoscale structure of the cold air damming event (Stauffer and Warner 1987). The study found a strong relationship between the wedge of high-pressure along the mountain slope and the maintenance of the cold pool within the damming region. Parcel trajectories within the mesoscale model also highlighted the overrunning warm air co-located just above the cold pool concurrent with

the height of the inversion and its importance in helping to erode the surface cold air at the end of the cold-air damming event. Focus was also given to the Front Range of the Rocky Mountains in central Colorado (Dunn 1987) in which a model scheme depicted the creation of a meso-front and cold-air damming along the spine of the Front Range like the setup found in the southern Appalachians save for the lack of temperature gradient associated with the land-sea contrast found in the Mid-Atlantic region. These mesoscale conditions were found to be in concert with the presence of an anticyclone to the north-northeast and often a low-pressure system over the Panhandles region.

The landmark research associated with cold-air damming (Bosart and Bell 1987) brought focus back to the Appalachians with a 3-part study including a 50-year monthly climatology of cold-air damming events in the region, a synoptic investigation of a March 1985 cold-air damming case study, and a dynamic study on flow structure and force balances associated with the planetary boundary layer during cold-air damming events. Damming of the easterly flow, specifically over the coastal regions of the Carolinas to the east of the ridge, was found to halt the northward progression of warm fronts over the region. The directing of this statically stable flow southward led to an increased stabilization of the region below 850 hectopascals (hPa) directly east of the mountain chain. The inversion strengthened over the course of time as frigid air continued to filter into the lowest levels of the atmosphere below the shallow layer of warm air. Variables that played a role in the formation of these coastal fronts include topography, the configuration of the coastline, the contrast of temperatures between the land and the ocean, and friction. A 15-20°C difference between the colder land mass and the warmer

ocean existed especially along the Carolina coast with the presence of the Gulf Stream just offshore.

Forecasting diagnostic implications for cold-air damming included the importance of the lapse rate below 850 hPa being less than the moist adiabatic lapse rate and the low-level flow becoming perpendicular to the featured terrain contours producing an uphill component at the surface. Another theoretical approach to cold-air damming, specifically the persistence and maintenance of the surface cold dome, was undertaken (Xu 1990) and found that in using a multi-oriented steady-state model the force of friction is paramount to maintaining the cold dome as Coriolis force is negated by the topographic feature (in that case the southern Appalachians). The study concluded that without friction slowing the pressure gradient-induced mountain barrier jet that formed normal to the linear topography, the jet would overcome the surface cold air and eliminate the cold dome, thus negating cold-air damming. This is the case for a north-south barrier such as the Appalachian Mountains, but there is implication in the study that this would apply to an east-west oriented barrier under the correct synoptic conditions.

A cloud physics study of damming events (Fritsch et al. 1992) determined that the existence of low-level cloud cover was necessary in helping to maintain the stable layer and associated cold pool. In the absence of clouds, the daytime lapse rates may increase to the point of destroying the surface stable layer and ultimately the cold-air damming event. Additionally, radiational and evaporative cooling in the presence of low-level cloud cover can help to persist and even enhance a cold-air damming event.

A research summary (Keeter et al. 1995) described the challenges of forecasting for cold-air damming events, as well as the various impacts of the weather phenomenon, not only in the elevated region directly under the dammed cold air but also coastal impacts along the Virginia and Carolina coasts. A more recent study (Bailey et al. 2003) enlisted the use of a classification scheme to distinguish synoptically forced cold-air damming events from those events that are governed by diabatic processes. This study attempted to categorize all cold-air damming events into these classifications and find pattern recognition for forecasting purposes in terms of "high impact" events (those that feature ice storm characteristics) and "low impact" events. Most recently, research was undertaken (Rackley and Knox 2016) updating climatology including station-to-station cold-air damming event frequency and intensity data for southern Appalachian events.

2.2 Case Selection

Research surrounding the hypothesis that the Ozark Plateau produces cold-air damming events is segmented into three study phases. The first phase of research centers around a singular case that occurred on 04 March 2014. Based upon observational data and reports from local newspapers, as well as anecdotal evidence from the trucking industry, this case created a high impact in the eastern Arkansas region of interest when motorists became stranded overnight on portions of Interstates 40 and 55 in the region. It is this high impact situation that provides the motivation to make this case the focal point for the first sequence of study and establish cold-air damming as one cause of the event.

The second phase of research expands upon atmospheric conditions discovered in the first phase of study during the cold-air damming event and brings these conditions to bear as discriminating conditions on a 5-year study of cold-air damming frequency and intensity within the region of interest. Due to the severity of impacts on local roads and interstate highways in the region of interest during the initial case study, the second phase of research is ultimately driven by a search to find other instances of similar sensible weather effects. The 5-year study takes place between 01 January 2016 and 31 December 2020. To identify potential cases of cold-air damming within the portion 6 datasets of Meteorological Aerodrome Report (METAR) code are analyzed from 6 Automated Surface Observing Systems (ASOS) stations located across the region of interest. These stations (seen in Fig. 2.1) are Little Rock, Arkansas (KLIT), West Memphis, Arkansas (KAWM), Memphis, Tennessee (KMEM), Blytheville, Arkansas (KHKA), Kennett, Missouri (KTKX), and Poplar Bluff, Missouri (KPOF).

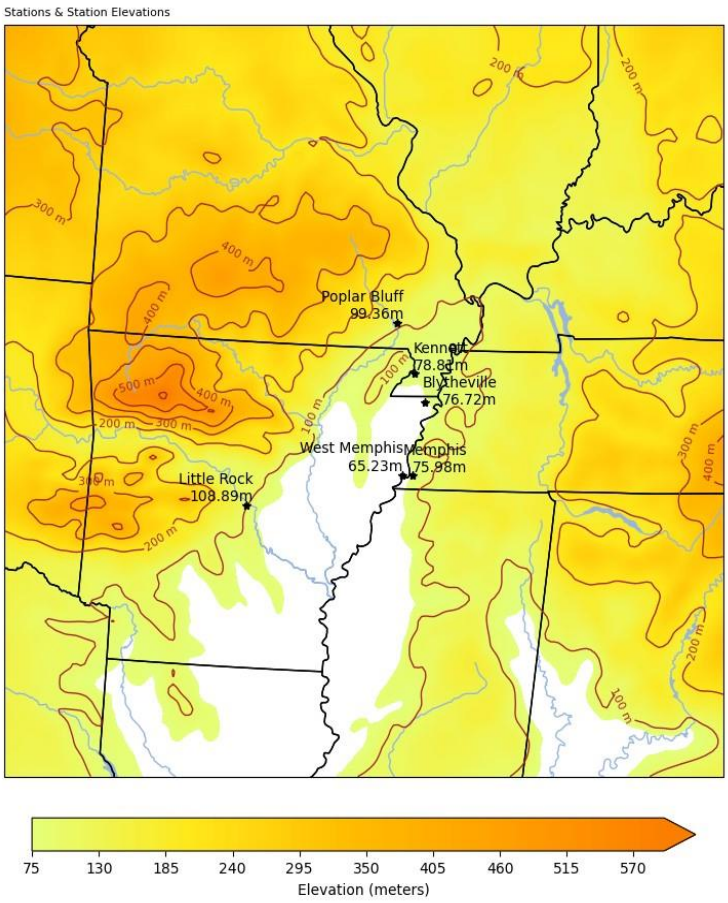

Figure 2.1 - Map of ASOS station locations and their elevations. The topography of the region is color coded (see legend) for elevations from 75 m to elevations above 570 m found at the highest extent of the Ozark Plateau and its associated mountain chains. Elevations below 75 m are not included in the color coding.

Within the METAR report the Present Weather portion of the report is examined to find specific codes that coincide with cold-air damming events. While freezing fog was the main culprit of the initial case study in the first phase, other weather codes were included in the METAR report search. These codes include light freezing rain (-FZRA), freezing fog (FZFG), freezing drizzle (FZDZ), and light snow/mist (-SN BR). A case study is

defined by the 6-hour time marker (00 UTC, 06 UTC, 12 UTC, 18 UTC) prior to the first cold-air damming present weather indicator and the 6-hour time marker immediately following the final cold-air damming present weather indicator. In total, 34 potential cold-air damming cases were identified for the second phase of research. *It should be noted here that the choice of a 5-year period and the six locations used were based on data availability. Prior to 2016 large gaps in ASOS data were found within the region of interest. These 6 locations represent the most complete data sets found in the region between 2016 and 2020.*

Table 2.1 - A list of case studies taken from the 5-year analysis of METAR reports between 01 January 2016 and 31 December 2020.

Case Study Date	Location(s) Reporting Observations	Case Study Date	Location(s) Reporting Observations
1/20/2016	KPOF, KHKA, KLZK, KAWM, KMEM	11/12/2018	KHKA, KLZK, KAWM, KMEM
2/2/2016	KAWM	11/21/2018	KTKX, KAWM
2/14/2016	KPOF, KHKA	12/6/2018	KHKA, KLZK, KAWM, KMEM
11/14/2016	KAWM	12/22/2018	KTKX
11/26/2016	KPOF, KTKX, KLZK, KAWM	1/11/2019	KPOF
11/27/2016	KLZK	1/16/2019	KPOF
12/18/2016	KPOF, KAWM, KMEM	1/19/2019	KPOF, KHKA, KLZK, KAWM
12/21/2016	KPOF	2/15/2019	KPOF, KHKA, KMEM
1/6/2017	KLZK, KAWM, KMEM	2/28/2019	KPOF
1/24/2017	KHKA	3/3/2019	KPOF, KHKA
3/11/2017	KHKA, KLZK, KAWM	11/11/2019	KHKA, KLZK, KAWM, KMEM
1/11/2018	KPOF, KHKA, KLZK, KAWM, KMEM	12/7/2019	KHKA
1/16/2018	KHKA, KLZK, KAWM, KMEM	12/14/2019	KPOF, KTKX, KHKA, KAWM
1/29/2018	KAWM	12/17/2019	KPOF, KMEM
2/4/2018	KPOF, KHKA, KLZK	1/22/2020	KPOF
2/11/2018	KPOF	2/6/2020	KAWM, KMEM
2/18/2018	KPOF, KTKX	2/20/2020	KLZK, KAWM, KMEM
4/7/2018	KPOF, KHKA, KLZK	12/16/2020	KHKA, KLZK

Due to the use of present weather reports as the impetus for discovery of potential cold-air damming events, dates between the beginning of May through the end of September were omitted due to lack of freezing conditions during that portion of the year. Also, without any significant freezing weather ever occurring during these months cold-air damming is hard to identify. However, the study recognizes that cold-air damming can occur during these omitted dates, but the focus here is on impactful cold-air damming events that feature the adverse effects of freezing and icy conditions and so the focus of the study is on dates in which these freezing conditions can occur.

The third and final phase of research shifts from an observational approach to a more numerical modeled approach. The Weather Research and Forecasting (WRF) Model is utilized to identify the role of terrain in cold-air damming events associated with the Ozark Plateau. For this phase, two case studies were chosen for evaluation. The first study is the initial case study from the first phase of study dated 04 March 2014 totaling 60 simulation hours from 00 UTC on 03 March 2014 until 12 UTC 05 March 2014. The other study was taken from results found in the second research phase: a case that impacted the Kennett, Missouri station on 27 November 2016 simulating 18 hours between 0000 UTC on 27 November 2016 and 1800 UTC 27 November 2016.

CHAPTER 3. DATA AND METHODS

3.1 Initial Case Study: 04 March 2014

The initial case study serves as both the impetus for the overall research surrounding Ozark based cold-air damming as well as the foundation for later phases of study. The first phase of study is purely observational and seeks to satisfy two objectives. The first objective aims to establish that cold-air damming did, in fact, occur, based on analysis of various resources during times of observed impact including synoptic surface maps, mesoscale 10-m wind and relative humidity maps, observed upper-air soundings from the Weather Forecasting Office (WFO) of the National Weather Service based in North Little Rock, Arkansas (LZK), and meteorograms from various locations in the affected region. The second objective (provided that the first objective is satisfied) is to identify characteristics needed to establish the presence of Ozark-based cold-air damming in other case studies. Observational analysis of maps and charts took place at 6-hour increments beginning at 0000 UTC on 03 March 2014 and finishing at 1200 UTC on 05 March 2014 totaling 60 hours of observation for this initial case. Within the timeframe of analysis is the passage of the initial mid-latitude cyclone and associated cold front through the region of interest followed by the evolution of the parent anticyclone to the north-northeast as the impact of cold-air damming is observed at the 6 locations defined earlier in Chapter 2 (Section 2.2 – Case Selection).

3.1.1 Radar Composite CONUS Surface Pressure Maps

Observational analysis of the initial case study began at the synoptic scale level with the usage of continental United States (CONUS) spatially sized surface maps. This series of maps is sourced from the Weather Prediction Centers (WPC) National Centers for Environmental Prediction (NCEP) archive website (WPC Surface Analysis Archive (noaa.gov)). An example is shown in Figure 3.1. These maps show a variety of features useful in diagnosing cold-air damming at the synoptic level, in this case present over the central and eastern CONUS.

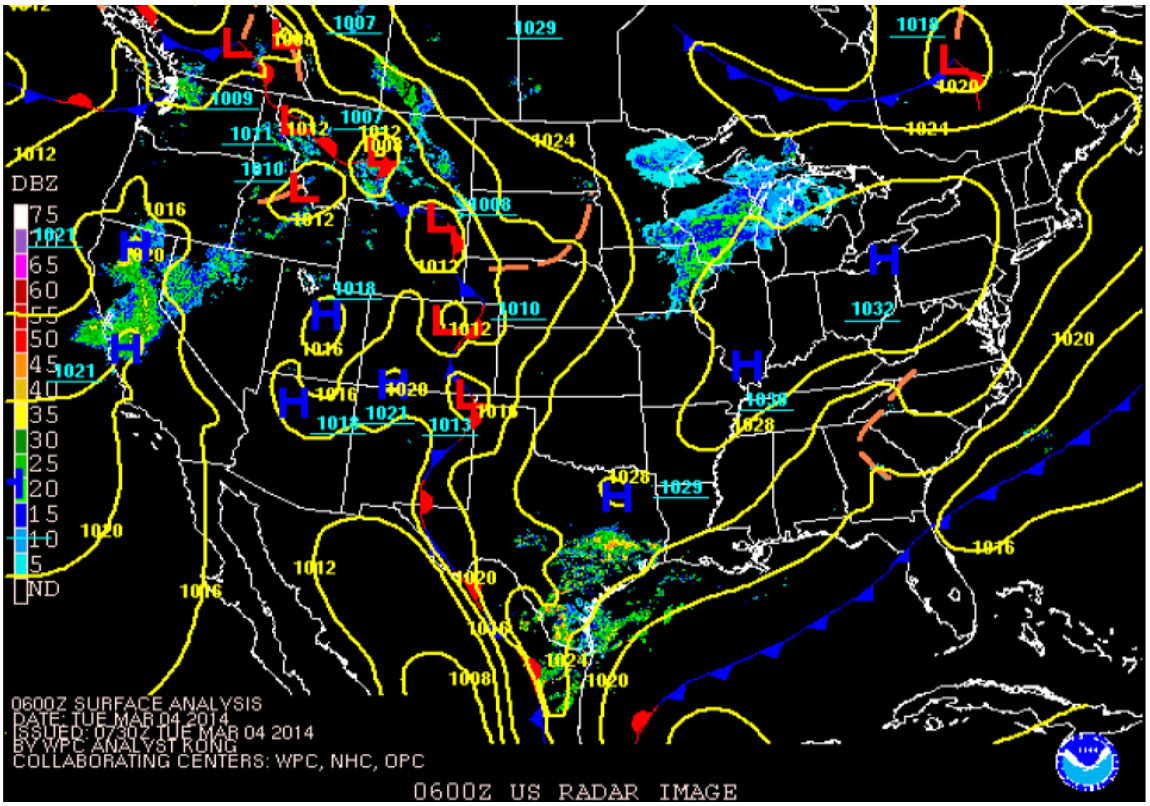

Figure 3.1 – A radar-overlayed surface pressure map from the initial case study at 0600 UTC on 04 March 2014. The solid yellow lines are isobars with associated blue H's representing centers of high-pressure and red L's symbolic of centers of low-pressure. These surface maps also contain traditional frontal symbols with blue-pipped lines representing cold fronts, red-pipped lines for warm fronts, alternating red-blue pipped lines for stationary fronts, and orange dashed lines for pressure troughs. An overlaid radar composite taken from the National Weather Service's network of WSR-88D radar stations depicts areas of precipitation across the CONUS from 0 to 75 dBz. Chart courtesy of NOAA/NWS.

The radar overlay was an important feature of these charts in that it allowed for analysis of present weather coding found in the METAR data. The radar overlay depicted if the present weather being described is associated with actual precipitation seen in the radar data or the potential cold-air damming event. This analysis was reinforced by analyzing archive radar data using the Interactive Radar Tool on the National Center for Environmental Information's website (Radar Data (noaa.gov)). Using this resource, the study determined if present weather coding is a result of precipitation falling at the time of observation or if the coding is a result of another phenomenon (e.g. freezing fog), possibly related to the cold-air damming event in progress. This analysis comes with an understanding that the Radar Tool uses a mosaic of the WSR-88D radar network maintained by the National Weather Service (NWS) and lowest beam heights vary over the 6 ASOS stations used for the study.

The other utility of the surface maps is to analyze the placement and evolution of the parent anticyclone as the cold-air damming event progresses. For the region of interest associated with this study, the ideal location for high-pressure centers to be associated with cold-air damming events would be to the north-northeast of southeastern Missouri and eastern Arkansas. Ideally, centers of high-pressure should be found in a region from eastern Missouri into Illinois and further east into the Ohio River Valley to expose the region of interest to the southern flank of the anticyclone placing said region in east-to-west 10-m wind flow.

3.1.2 Archived Regional 10-m Wind Maps

The online archive database kept by Plymouth State (Make Your Own - Surface Data; plymouth.edu)) allowed for the creation of specific variable surface maps. Archived regional surface maps were created for each 6-hour time step (example of a wind map in Figure 3.2) involved in the initial case study from 0000 UTC 03 March 2014 through the end of the event at 1200 UTC 05 March 2014. The wind maps focused on the region of interest (the southeastern flank of the Ozark Plateau and the Mississippi River flood plain in southeast Missouri and eastern Arkansas) and featured 2 variables used to diagnose 10-m wind flow and speed.

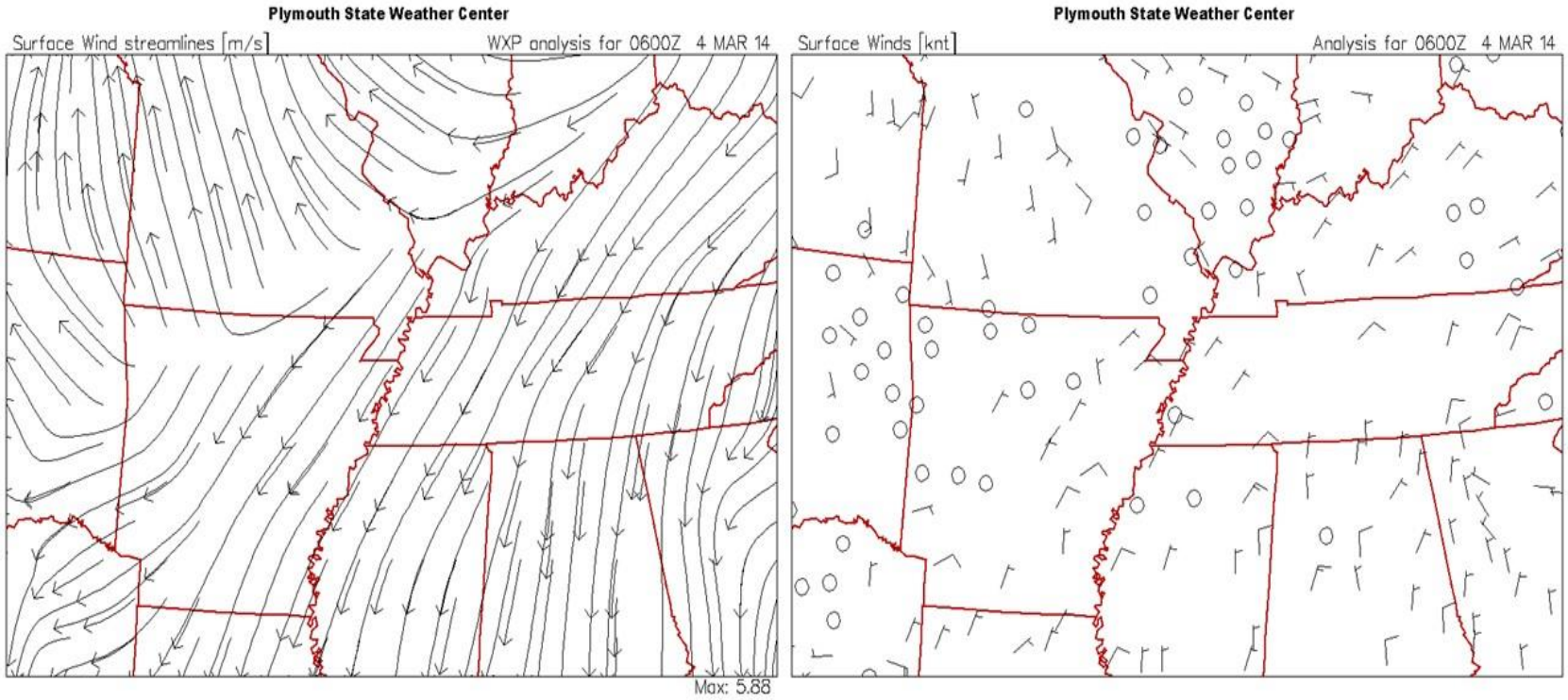

Figure 3.2 - Maps of observed surface winds from the initial case study at 0600 UTC on 04 March 2014. Map (a) features streamlines denoting surface wind flow (m s $^{-1}$) and direction. Map (b) features plotted wind barbs placed at high density adding observed wind speed in knots to the analysis. Charts created using Plymouth State Weather Center data archive (https://vortex.plymouth.edu/).

The maps provided guidance on 10-m wind behavior observed during the cold-air damming event. For example, preferred wind direction during the event features a terrain-orthogonal component or on the directional compass any wind direction between 40 and 220 degrees. These numbers were signified based on the alignment of the southeastern flank of the Ozark Plateau. The Ozark Plateau as a whole, features an upside-down bowl-shape though the southeastern flank just west of the Mississippi River flood plain is oriented more like the traditional spine of a mountain chain, such as the southern extent of the Appalachian Mountains. Wind directions within the conditions stated above would favor cold-air damming as the 10-m wind flow within the surface stable layer would promote pushing the cold dome of air up against the edge of the Plateau. Through observation it was established that light 10-m wind speeds of approximately 5 kts or less were preferred for cold-air damming events as the flow was too weak for the cold, dense air trapped at the surface to overcome the topographic feature. 5-kt wind speed became the theoretical threshold for preferable cold-air damming wind speed based on results of numerical analysis in which flow strength to overcome an obstacle (topography in this case) was calculated. In the flow strength calculations, cold-air damming occurred when wind speeds were 5 kts or less.

3.1.3 Archived Surface Relative Humidity Maps

The same online archive database provided by Plymouth State was utilized to create surface relative humidity maps at 6-hours intervals during the initial case study from 0000 UTC 03 March 2014 through the end of the event at 1200 UTC 05 March

2014. Focused on the region of interest, the surface relative humidity maps (Fig. 3.3) showed the presence of moisture (or lack thereof) within the impacted region during cold-air damming events.

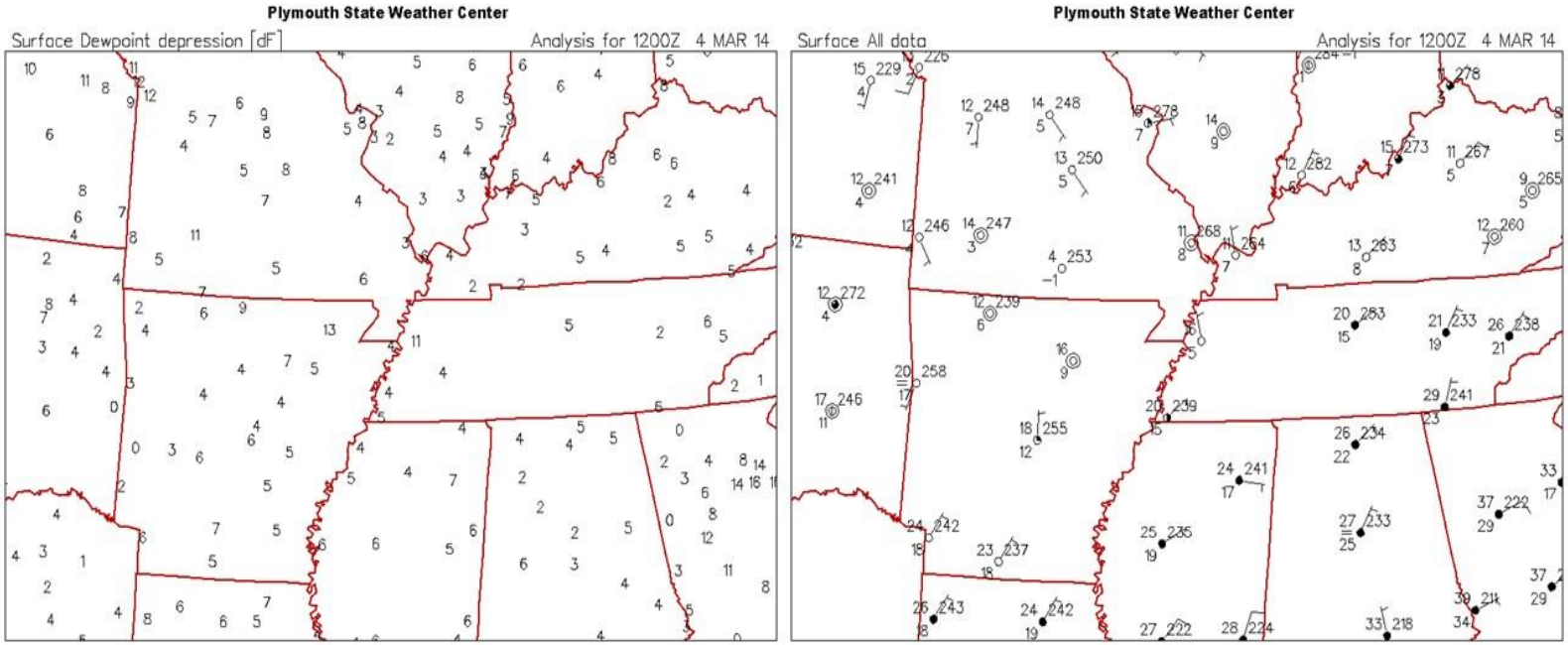

Figure 3.3 – Maps depicting surface relative humidity from the initial case study at 1200 UTC on 04 March 2014. Map a features dewpoint depressions (Fahrenheit) at high density. Map b features station model plots in medium-to-low density across the map. The standard station model plot is employed to contextualize the values shown in map a. Charts created using Plymouth State Weather Center data archive (https://vortex.plymouth.edu/).

Due to chart analysis convention, dewpoint depressions of 5°F or less were observed as moisture rich conditions at the surface. The amount of moisture present during a cold-air damming event did not face the same scrutiny as wind speed and direction in that a moisture rich surface layer was not necessary for a cold-air damming event to take place. However, the presence of moisture in the stable surface layer was an indication that the cold-air damming event was more impactful especially when accompanied by freezing or below-freezing temperatures.

3.1.4 Observed and Modeled Upper-Air Soundings

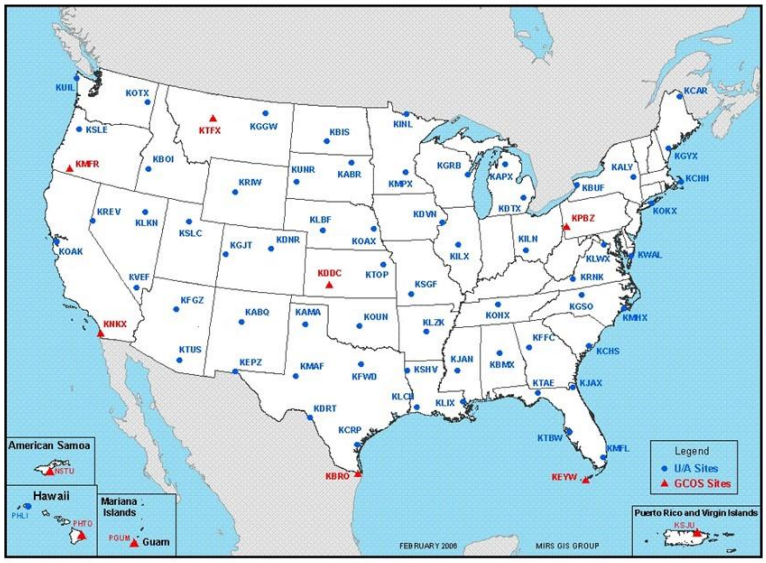

Figure 3.4 - A map of National Weather Service offices that fly twice daily radiosondes at 0000 and 1200 UTC to create a network of observed upper-air soundings.

Upper-air soundings were an important analysis tool in the studies' objective to identify cold-air damming in the Ozarks region. Figure 3.4 depicts a map of NWS offices that make up the network of upper-air soundings flown and observed twice a day at 0000 and 1200 UTC.

The 2 locations closest to the region of interest are the Springfield, Missouri office (KSGF) and the Little Rock, Arkansas (KLZK) office which is located near one of the 6 ASOS station locations (KLIT) included in the METAR report portion of the study. The other 5 stations are not located near an observed sounding source and modeled soundings were verified (discussed later) and utilized to cover the lack of observed data in these locations.

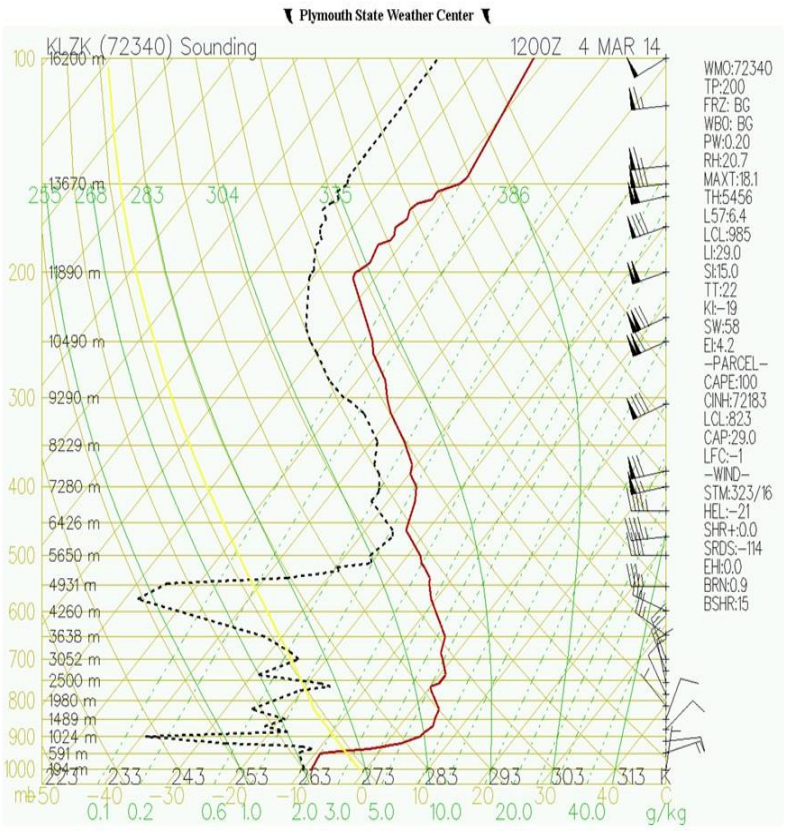

Figure 3.5 - An observed upper-air sounding from the Little Rock, Arkansas National Weather Service office (KLZK) at 1200 UTC on 04 March 2014. Charts created using Plymouth State Weather Center data archive (https://vortex.plymouth.edu/)

The upper-air soundings, specifically the lowest levels of the soundings (Fig. 3.5),

revealed certain characteristics commonly associated with the presence of a cold-air damming event. The wind profile during cold-air damming events typically will feature light easterly winds particularly below another cold-air damming feature: the temperature inversion. The initial increase in air temperature that represents the base of the temperature inversion signifies the top of the dome of cold, dense air found in the stable surface layer that becomes “trapped” near the surface up against the elevation change of a topographic feature. The inversion can become quite strong at times, as the air temperature can climb well above freezing as wind flow above the stable layer reverts to westerly flow above the terrain feature and diabatic processes increase the temperature

above the trapped cold air. Typically, the stronger the inversion the more persistent and longer-lasting the cold-air damming event tends to be. The temperature profile will revert to common lapse rate behavior near the end of a cold-air damming event as the cold, stable layer at the surface is eroded away. The lowest level of the sounding can also reveal the depth and extent of moisture trapped at the surface with the cold air. To reiterate, the presence of moisture in the stable layer is not direct evidence of cold-air damming but when present during these events can indicate intense impacts observed at the surface.

3.1.4.1 Modeled Upper-Air Sounding Verification Process

Noted above, the region of interest throughout this research sequence contains only one NWS office in which observed upper-air soundings are flown twice daily (Little Rock, AR). To overcome the limitations of observed upper-air soundings, 12-km North American Model (NAM) soundings are used in the other five locations (KPOF, KHKA, KTKX, KAWM, and KMEM) where METAR reports from these ASOS stations is utilized. An online archive of upper-air atmospheric data (READY Archived Meteorology (noaa.gov)) provided by NOAA's Air Research Laboratory provided the model output necessary to analyze these soundings. Initial field model output for each sounding taken at 6-hour intervals was concurrent with the other analysis resources (surface maps, meteorograms, etc.). Due to the use of model output in analysis that was mainly based in observation, verification was necessary to ensure the quality of the model output in question. For the initial March 2014 case study, NAM 12-km sounding output was

gathered for the KLZK, KPOF, and KHKA stations between 0000 UTC 03 March 2014 and 1200 UTC 05 March 2014 at 6-hour intervals. Observed soundings from the KLIT NWS office were also gathered, though with only 2 radiosonde flights per day; this observed sounding data did not match the 6-hour temporal resolution of the modeled sounding output. *It is understood that there was interpolation between the verification at the Little Rock, AR station and the other 5 stations, as well as only verifying every 12 hours. Due to the use of initialized model output, only as long as the Little Rock verification achieved specific thresholds for specific atmospheric variables, then the model output was considered satisfactory for analysis to continue*. Variables for verification included temperature, dewpoint temperature, wind direction, and wind speed (knots). Observed data was compared to modeled output at 7 levels of atmospheric pressure: 250 hPa, 500 hPa, 700 hPa, 850 hPa, 900 hPa, 950 hPa, and 1000 hPa. The study then computed a difference in variables for each pressure level. These variable differences were then averaged, and the average was compared to specific thresholds for each variable.

Table 3.1 - A list of model sounding verification thresholds for comparing observed weather characteristics to modeled characteristics. Weather characteristics include temperature, dewpoint temperature, wind speed, and wind direction.

Variable Thresholds for Comparative Analysis of Model Output	
2-m Temperature	1.5° C
2-m Dewpoint Temperature	4.5° C
Wind Direction	10°
Wind Speed (kts)	2 kts

3.2 5-Year Cold-Air Damming Frequency Study

To better understand the frequency of cold air damming events in the Ozark Plateau region, observations of freezing weather conditions were used to ascertain when these events take place. To obtain these observations an archive of METAR reports from 6 ASOS station locations within the region of interest were analyzed (discussed previously in Case Selection). These ASOS stations are an excellent source of archived observed data as they regularly observe many weather characteristics including the present weather coding utilized for this research sequence.

Following the evaluation of the METAR reports from each station, 34 potential cases of cold-air damming were identified and given specific time frames. Each case begins at the 6-hour synoptic time prior to the first METAR observed report of freezing weather and ends at the 6-hour synoptic time after the last report of freezing conditions (freezing conditions discussed previously in Case Selection). The same resources as described in the initial case study data and methods section including radar-overlayed surface maps, 10-m wind maps, surface relative humidity maps, and NAM 12-km modeled upper-air soundings were gathered at each 6-hour time interval contained within each case study. All 34 case studies were then analyzed in the same manner as the initial case study of the first sequence of research.

Each case study was also evaluated numerically using the Froude number. The established and efficient way to study cold-air damming phenomena involved calculations of the Brunt-Väisälä frequency and the Froude number. The Brunt-Väisälä frequency was defined as the frequency at which a displaced air parcel will oscillate

when displaced vertically within a statically stable environment (Stull, 1995). It is calculated using:

$$N = \sqrt{\frac{g}{\theta_v} * \frac{\partial \theta_v}{\partial z}} \qquad (1)$$

Where:

- N represents the Brunt-Väisälä frequency
- g is the gravitational constant valued at 9.8 m s^{-1}
- θ_v is the ambient virtual potential temperature
- $\frac{\partial \theta_v}{\partial z}$ is the gradient of ambient virtual potential temperature with geopotential height (z) whose values are taken from the model sounding output.

The ambient virtual potential temperature is calculated using:

$$\theta_v = \theta(1 + 0.61 * w_s) \qquad (2)$$

Where:

- θ is the actual potential temperature (calculated empirically using sounding temperature output).
- w_s is the saturation mixing ratio (also calculated empirically from sounding temperature output).

Finally, the Froude Number is defined by the A.G. as a measure of whether there will be an upstream-propagating region of decelerated flow. The Froude number describes flow in this way over any given spatial area and so a singular Froude number is efficient for

flow evaluation. In cases where the Froude number was calculated at a point location (or several point locations) using averages of U-wind speed and Brunt-Väisälä frequency in the vertical direction over the location, an average of these Froude number calculations was used to arrive at a singular value for the Froude number. When the Froude number is >>1 the flow will ascend over the obstacle with no upstream deceleration. When the Froude number is << 1, a region of upstream flow deceleration forms that may propagate continuously upstream with time. Froude number values around 1 (1.00 to 1.20) signaled that the flow could be disrupted where elevation heights are taller or uninterrupted in cases of lower elevation values. The Froude number was calculated using:

$$Fr = \frac{U^2}{(N * h)^2} \qquad (3)$$

Where:

- Fr represents the Froude number
- U is the incoming wind speed (m s^{-1}) (taken from model sounding output)
- N is the Brunt-Väisälä frequency
- h is the height against relief in meters

Using this form of the Froude number allowed for the evaluation of a flow field. Bosart and Bell (1988) related this form of the Froude number to "the kinetic energy of the horizontal flow and the potential energy represented by buoyant forces" or more simply "the ratio of kinetic energy of the ambient flow to the energy needed to get the air parcel above the mountain top". Here, the mountain top in question is the maximum height of the Ozark Plateau. For h, each station's elevation is subtracted from the tallest elevation

height of the Ozark Plateau which was found to be approximately 2,300 ft in a study performed by the US Geological Survey (Adamski et. al 1995).

3.2.1 Characteristics for Classifying Cold-Air Damming Events

To quantifiably classify all 34 cases of potential impactful cold-air damming, a list of identifying characteristics was created to determine if conditions observed by the 6 ASOS stations used in this study were the result of cold-air damming occurring up against the Ozark Plateau. The list of characteristics was comprised of conditions that are observed during a cold-air damming event, and characteristics that would make the cold-air damming an impactful event on the region of interest. It should be noted that these characteristics were born of observations found in the initial cold-air damming case study from the first phase of research. Observations of that referenced cold-air damming event were used as characteristics to identify other cases of cold-air damming associated with the Ozark Plateau. Due to this, the research focused only on impactful freezing conditions resulting from cold-air damming. It is understood, however, that cold-air damming can occur when temperatures are above freezing, though for this research those instances were omitted. Each potential case study was analyzed using the tools listed above to clarify if the necessary conditions were present to justify cases of cold-air damming.

Cases that met all necessary cold-air damming characteristics and necessary high impact cold-air damming conditions are deemed red cases. A classification scheme was introduced to categorize cold-air damming by intensity/impact. Cases that met all necessary cold-air damming conditions, but not high impact cold-air damming

characteristics were classified to be yellow cases. Finally, cases that did not meet all the necessary cold-air damming conditions were designated as green cases.

The list of characteristics used to identify a cold-air damming event is as follows:

1. Favorable parent anticyclone placement
2. Terrain-orthogonal 10-m wind component
3. Model sounding temperature profile inversion above the PBL
4. Model sounding terrain-orthogonal surface layer wind profile
5. Lack of significant radar reflectivity
6. Favorable Froude number calculation

Favorable parent anticyclone placement for the region of interest that includes southeastern Missouri and eastern Arkansas places a high-pressure zone that extends as far west as the western borders of Missouri and Iowa and as far east as the eastern border of Ohio. The high-pressure center must reside within the zone while the region is experiencing cold-air damming conditions. It should be noted that the high-pressure zone is not rigid as some anticyclones cover a larger surface area than others. In these cases, special treatment of anticyclone placement is taken to ensure that the region of interest resides in the southern flank of the pressure center and that special treatment is noted in the following 5-Year Analysis Results Section.

A terrain-orthogonal wind component is a crucial ingredient in the creation and evolution of cold-air damming events. As described above, the southeastern flank of the Ozark Plateau resides just west of the vast floodplain created by the Mississippi River. With these two areas of elevation contrast located directly next to one another the terrain-

orthogonal wind component pushing cold, dense air up against the elevation of the Plateau becomes even more important in Ozark Plateau cold-air damming events. To evaluate wind direction several resources are utilized. Synoptically, the surface pressure maps provide a general overview of where terrain-orthogonal wind components can be found in the southern flank of anticyclones, even when assuming non-geostrophic 10-m wind flow. Regionally, the 10-m wind maps described previously depicted the general flow of the 10-m wind pattern across the region as well as wind barbs observing speed in knots to give a better observation of how fast the wind is blowing. This was important when calculating the Froude number, another characteristic used in determining the existence of cold-air damming. A deterministic approach to terrain-orthogonal wind component utilized NAM-12 km model sounding output at each impacted ASOS station. Evaluating the wind profile of each time-stepped sounding allowed understanding of the directional evolution above and below the temperature inversion, and how the stratified layers of the cold-air damming event responded to both speed and directional changes of the wind profile. This deterministic approach satisfied the fourth characteristic for cold-air damming events as well. Cases in which a terrain-orthogonal component did not exist (directional degree resides outside of the 40-to-220-degree wind direction zone) during times of observed impact resulted in the case being labeled as a green case.

The NAM-12 km model soundings were useful in evaluating the wind profile, as well as the presence of the necessary temperature inversion during cold-air damming events. The importance of the inversion is described above and the mere presence of the temperature inversion during the time steps coinciding with observed impact times was

enough to satisfy this cold-air damming condition. Any case that did not possess a temperature inversion during impact times was deemed a green case.

The initial cold-air damming case study analyzed in the first phase of research showed the impact of icy road conditions occurring even when frozen precipitation was not observed on local radar reflectivity. To keep consistent with the first phase the 34 potential cold-air damming case studies face radar reflectivity imagery scrutiny. To perform this analysis, radar reflectivity data was collected from NOAA's National Center for Environmental Information online data archive (Radar | National Centers for Environmental Information (NCEI) (noaa.gov)). This data was then downloaded into Gibson Ridge (GR) software and displayed. The location of impact was evaluated for the presence of hydrometeor reflectivity directly over the ASOS station location during the time of impact. In cases that featured prominent reflectivity at those impact times, the case was removed from further study and classified as green. An unintentional benefit of not having a radar station co-located with 4 of the 6 ASOS stations (Fig. 3.6) was that any reflectivity observed over those locations was determined though sounding analysis to be occurring above the stable surface layer containing the potential cold dome.

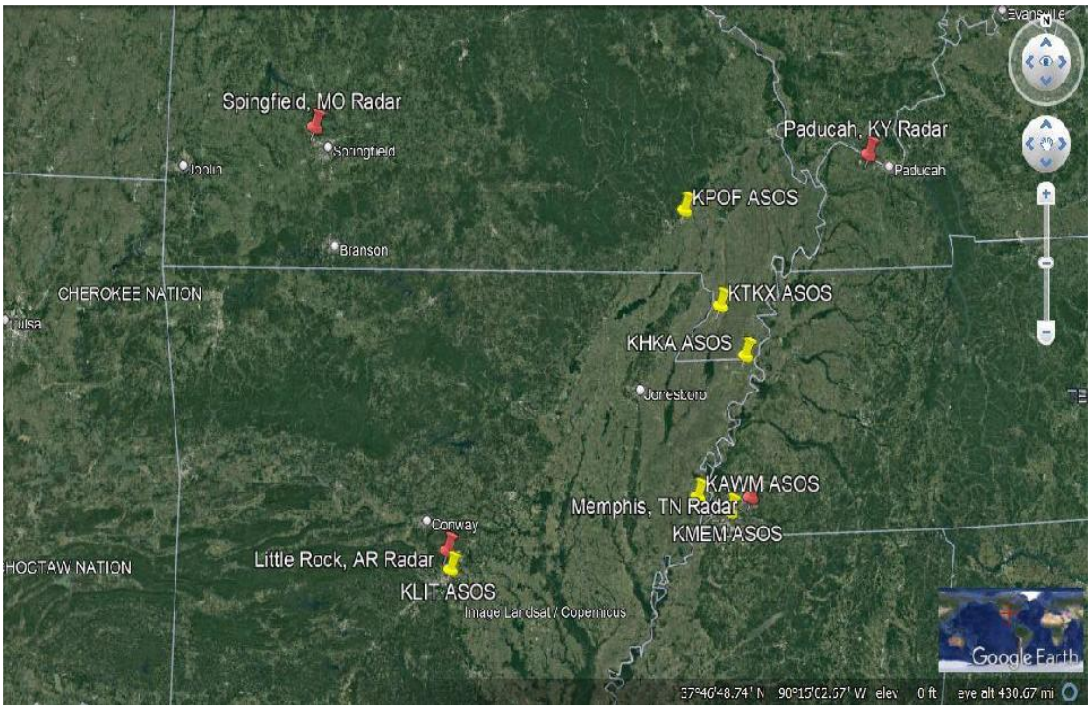

Figure 3.6 – A map showing the 6 ASOS station locations and the local network of National Weather Service WSR-88D radar towers. Yellow markers represent the ASOS stations. Red markers represent the NWS radar towers. Image created using Google Earth.

In the cases of the (KLIT) Little Rock, AR and the (KMEM) Memphis, Tennessee station the radars employed are far enough away (12 km and 17 km respectively) from the KLIT and KMEM ASOS station locations that this analysis was still pertinent. Table 3.1 details the radar beam height above each ASOS station's location.

Radar beam height was calculated using the following equation:

$$h = \sqrt{[(\frac{4}{3} * R)^2 + r^2 + 2r\left(\frac{4}{3}R\right) * \sin\varphi]} + \left(\frac{4}{3}R\right) + H_0 \qquad (4)$$

Table3.2 - Height of the center of closest radar location radar beams above the 6 ASOS station locations.

Station	Closest Radar Location	Distance Between	Lowest Beam Height at ASOS Station
Poplar Bluff, MO (KPOF)	Paducah, KY (KPAH)	141.82 km	2450 m
Kennett, MO (KTKX)	Memphis, TN (KMEM)	121.70 km	1960 m
Blytheville, AR (KHKA)	Memphis, TN (KMEM)	87.47 km	1240 m
Little Rock, AR (KLIT)	Little Rock, AR (KLZK)	12.36 km	150 m
West Memphis, AR (KAWM)	Memphis, TN (KMEM)	39.52 km	470 m
Memphis, TN (KMEM)	Memphis, TN (KMEM)	17.66 km	200 m

Where:

- h = Radar beam center height
- R = Radius of the Earth (6378 km)
- r = Range from radar tower to ASOS station location
- φ = Elevation angle of lowest radar beam (~0.5°)
- H_0 = Height of radar above the ground (30.5 meters)

The final characteristic for identifying the existence of cold-air damming took a numerical approach to analysis involving the Froude number. Described above in section 3.2.1, the Froude number calculation was a resourceful tool for determining if 10-m wind flow was strong enough to overcome the terrain barrier in question (in this case the Ozark Plateau). Values of Froude number greater than 1 suggested that the flow overcomes the barrier. Otherwise, Froude number values less than or equal to 1 implied that the flow cannot overcome the barrier, and either was forced around the obstacle or became trapped up against the obstacle. This Froude number calculation was performed for all 34 potential cases of cold-air damming at each 6-hour time step of analysis for each case. This not only calculated a specific Froude number per time-step but also showed how the

flow evolved over the course of the potential cold-air damming event. Red cases were those in which the Froude number is 1 or less, and green cases were those in which the Froude number was greater than 1.20.

The other characteristics of evaluation for this 5-year study were those that were needed for ***impactful*** cold-air damming events. These conditions are as follows:

1. Moisture rich surface layer
2. 2-m temperatures at or below freezing
3. The existence of cloud cover over impacted stations

To evaluate surface level moisture a variety of resources were employed. The archived observed surface maps of dewpoint depressions and station model plots were used to analyze not only surface moisture in the region of interest at the time of impact but also if there existed a steep gradient in the moisture field between the floodplain of the Mississippi River and the top of the Ozark Plateau. The station model plots featured on these maps also depicted a numerical understanding of available moisture with the listing of both air temperature and dewpoint temperature. In locations where the difference between the 2 variables (dewpoint depression) is 5°F or less the location was understood to be near saturation, and thus moisture laden. High impact cold-air damming events needed to have a dewpoint depression of 5°F or less to be considered as such. The NAM-12 km model soundings (described previously in Data & Methods) also gave a vertical resolution to both dewpoint and air temperature. Typically, in high impact cold-air damming events, a moisture-rich surface layer dries out quickly as height increases, especially in the presence of a strong temperature inversion often observed just above the

cold, stable surface layer. In these existences the 5°F dewpoint depression rule was once again employed to determine the extent of moisture availability at the surface. For the cases that exhibited moisture availability at the surface a red case classification was given. For those cases that did not possess significant moisture at the surface a yellow classification was given.

Coinciding with a moisture rich environment, freezing or below freezing temperatures are necessary for the cold-air damming event to have a significant impact felt at the surface. 2-m temperatures are evaluated in several ways. The surface relative humidity maps give a regional sense of the surface moisture gradients through the placement of the station model plots throughout the map. For a deterministic solution, the NAM-12 km soundings are employed to evaluate the vertical temperature profile at a singular location. For each potential case study, a primary location of impact is chosen based on METAR report analysis. For those cases in which multiple stations are impacted a location is chosen amongst the impacted station based upon the duration of impact for each station. The station that experienced the longest time of impact is selected as the

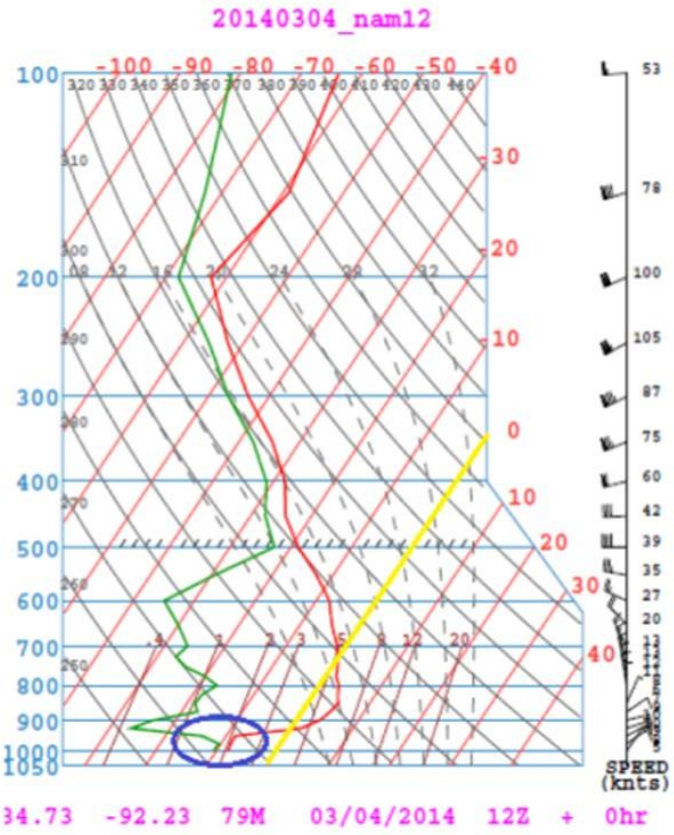

Figure 3.7 - A model NAM-12 km sounding from the initial case study at 1200 UTC on 04 March 2014 located at the Blytheville, Arkansas station (KHKA). The temperature profile (red line) is evaluated at the surface (circled in blue) to be below the 0°C freezing isotherm (denoted in yellow). Sounding created courtesy of NOAA's Air Resources Laboratory.

primary location for the case study. At this location the model sounding is evaluated to determine if freezing or below freezing temperatures existed in the stable surface layer. Figure 3.7 shows a model sounding in which temperatures were in fact below freezing at the surface, supporting an impactful cold-air damming event.

Finally, meteorograms from the impacted ASOS locations provided a good account of 2-m temperature over the course of a 24-hour period and how the temperature evolved over that same period. For point locations, meteorograms were an excellent resource for understanding how observed weather was experienced and how it changed over the course of a day. Observed meteorograms were collected for each potential case study at

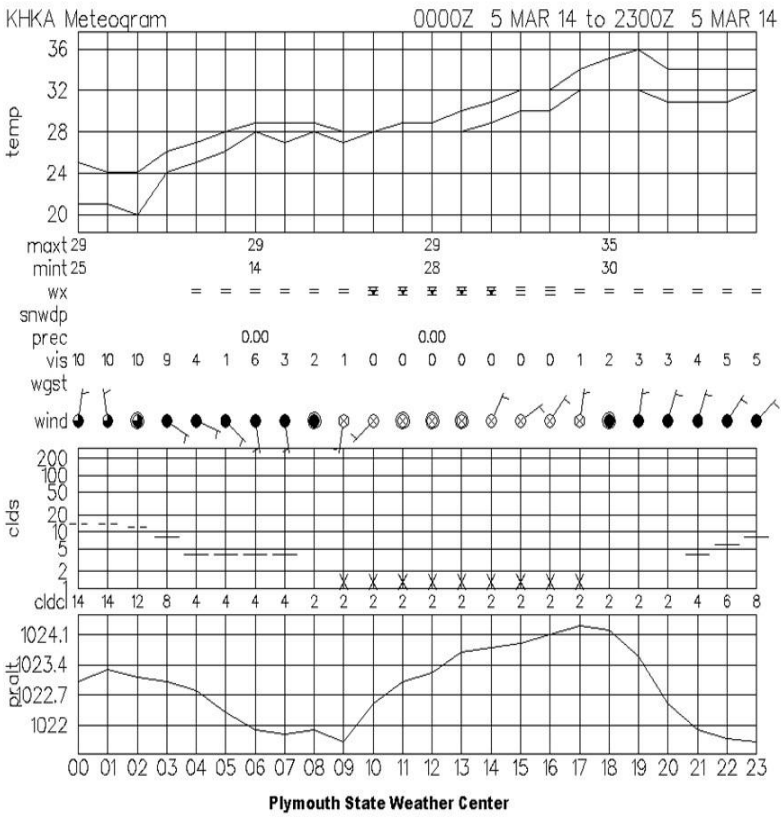

Figure 3.8 - A meteorogram from the initial case study taken from the Blytheville, Arkansas (KHKA) location for 05 March 2014. The meteorogram displays observed weather characteristics between 0000 UTC and 2300 UTC on that day. Weather characteristics include temperature, dewpoint temperature, present weather, precipitation accumulation, visibility, wind speed, wind direction, cloud cover, cloud altitudes, and surface pressure. Meteorogram created using Plymouth State Weather Center data archive (https://vortex.plymouth.edu/)

each impacted ASOS station location for each day cold-air damming weather reporting was observed. Meteorograms provide several observed characteristics (Fig. 3.8) including cloud cover, the third and final impact condition in the analysis of potential cold-air damming.

The analysis of cloud cover reinforces the analysis of low-level moisture present during the cold-air damming event. Cloud cover implies saturation and subsequent condensation at the altitude at which cloud cover was present. Cloud cover also helps potential cold-air damming events to persist by limiting the effects of daytime heating and poor ground conditions in the case of freezing fog. Freezing fog can contribute to

riming on objects and ground surfaces persisting and helping to maintain hazardous conditions. In cases where cloud cover was found in the lower levels of the atmosphere the event was determined to be impactful if the other 2 impact conditions were also satisfied. Events in which cloud cover persisted were regarded as longer lasting cold-air damming events and impacts were felt at the surface over a longer period.

3.3 WRF Methods for Evaluating Terrain Interaction in Cold-Air Damming Events

3.3.1 Model Overview and Specifications

The third phase of research on cold-air damming took a numerical modeling approach to the burden of evaluating cold-air damming events in the Ozarks. To complete this task the Weather Research and Forecasting Model (WRF) was utilized to manipulate the scale of the Ozark Plateau. Developed by the National Center for Atmospheric Research (NCAR) the WRF is an atmospheric modeling system that uses a variety of physics options, fully compressible nonhydrostatic equations, domain nesting capabilities, an Arakawa C-grid, and Runge-Kutta 2nd and 3rd order time integration options (Skamarock et al. 2021). The WRF was an excellent resource for this approach as its small resolution and high computation power allows the ability to estimate the changes to cold-air damming events when the elevation of topography is altered.

The study uses 2 simulations (detailed in Section 2.2 - Case Selection) to evaluate the role of terrain in these cold-air damming events. The model output, parametrization schemes, and nested domain grids are unaltered for each simulation. Model initial conditions for these simulations come from the Global Forecasting System (GFS). Table

3.2 is a list of the parameterization schemes utilized for both simulations. Three nested domain grids were used for the 2 simulations (Figure 3.9) with the largest domain (d01) encompassing the eastern half of the continental United States containing 25-km grid spacing affording a 120x120 grid point field. The second domain (d02) focused more on a regional scale over the Lower Mississippi River Valley with 5-km grid spacing giving a 181x181 grid point field. The innermost domain (d03) truncated down to the region of interest centered over extreme southeastern Missouri and northeastern Arkansas containing 1-km grid spacing and a 231x231 grid point field.

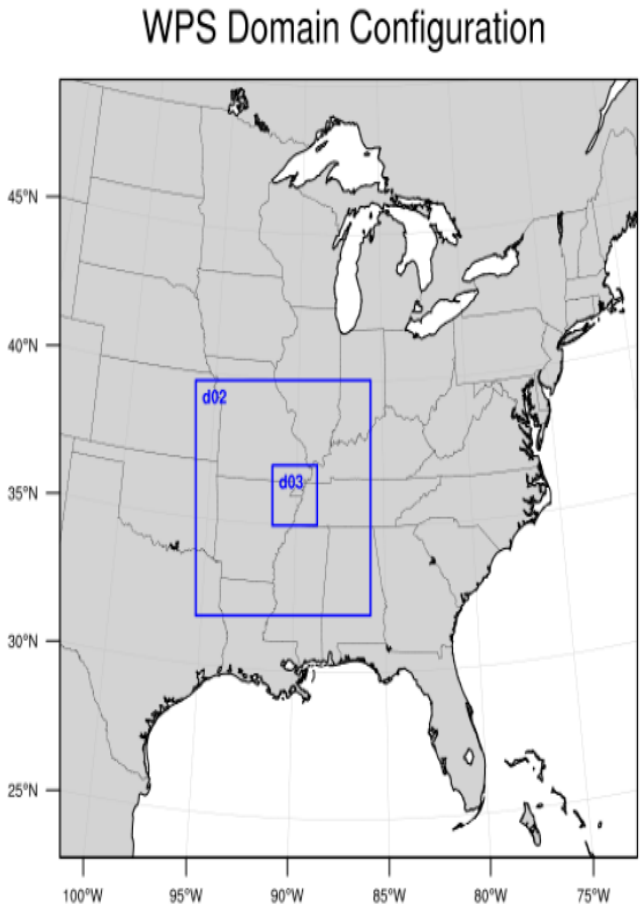

Figure 3.9 – A map of the nested grid domain used in the three WRF simulations modeling cold-air damming events in the Ozarks. The outermost domain (d01) employs 25-km grid spacing, the second regional domain (d02) contains 5-km grid spacing, and the innermost domain (d03) uses the finest spatial resolution at 1-km grid spacing.

The domains were “nested” due to the initial and boundary conditions for each domain. For each simulation the outermost domain (d01) begins 6 hours prior to the d02 which begins 6 hours prior to the innermost domain (d03). Boundary conditions for d01 were taken from the GFS-25 model output detailed above. Initial boundary conditions for the inner 2 domains were taken from the higher ordered domain at the start time of the inner domain’s simulation. This allowed the model to spin-up conditions in the innermost domain that were most ideal for fine spatial resolution modeling techniques. For each case study an actual-terrain simulation was performed and used as a baseline control for all other simulations of the case study in which the topography elevation was altered. The first alteration completely flattened the elevation of the Ozark Plateau multiplying terrain elevation by 0.001. The other alterations multiplied terrain elevation by factors between 0.1 and 2.0 (including the baseline control factor 1.0) which provided a dataset of elevation-iterated model output. *The 26 November 2016 case only simulated the benchmark runs (0.001, 0.5, 1.0 and 2.0 iterations).* In total, 46 WRF simulations were performed in the third phase of research across the 2 case studies involved.

3.3.2 WRF Modeling-Based Charts for Analysis

Following the completion of WRF simulations, a series of charts were created to help contextualize and analyze data created during the simulations. Using the PYTHON computer programming language, a series of surface charts were created for each WRF simulation at 6-hour synoptic times (0000 UTC, 0600 UTC, 1200 UTC, 1800 UTC) contained within each case study time frame. An example of the 10-m wind streamlines charts can be seen in Figure 3.10. Two sets of streamline charts were created for each

case study. Figure 3.10 features the streamline chart that captured wind flow in the regional domain (d02) as well as streamline charts associated with the innermost domain (d03).

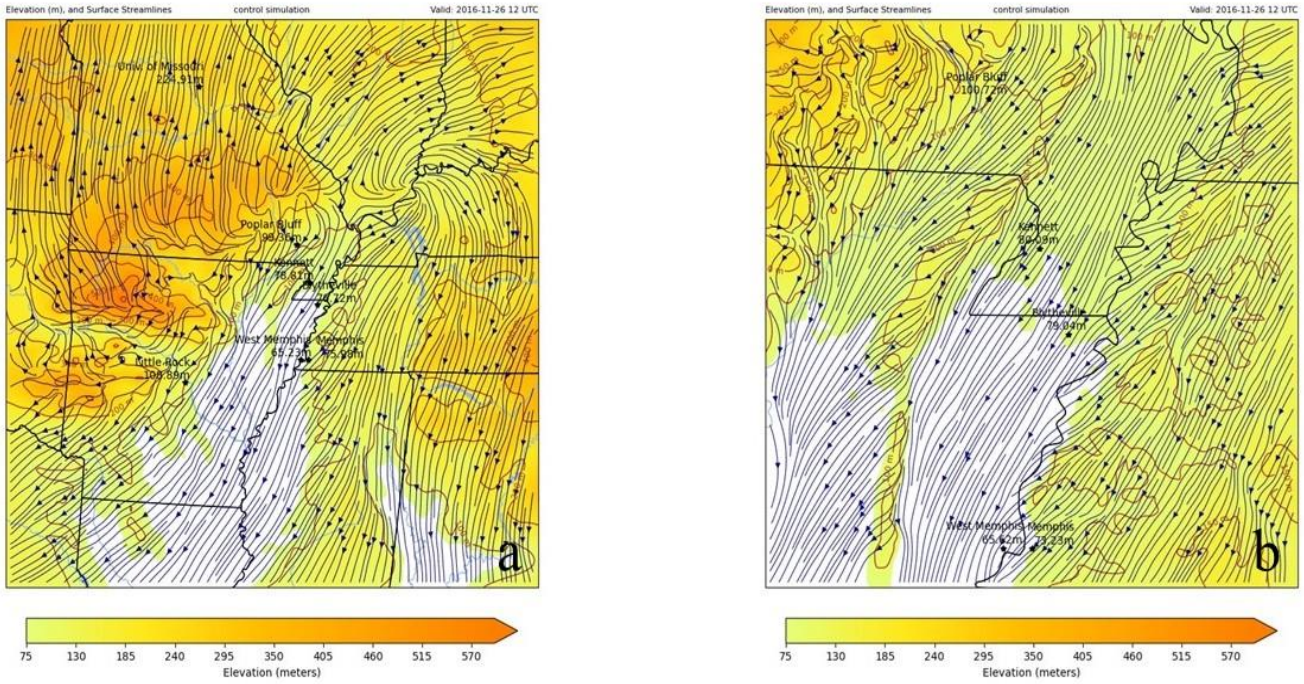

Figure 3.10 – Surface streamline charts created from WRF model-simulated output from the 26 November 2016 case study at 1200 UTC. Both charts feature ASOS station locations and elevations, surface wind streamlines (dark blue), and color shaded terrain elevation between 75 and >570 m. Map (a) includes the regional (d02) streamline chart. Map (b) contains the innermost (d03) streamline chart.

These charts were useful in understanding how the model simulated 10-m wind flow and how that 10-m wind flow evolved over time. Altering terrain height within the WRF model gave a comparative analysis of 10-m wind flow and how that flow was manipulated both at a regional scope and within the region of interest when terrain elevation was altered. Figure 3.11 gives an example of comparative analysis between the 4 benchmark alterations for the streamline charts. These 4 charts were all created using the innermost (d03) domain.

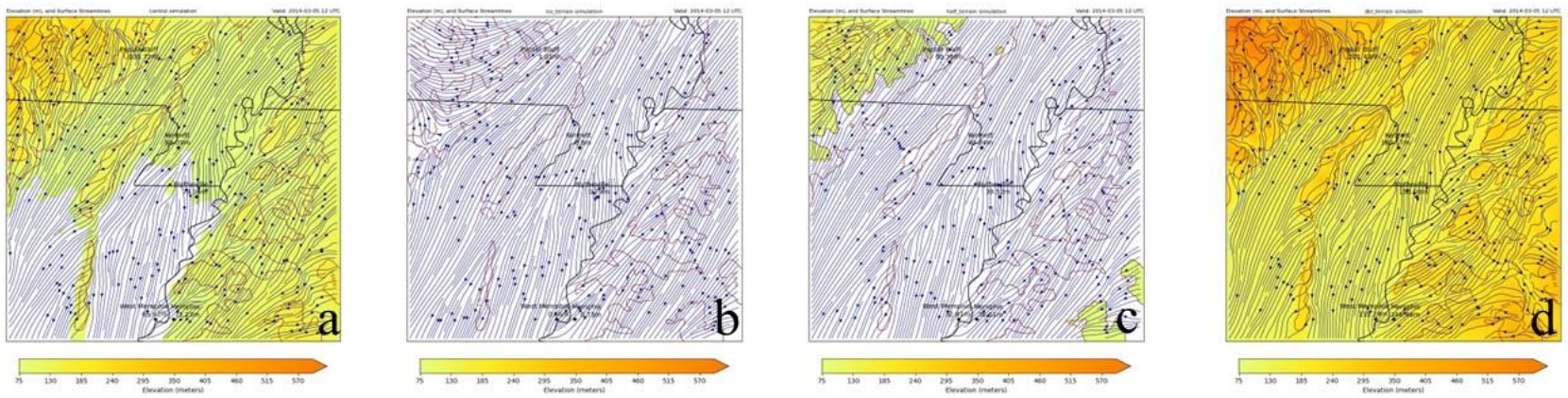

Figure 3.11 – A 4-panel featuring d03 streamline charts at 1200 UTC from 05 March 2014. All charts feature ASOS station locations and elevations, surface wind streamlines (dark blue) and color shaded terrain elevations between 75 and >570 meters. Map (a) is the 1.0 (actual-terrain) simulated streamline chart. Map (b) is the 0.001 (no_terrain) simulated streamline chart. Map (c) is the 0.5 (half_terrain) simulated streamline chart. Map (d) is the 2.0 (dbl_terrain) simulated streamline chart.

Another set of charts created from WRF model-simulated output depicted 2-m temperatures. These charts help to analyze how temperature evolved during the 2 cases studies and how that evolution was manipulated when the terrain elevation was altered. Again, charts were created at 6-hour intervals of synoptic times (0000 UTC, 0600 UTC, 1200 UTC, and 1800 UTC) contained within the time frame for each case study. Figure 3.12 provides an example of these 2-m temperature maps, one of which features the regional (d02) 2-m temperature map and the other the innermost (d03) 2-m temperature map.

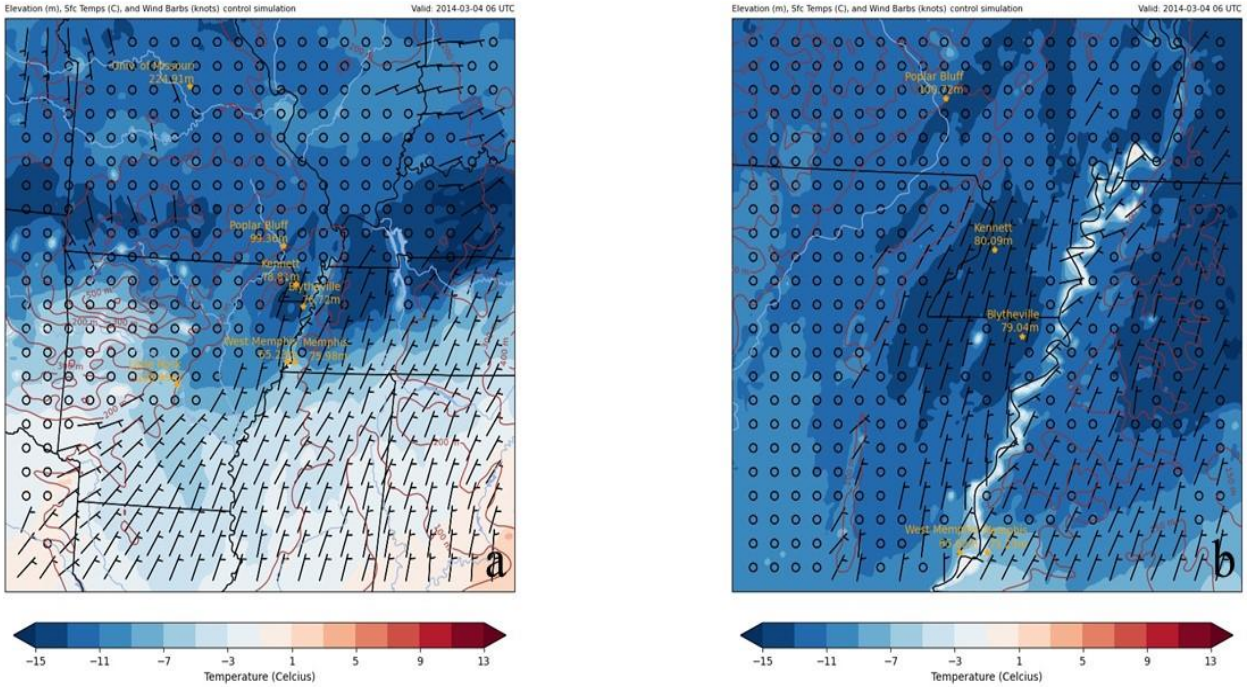

Figure 3.12 – 2-m temperature charts created from WRF model-simulated ouput at 0600 UTC on 04 March 2014. Each chart features ASOS station locations and elevations (orange), terrain elevations (light brown), 10-m AGL surface wind barbs in knots (black), and color shaded 2-m temperature between < -15°C and > 13°C. Map (a) is a regional (d02) 2-m temperature chart. Map (b) is the innermost (d03) 2-m temperature chart.

The presence of 10-m AGL wind barbs on the 2-m temperature maps allowed understanding the evolution of 10-m wind flow in concert with the changing of the 2-m temperature field with each terrain elevation alteration. Figure 3.13 gives an example of a comparative analysis of 2-m temperature between the 4 benchmark terrain alterations.

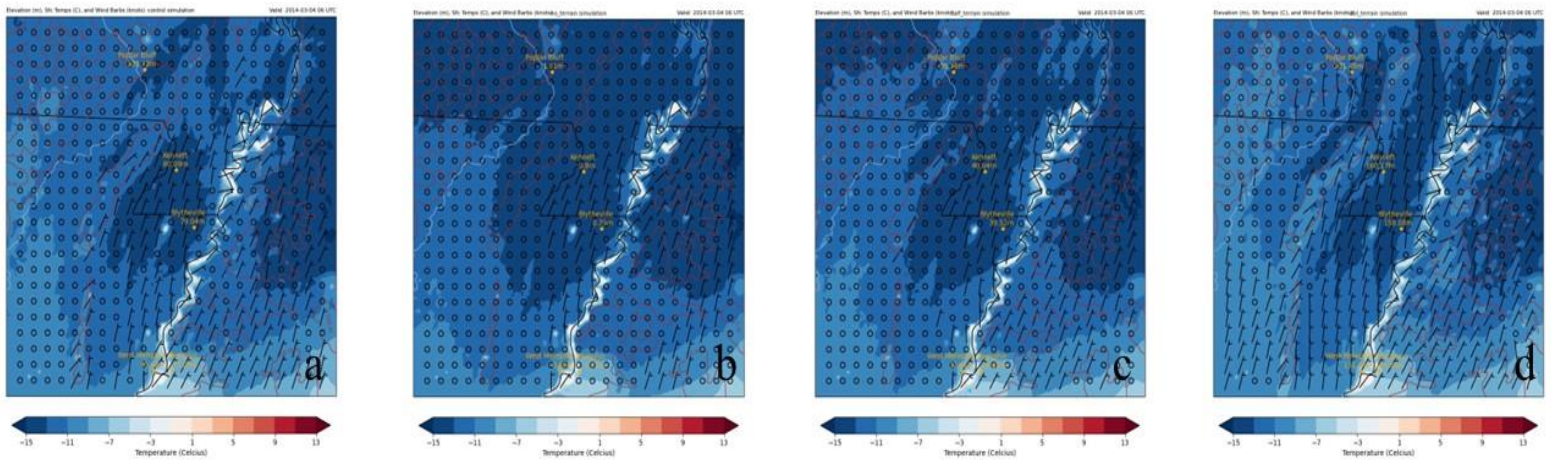

Figure 3.13 – A 4-panel of 2-m temperature charts created from WRF model-simulated output at 0600 UTC on 04 March 2014. Each chart features ASOS station locations and elevation (orange), terrain elevation (light brown), 10-m surface wind barbs (black), and color shaded 2-m temperatures between < -15°C and > 13°C. Map (a) is the 1.0 (actual-terrain) simulation 2-m temperature chart. Map (b) is the 0.001 (no_terrain) simulation 2-m temperature chart. Map (c) is the 0.5 (half_terrain) simulation 2-m temperature chart. Map (d) is the 2.0 (dbl_terrain) simulation 2-m temperature chart.

The final group of charts created for analysis in the third phase of research were WRF model simulation upper-air soundings. Like the other charts created for analysis the simulated upper-air soundings were created at 6-hour intervals coinciding with synoptic hours (0000 UTC, 0600 UTC, 1200 UTC, 1800 UTC) contained within the time frame of each case study. Unlike the other charts, the simulated soundings were point located and required a latitude and longitude coordinate. For the 04 March 2014 case study, the Blytheville, AR station was designated as the point location making its latitude and longitude the coordinate used for its simulated soundings. Kennett, Missouri being the sole station impacted during the 26 November 2016 event is designated as the point location for that case study. Each sounding lists its coordinate along with its time stamp at the top of the chart (Fig 3.14).

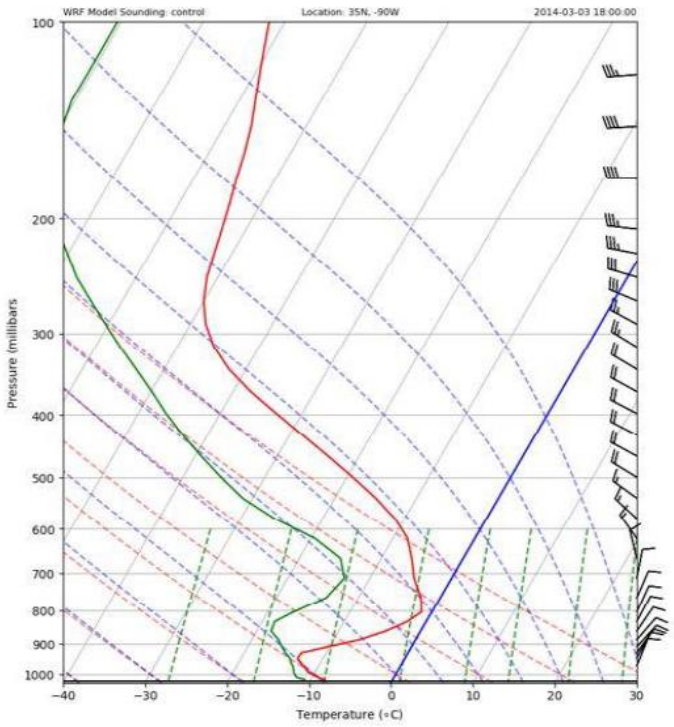

Figure 3.14 – A WRF model simulated upper-air sounding at 1800 UTC on 03 March 2014 located at the Blytheville, Arkansas station (KHKA). The profile features an air temperature vertical profile (red line), dew point temperature vertical profile (green line), and a vertical wind profile (black wind barbs; right side). The x-axis is temperature in Celsius with the 0°C freezing line highlighted in blue. The y-axis features logarithmic ascending pressure values in millibars. The sounding also contained low-level mixing ratio lines (dashed green), saturation adiabat lines (dashed blue), and dry adiabat lines (dashed purple).

The simulated upper-air soundings created in the third phase of research were analyzed like the upper-air soundings of the previous 2 phases. Verification (described above) of the WRF-model soundings was restricted to only the actual-terrain simulations.

3.3.3 WRF Model Froude Calculations

The Froude number analysis was employed once again in the third phase of research to numerically quantify the topography's ability to impede 10-m wind flow

during cold-air damming events. For each case study in the third phase, 2 Froude numbers were calculated: one associated with the regional domain (d02), and one with the innermost domain (d03). A singular Froude number was calculated for each of these domains in every simulation run. The Brunt-Väisälä frequency (N) and 10-m wind speed values (U) were averaged over each domain's grid point values and these averages were used to calculate the Froude number. Output tables containing Froude number values for every simulation run of each case study can be found later in Chapter 6 – Third Phase: WRF Modeling.

CHAPTER 4. FIRST PHASE: INITIAL CASE STUDY

4.1 Introduction

The initial phase of research analyzed a case study taken from observed weather events and reported impacts on travel in the region of interest for this study: southeastern Missouri and eastern Arkansas. On 04 March 2014, after the passage of a late-winter mid-latitude cyclone that brought snow and freezing rain to the state of Arkansas as well as a snowpack to the northeast over southern Illinois and Kentucky, motorists traveling on Interstates 40 and 55 in eastern Arkansas became stranded as traffic came to a standstill due to icy road conditions. These adverse road conditions occurred well after precipitation associated with the cyclone traversing the southern United States had ceased over the region of interest. As stated previously, local authorities in concert with the Arkansas National Guard worked throughout the evening of 04 March 2014 and the morning hours of 05 March 2014 to bring necessary medicines, supplies, and, when necessary, evacuation to those stranded on the highways and roads impacted throughout the region.

It is this scenario that acted as the impetus for this research project, and ultimately culminated in supporting evidence for the presence of Ozark Plateau-induced cold-air damming. The following is an analysis of the 04 March 2014 cold-air damming case and results of that analysis were used as a template for identifying Ozark cold-air damming in later phases of research.

4.2 Synoptic Overview

Radar-overlayed surface maps acted as a visual resource to understand the synoptic setup and evolution of the synoptic pattern through the cold-air damming event. The initial surface maps (Figure 4.1) showed precipitation associated with the frontal passage propagating across and to the east away from the Lower Mississippi Valley and the region of interest in eastern Arkansas at 0000 UTC and 0600 UTC on 03 March 2014.

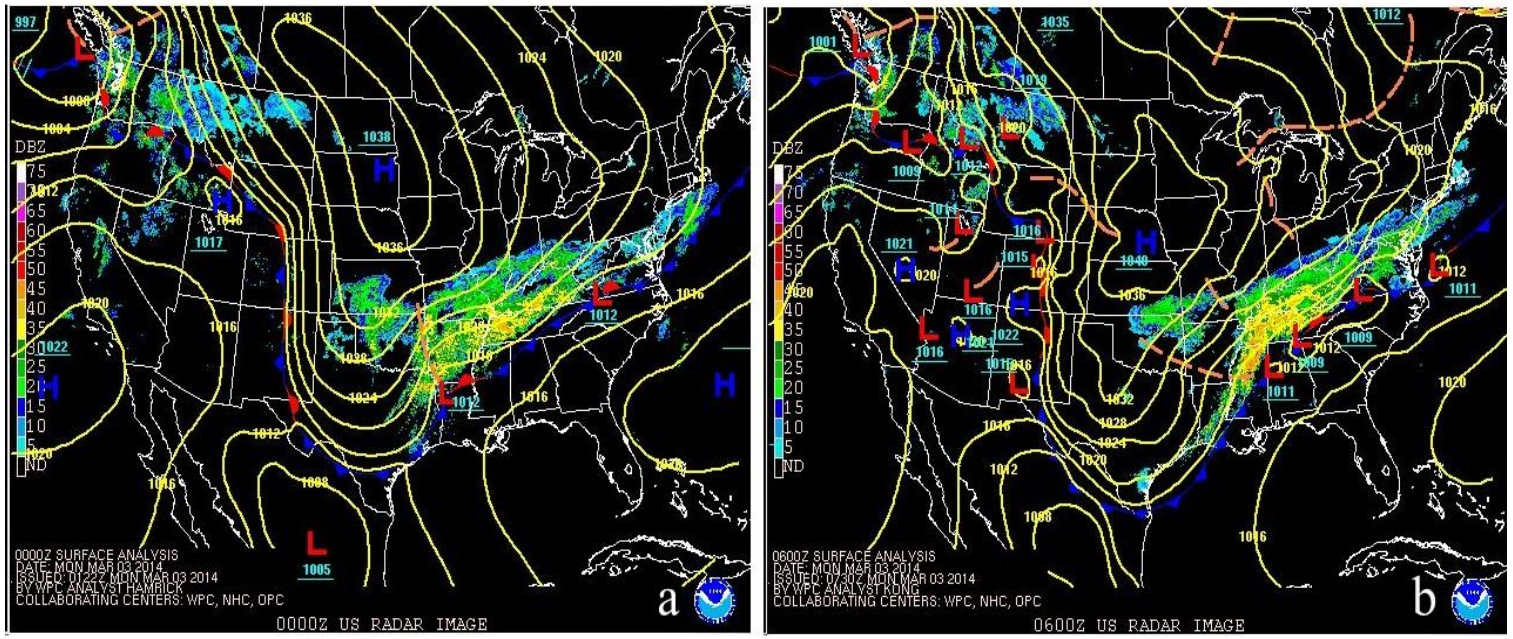

Figure 4.1 – Radar-overlayed surface pressure maps from the initial case study. These maps feature the mid-latitude cyclone traversing over and just past the region of interest in eastern Arkansas. Map (a) is analyzed at 0000 UTC on 03 March 2014. Map (b) is analyzed at 0600 UTC on 03 March 2014. Maps courtesy of NOAA/NWS.

An important feature of these initial maps was the presence of an anticyclone building into the Central Plains. The anticyclone was crucial for the creation of cold-air damming and its placement initially over the Dakotas (Fig. 4.1a), and then 6 hours later just to the northwest of Missouri (Fig. 4.1b) coincided with the timing of a cold-air damming event later in this analysis. This placement led to the establishment of northeasterly 10-m wind flow in eastern Arkansas on the morning of 03 March 2014 where northeasterly flow at the surface flowed around the anticyclone to the northwest. At these times of analysis, the cold-air damming event had yet to begin, though eastern Arkansas was experiencing winter weather in the form of freezing rain and snowfall (specifically in the northeastern corner of the state) as precipitation associated with the cyclones passed through the area.

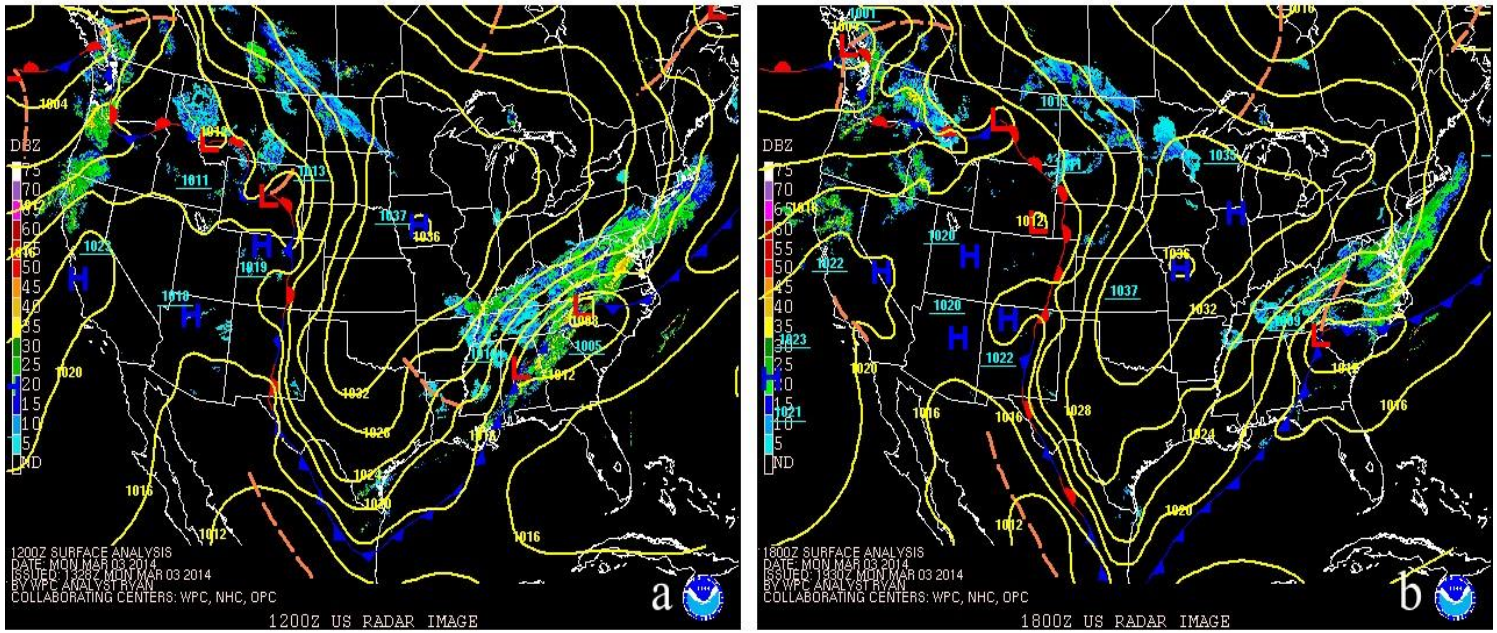

Figure 4.2 – Radar-overlayed surface pressure maps from the initial case study. These maps serve as a "buffer" time period between the passage of the mid-latitude cyclone and the onset of the cold-air damming event. Map (a) is analyzed at 1200 UTC on 03 March 2014. Map (b) is analyzed at 1800 UTC on 03 March 2014. Maps courtesy of NOAA/NWS.

The second set of surface pressure maps in Figure 4.2 served as a “buffer” period between the passage of the mid-latitude cyclone early on 03 March 2014 and the onset of the cold-air damming event which was established at 0000 UTC on 04 March 2014. Some residual precipitation existed over the region of interest in the morning hours (Fig 4.2a) but propagated to the east by 1800 UTC (Fig. 4.2b). Propagation of the parent anticyclone slowed over the course of the day on 03 March 2014, though the center of high-pressure was in a favorable position over northern Missouri at 1800 UTC on 03 March. This positioning continued to allow for northeasterly 10-m wind flow over the region of interest according to the closed isobars around the anticyclone shown on both maps (Fig. 4.2).

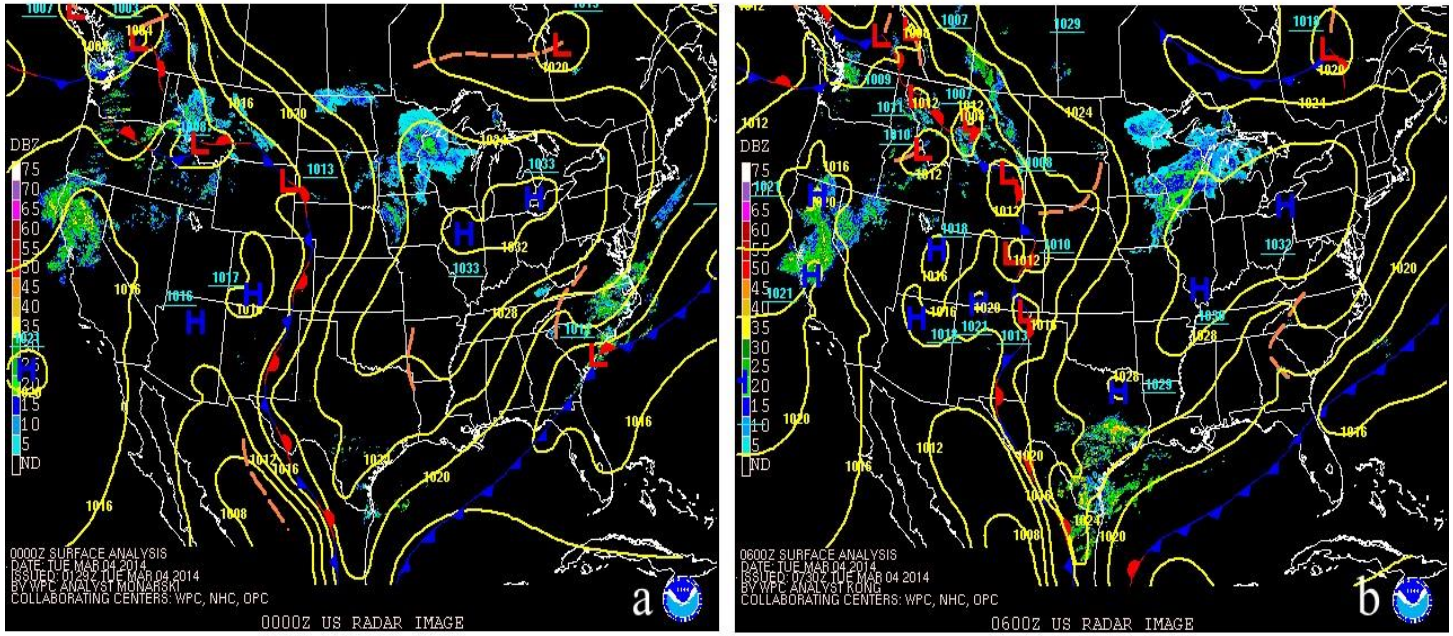

Figure 4.3 – Radar-overlayed surface pressure maps from the initial case study. These maps represent the onset of the cold-air damming event in eastern Arkansas according to corresponding METAR codes observing cold-air damming weather characteristics. Map (a) is analyzed at 0000 UTC on 04 March 2014. Map (b) is analyzed at 0600 UTC on 04 March 2014. Maps courtesy of NOAA/NWS.

The next set of maps (Fig. 4.3) showed surface pressure at 0000 UTC and 0600 UTC on 04 March 2014. Notable in these surface maps was the absence of radar reflectivity over the region of interest despite this set of maps representing the beginning of the period in which road conditions began to deteriorate across eastern Arkansas, stranding motorists in the area. The parent high-pressure system had tracked to northern Illinois (Fig. 4.3a) and the region of interest was now firmly entrenched in north-northeasterly wind flow according to surface isobars. By 0600 UTC on 04 March 2014 (Fig. 4.3b), the high-pressure system responsible for cold-air damming impacting the region had strengthened with its center located on the Indiana/Ohio border. This continued to promote northeasterly wind flow still influencing the region of interest.

Complicating matters along Interstate 55 and Interstate 40 in eastern Arkansas was the snowpack left behind by the mid-latitude cyclone propagating to the east on the morning of 03 March 2014.

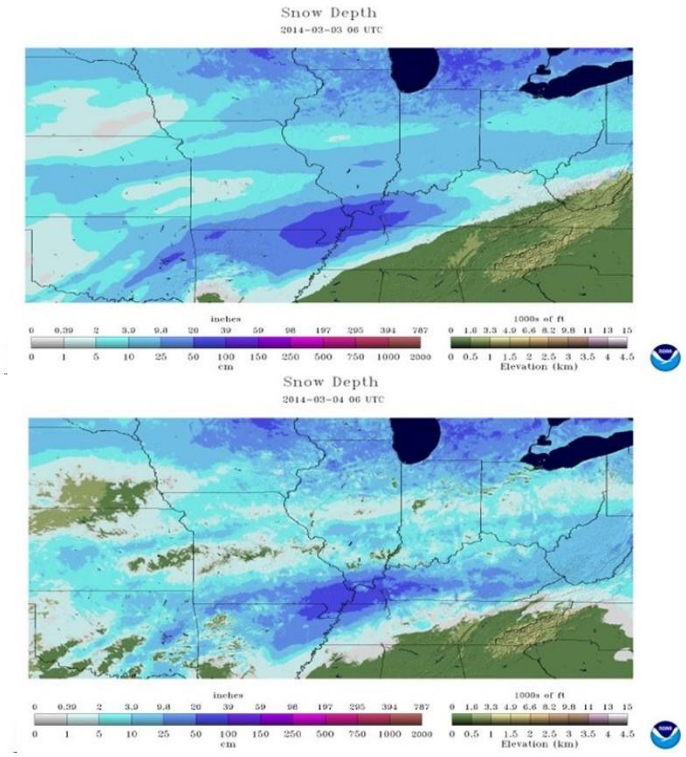

Figure 4.4 – Maps of snowpack depth from the initial case study at 0600 UTC on 03 March 2014 (top) and 0600 UTC on 04 March 2014 (bottom). The snowpack is color coded between 0 and 787 inches of snow pack. Maps courtesy of NOAA/NWS.

Figure 4.4 reveals that the largest snowfall accumulations from the late winter storm occurred over extreme northeastern Arkansas, the bootheel of Missouri, western Kentucky, and extreme southern Illinois. The accumulation maps featured in Figure 4.4 extend snowfall accumulations southward into eastern Arkansas as far south as the Interstate 40 corridor in eastern central Arkansas. However, it was inferred that the largest snowpack located to the northeast aided the northeasterly flow provided by the parent anticyclone to the north-northeast in advecting additional cold air and moisture into an already containing a freezing surface air mass. This conclusion was reached because of the lack of snowmelt between 0600 UTC on 03 March 2014 and 0600 UTC 04 March 2014, when the cold-air damming event was occurring.

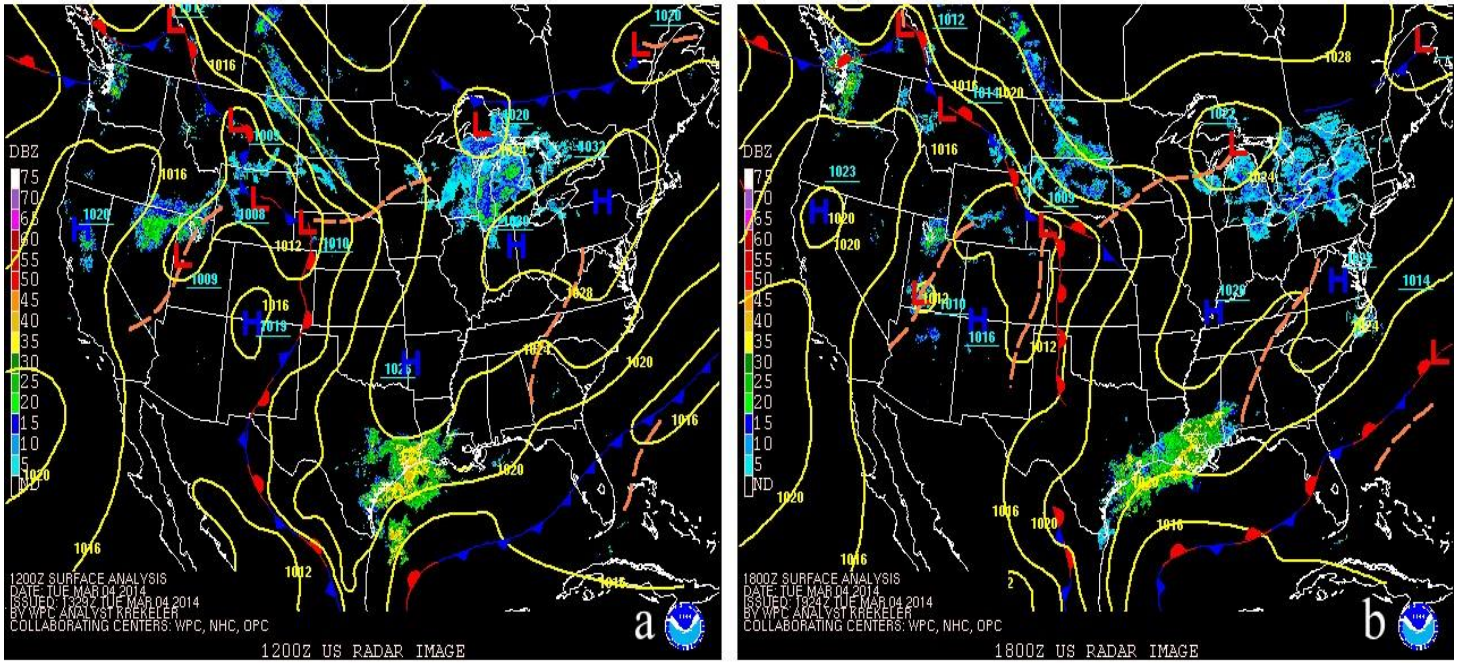

Figure 4.5 – Radar-overlayed surface pressure maps from the initial case study. These surface maps feature the resilience of the parent anticyclone and continued lack of radar reflectivity over the region of interest. Map (a) is analyzed at 1200 UTC on 04 March 2014. Map (b) is analyzed at 1800 UTC on 04 March 2014. Maps courtesy of NOAA/NWS.

The next set of surface pressure maps used for analysis rounded out the time steps of 04 March 2014 (Figure 4.5). This cold-air damming event concluded shortly after 0000 UTC on 05 March 2014 and these maps featured the reasoning behind the longevity of the event. High pressure remained in place over the Ohio River Valley slowly pushing to the east-northeast giving the cold-air damming event its longevity. Isobars around the anticyclone spread out across the eastern half of the United States, diminishing the speed of 10-m wind flow while still providing a terrain-orthogonal flow environment needed for the cold-air damming event to maintain over the region. This arrangement was inferred from a synoptic spatial point of view and further investigation of other resources (mesoscale 10-m wind maps, soundings, meteorograms, etc.) was needed to confirm 10-m wind flow patterns. There was a lack of radar reflectivity over the region of interest though a large swath of radar reflectivity was observed to the south over the Gulf Coast associated with the frontal boundary to the south.

Synoptic analysis concluded with the first two 6-hour time steps of 05 March 2014. Figure 4.6 shows the surface pressure maps that signaled the end of the cold-air damming event over the region of interest.

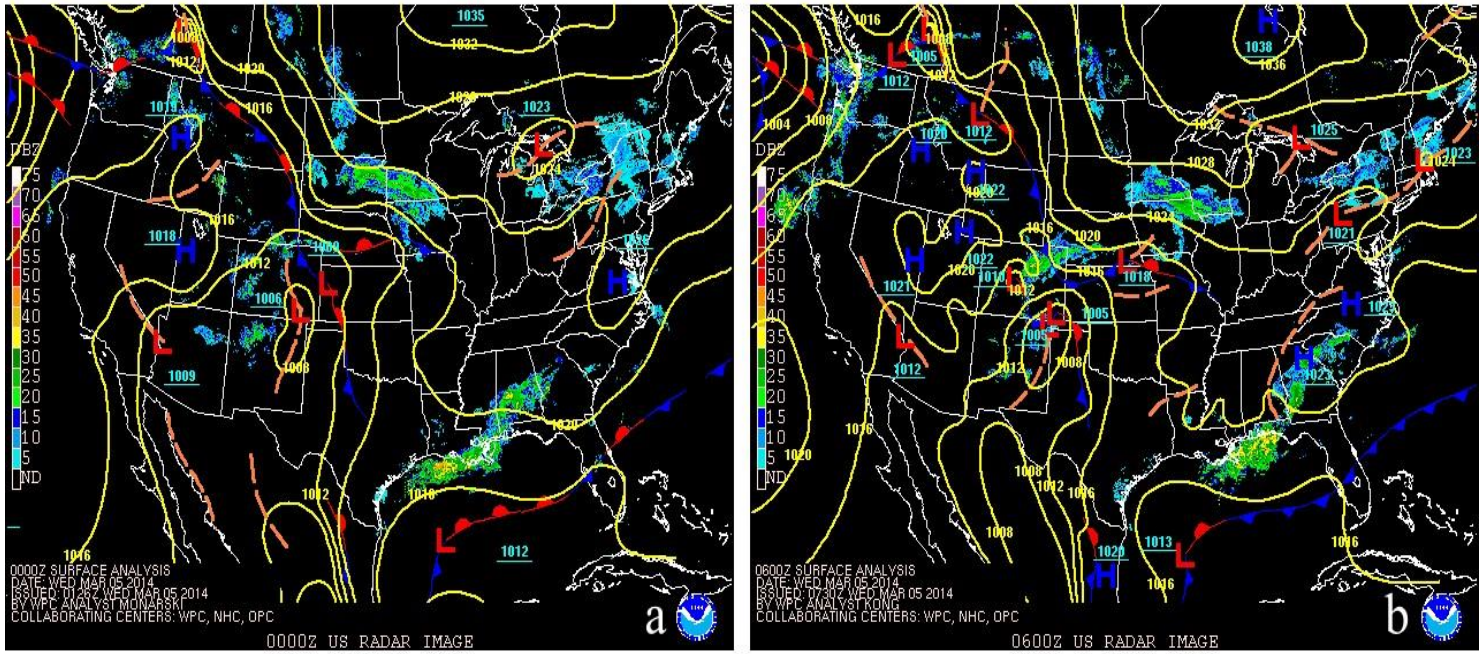

Figure 4.6 – Radar-overlayed surface pressure maps from the initial case study. These surface maps signal the end of the cold-air damming event over the region of interest. Map (a) is analyzed at 0000 UTC on 05 March 2014. Map (b) is analyzed at 0600 UTC on 05 March 2014. Maps courtesy of NOAA/NWS.

The 0000 UTC surface map from 05 March 2014 (Fig. 4.6a) depicted that the pressure center of the parent anticyclone to the cold-air damming event over eastern Arkansas had moved to the east of the favorable zone needed for the event to sustain over the region of interest and was centered over the Mid-Atlantic region. While radar reflectivity continued to remain away from eastern Arkansas the 0600 UTC 05 March 2014 surface map (Fig. 4.6b) demonstrated the formation of a new system set to invade the Midwest maturing over the northern Plains.

4.3 10-m Wind Map Analysis

10-m wind maps were created for each synoptic time step of the initial case study to understand the 10-m wind velocity field over the course of the cold-air damming event. With that being the emphasis of study analysis, wind maps were restricted to those time steps in which cold-air damming occurred. Those time steps began at 0000 UTC on 04 March 2014 and concluded as the event ended by 0600 UTC on 05 March 2014.

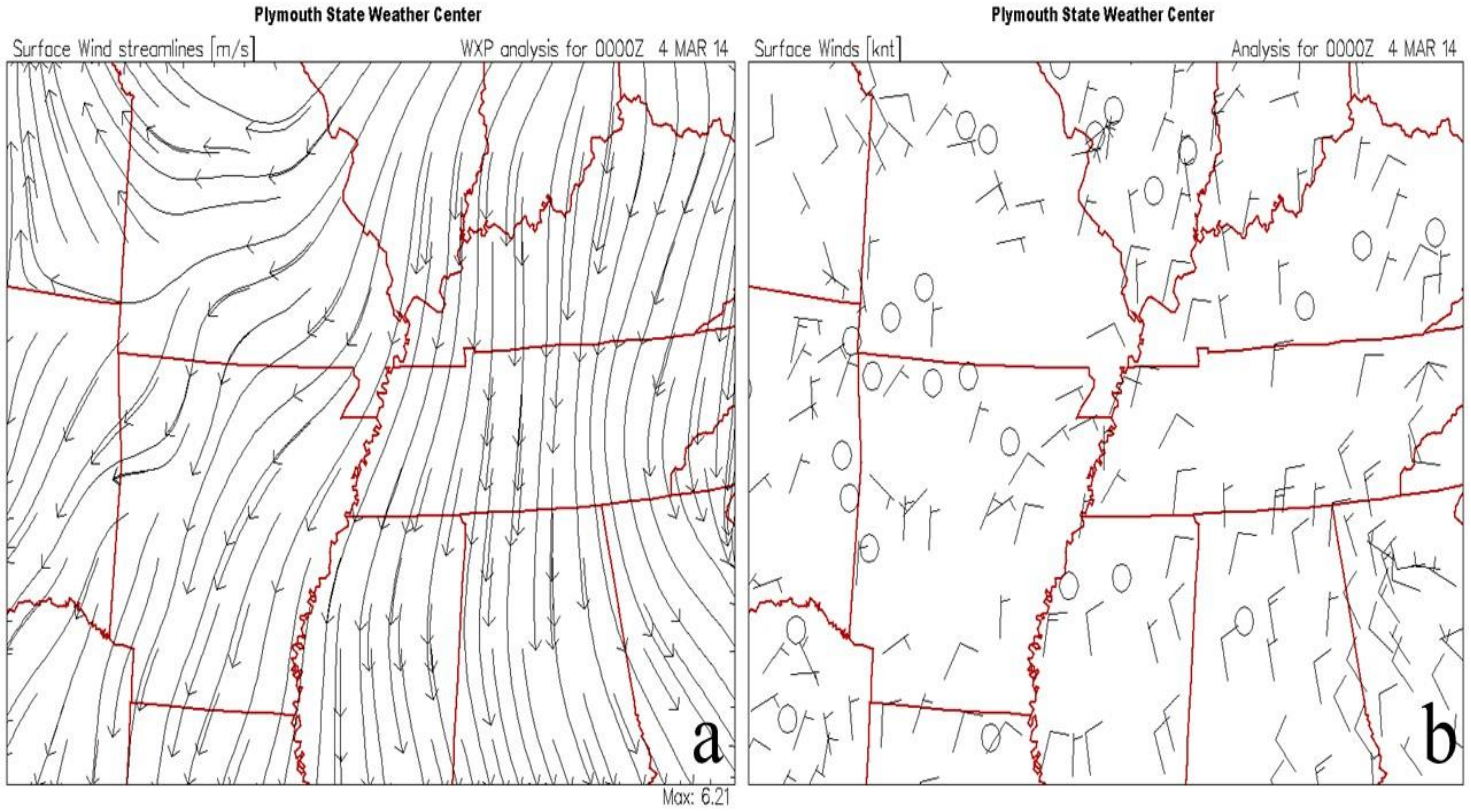

Figure 4.7 – 10-m wind maps created for the initial case study at 0000 UTC on 04 March 2014. Map (a) features the region of interest with 10-m wind flow streamlines (m s-1). Map (b) features observed 10-m wind barbs (knots). Maps courtesy of Plymouth State Weather Center data archive (https://vortex.plymouth.edu/).

Figure 4.7 contains the first time of the 04 March 2014 event as cold-air damming began to impact the region of interest.

The influence of the anticyclone was noted in Figure 4.7 which features a pair of 10-m wind charts from the region of interest in eastern Arkansas at 0000 UTC on 04

March 2014. The 0000 UTC charts show the observed 10-m wind flow field at the onset of the cold-air damming event and featured northeasterly flow beginning to influence the region of interest pushing the post-frontal northerly flow associated with the cold front out of the area.

The chart at 0600 UTC (Figure 4.8) on 04 March 2014 continued a trend of decreased wind speeds as calm to 5-kt northeasterly winds were observed in the region of interest at that time. This was indicative of what was analyzed synoptically as the calmer surface flow of the parent anticyclone replaced the stronger post-frontal flow propagating to the southeast.

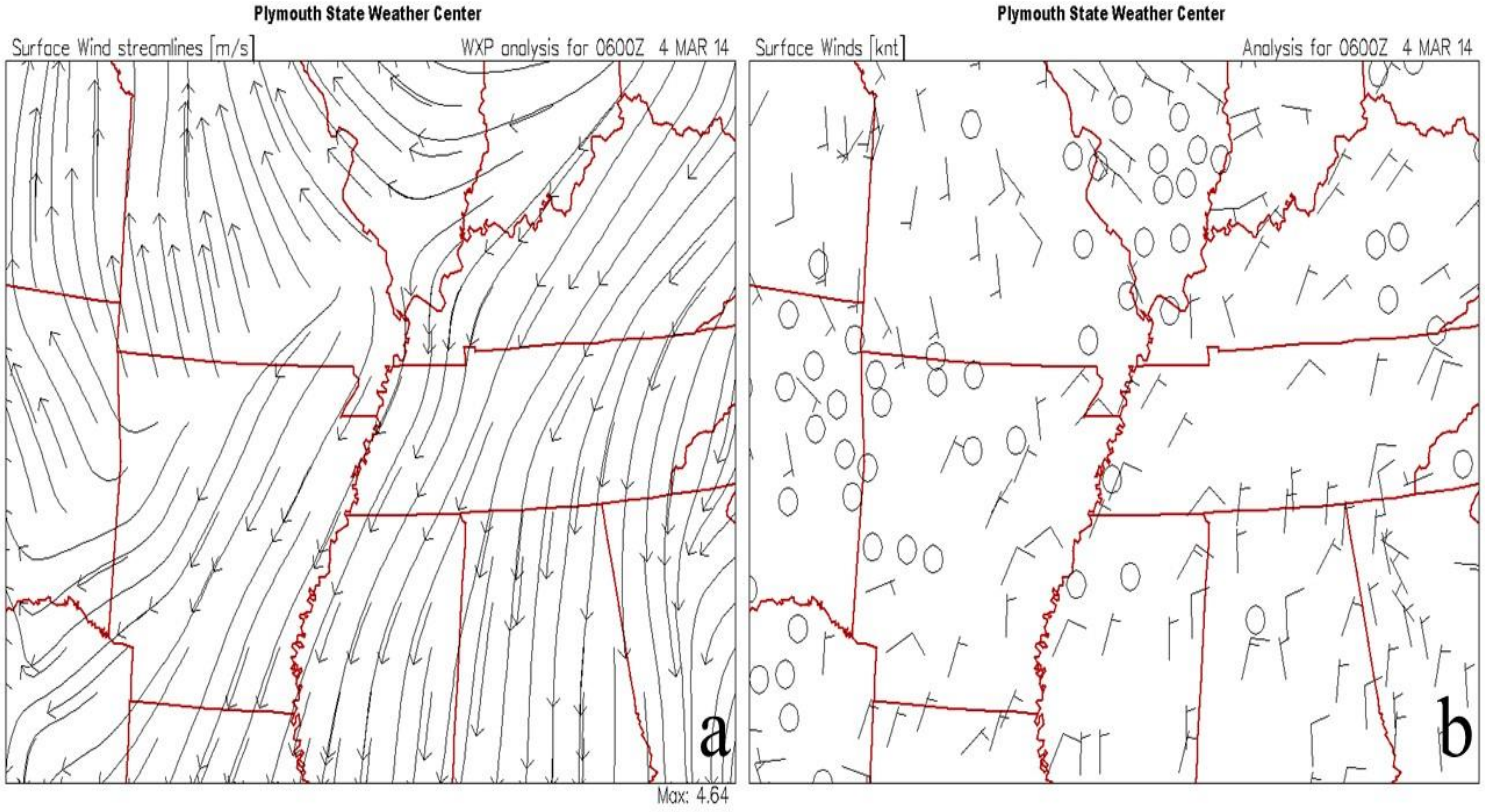

Figure 4.8 – 10-m wind maps created for the initial case study at 0600 on 04 March 2014. Map (a) features the region of interest with 10-m wind flow streamlines (m s-1). Map (b) features observed 10-m wind barbs (kts). Maps courtesy of the Plymouth State Weather Center data archive (https://vortex.plymouth.edu/).

Figure 4.9 occurs at 1200 UTC on 04 March 2014 around sunrise. These maps continued to feature the weak northeasterlies at the surface as well as a col point, or saddle point, in the wind direction that constitutes a deformation zone (Fig. 4.9a) over the region of interest. By 1800 UTC on 04 March 2014 (Fig. 4.10) the col point persisted.

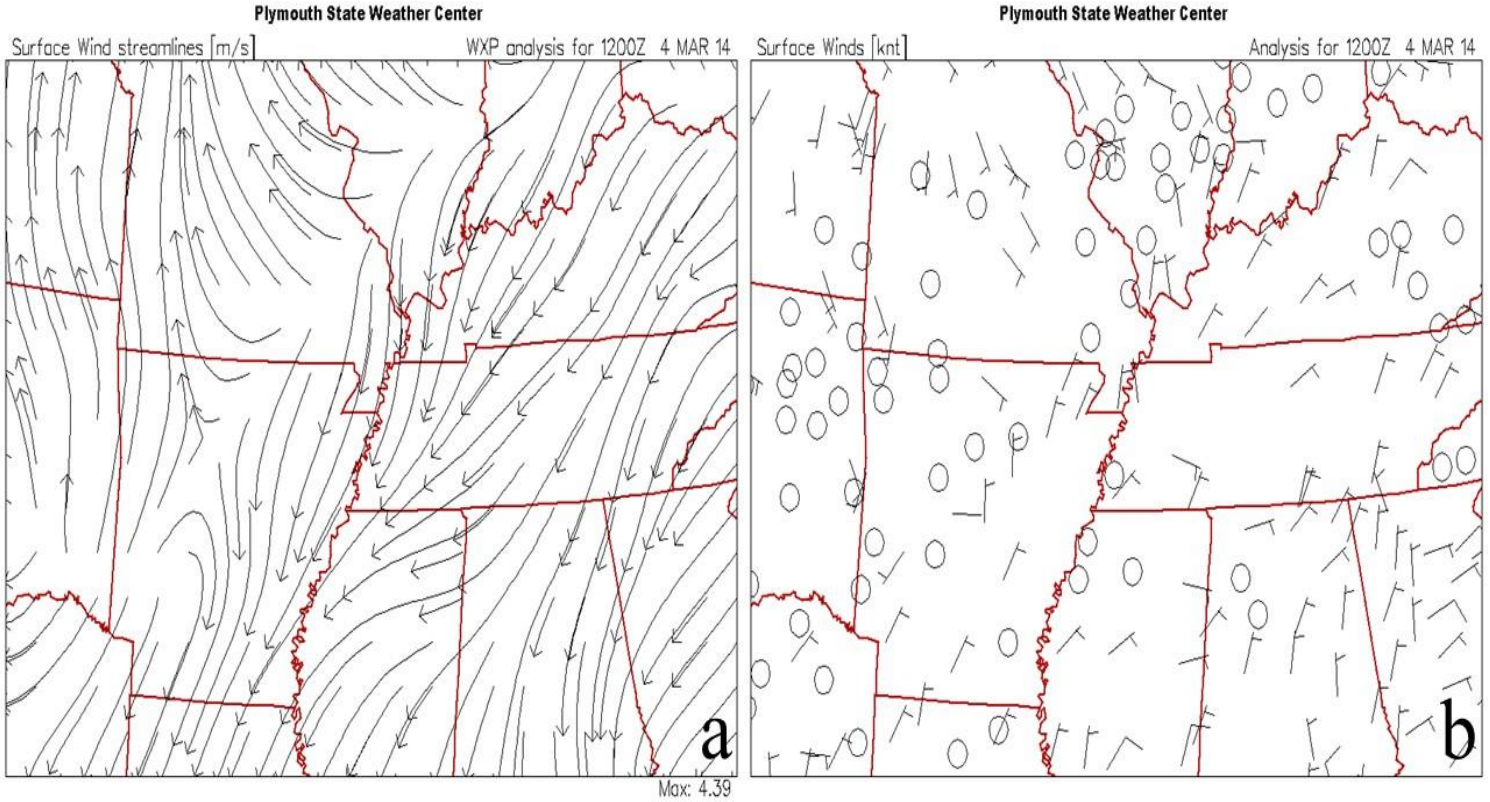

Figure 4.9 – 10-m wind maps created for the initial case study at 1200 UTC on 04 March 2014. Map (a) features the region of interest with 10-m wind flow streamlines (m s-1). Map (b) features observed 10-m wind barbs (kts). Maps courtesy of the Plymouth State Weather Center data archive (https://vortex.plymouth.edu/).

Disorganized flow over the region of interest was observed with some stations reporting calm conditions, while others were oriented in either a southeast or northeast fashion between 5-10 kts. The last of the observed 10-m wind maps used for analysis appear in Figure 4.11 and Figure 4.12, by 05 March 2014 as the cold-air damming event over the region comes to an end.

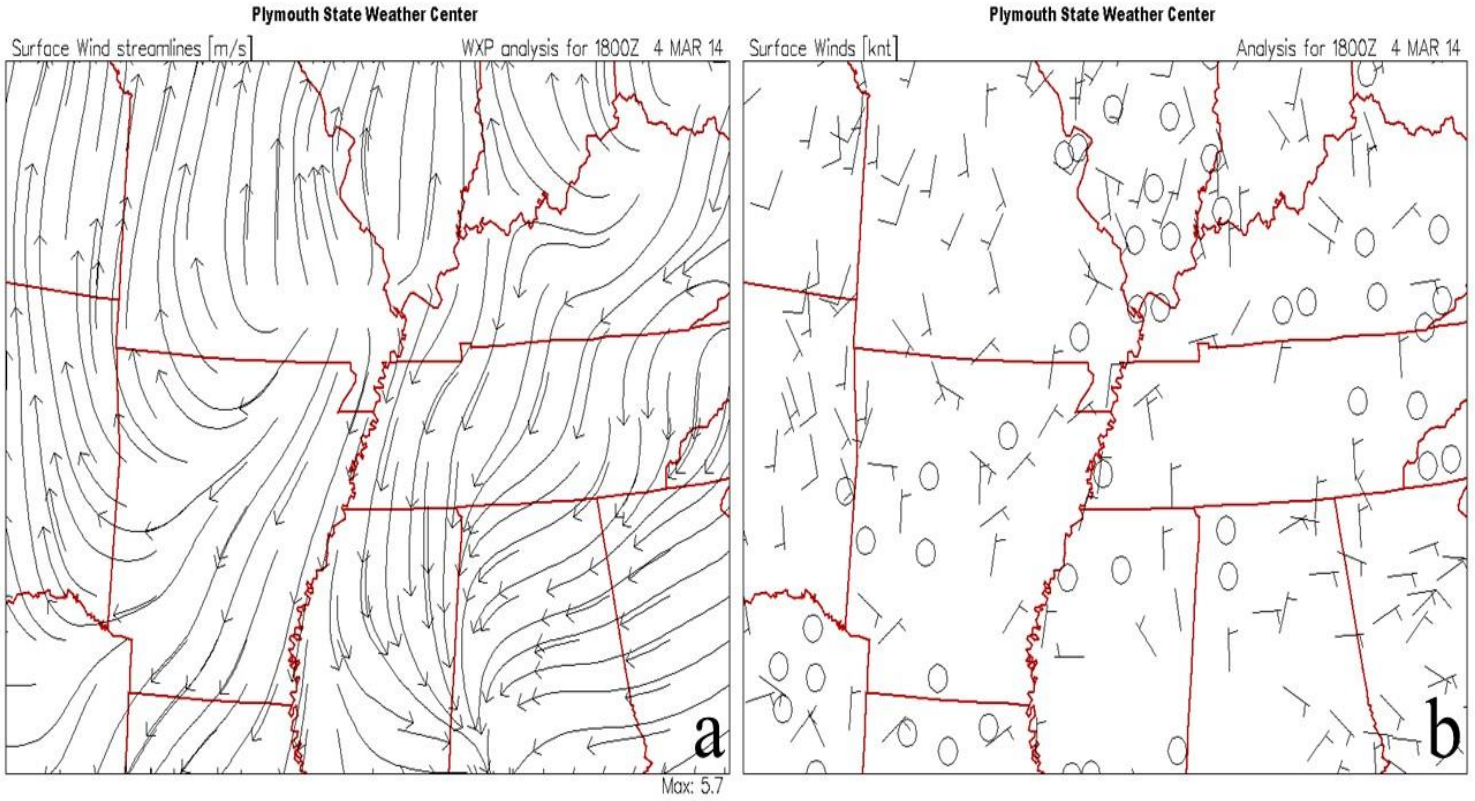

Figure 4.10 – 10-m wind maps created for the initial case study at 1800 UTC on 04 March 2014. Map (a) features the region of interest with 10-m wind flow streamlines (m s-1). Map (b) features observed 10-m wind barbs (kts). Maps courtesy of the Plymouth State Weather Center data archive (https://vortex.plymouth.edu/).

10-knot wind barbs in or near the region of interest were non-existent on each map (Fig. 4.11 or Fig. 4.12) as night fell on 05 March 2014 and 10-m winds calmed over the region and oriented out of the southeast. Observed wind turned to a more southerly course which signaled the movement of the parent anticyclone further to the east opening the region of interest up to the western flank of surface flow around the anticyclone.

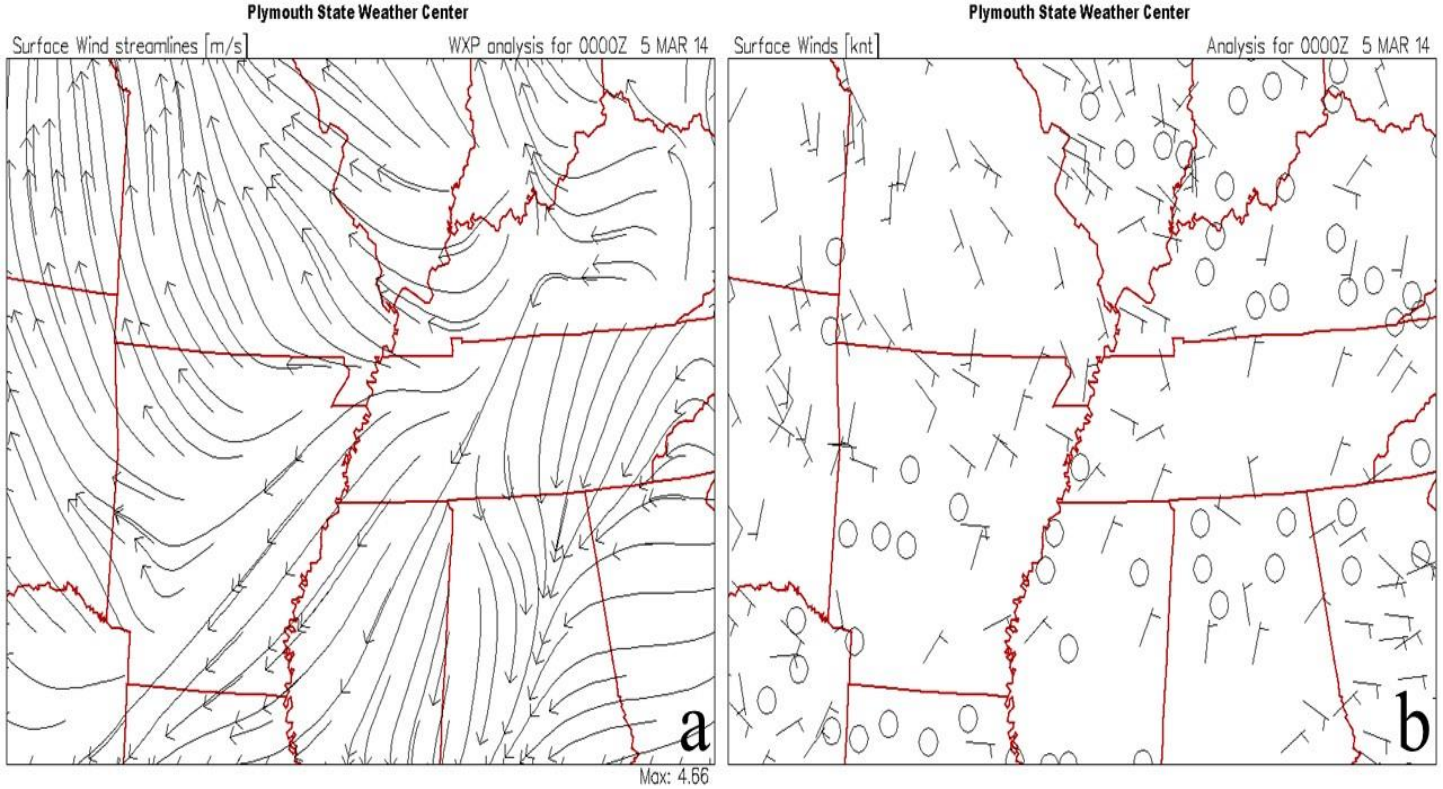

Figure 4.11 – 10-m wind maps created for the initial case study at 0000 UTC on 05 March 2014. Map (a) features the region of interest with 10-m wind flow streamlines (m s^{-1}). Map (b) features observed 10-m wind barbs (kts). Maps courtesy of the Plymouth State Weather Center data archive (https://vortex.plymouth.edu/)

4.4 Upper-Air Sounding Analysis

The analysis of the cold-air damming event continued with a deterministic vertical profile of the atmosphere. It was understood that generally the temperature decreases with altitude in the atmosphere save for an instance when air temperature briefly increases with altitude near the surface. These instances are known as temperature inversions. In the case of cold-air damming, inversions are necessary in helping to trap the cold dome of air at the surface thereby maintaining the cooler conditions and prolonging the event.

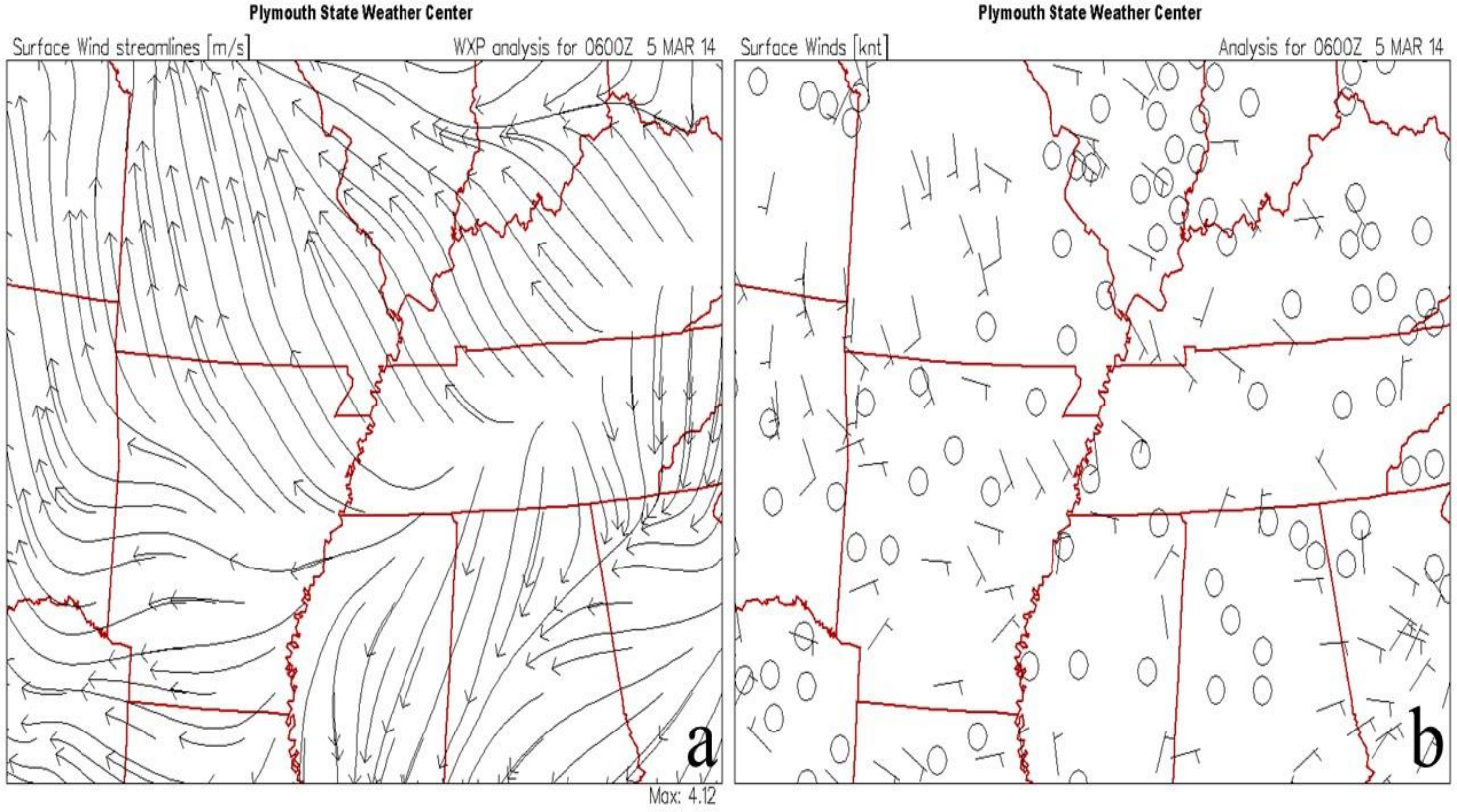

Figure 4.12 – 10-m wind maps created for the initial case study at 0600 UTC on 05 March 2014. Map (a) features the region of interest with 10-m wind flow streamlines (m s-1). Map (b) features observed 10-m wind barbs (kts). Maps courtesy of the Plymouth State Weather Center data archive (https://vortex.plymouth.edu/)

Figure 4.13 represents a series of these soundings in the form of skew-T/log P diagrams. Each of the soundings was observed by balloon radiosonde flights flown from the National Weather Service office in Little Rock, Arkansas (KLZK). Little Rock, Arkansas is the only upper-air station in the state (and within the region of interest) that flies regular balloon flights and so this station, located on the western fringe of the region of interest, is the best source for observed upper-air soundings (and the observation platform needed for model sounding verification described above). The first observed sounding was from the morning of 03 March 2014 at 1200 UTC (Figure 4.13a). The temperature profile (red line) and dewpoint profile (dashed line) were well below freezing, with some low-level moisture present. The presence of a rather strong temperature inversion existed as early as the morning of 03 March 2014 from altitudes of approximately 600 to 2500 m. Additionally, in the wind profile northerly wind flow up to 10 kts was observed near the surface as expected after a frontal passage like the one experienced early on 03 March 2014.

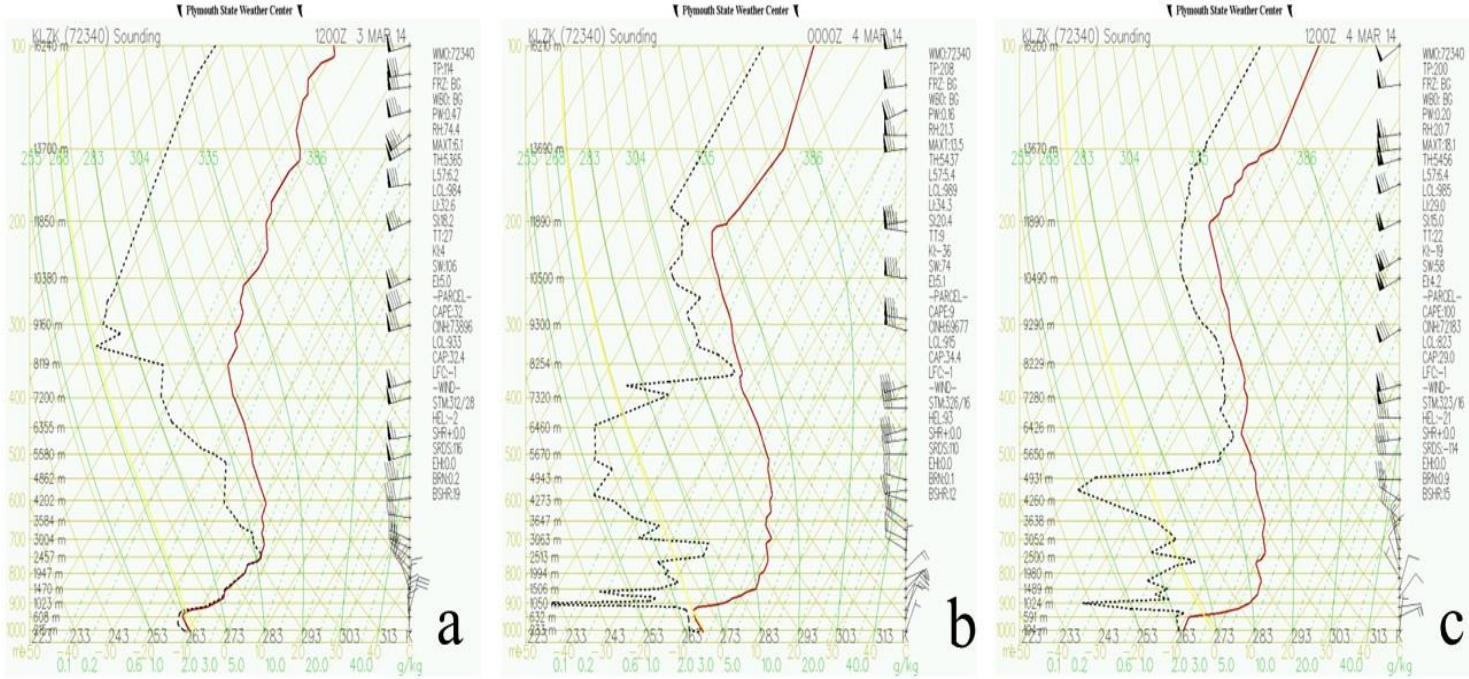

Figure 4.13 - Observed upper-air soundings from Little Rock, Arkansas (KLZK) at 1200 UTC on 03 March 2014 (chart a), 0000 UTC on 04 March 2014 (chart b), and 1200 UTC on 04 March 2014 (chart c). The y-axis of each chart is decreasing logarithmic atmospheric pressure with height. The x-axis of each chart is air temperature in ºC. The red line represents observed air temperature with height while the green line represents observed dew point temperature with height. The vertical wind profile featuring black wind barbs (kts) is found just right of the upper-air sounding. Charts courtesy of the Plymouth State Weather Center data archive (https://vortex.plymouth.edu/).

12 hours later, the second sounding was observed at 0000 UTC on 04 March 2014 (Fig. 4.13b). The temperature profile continued to exhibit an inversion just above the surface. At that time the inversion was not quite as deep, ranging in altitude from approximately 650 to 1500 m. The entire profile was also much drier in Little Rock, Arkansas than observed 12 hours prior, though surface moisture was still evident at that time. The wind profile depicted what was analyzed on the 10-m wind maps: light 5-kt wind flow out of the northeast. The final sounding (Fig. 4.13c) was observed 12 hours later the morning of 04 March 2014 at 1200 UTC. This sounding was like the second sounding with a dry overall profile save for some near-surface moisture. The inversion was still in place ranging from approximately 600 to 1000 m; the shallowest inversion layer of the 3 observed in Figure 4.13. The wind profile still showed light north-northeasterly wind flow at 5 kts, though just above the surface stronger easterly flow at 20 kts existed perhaps signaling the end of the high-pressure influence in central Arkansas. Overall, these 3 soundings show the ingredients necessary to not only create, but sustain, a cold air damming event.

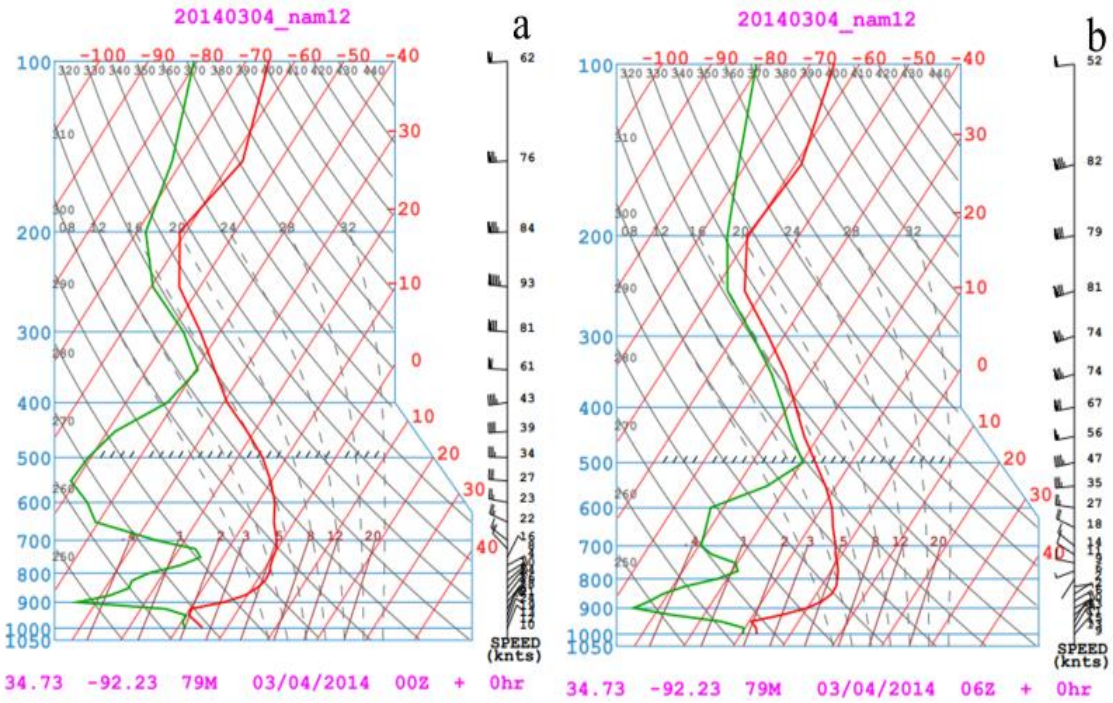

Figure 4.14 - Upper-air modeled NAM-12km soundings from the initial case study for the Blytheville, Arkansas station (KHKA). The y-axis decreases logarithmic atmospheric pressure with height. The x-axis is the air temperature in °C. The red line represents air temperature with height while the green line represents dewpoint temperature with height. The vertical wind profile is shown to the right of each chart with black wind barbs (kts). Chart (a) is from the model initial fields at 0000 UTC on 04 March 2014. Chart (b) is from the model initial fields at 0600 UTC on 04 March 2014.

After model verification practices were satisfied, a series of NAM-12km upper-air model soundings were analyzed during the time steps of the cold-air damming event on 04 March 2014. For this initial case study, the Blytheville, Arkansas station (KHKA) was chosen as the point station for analysis of deterministic resources. The time steps for analysis were again those in which cold-air damming was impacting the region which includes 0000 UTC of 04 March 2014 through 0600 UTC of 05 March 2014. Figure 4.14 contains the first 2 modeled soundings from the Blytheville, Arkansas station at the onset of the cold-air damming event.

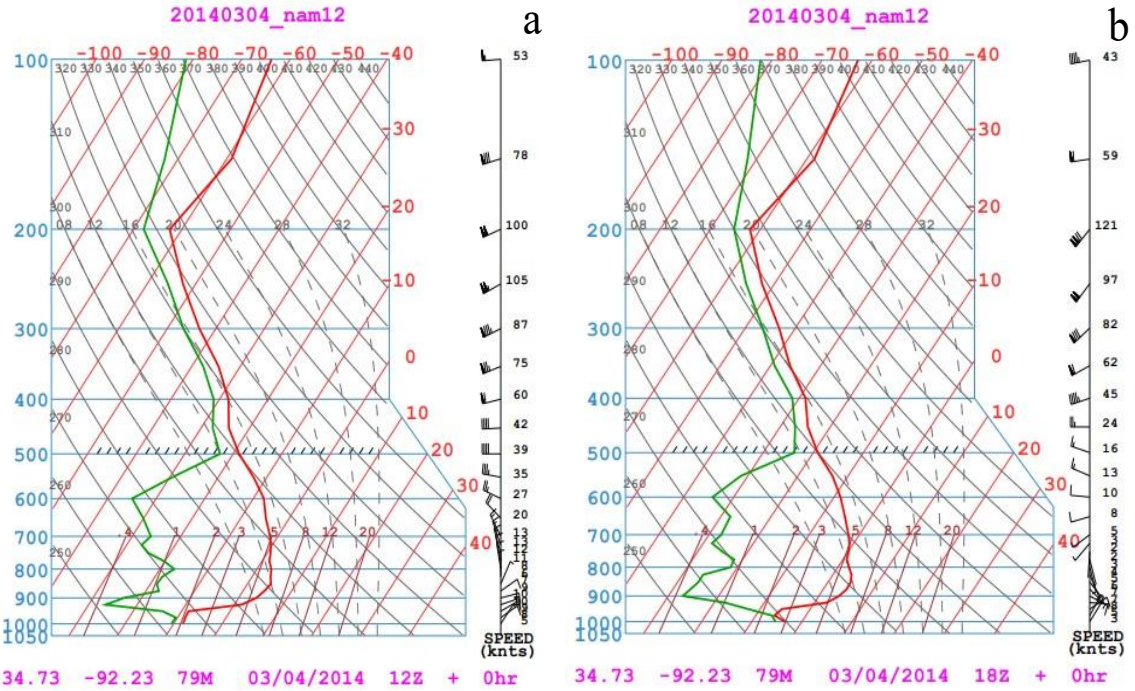

Figure 4.15 - Upper-air modeled NAM-12km soundings from the initial case study for the Blytheville, Arkansas station (KHKA). The y-axis decreases logarithmic atmospheric pressure with height. The x-axis is the air temperature in °C. The red line represents air temperature with height while the green line represents dewpoint temperature with height. The vertical wind profile is shown to the right of each chart with black wind barbs (kts). Chart (a) is from the model initial fields at 1200 UTC on 04 March 2014. Chart (b) is from the model initial fields at 1800 UTC on 04 March 2014.

Figure 4.14 is modeled at 0000 UTC on 04 March 2014 (Fig. 4.14a) and depicts a 2-m temperature profile that was several °C below freezing. This was expected of the temperature observation for this time of year less than 24 hours after the passage of a mature mid-latitude and associated strong cold front. A very shallow layer of moisture existed at the surface beneath the temperature inversion likely associated with the snowpack left behind from the previous days' precipitation. A strong temperature inversion was already in place just above the moist surface layer with temperatures creeping just above freezing between 850 and 750 hPa. 10-m winds were northeasterly at 10 kts up through 800 hPa. The other upper-air sounding modeled 6 hours later at 0600

UTC on 04 March 2014 (Fig. 4.14b) depicts a shallow temperature inversion slightly below 750 hPa though the warm nose was now several °C warmer than freezing.

Surface moisture persisted through the night with temperatures dropping to nearly 10°C below freezing. The wind profile had shifted slightly eastward which was more favorable in terms of terrain orthogonal wind for cold-air damming. Some moisture began to fill in the upper levels of the profile though this new feature did not impede or enhance the cold-air damming event taking place.

Figure 4.15 rounds out the 04 March 2014 time steps at 1200 and 1800 UTC respectively. The 1200 UTC time step (Fig. 4.15a) continued nearly 10°C below-freezing 2-m temperatures along with the persistent surface moisture associated with the snowpack. The inversion was at its strongest with a warm nose near 5°C above freezing and a temperature differential of nearly 15°C between the 2-m temperature and the top of the inversion as expected with diurnal processes also in progress during the cold-air damming event. More easterly 10-m winds continued up through the inversion with backing winds to a northerly direction above 850 hPa. By 1800 UTC (Fig. 4.15b) 2-m temperatures still resided below freezing though nearly 5°C warmer than 6 hours previous in part due to diurnal processes continuing through the day. Due to this slight warming the inversion was not quite as strong as previously seen though the warm nose continued to persist and was nearly 5°C above freezing. While some northeasterly wind barbs were observed near the surface, just above the surface still within the height of the inversion winds began to shift to the southeast as the parent anticyclone began to trek away from its favorable position to the east.

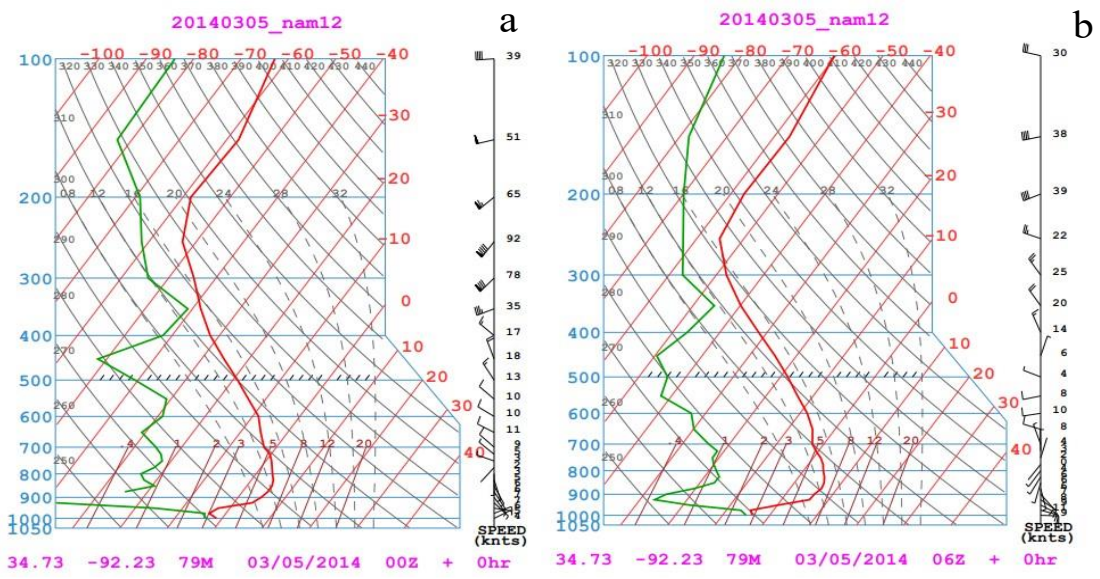

Figure 4.16 - Upper-air modeled NAM-12km soundings from the initial case study for the Blytheville, AR station (KHKA). The y-axis decreases logarithmic atmospheric pressure with height. The x-axis is the air temperature in °C. The red line represents air temperature with height while the green line represents dewpoint temperature with height. The vertical wind profile is shown to the right of each chart with black wind barbs (kts). Chart (a) is from the model initial fields at 0000 UTC on 05 March 2014. Chart (b) is from the model initial fields at 0600 UTC on 05 March 2014.

Model sounding analysis was complete with the last set of charts (Figure 4.16). Limited daytime heating yielded the smallest temperature inversion of the event with only an approximately 7°C difference between the nearly freezing 2-m temperature and the warm nose of the inversion which continued to persist at about 5°C. Most wind barbs near the surface were observed to be calm and southeasterly with only a couple of barbs observed at an easterly component. Due to the axis of terrain of the southeastern flank of the Ozark Plateau these winds barbs continued to favor cold-air damming. Moisture found at higher altitudes in previous soundings was no longer present by 0000 UTC on 05 March 2014. Six hours later, after the sun had set, 2-m temperatures began to fall back below freezing, strengthening the temperature inversion somewhat as the warm nose at the top of the inversion continued to run nearly 5°C above freezing. Surface moisture continued to be persistent under the assumption that cold 2-m temperatures over the

course of the previous day did little to melt the existing snowpack. The remainder of the profile remained significantly dry above the temperature inversion. The wind profile at the surface was predominantly out of the southeast though just above the temperature inversion winds had shifted to a southwesterly course.

4.5 Froude Number Numerical Analysis

Supplementing the map and chart analysis of the initial 04 March 2014 case study was a numerical analysis of Froude Numbers evaluating the ability of 10-m wind flow to overcome terrain obstacles. Calculations for this analysis were taken from 3 locations within the region of interest: Poplar Bluff, Missouri (KPOF), Blytheville, Arkansas (KHKA), and Little Rock, Arkansas (KLIT). For purposes of continuity, model output used for the calculations was gathered from the model NAM-12km soundings despite the Little Rock station having observed data. As stated previously (Chapter 3, Section 3.1.4.1), the model soundings were verified using the observed upper-air data from the Little Rock, Arkansas observed sounding. This allowed for said continuity and to conduct calculations at a 6-hour interval. Variables in the Froude equation were averaged vertically between the surface and the top of the inversion at each station. Therefore, the layer height for each calculation may change as the inversion height evolved through the cold-air damming event, though the averaging of variables accounts for this height change and produced a valid Froude number at each station per time step.

Table 4.1 – Froude number calculations for the Poplar Bluff, Missouri (KPOF) station for the initial case study. Calculations were taken from NAM-12km initial fields modeled upper-air sounding output at 6-hour intervals between 12 UTC on 03 March 2014 and 06 UTC on 05 March 2014.

KPOF Froude Number Calculations

Date	Time	Z-BOT (m)	ZZ-TOP (m)	Layer Height (m)	Wind Dir	Wind Spd (m s^{-1})	N	Fr
3/3/2014	12Z	123	2183	2060	87.1	11.9	0.0043	1.4055
3/3/2014	18Z	123	1975	1852	27.7	9.7	0.0043	1.3079
3/4/2014	00Z	123	1981	1858	40.9	7.8	0.0041	1.0844
3/4/2014	06Z	123	1742	1619	116.0	4.0	0.0045	0.5811
3/4/2014	12Z	123	1491	1368	158.7	2.8	0.0049	0.4347
3/4/2014	18Z	123	1494	1371	123.0	1.3	0.0042	0.2349
3/5/2014	00Z	123	1024	901	124.5	2.1	0.0044	0.5488
3/5/2014	06Z	123	1020	897	141.1	4.1	0.0051	0.9440

Surface Flow is Impeded Surface Flow May be Impeded Surface Flow is Unimpeded

4.5.1 Poplar Bluff, Missouri (KPOF) Froude Number Analysis

Froude number calculations for the KPOF station yielded favorable results for the presence of cold-air damming. The first 2 time steps in which surface flow was unimpeded are expected as the station was in a post frontal flow regime immediately following the passage of the cold front. By 0000 UTC of 04 March 2014 the Froude number began to resolve numbers more indicative of a surface flow being blocked or redirected around an obstacle. Initially, the number 1.0844 at 0000 UTC on 04 March 2014 did fall into the gray area associated with Froude number, but the trend and results of later time steps revealed how the surface flow both in speed and direction became favorable for a cold-air damming event to take place in the region. Unlike the other 2 stations, the wind directional component fell into the favorable 40-to-220-degree zone for

terrain orthogonal efficiency in producing a cold-air damming event. Initially, 10-m wind velocity was not favorable for cold-air damming to take place but as the anticyclone propagated into a favorable zone for influence this allowed 10-m wind velocities to relax, and the Froude number calculations bear this out.

4.5.2 Blytheville, Arkansas (KHKA) Froude Number Analysis

Results for Froude number calculations over the Blytheville, Arkansas station were similar to those of the Poplar Bluff, Missouri station. Wind direction was favorable save for 1800 UTC on 03 March 2014. The Froude number favored cold-air damming during impact times except for the 0000 UTC 04 March 2014 time step in which the 1.2461 value suggested the flow was unimpeded. The Froude number did shift back to favorable for cold-air damming and remained favorable until the final time step evaluated at 0600 UTC on 05 March 2014. The Blytheville, Arkansas station resides the furthest to the east meaning the station endured the cold front and ensuing post-frontal wind regime at slightly later times than the other 2 analyzed stations. This may explain some of the differences in values or timing of Froude number values at the Blytheville, Arkansas station.

Table 4.2 – Froude number calculations for the Blytheville, Arkansas (KHKA) station for the initial case study. Calculations were taken from NAM-12km initial fields modeled upper-air sounding output at 6-hour intervals between 1200 UTC on 03 March 2014 and 0600 UTC on 05 March 2014.

KHKA Froude Number Calculations

Date	Time	Z-BOT (m)	ZZ-TOP (m)	Layer Height (m)	Wind Dir	Wind Spd (m s^{-1})	N	Fr
3/3/2014	12Z	78	2729	2651	220.9	13.1	0.0042	1.2559
3/3/2014	18Z	78	2493	2415	18.5	8.0	0.0040	0.8770
3/4/2014	00Z	78	1980	1902	36.9	9.4	0.0043	1.2461
3/4/2014	06Z	78	1741	1663	67.3	6.7	0.0045	0.9723
3/4/2014	12Z	78	1255	1177	77.5	5.8	0.0052	1.0618
3/4/2014	18Z	78	1260	1182	49.8	3.5	0.0047	0.7054
3/5/2014	00Z	78	1254	1176	79.5	2.5	0.0044	0.5289
3/5/2014	06Z	78	797	719	129.3	5.2	0.0058	1.4290

Surface Flow is Impeded Surface Flow May be Impeded Surface Flow is Unimpeded

Table 4.3 - Froude number calculations for the Little Rock, Arkansas (KLIT) station from the initial case study. Calculations were taken from NAM-12km initial fields modeled upper-air sounding output at 6-hour intervals between 1200 UTC on 03 March 2014 and 0600 UTC on 05 March 2014.

KLIT Froude Number Calculations

Date	Time	Z-BOT (m)	ZZ-TOP (m)	Layer Height (m)	Wind Dir	Wind Spd (m s^{-1})	N	Fr
3/3/2014	12Z	81	2459	2378	215.1	12.9	0.0043	1.3428
3/3/2014	18Z	81	2493	2412	18.5	8.0	0.0041	0.2857
3/4/2014	00Z	81	1991	1910	43.0	8.6	0.0042	1.1731
3/4/2014	06Z	81	1505	1424	56.2	5.9	0.0048	0.9700
3/4/2014	12Z	81	1493	1412	60.7	4.5	0.0050	0.6948
3/4/2014	18Z	81	1264	1183	78.6	3.4	0.0047	0.6817
3/5/2014	00Z	81	1250	1169	107.5	3.3	0.0045	0.6842
3/5/2014	06Z	81	1248	1167	120.1	4.5	0.0049	0.8520

Surface Flow is Impeded Surface Flow May be Impeded Surface Flow is Unimpeded

4.5.3 Little Rock, Arkansas (KLIT) Froude Number Analysis

The final Froude number analysis involved the Little Rock, Arkansas (KLIT) station. Results of these Froude number calculations resemble more so the results from the Poplar Bluff, Missouri station. This may be the result of several factors. It is hypothesized that perhaps proximity to the escarpment of the Ozark Plateau (which is very similar to the Poplar Bluff, Missouri station) may influence the results. Also, the Little Rock, Arkansas station falls along a similar axis of frontal passage regarding the cold front that passed through the region early on 03 March 2014. The timing of influence of the cold front resembled more the timeline of events at the Poplar Bluff, Missouri station rather than the Blytheville, Arkansas station which lies furthest east.

The early time steps of 03 March 2014 observed a Froude number value of 1.3428 indicating a surface flow that was unimpeded. This was expected as the post-frontal wind regime was stronger at that time in the hours just after frontal passage. 6 hours later the Froude number was more favorable at 0.2857, but the wind direction was too northerly at 18.5° for a weak 10-m wind flow to matter, as at that direction the wind was not terrain-orthogonal and more terrain-parallel with the southeastern flank of the Plateau. Despite these early issues with wind directional component, like the numerical analysis of the Poplar Bluff, Missouri station, by 0000 UTC on 04 March 2014 the Froude number trended towards a favorable value with a favorable wind direction through the last time step of numerical analysis. These favorable Froude numbers, seen at all 3 stations in this analysis, are some of the most compelling evidence for Ozark Plateau induced cold-air damming for this initial case study.

4.6 Surface Moisture Map Analysis

Analysis up to this point has focused on examining conditions necessary to produce a cold-air damming event. From this point on the focus will shift (slightly) to examining characteristics necessary to produce an ***impactful*** cold-air damming event. This analysis began with an examination of available surface moisture. Upper-air sounding model output from the Blytheville, AR station analyzed previously indicated a persistent, extremely shallow layer of moisture that the study links to an existing snowpack both in the northern portions of the region of interest as well as points to the northeast (Figure 4.4). To investigate further, surface moisture maps were utilized during

the cold-air damming impact time steps of 0000 UTC 04 March 2014 through 0600 UTC 05 March 2014.

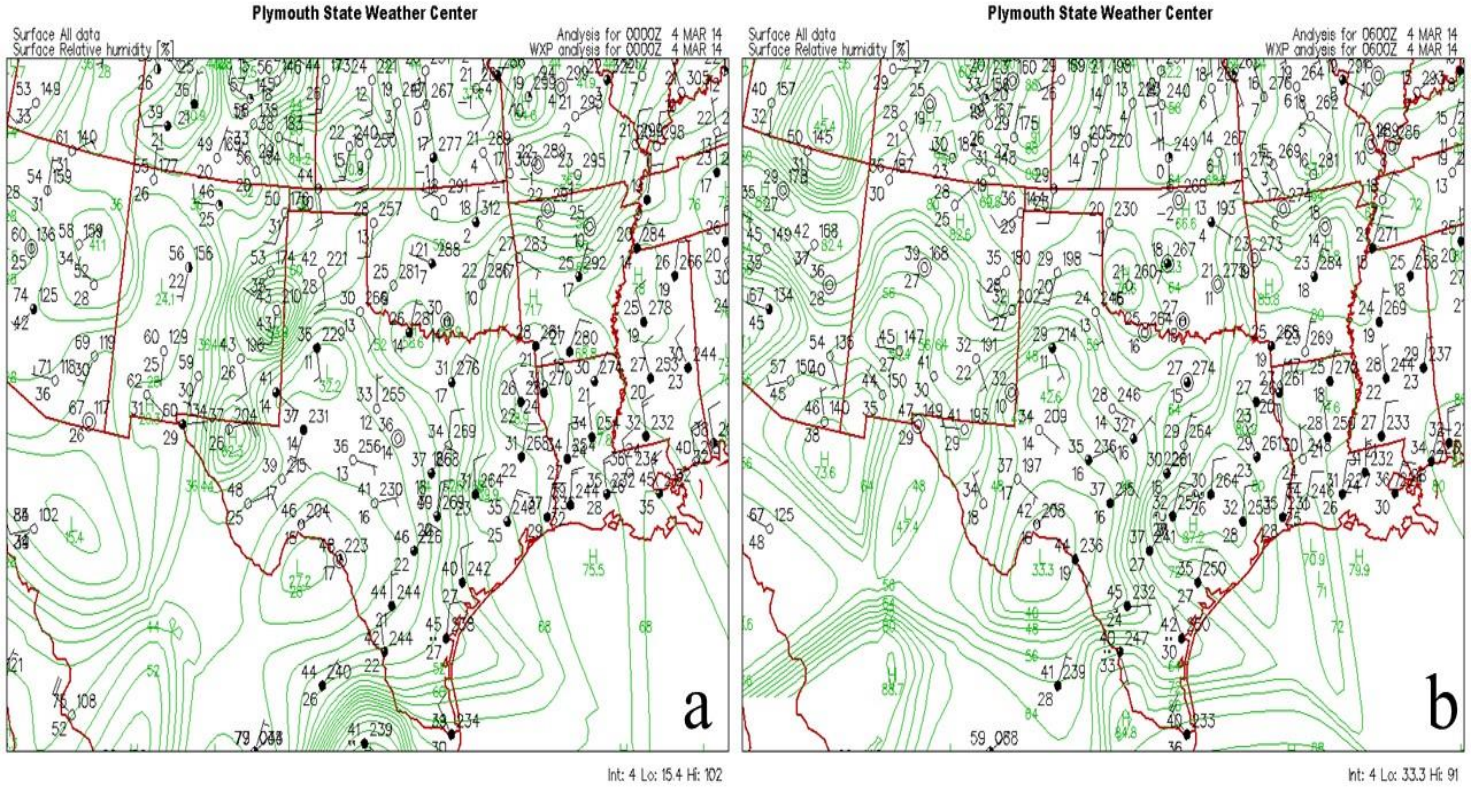

Figure 4.17. Observed surface moisture maps created for the initial case study. These maps feature Southern Plains states in red, green isohumes (%) of relative humidity at intervals of 4%, and black station model plots that include air temperature (°F) (top left), dewpoint temperature (°F) (lower left), cloud cover (center), wind barbs (kts), and sea level pressure abbreviated as tens, ones, and tenths (mb) absent the decimal (top right). Map (a) was analyzed at 0000 UTC on 04 March 2014. Map (b) was analyzed at 0600 UTC on 04 March 2014. Maps courtesy of the Plymouth State Weather Center data archive (https://vortex.plymouth.edu/)

At 0000 UTC on 04 March 2014 (Fig 4.17a) a pocket of dry air existed over southwest Missouri with a steep moisture gradient over the region of interest leading to a rich moisture field over western Tennessee, closer to the retreating mid-latitude cyclone. Dewpoint depressions of 6, 8, and 10°F across the region fall outside of the 5°F threshold for an impactful cold-air damming event at that time despite numerous station model plots reporting cloudy skies. Northeasterly winds helped to decrease these dewpoint depressions 6 hours later at 0600 UTC on 04 March 2014 (Fig. 4.17b). The dry pocket of surface air over southern Missouri still existed though depressions within the region of interest were now within that 5°F threshold with values of 3 and 5°F as northeasterly surface flow and cloudy conditions continued over the region.

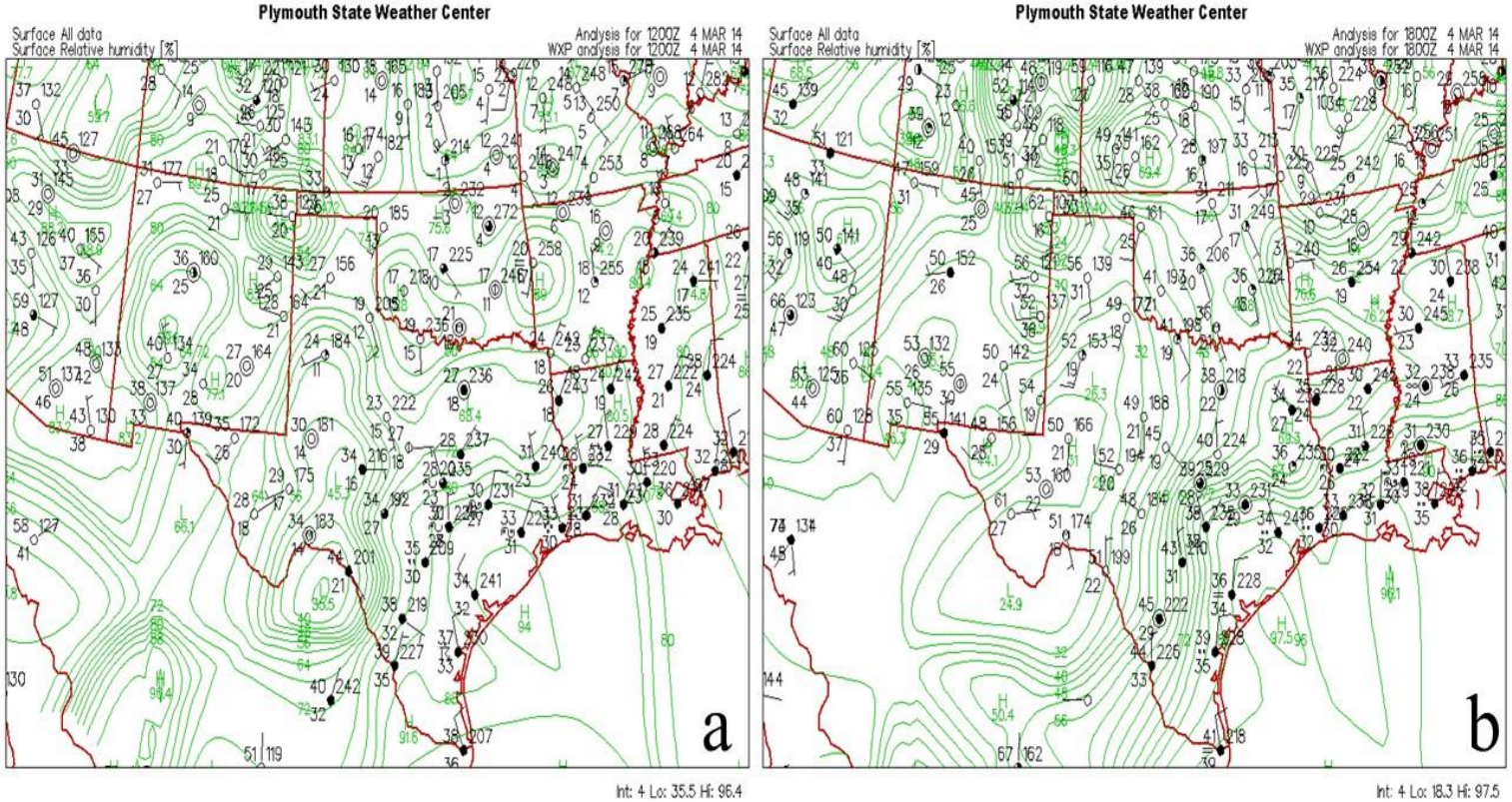

Figure 4.18 - As in Figure 4.17, but valid at a) 1200 UTC 04 March 2014, and b) 1800 UTC 04 March 2014. Maps courtesy of the Plymouth State Weather Center data archive (https://vortex.plymouth.edu/)

By morning (Fig 4.18a), isohumes lost their gradient characteristics and became disorganized across the region of interest. Station model plots in the southern extent of the region (Little Rock, Arkansas and Memphis, Tennessee) remained somewhat moist (6 and 2°F dewpoint depressions) while the northern extent of the region of interest dried out as the dry pocket of air propagated across southern Missouri.

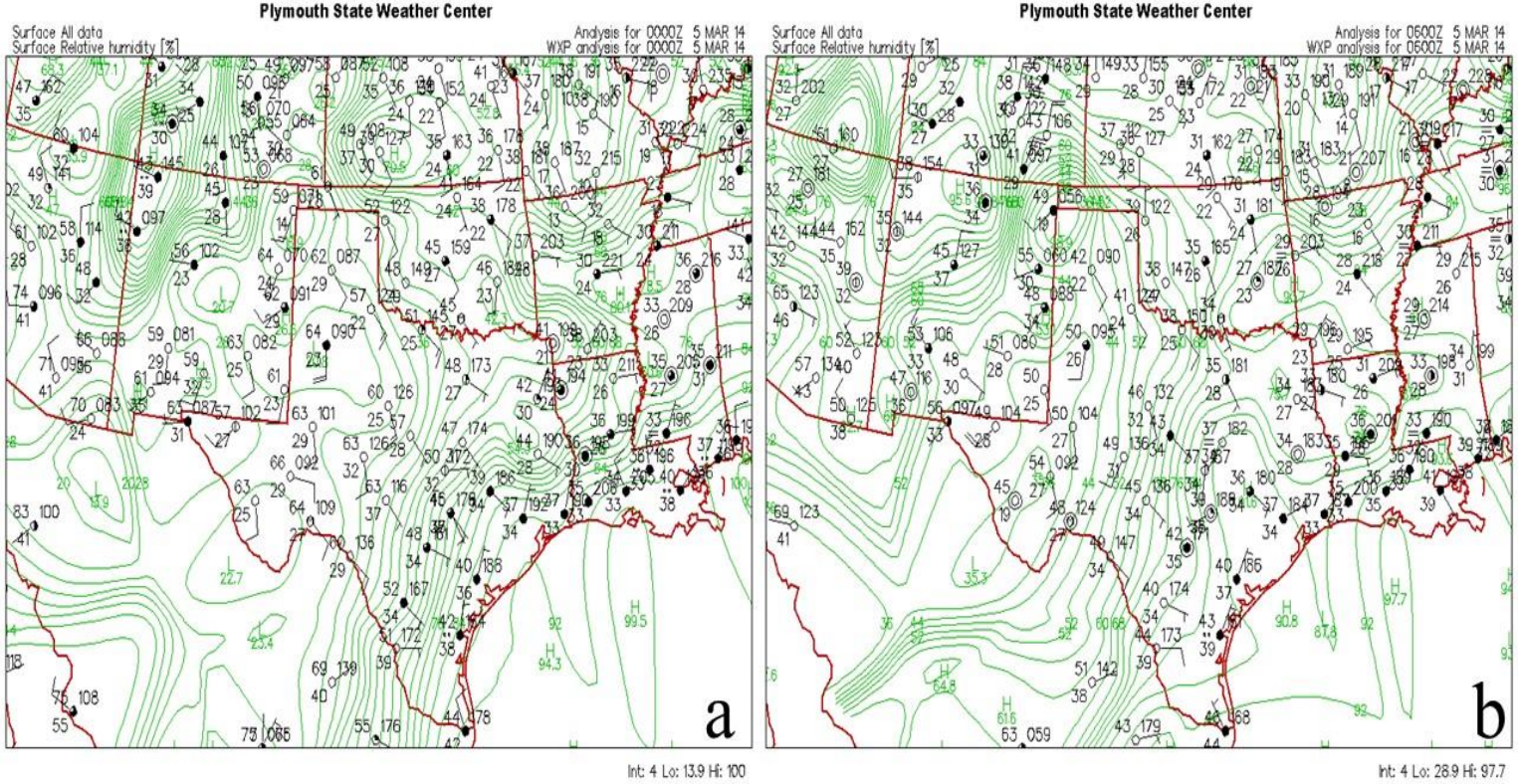

Figure 4.19 - As in Figure 4.17, but valid at a) 0000 UTC 05 March 2014, and b) 0600 UTC 05 March 2014. Maps courtesy of the Plymouth State Weather Center data archive https://vortex.plymouth.edu/)

A more easterly flow pushed surface moisture back into the region as cloudy skies and moisture rich dewpoint depressions were observed at 1800 UTC on 04 March 2014 (Fig 4.18b). A north-to-south moisture gradient had set up over the region of interest with more moisture to the south.

The final set of analyzed surface moisture maps (Figure 4.19) show the 2 time steps of 05 March 2014 involved in the cold-air damming event. By 0000 UTC on 05 March 2014 (Fig. 4.19a) the moisture gradient between southern Missouri and central Arkansas had tightened and cloudy skies presided over the southern extent of the region of interest. 10-m winds continued to shift to a more east-southeast flow. By the end of analysis at 0600 UTC of 05 March 2014 (Fig. 4.19b) fog was reported at the Memphis, Tennessee station model plot with favorable dewpoint depressions observed across the region. Southeasterly flow and cloudy skies persisted with a steep moisture gradient in place over the region between the dry air over Missouri and the moist air over central Arkansas and western Tennessee.

4.7 Creation of Characteristics for Phase Two

From these observations of synoptic and mesoscale conditions before, during, and after the 04 March 2014 cold-air damming event a list of characteristics was created to identify other instances in which cold-air damming was impacting the region of interest for this research. These characteristics are listed above in Data & Methods and were the quantitative checklist for the second phase of research in which 34 potential cold-air damming events were scrutinized over the course of a 5-year period. Each potential

event's ability to resemble the observations of this initial phase determined if each case was indeed a cold-air damming event and in that event, if the cold-air damming event was an impactful cold-air damming event.

CHAPTER 5. SECOND PHASE: 5-YEAR STUDY

5.1 Introduction

After the initial phase of research analyzing and concluding that cold-air damming did in fact occur and impact the region in and around eastern Arkansas on 04 March 2014, the next logical question becomes how often does the Ozark Plateau create these cold-air damming events? An important follow-up question to the initial inquiry is then how many of these events are impactful in terms of creating adverse, hazardous, icy conditions in the region.

To carry out this second phase of research the initial case study of the first phase was employed as a template. Characteristics of observed conditions from the 04 March 2014 event were established as baselines for confirming other cases of cold-air damming within the region. To identify potential cases an investigation of METAR reports from the 6 ASOS station locations (Table 3.1) within the region of interest was performed searching for the same present weather reports observed during the initial case study. The METAR investigation was limited to months in which freezing observations are possible in the region: a period between the beginning of October and the end of April. The months of May through September were omitted from the investigation, though the author recognizes that cold-air damming is possible during these months. However, to identify potential case studies based on freezing conditions, these warmer months were omitted from consideration.

In total, 9 characteristics were used to identify these potential cold-air damming cases. The first 6 characteristics tended to the primary question of whether the Ozark

Plateau can create cold-air damming events. The final 3 characteristics focus more on the secondary question of impactful cold-air damming cases. The characteristics were analyzed independently of each other. For instance, if a case did not feature appropriate terrain-orthogonal 10-m winds but did feature a supportive Froude number then the Froude number condition is still satisfied. Despite the satisfaction of the Froude number characteristic the lack of terrain-orthogonal 10-m winds would prevent the case from being a cold-air damming event. For a case to be deemed a red case (impactful cold-air damming event) all 9 characteristics must be satisfied. Yellow cases were those cases in which the first 6 conditions were met, but one of the final 3 conditions was not. In those cases, a cold-air damming event was occurring but was not impacting the region in an adverse way due to a lack of one of the characteristics. Green cases were those cases in which one of the first 6 characteristics was not satisfied and therefore the Ozark Plateau was not creating a cold-air damming event. In these green cases, the freezing conditions were brought about by a different atmospheric mechanism.

5.2 Cold-Air Damming Characteristics

Scrutiny of the 34 potential cold-air damming events took place using the archived surface maps with radar overlay to diagnose favorable parent anticyclone placement which is the first characteristic. This synoptic approach analyzed continental surface maps to identify the existence of anticyclones to the north of the region of interest in a favorable zone detailed in section 3.2.2 of Chapter 3. After analysis, 22 of the 34 case studies (65%) exhibited favorable placement of the anticyclone driving easterly 10-m winds. Almost all of the cases that did not satisfy the conditions involved a low-pressure

system emerging from the Gulf Coast and moving up into the region of interest to cut off flow from any associated anticyclone to the north. Otherwise, for favorable cases the anticyclone and its associated closed isobars were oriented in a position that supported favorable 10-m wind flow.

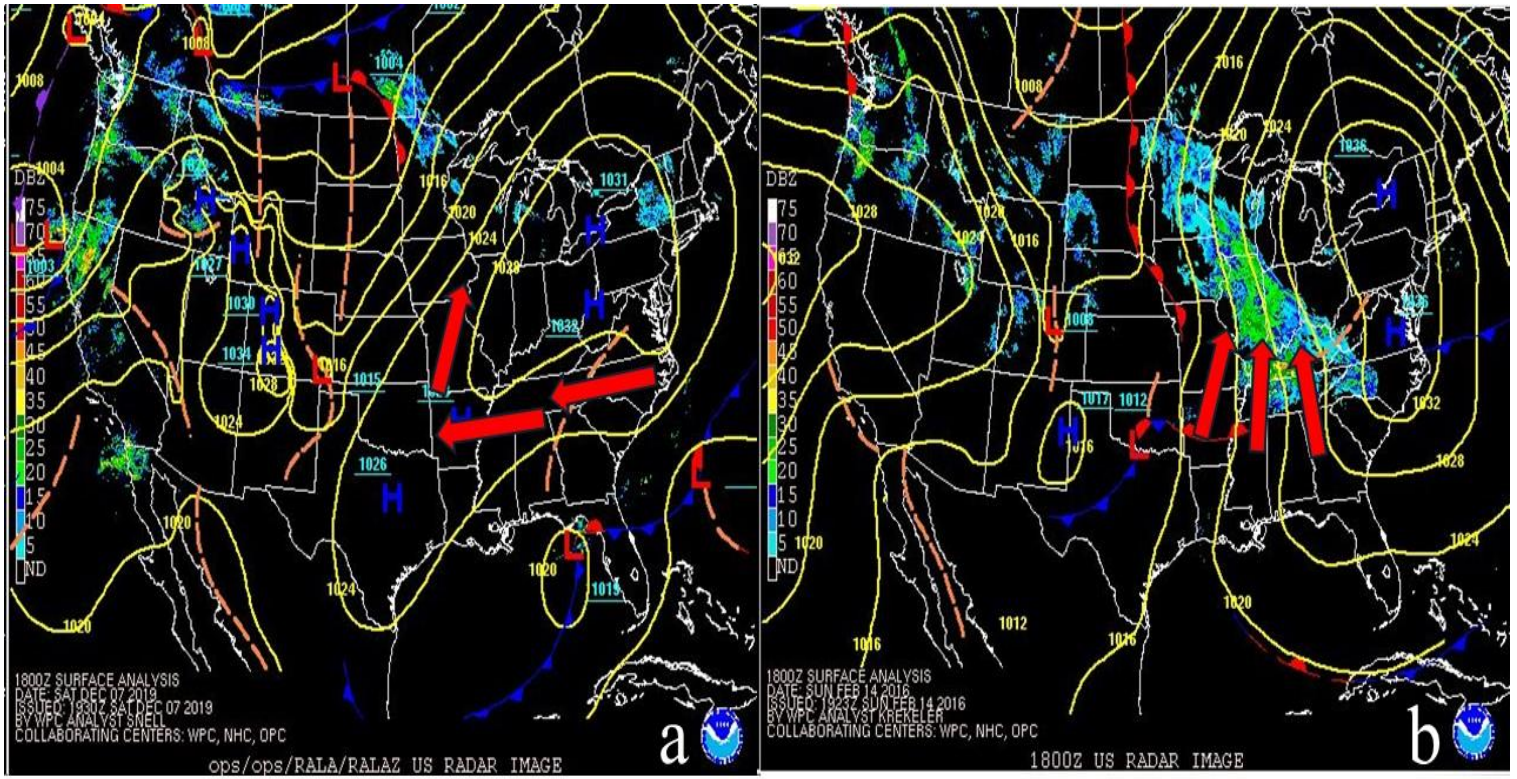

Figure 5.1 - Samples of synoptic analysis involved in the 5-year case study. Map (A) is a surface pressure chart from 18 UTC on 07 December 2019. Map (B) is a surface pressure chart from 18 UTC on 14 February 2016. Red arrows on each chart symbolize assumed non-geostrophic surface flow around the parent anticyclone near the region of interest.

Favorable terrain-orthogonal 10-m winds were the second characteristic of analysis. METAR reports were used to evaluate this characteristic in which a numerical wind direction value was analyzed for each METAR report where freezing conditions were observed. Numerical values of wind direction had to be in the favorable terrain-orthogonal wind direction component "zone" of 40-to-220°. In conclusion, 20 of 34 potential cases (59%) exhibited favorable terrain-orthogonal 10-m winds. For those cases in which the 10-m wind direction component fell outside of the required directional degree zone, northerly flow associated with a frontal passage or other encroaching boundary were the main detractors keeping potential cases from becoming cold-air damming events.

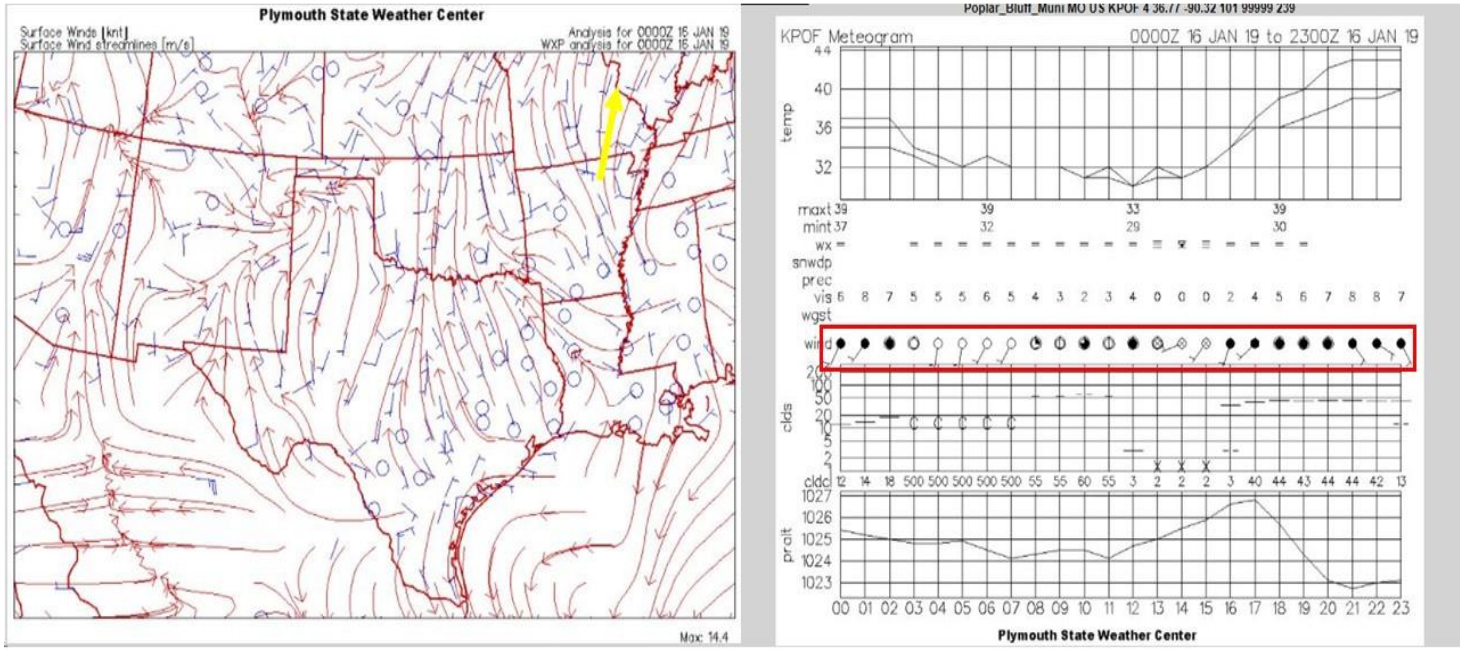

Figure 5.2 – An example of resources used for determining favorable terrain orthogonal surface wind flow in the 5-year case study analysis. The left chart is a surface wind map featuring surface wind flow streamlines and surface wind barbs from 0000 UTC on 16 January 2019. The yellow arrow over the region of interest depicts analyzed surface wind flow based on observations from the chart. The right chart is a meteorogram from the Poplar Bluff, MO station (KPOF) listing observations from 0000 to 2300 UTC on 16 January 2019. The red box on the meteorogram highlights the observed surface wind barbs at 1-hour time intervals during that 24-hour period. Maps courtesy of the Plymouth State Weather Center data archive (https://vortex.plymouth.edu/).

The third and fourth characteristics brought model initial field sounding output into the 5-year case analysis. Atmospheric conditions within the planetary boundary layer are critical to the development and maintenance of these cold-air damming events. The third characteristic involved the existence of a temperature inversion near the surface helping to trap the cold air near the ground and maintain the event. The analysis concluded that an overwhelming 29 of 34 (89%) of the case studies exhibited the necessary temperature inversion near the surface. This third characteristic was the most satisfied characteristic of the 9 involved in the 5-year study. The fourth characteristic analyzed the behavior of the winds at the surface and near the surface up through the inversion. Again, this condition is critical not only to the establishment of the cold-air damming event but also its maintenance and longevity. The cold-air damming event will erode when 10-m winds fail to support the "trapping" of the cold air against the terrain feature. After analysis, only 15 of 34 (44%) of the cases in the 5-year study exhibited favorable sounding surface layer winds. This characteristic featured 6 fewer satisfied cases than the terrain-orthogonal 10-m wind direction component characteristic described previously. This was attributed mainly to the fact that the model initial field sounding surface layer winds characteristic considers winds of the layer between the inversion and the surface, which can vary in size, and can contain several measurements of wind speed and direction as opposed to the previous characteristic in which a singular wind flow observation at 10 meters was analyzed. The example sounding in Figure 5.3 shows this low-level layer of the modeled wind environment associated with the sounding surface layer wind characteristic.

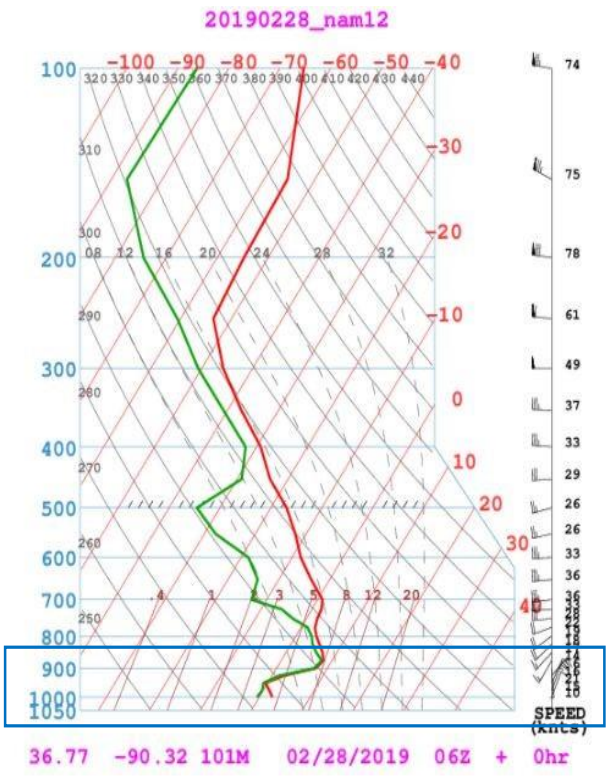

Figure 5.3 – An example of a NAM-12km model sounding used for analysis in the 5-year case study from the Poplar Bluff, Missouri (KPOF) station. This sounding taken from 0600 UTC on 28 February 2019 is similar to the sounding described in Figure 4.13. Here the inversion layer of the sounding is highlighted (in blue) to showcase the area in which the sounding temperature inversion associated with the third characteristic and the sounding surface level wind barbs associated with the fourth characteristic are located. Sounding data courtesy of NOAA's Atmospheric Upper-Air Laboratory.

Radar reflectivity was the focus of the fifth characteristic of the 5-year case study. This characteristic was created directly from lack of radar reflectivity observed during the time of impact of the initial case study in the first phase of research. In that case, conditions at the surface deteriorated, specifically on road surfaces, almost 12 hours after precipitation associated with the passing mid-latitude cyclone had exited the region of interest. Lack of any radar reflectivity over the region as icy conditions set in during the cold-air damming event associated with the initial case study is an observed condition that led to a characteristic of cold-air damming events in which a lack of radar reflectivity over the station associated with each case study within the 5-year study was required to

satisfy the fifth characteristic. This was used to discriminate between those cases in which the freezing present weather conditions observed in the METAR reports were related to cold-air damming taking place over the station observing the freezing conditions and not some other atmospheric phenomena such as organized precipitation. Reflectivity values of 15 dBZ or above were considered organized areas of precipitation (Liu et al. 2008) and in those cases the freezing conditions observed by the station's ASOS system were associated with the precipitation and not with any potential cold-air damming event. After analysis, only 14 of 34 (41%) cases exhibited a lack of radar reflectivity over the station of interest. This eliminated potential cold-air damming cases in which a present weather code reported freezing rain (FZRA) or light freezing rain (-FZRA) was observed.

The final condition of analysis to determine the presence of a cold-air damming event was a numerical analysis involving the Froude number. To reiterate, the Froude number is a unitless number used to determine if a wind is strong enough to flow over an obstacle of a given height. For Froude number values much less than 1 the flow is said to be insufficient to overcome the said obstacle. For Froude number values much greater than 1 the flow is said to be strong enough to flow over the given obstacle. For Froude number values around 1 the surface flow is said to be somewhat impeded, though given a situation in which topographic values are inconsistent the surface flow may crest lower elevation height values. For the 5-year study the Froude number was evaluated using an average of 10-m wind speeds found on the 10-m wind maps. This was a different process from other Froude number calculations performed in other phases of this research but was appropriate for the 5-year case study given the resources utilized for analysis. For

Table 5.1 - Elevation height against relief values used for Froude number calculation in the first and second phases of research. Each height value is calculated subtracting the elevation of the 6 ASOS station's elevation used in the second phase of research from the maximum elevation height of the Ozark Plateau (701 m).

Point Station Location	Elevation	Froude Number Height (h) Value
Poplar Bluff, MO (KPOF)	99.36 m	602 m
Kennett, MO (KTKX)	78.81 m	622 m
Blytheville, AR (KHKA)	76.72 m	624 m
Little Rock, AR (KLZK)	108.89 m	592 m
West Memphis, AR (KAWM)	65.23 m	636 m
Memphis, TN (KMEM)	75.98 m	625 m

each case the height variable was taken from the point location station's elevation subtracted from a value of 2,300 ft (701 m), which was defined by a study performed by the U.S. Geological Survey (Adamski et. al 1995). Table 5.1 contains a list of elevation height against relief values for Froude number calculation for each point location station used in the second phase of research. After analysis, 13 of 34 (38%) cases exhibited favorable Froude number results. The Froude number characteristic was the strongest opponent of cold-air damming amongst the 6 characteristics associated with identifying cold-air damming events.

After analysis of these first 6 characteristics, only 6 of the 34 (18%) cases involving potential cold-air damming satisfied all 6 of the characteristics, which was the requirement for a case to be considered a red case. Two cases (20 January 2016 and 11 March 2017) were disqualified based on the radar reflectivity condition that otherwise would have been considered for red cases. These cases were reevaluated, and it was determined that, based on beam height, the reflectivity was occurring above the inversion layer and therefore, METARS reports of freezing precipitation were not associated with a cold-air damming event. After analysis of these initial 6 characteristics was completed a

new analysis of 3 additional characteristics was undertaken to determine if potential cold-air damming events had an impact on surface conditions, such as the initial case study of 04 March 2014.

5.3 Impactful Cold-Air Damming Characteristics

While only 6 cases were identified for potential cold-air damming events from the initial 6 cold-air damming characteristics, all 34 cases were analyzed again for being impactful cold-air damming events for completeness. The final 3 characteristics include surface moisture, 2-m temperature, and cloud cover. These characteristics were chosen based upon observations from the initial case study of 04 March 2014, in which surface moisture, below freezing 2-m temperatures, and low-level cloud cover were present over the region of interest while the cold-air damming event was having a major impact on roadways and ground surfaces as described in Chapter 1.

The surface moisture characteristic was evaluated using both surface relative humidity maps in concert with meteorograms from the impacted stations. The surface relative humidity maps included isohumes of relative humidity as well as station model plots containing both temperature and dewpoint temperature. Surface moisture was said to be present if the difference between temperature and dewpoint temperature is 5°F or less. The surface relative humidity maps were the first pass analysis of surface moisture. For a more deterministic result, the meteorograms were used from the station of focus for each case study. Figure 5.4 highlights the portion of the meteorograms observing both temperature and dewpoint temperature in the same graph and how they evolved over the

course of a 24-hour period. These meteorograms helped fill the 6-hour gaps between what was analyzed on the surface relative humidity maps which were evaluated every 6 hours at 0000, 0600, 1200, and 1800 UTC during the potential cold-air damming event. After analysis, 25 of 34 (74%) cases contained sufficient surface moisture as to have an impact on surface conditions during a cold-air damming event.

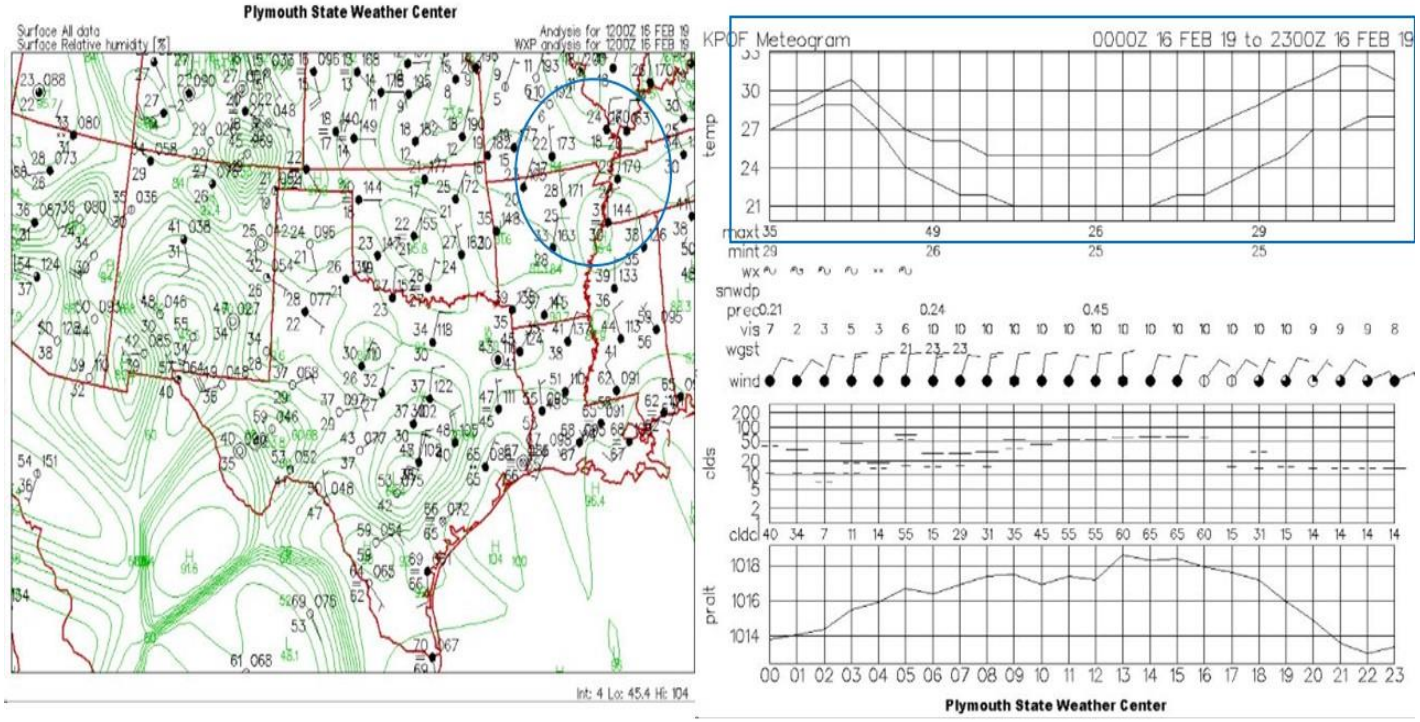

Figure 5.4. Examples of resources used to analyze impact characteristics for the 5-year study. The left-hand chart is a surface relative humidity map with green isohumes of relative humidity and station model plots used to identify areas of sufficient moisture. The blue circle highlights the area of interest. Station model plots and isohumes within the circle are used to understand the surface moisture profile as well as the presence of below freezing temperatures. The right-hand chart is a meteorogram from the Poplar Bluff, Missouri station on February 2019. The upper portion of the meteorogram (highlighted by the blue rectangle) records observed temperature and dewpoint temperature over the course of the 24-hour time period.

The second impact characteristic focused on below-freezing 2-m temperatures. Arguably the most important of the impact characteristics, below-freezing 2-m temperatures were necessary for icy conditions to be experienced during cold-air damming events. The same resources highlighted in Figure 5.4 were again utilized for this second impact characteristic. In using the meteorograms, for cases in which the temperature was observed around the freezing mark, (32°F in the case of the meteorograms) the temperature must be below freezing for at least 50% of the period in which freezing conditions were observed by the station's ASOS system. This meticulous study of 2-m temperatures reiterated the importance of the meteorograms role in this research. After analysis, 18 of 34 (53%) cases exhibited below freezing temperatures during the cold-air damming event.

The final characteristic involved cloud cover as a necessary component to impactful cold-air damming events. Cloud cover was considered in the study as representative of long-lasting events. It is understood that a cold-air damming event with surface impacts can occur without cloud cover though typical, long-lasting, impactful cold-air damming events (such as the initial case study from the first research phase) exhibit a layer of clouds that helps to maintain freezing conditions at the surface especially during the day when incoming solar radiation may erode the freezing surface layer over the course of daytime hours during a cold-air damming event. During nighttime hours when stable layers typically develop and 2-m temperatures are lowest, cloud cover may inhibit some radiational cooling. Because of this potential effect it is important to evaluate the 2-m temperature characteristics separate from the cloud cover characteristic. To evaluate cloud cover, meteorograms were again used as they were a

versatile resource and record cloud observations over a 24-hour period. Figure 5.5 gives an example of how meteorograms show cloud cover in a way that is beneficial for this research. After analysis, 27 of 34 (79%) cases experienced sufficient cloud cover during the cold-air damming event period to promote a long-lasting event provided other characteristics are also satisfied.

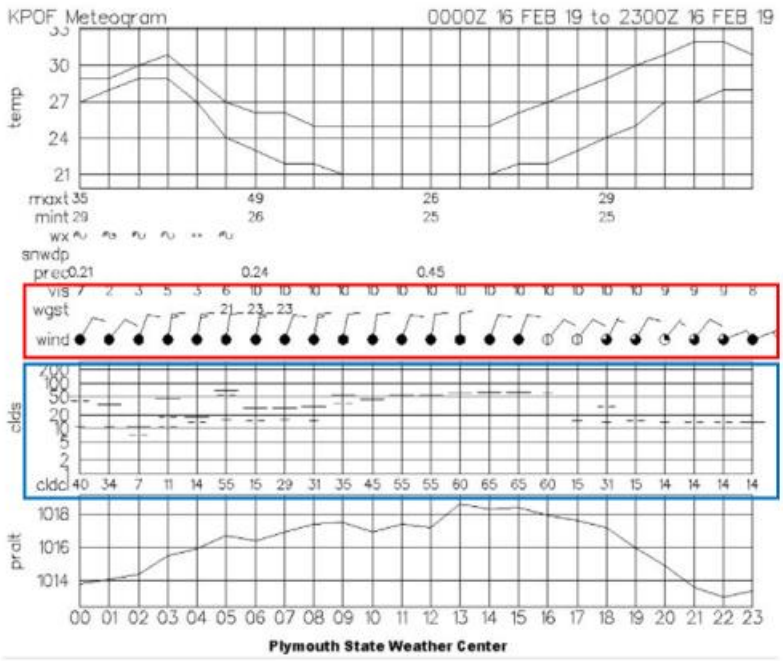

Figure 5.5 – An example of a meteorogram used for analysis during the 5-year study. Here the meteorogram from the Poplar Bluff, Missouri station on 16 February 2019 highlights the cloud observations from the ASOS station. The red rectangle showcases the wind barbs with a center circle indicating presence and percentage of sky cover. The blue rectangle represents cloud altitude levels when clouds are present overhead. Chart courtesy of the Plymouth State Weather Center data archive (https://vortex.plymouth.edu/).

5.4 Results and Conclusions

Upon completion of analysis, 4 red cases, 2 yellow cases, and 28 green cases are the results of the 5-year study. Table 5.1 is a detailed explanation of analysis results for not only each characteristic of focus plus the resulting conclusion for each case study in question. While only having 4 red and 2 yellow cases was not an overwhelming indictment for Ozark Plateau induced cold-air damming event, that there were 6 cases in a 5-year period does suggest that it is possible to experience these cold-air damming events in this region when specific conditions do exist. The frequency and intensity of these events pales in comparison to their Appalachian and Rocky Mountains counterparts, but the goal of this study phase was not to compare events to the well-recognized cold-air damming regions, but rather (and specific to the second phase) to identify if the Ozark Plateau region could produce cold-air damming events as well.

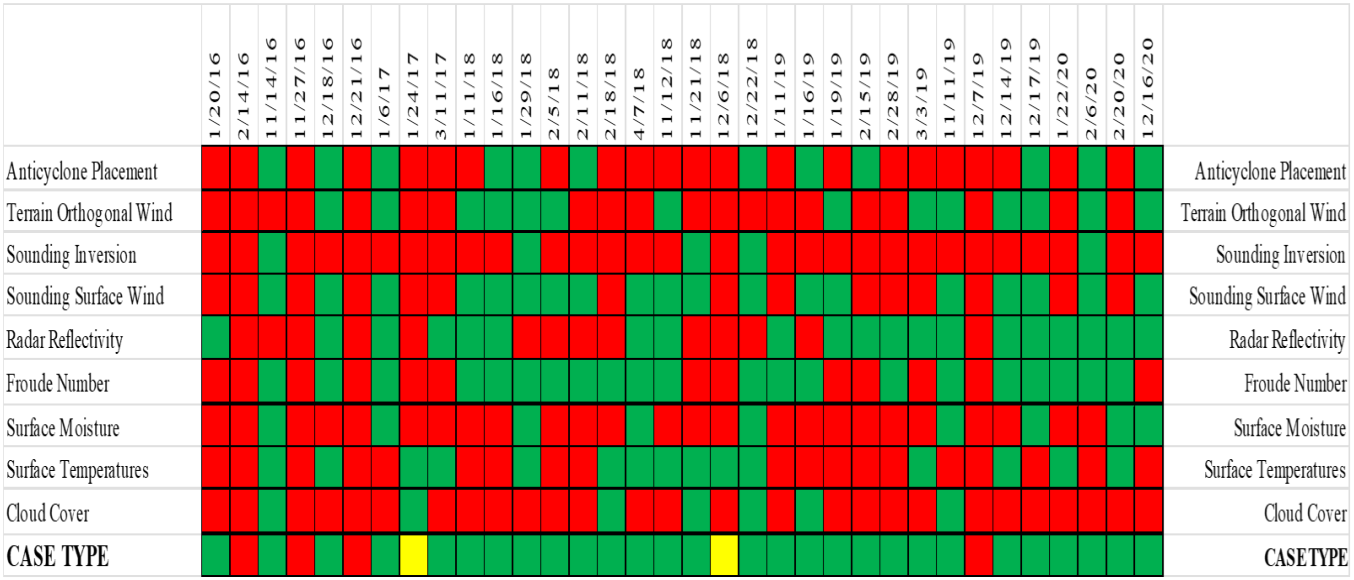

Table 5.2 - A table of results from the 5-year case study. The 9 characteristics of analysis are listed to the left and right of the color -coded chart. The 6 cold-air damming characteristics are separated from the 3 impact characteristics by a solid black line. The case type color-coded conclusion from the study is separated by an additional solid black line. A square is shaded red if the case satisfies the characteristic in question for cold -air damming. A square is shaded green if the case does not satisfy that characteristic and cold-air damming is not possible. Red cases are those in which are 9 characteristics are satisfied for an impactful cold -air damming event. Yellow cases are those in which cold -air damming is occurring, but the impact characteristics were not all satis fied. Green cases are those cases in which at least a portion of the 6 cold -air damming characteristics are not satisfied and cold -air damming is not occurring

CHAPTER 6. THIRD PHASE: WRF MODELING

6.1 Introduction

To adequately evaluate the impact of topography on cold-air damming events the Weather Research & Forecasting (WRF) model was employed. The characteristics and conditions used for each simulation are detailed earlier in Section 3.3 of Chapter 3 - Data and Methods. The model produced 6-hour time step output for the outer grid (domain 01 or d01), 1-hour time step output for the regional nested grid (domain 02 or d02), and 15-minute time step output for the innermost nested grid focused on this study's region of interest (domain 03 or d03). Despite the fine temporal resolution, the case studies evaluations were documented at 6-hour time increments to remain consistent within the 3 domains. The model simulated 2 cases: the initial case study of 04 March 2014 and a case study chosen from the 5-year study that occurred on 27 November 2016. For each case the model was tasked to simulate terrain heights altered between 0.0001 and 2x terrain height for every tenth iteration (0.1, 0.2, 0.3, etc.) which totaled 21 simulation model runs per each case or 42 model runs total. The focus of this text will keep to the actual-terrain model run (terrain height * 1.0), no-terrain (terrain height * 0.0001), half-terrain (terrain height * 0.5), and double-terrain (terrain height * 2.0), here to be known as the main simulations.

6.2 04 March 2014 Case Study

The first case study for this modeled focus was the case study of 04 March 2014 detailed earlier in Chapter 4 of this research study. The spot location for this case study

was the Blytheville, Arkansas station (KHKA) based upon its proximity to Interstate 55, though incident reports and impacts occurred in much of the region of interest of d03. Maps and soundings were analyzed at 6-hour time increments beginning at staggered start times depending on which domain the analysis output was taken from until the last time of model output at 1200 UTC on 05 March 2014. To allow the WRF model to properly analyze the event the 3 domains were staggered in starting times by 6 hours starting with the largest domain (d01) beginning at 0000 UTC on 03 March 2014, followed by the second or regional domain (d02) at 0600 UTC on 03 March 2014, and finishing with the smallest or region of interest domain (d03) starting at 1200 UTC on 03 March 2014.

6.2.1 Actual-Terrain versus No-Terrain Comparison

To best represent the results of the WRF modeling simulations for each of the 3 case studies, a comparison of the 3 altered main simulations to the actual-terrain simulation of each case was analyzed. The early time steps mainly associated with 03 March 2014 feature weather conditions typical of a post-frontal regime so comparison will begin at the 0000 UTC of 04 March 2014 time step, which is understood to be the onset of the cold-air damming event in the initial case. The first comparison features the actual-terrain simulation runs and the no-terrain simulation runs in which the elevation of the Ozark Plateau was essentially flattened when terrain height is multiplied by 0.001.

6.2.1.1 0000 UTC 04 March 2014

The analysis began with the d02 streamline maps from the actual-terrain simulations and the no-terrain simulations. At 0000 UTC the regional maps showed consistent 10-m wind streamlines on both maps (Figure 6.1) out of the northeast uniform across the region of interest in northeastern Arkansas. The difference in the 2 maps was the lack of terrain shading on the no-terrain map (Fig. 6.1b). Less obvious was the bending and deviation of the 10-m wind streamlines on the actual-terrain map (Fig. 6.1a) as surface flow navigated the elevation of the Ozark Plateau west of the region of interest. Here is where terrain influence on 10-m wind flow was first observed in the streamlines.

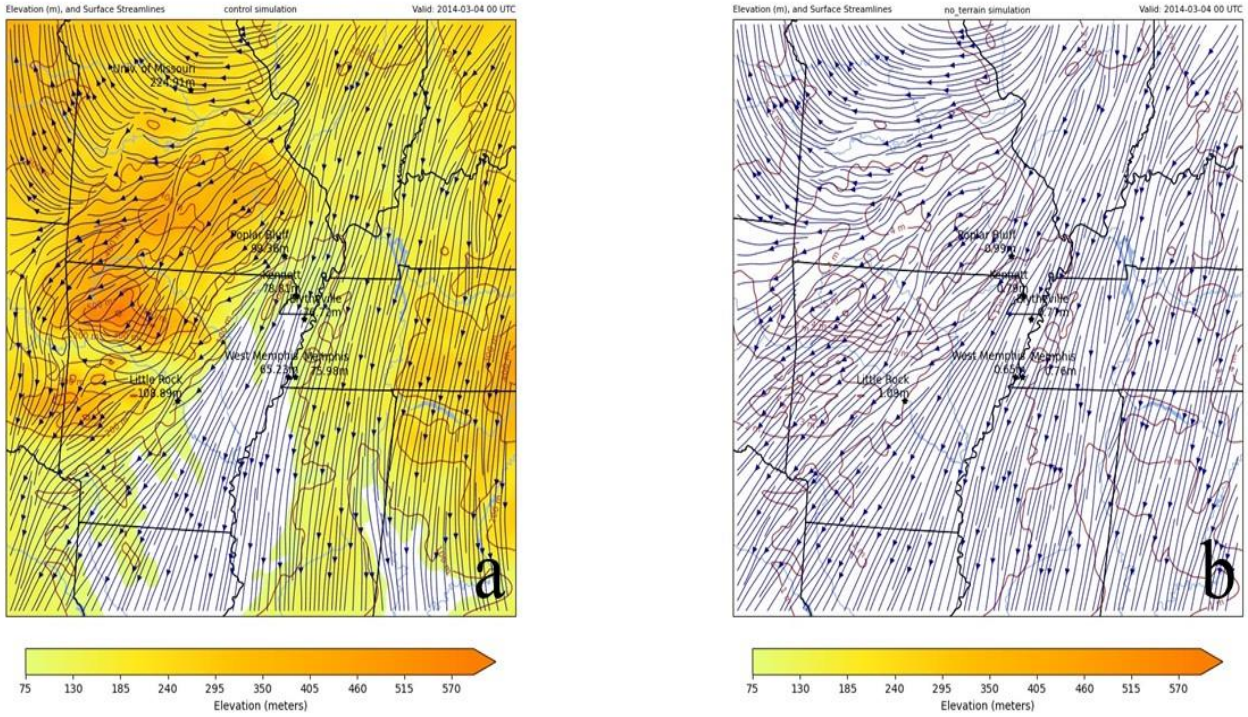

Figure 6.1 – d02 streamline maps from 0000 UTC on 04 March 2014. Map (a) is from the actual-terrain simulation run. Map (b) is from the no-terrain simulation run. Surface wind streamlines are depicted in navy blue on each map. The elevation heights are shaded from 75 m up through 570 m. Topographic lines are shaded in dark brown.

The d03 streamlines focused attention to the region of interest over the Missouri bootheel region and extreme northeastern Arkansas (Figure 6.2). Like the regional streamline maps of the d02 streamline maps (Figure 6.1). the surface flow through the flood plain was consistently out of the northeast. The d03 streamline maps, however, featured more deviation around the elevation associated with Crowley's Ridge just west of Blytheville, Arkansas. Surface flow on the no-terrain map (Figure 6.2b) remained northeasterly and uniform across the flood plain while on the actual-terrain simulation (Figure 6.2, a) the surface flow did deviate around the ridge as it traversed from northeast to southwest. This deviation around the ridges was in response to damming occurring in a limited capacity at the northeastern point of the embedded ridges. This was a common observation in the early time steps of this March 2014 case study before the shift to a more easterly direction occurred in the morning hours of 04 March 2014.

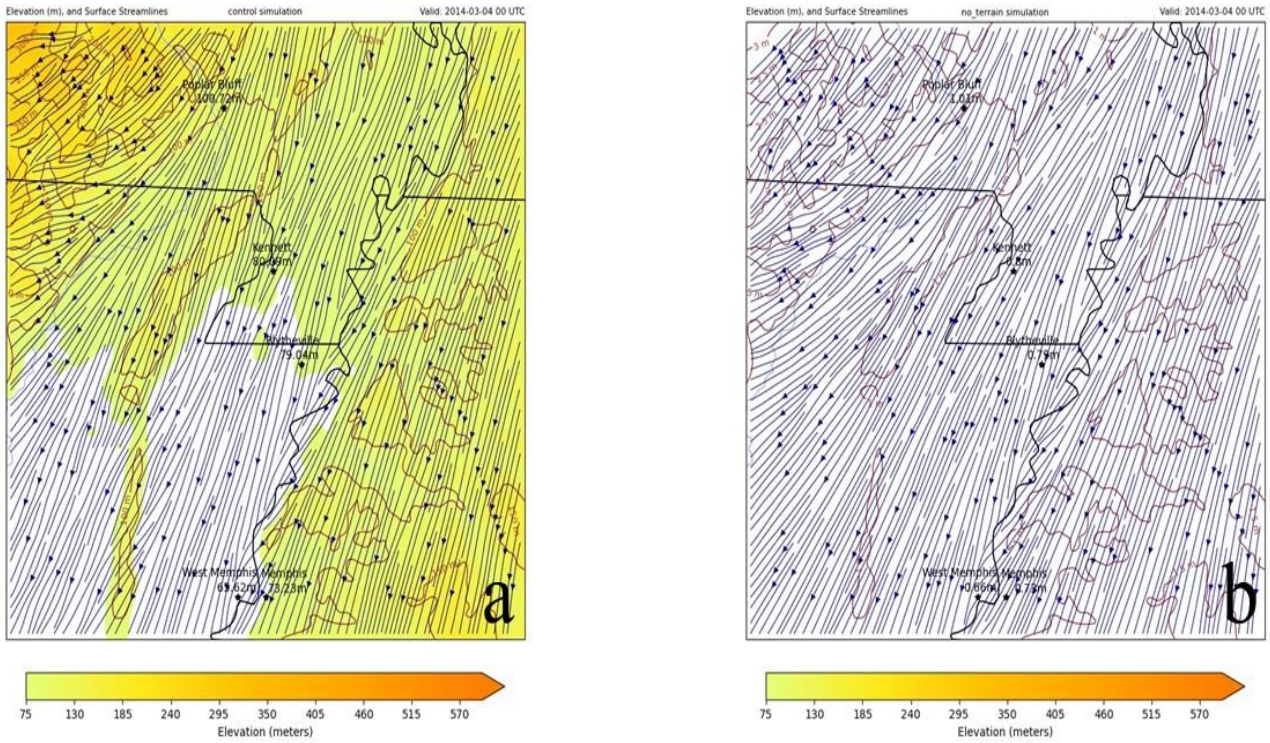

Figure 6.2 – d03 streamline maps from 0000 UTC on 04 March 2014. Map (a) is from the actual-terrain simulation runs. Map (b) is from the no-terrain simulation runs. Surface wind flow streamlines are featured in navy blue on each map. The elevation is shaded from 75 m up through 570 m. Topographic lines are featured in dark brown.

The regional temperature maps at 0000 UTC on 04 March 2014 (Figure 6.3) showed below-freezing temperatures across northern Arkansas and Missouri with a temperature gradient to warmer temperatures further south. There appeared to be a nose of freezing temperatures extending southwestward down into eastern Arkansas on both maps, even though warmer temperatures existed at that same latitude to the west over the Plateau and to the east over southern Tennessee. From a regional viewpoint the differences between the actual-terrain simulation and the no-terrain simulation were subtle. Wind barbs on the d02 temperature map at 0000 UTC were observed to calm over the Ozark Plateau though 5 kt northeasterly flow still existed in the region of interest. The temperature gradient was featured on both simulation maps as well as the freezing temperatures infiltrating the region of interest in northeastern Arkansas. The differences between the two maps show up more in the d03 temperature maps (Figure 6.4).

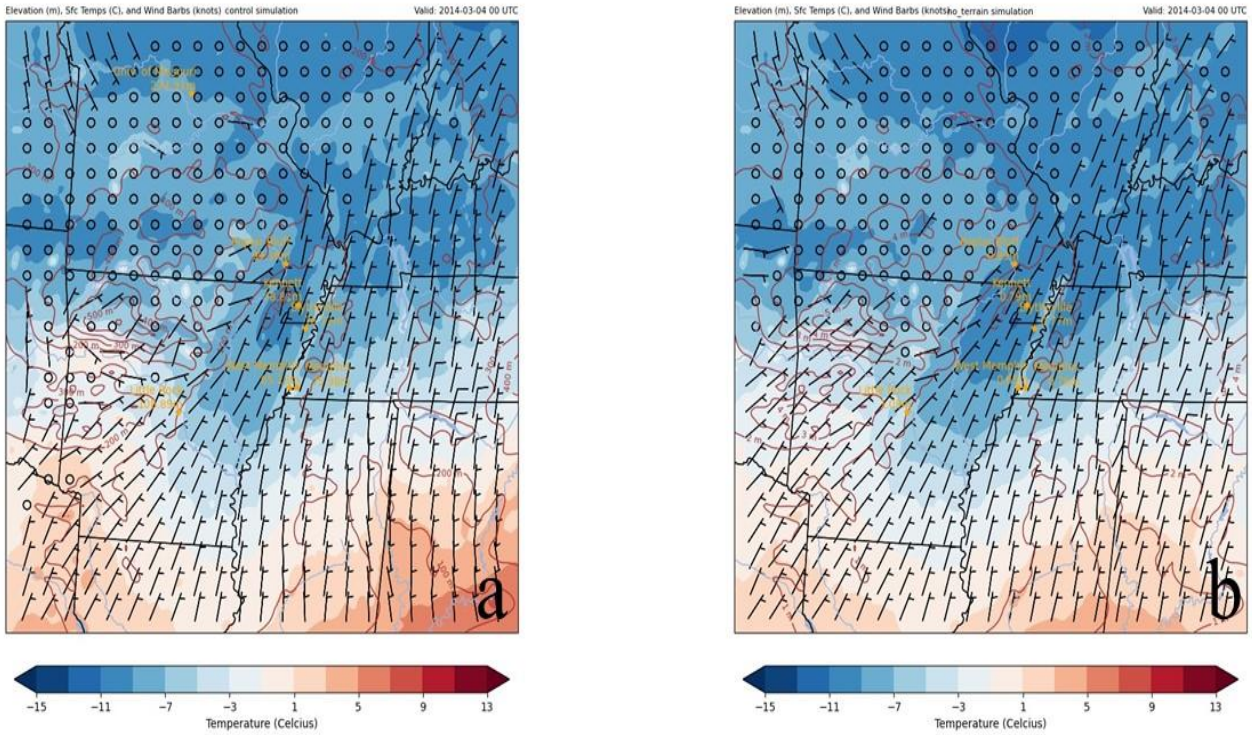

Figure 6.3 – d02 temperature maps from 0000 UTC on 04 March 2014. Each map features surface wind barbs (kts) in black, temperature shaded from blue to red from below -15°C up through 13°C. Topographic lines and values are featured on each map in dark brown.

On the d03 temperature map (Figure 6.4), the focus became the nose of below-freezing temperatures infiltrating the flood plain of eastern Arkansas. Most notable from these d03 maps was how the colder temperatures were more spread out in the no-terrain simulation (Fig. 6.4b) showing how the terrain of the region of interest has a "channeling effect" on colder, denser surface air. The coldest temperatures on the actual-terrain simulation run (Fig. 6.4a) were more confined to an area between the escarpment of the Plateau and the bootheel of Missouri. On the no-terrain simulation map, the colder temperatures were more widespread throughout the flood plain with even a localized area of temperatures a few °C colder than any temperatures found on the actual-terrain map. The channeling of colder air into the floodplain on the actual-terrain simulation while being blocked from spreading out as much as what was viewed on the no-terrain simulation map was another instance of terrain influence this time on the 2-m temperature field. It is inferred that the influence was due to the channeling because of damming occurring on the northeastern point of the ridges observed on the d03 streamline actual-terrain simulation map (Fig. 6.2a). The same influence was not observed on the no-terrain simulation maps.

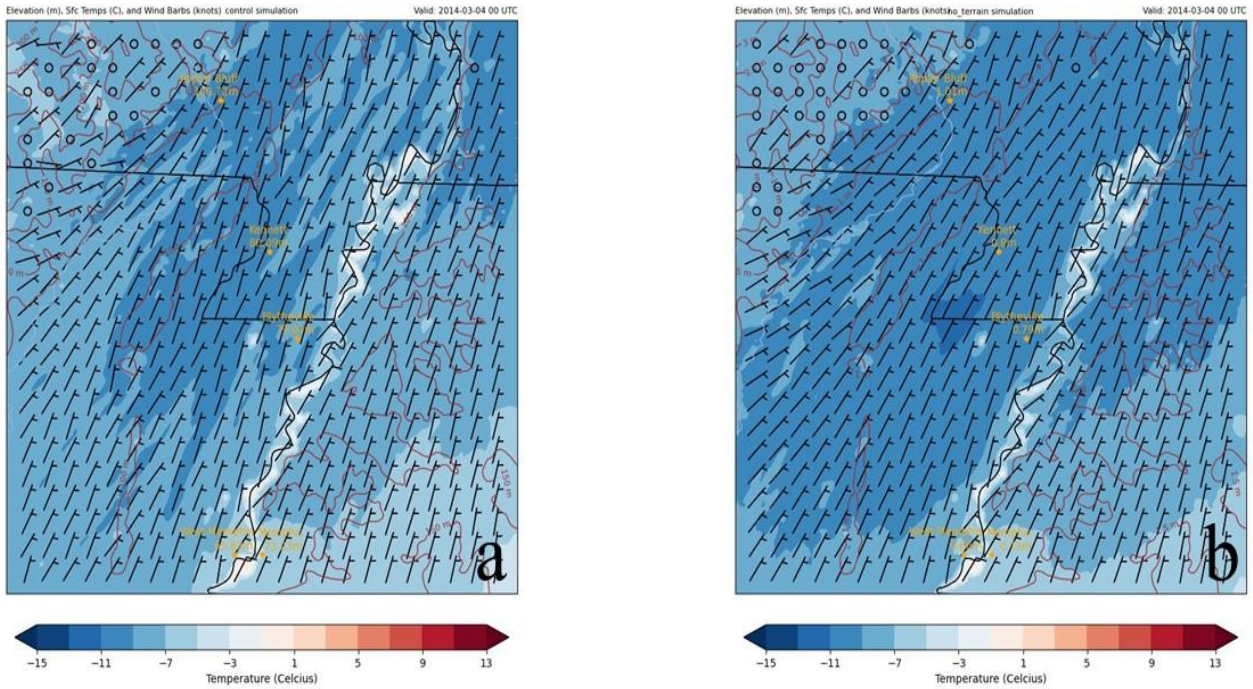

Figure 6.4 - d03 temperature maps from 0000 UTC on 04 March 2014. Each map features surface wind barbs (kts) in black, temperature shaded from blue to red from below -15°C up through 13°C. Topographic lines and values are featured on each map in dark brown.

6.2.1.2 0600 UTC 04 March 2014

The actual-terrain versus no-terrain comparison continued as the period moved into the overnight hours. At this point on the ground in the region of interest motorists were now stranded on icy roads as the sun had now fallen below the horizon for several hours and radiational cooling was driving 2-m temperatures well below freezing. Figure 6.5 shows a regional view of streamlined surface flow at 0600 UTC on March 2014. The regional d02 streamline maps (Figure 6.5) resolved continuous disorganized flow where winds were calm over the elevated topography and more organized evenly spaced flow across the floodplain from northeast to southwest. Flow over the region of interest was more northeasterly than 6 hours previously. The biggest difference between the 2 maps was the more easterly direction of surface flow just north over southern Illinois and Kentucky on the actual-terrain simulation run (Fig. 6.5a), whereas that same easterly turn occurred further north on the no-terrain simulation run (Fig. 6.5b).

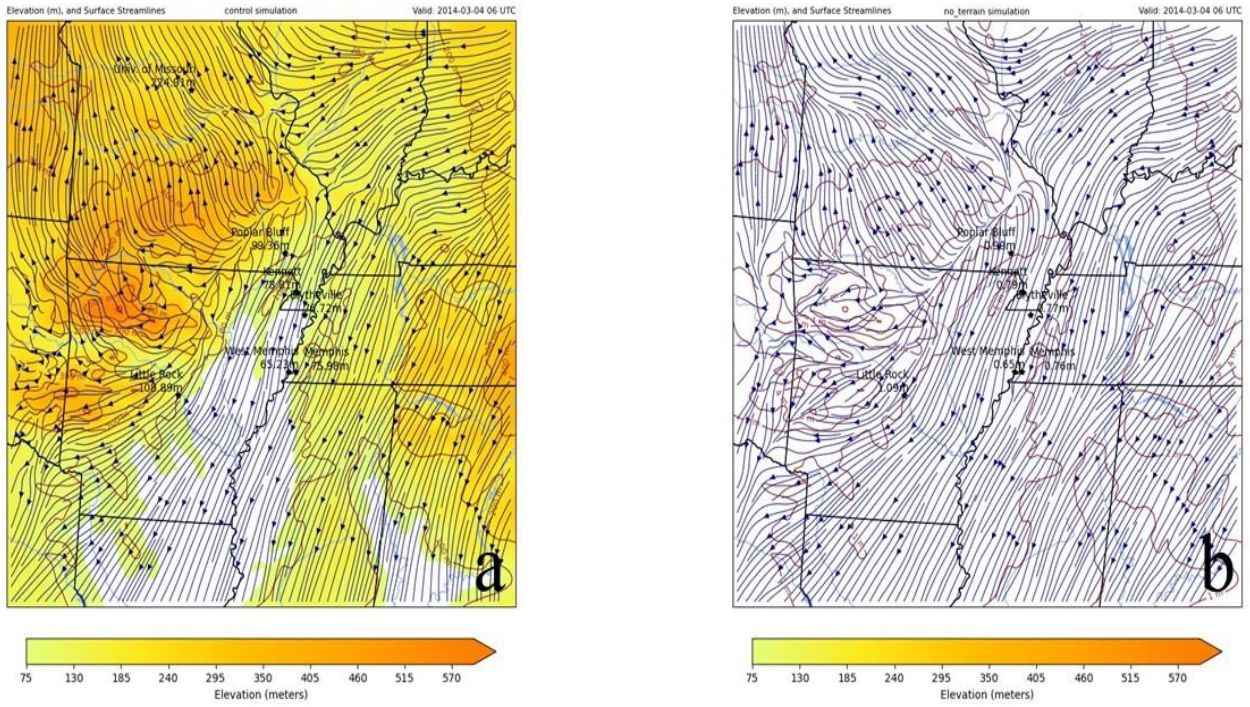

Figure 6.5 - d02 streamline maps from 0600 UTC on 04 March 2014. Map (a) is from the actual-terrain simulation run. Map (b) is from the no-terrain simulation run. Surface wind streamlines are depicted in navy blue on each map. The elevation heights are shaded from 75 m up through 570 m. Topographic lines are shaded in dark brown.

Regional analysis continued with d02 temperature maps (Figure 6.6) at 0600 UTC. These maps were consistent with analysis discussed previously at 0000 UTC. The same temperature gradient existed on both d02 maps from north to south with a nose of colder temperatures over eastern Arkansas. 10-m winds had calmed across the Ozark Plateau (or lack thereof in Fig. 6.6b). The difference observed on these maps is the extent of the cold temperatures. In the no-terrain simulation, the coldest temperatures were more widespread across southeastern Missouri, northeastern Arkansas, and to the east into Kentucky and Tennessee. On the actual-terrain simulation map (Fig. 6.6a) those coldest temperatures were more confined to areas east of the Mississippi River with only isolated areas of colder temperatures to the west over extreme northeastern Arkansas. It is inferred that this was in response to the elevation terrain of the Plateau just to the west containing this colder air from infiltrating further west.

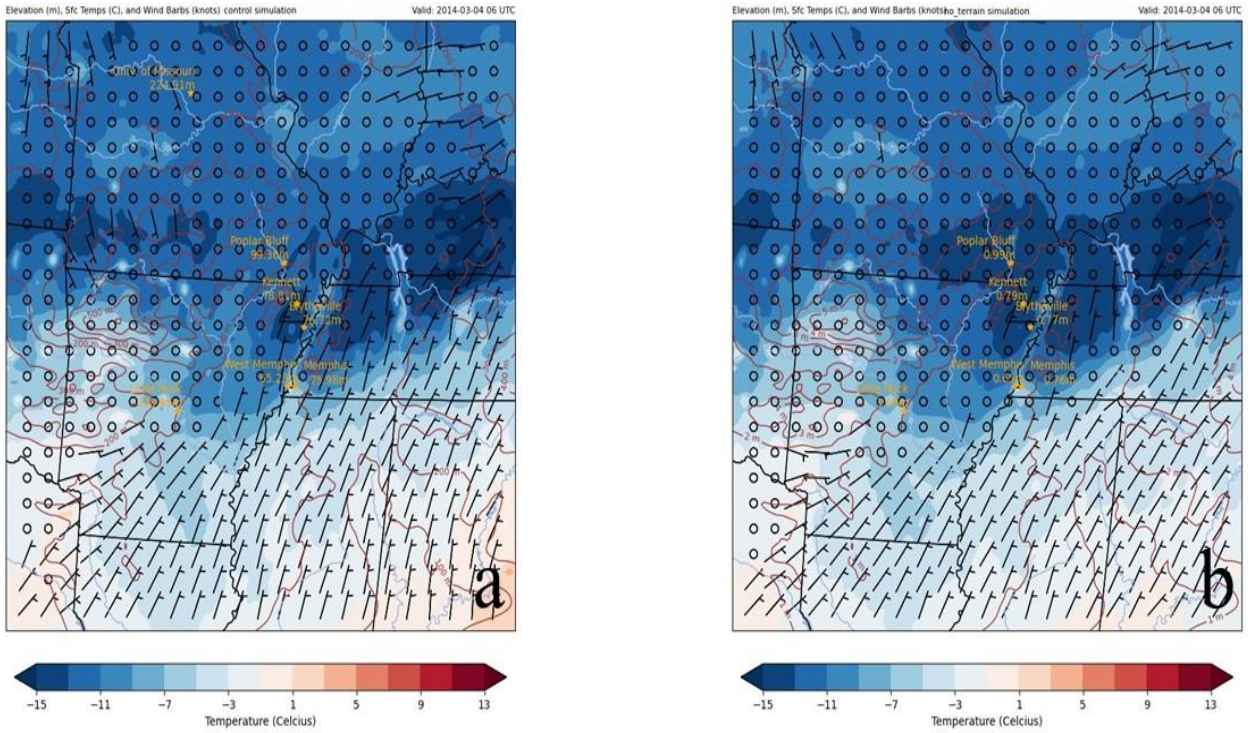

Figure 6.6 - d02 temperature maps from 0600 UTC on 04 March 2014. Each map features surface wind barbs (kts) in black, temperature shaded from blue to red from below -15°C up through 13°C. Topographic lines and values are featured on each map in dark brown.

The d03 streamline maps (Figure 6.7) reinforced calm winds in the region of interest as some streamlines across and around the embedded ridges of the plain were distorted much like their counterparts over the larger topographic feature both in the northwest corner of the d03 streamline maps and the larger extent of the d02 streamline maps. This distortion signaled that the change in terrain was influencing the calm 10-m wind flow across the region. The d03 streamline maps of 0600 UTC were almost entirely northeasterly and showed the same slight migration to a more easterly flow as seen in the d02 regional maps (Figure 6.6) discussed previously. The pattern of surface flow deviation around the ridge embedded within the flood plain, as seen 6 hours previously in the d03 streamline maps from 0000 UTC (Figure 6.3), still existed and included more disorganized streamline flow over the Ozark Plateau in the actual-terrain simulation run (Fig 6.7a). The no-terrain simulation run again featured a more uniform northeasterly flow over these terrain features with little to no deviation in northeasterly flow over the region of interest. This difference between the streamlines of these simulated maps was inferred to be due to terrain change.

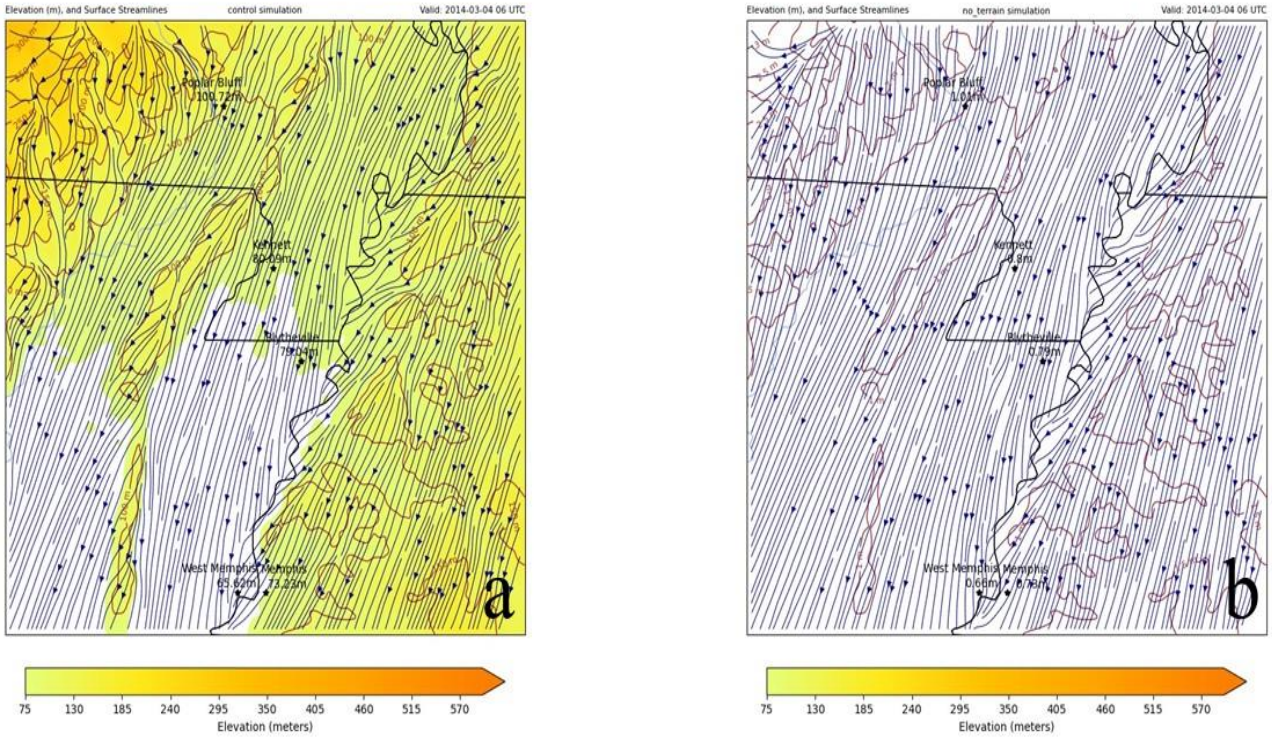

Figure 6.7 - d03 streamline maps from 0600 UTC on 04 March 2014. Map (a) is from the actual-terrain simulation runs. Map (b) is from the no-terrain simulation runs. Surface wind flow streamlines are featured in navy blue on each map. The elevation is shaded from 75 m up through 570 m. Topographic lines are featured in dark brown.

At 0600 UTC on 04 March 2014 the temperature plummeted below -11°C as seen on the d03 temperature map at that time step. Northeasterly 5-kt winds persisted in the flood plain though largely across the Ozark Plateau winds are calm. The d03 temperature maps (Figure 6.8) of 0600 UTC showed the sharpest contrast observed up to this point of analysis. While wind on both maps was relatively calm save for some 5-knot northeasterly barbs through the flood plain, the temperature shading showed significant differences. The actual-terrain simulation run (Fig. 6.8a) again featured a "channeling effect" on the surface air as the coldest temperatures were confined to a small region between the terrain elevation of the embedded ridge within the flood plain and the Mississippi River. This was again observed to be the result of damming occurring on the northeastern points of the ridges as the 10-m wind direction had not yet shifted to a more easterly course. The sharp rise in temperatures over and just near the river, easily viewed on both maps, speaks to the power of the WRF model and its ability to delineate between the heat capacities of the Mississippi River and the land surrounding the channel. This was commonly viewed on all 2-m temperature maps especially in below freezing conditions. The lack of channeling on the no-terrain simulation run map (Fig. 6.8b) was noticed as the northern half of the d03 map resolved the coldest temperatures viewed thus far.

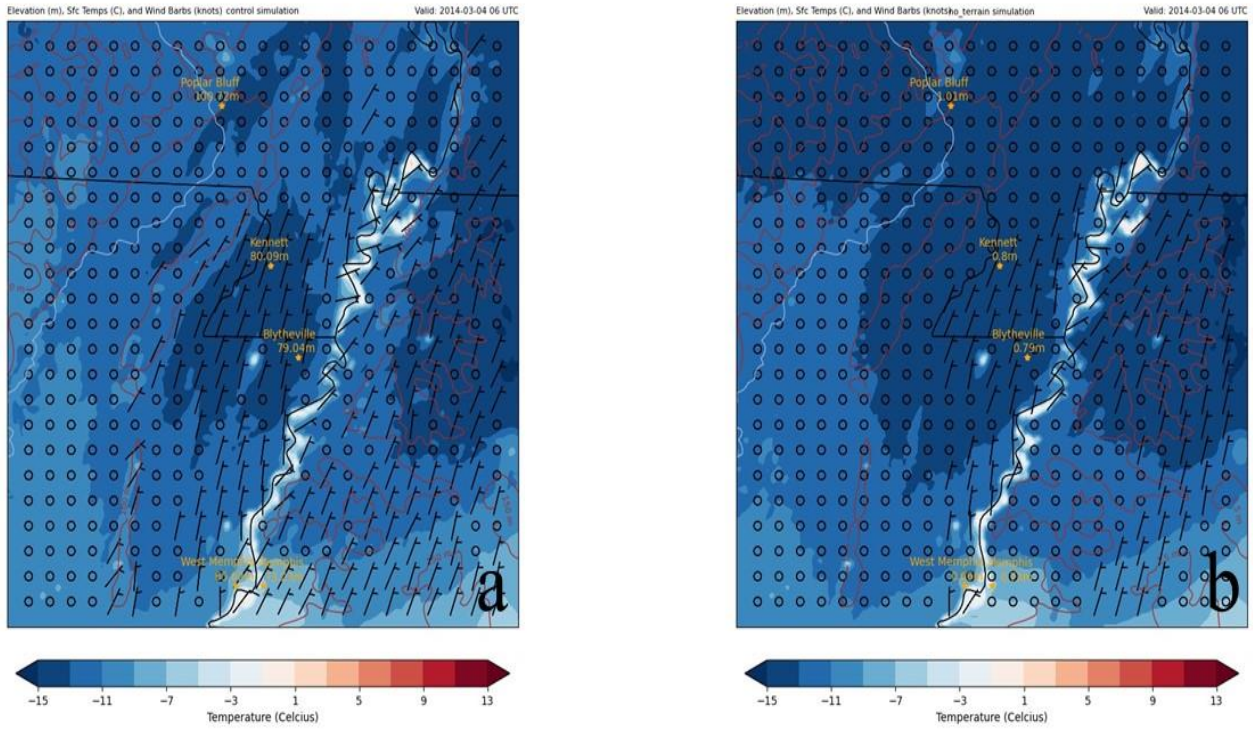

Figure 6.8 - d03 temperature maps from 00 UTC on 04 March 2014. Each map features surface wind barbs (kts) in black, temperature shaded from blue to red from below -15°C up through 13°C. Topographic lines and values are featured on each map in dark brown.

6.2.1.3 1200 UTC 04 March 2014

The analysis progressed into the morning hours of 04 March 2014 in which the coldest temperatures were observed in response to continued diurnal processes, in this instance radiational cooling. The regional d02 streamline maps (Figure 6.9) continued northeasterly flow over the region of interest, but now a divergent surface flow line develops over the edge of the escarpment at the base of the Ozark Plateau on both maps. This line separated the northeasterly flow to the southeast from southeasterly flow now observed over the Plateau and Missouri. Lack of elevation change on the no-terrain simulation run map (Fig. 6.9b) did not seem to influence this divergent flow pattern. The d02 streamline maps showed the flow across the region of interest steering to a more southerly flow across southern Missouri with a distinct wind shift just to the northwest of the Poplar Bluff, Missouri station though winds on the temperature map continued to resolve calm conditions over that region.

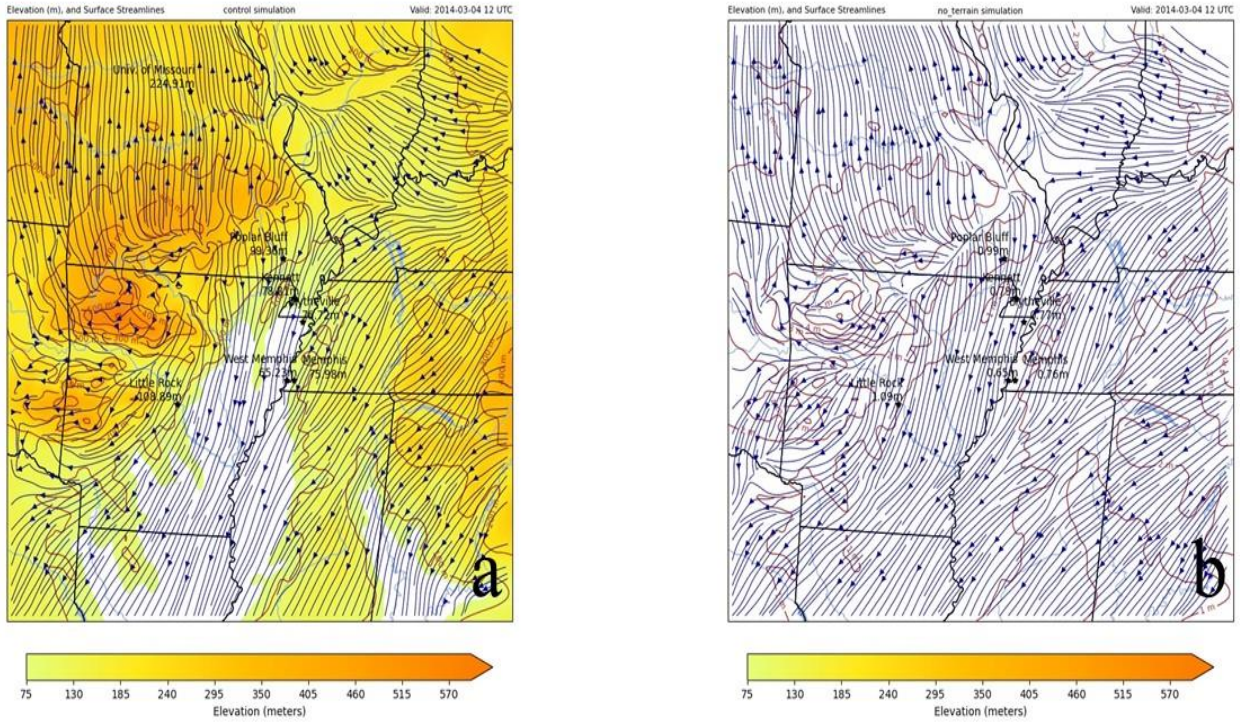

Figure 6.9 - d02 streamline maps from 1200 UTC on 04 March 2014. Map (a) is from the actual-terrain simulation run. Map (b) is from the no-terrain simulation run. Surface wind streamlines are depicted in navy blue on each map. The elevation heights are shaded from 75 m up through 570 m. Topographic lines are shaded in dark brown.

Regional temperature maps (Figure 6.10) from 1200 UTC on 04 March 2014 showed the coldest temperatures experienced during this cold-air damming event, as expected, due to diurnal processes. Again, the northern half of the maps, including the flood plain of eastern Arkansas, experienced well below-freezing temperatures just before the sun rose on 04 March. The pattern of more widespread colder temperatures on the no-terrain simulation map versus the more confined actual-terrain simulation runs continued into the morning hours of 04 March, highlighting the continued influence of terrain change on the simulations.

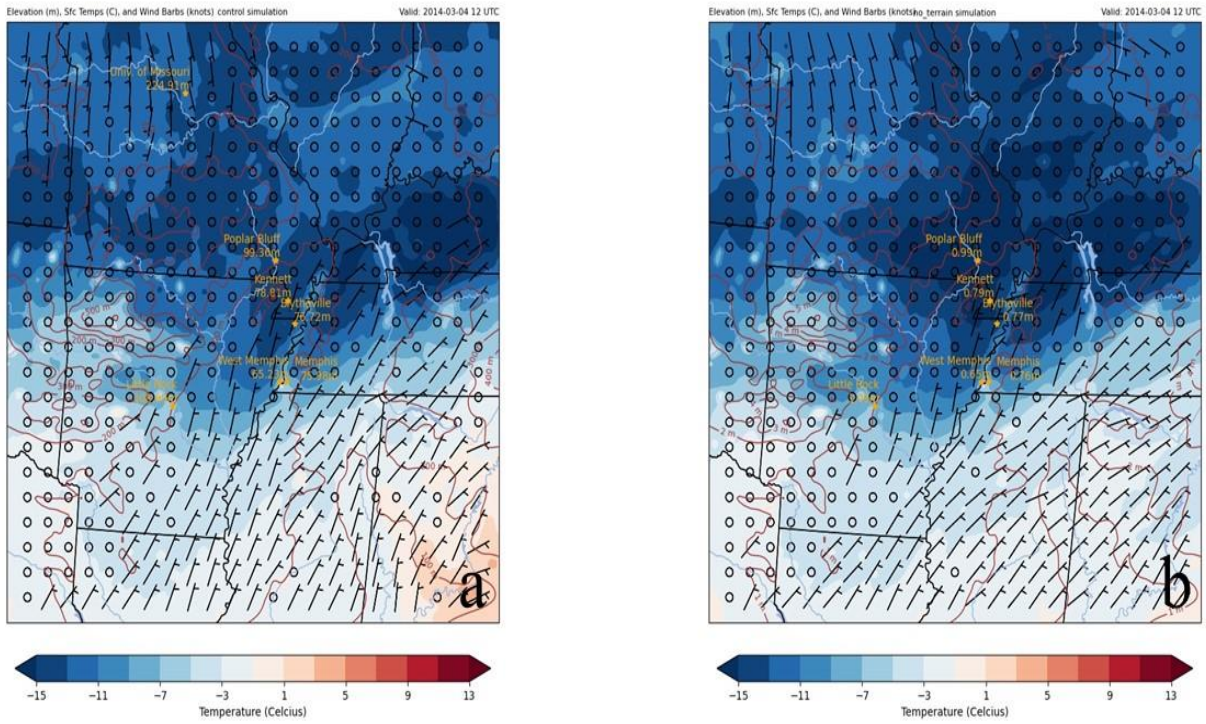

Figure 6.10 - d02 temperature maps from 1200 UTC on 04 March 2014. Each map features surface wind barbs (kts) in black, temperature shaded from blue to red from below -15°C up through 13°C. Topographic lines and values are featured on each map in dark brown.

The d03 streamline maps from 1200 UTC on 04 March 2014 showed one of the unique characteristics of this cold-air damming event. 10-m winds were still northeasterly and not yet in a favorable terrain-orthogonal direction, though the slow trend to a more easterly course continued through the morning hours as viewed on the d03 maps. What was unique was the flow supplying cold, moist air at the surface down into the flood plain where it was more contained on the actual-terrain simulation run, as seen in Figures 6.10 and 6.12, and more spread out in the no-terrain simulation due to lack of elevation just to the northwest.

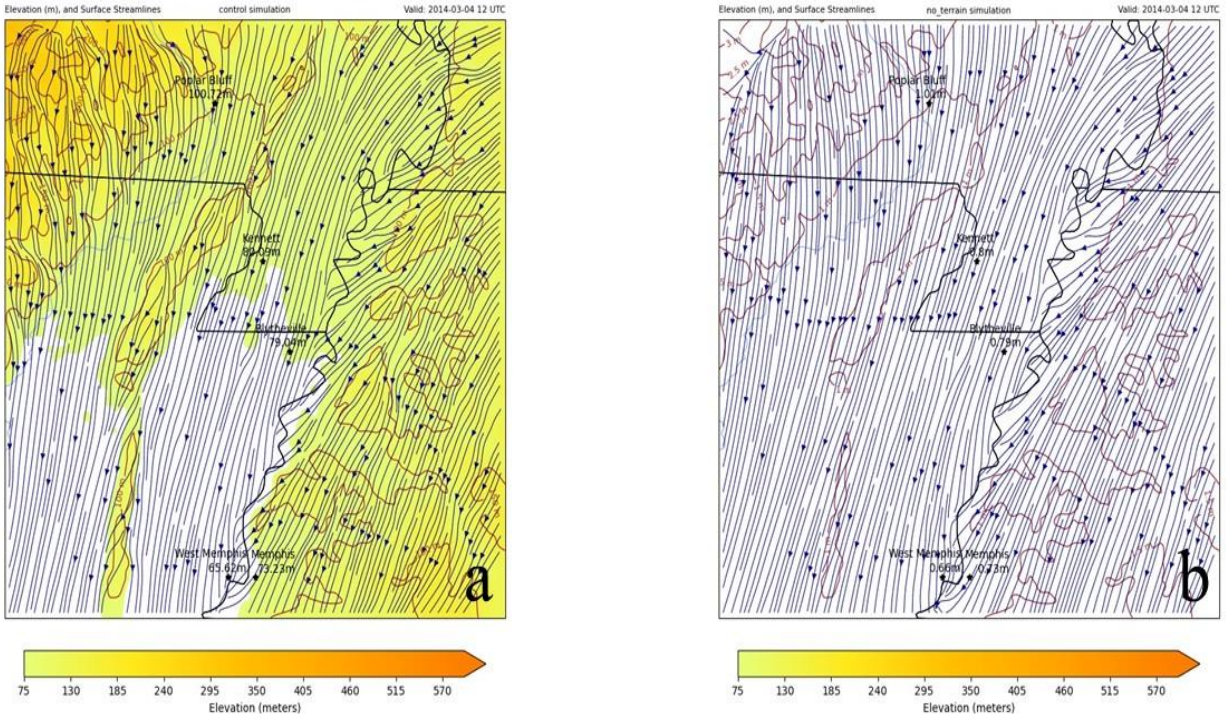

Figure 6.11 - a03 streamline maps from 1200 UTC on 04 March 2014. Map (a) is from the actual-terrain simulation runs. Map (b) is from the no-terrain simulation runs. Surface wind flow streamlines are featured in navy blue on each map. The elevation is shaded from 75 meters up through 570 meters. Topographic lines are featured in dark brown.

The d03 temperature maps of 1200 UTC on 04 March 2014 (Figure 6.12) featured the same calm winds over the Plateau despite obvious significant increases in elevation (actual-terrain simulation run) versus no increase in elevation (no-terrain) simulation run. The d03 temperature maps resolved again the “channeling effect” of the terrain in the actual-terrain simulation run in stark contrast to the widespread coldest temperature values (-13°C) from just west of Blytheville, Arkansas to much of the southern portion of Missouri in the no-terrain simulation run map.

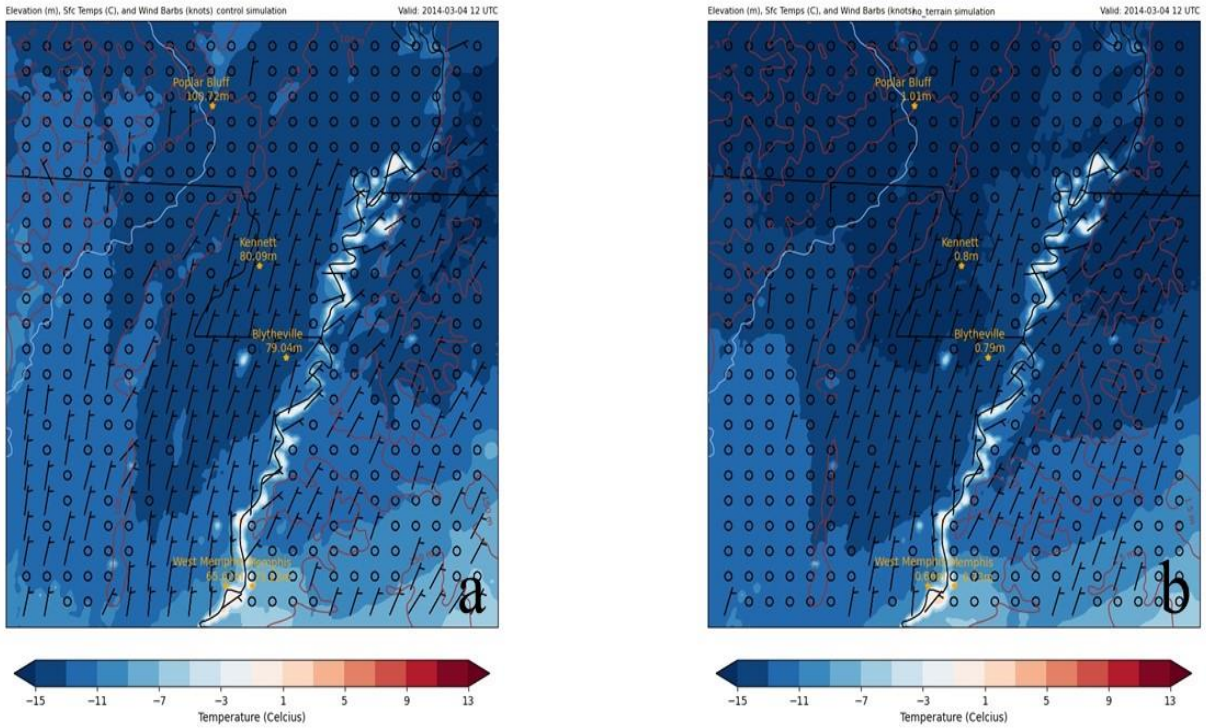

Figure 6.12 - d03 temperature maps from 1200 UTC on 04 March 2014. Each map features surface wind barbs (kts) in black, temperature shaded from blue to red from below -15°C up through 13°C. Topographic lines and values are featured on each map in dark brown.

6.2.1.4 1800 UTC 04 March 2014

The 1800 UTC series of maps were perhaps the most favorable for cold-air damming occurring in the region of interest. The d02 streamline maps (Figure 6.13) turned the northeasterly flow over the region of interest to a more easterly course over the Plateau. The southwestern flank of the parent anticyclone was apparent on both d02 maps as the high-pressure center had moved south enough for its southern edge easterlies to be terrain-orthogonal with the southeastern edge of the Plateau on both maps. Aside from some minor deviations on the actual-terrain simulation map in response to terrain elevation these maps were very similar in describing 10-m wind flow patterns.

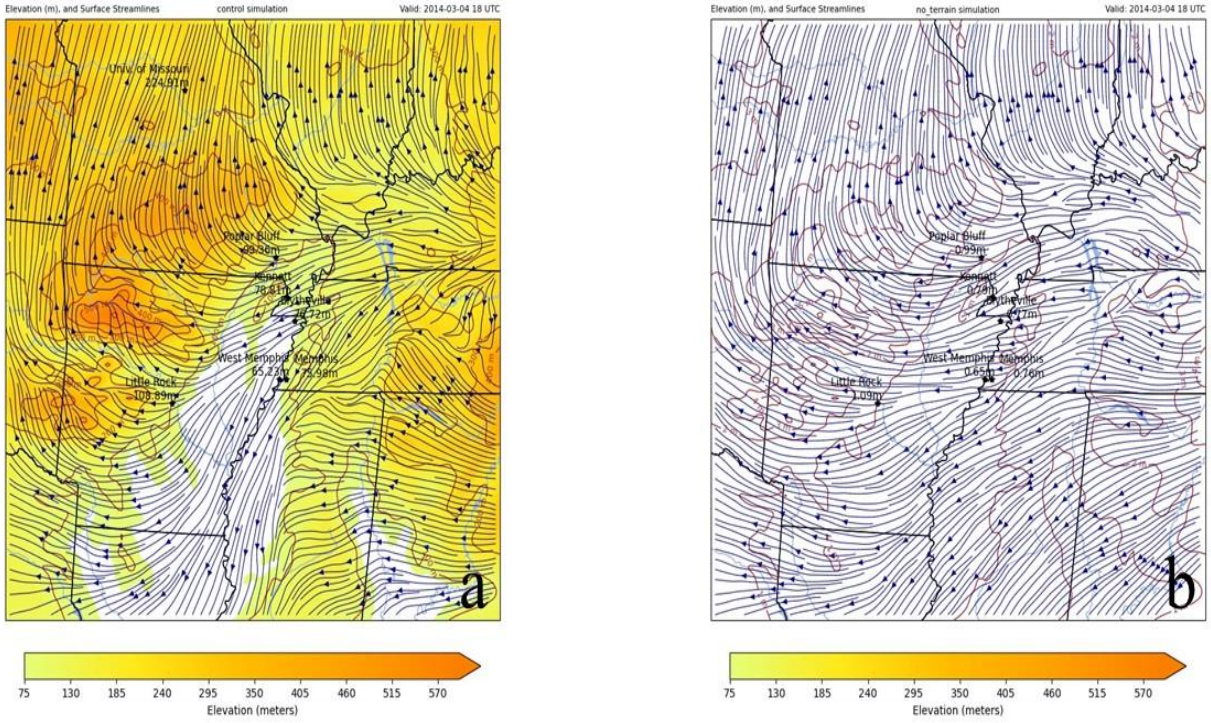

Figure 6.13 - d02 streamline maps from 1800 UTC on 04 March 2014. Map (a) is from the actual-terrain simulation run. Map (b) is from the no-terrain simulation run. Surface wind streamlines are depicted in navy blue on each map. The elevation heights are shaded from 75 m up through 570 m. Topographic lines are shaded in dark brown.

While the temperatures on the regional d02 maps (Figure 6.14) had rebounded to above freezing over much of Arkansas and southern Missouri, the temperatures in the region of interest remained below freezing even though they had warmed up to -5°C. Winds were calm over most of Arkansas except for the region of interest where 5-kt easterly flow was consistent with the streamline maps from this time step.

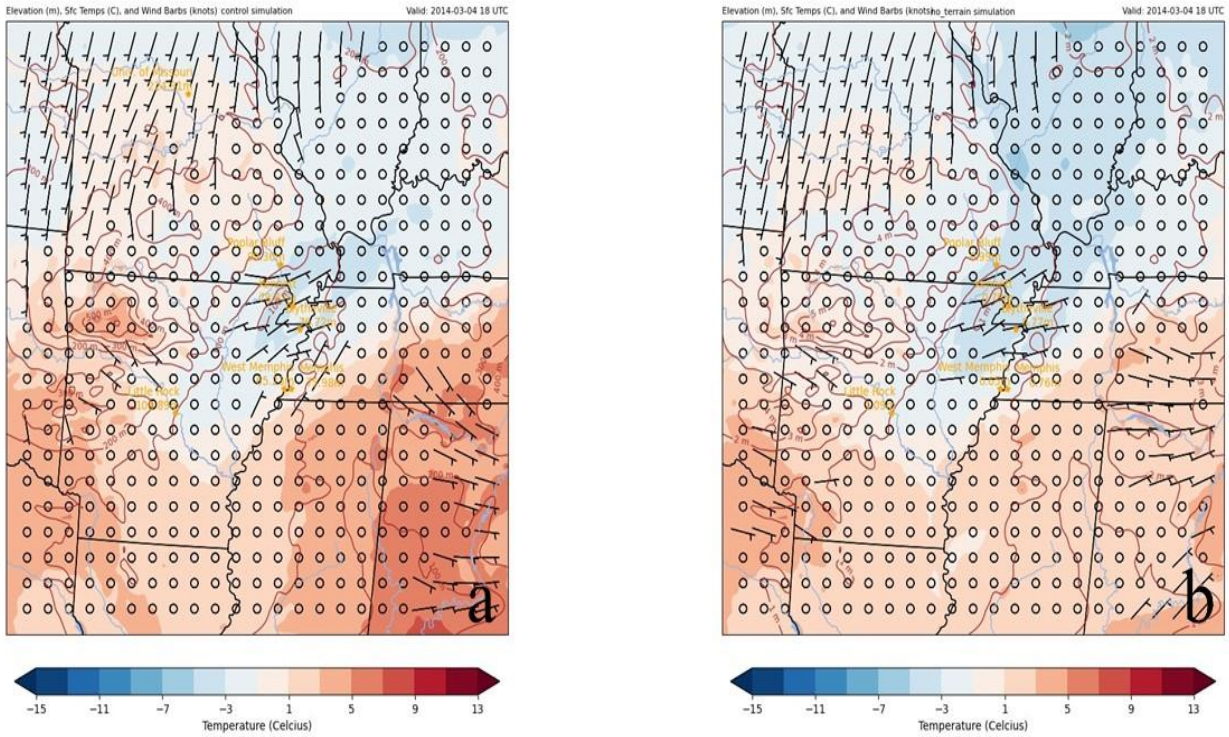

Figure 6.14 - d02 temperature maps from 1800 UTC on 04 March 2014. Each map features surface wind barbs (kts) in black, temperature shaded from blue to red from below -15°C up through 13°C. Topographic lines and values are featured on each map in dark brown.

Closer inspection of the region of interest from the d03 streamline maps (Figure 6.15) of the 1800 UTC time step showed that all streamlines associated with these maps contained a strong easterly component making even the calm winds viewed at this time very terrain-orthogonal and very conducive to a cold-air damming event taking place in the region. There was less deviation due to terrain on the actual-terrain run map than previously experienced due to a decrease in speed of the 10-m wind field at this time.

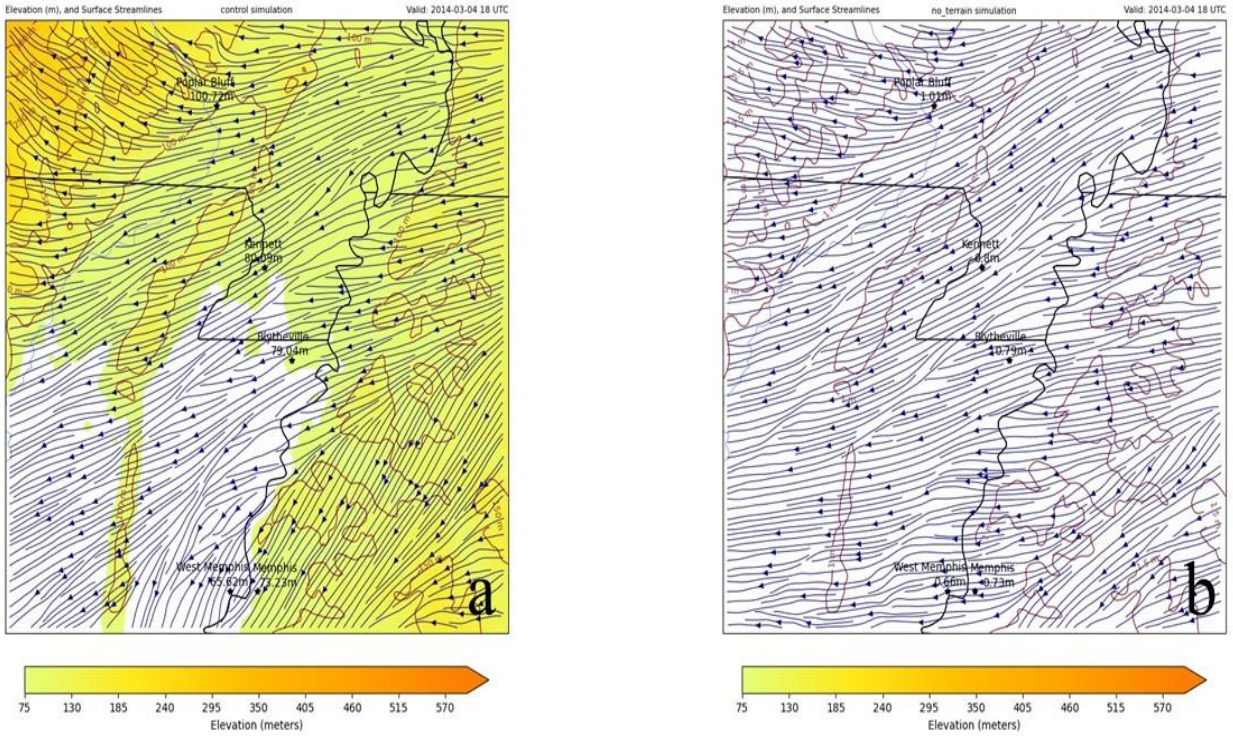

Figure 6.15 - d03 streamline maps from 1800 UTC on 04 March 2014. Map (a) is from the actual-terrain simulation runs. Map (b) is from the no-terrain simulation runs. Surface wind flow streamlines are featured in navy blue on each map. The elevation is shaded from 75 m up through 570 m. Topographic lines are featured in dark brown.

The d03 temperature maps (Figure 6.16) were the warmest viewed in this analysis thanks to the effects of diurnal processes as the sun reached maximum heating for the day. The relaxed wind field of either calm winds or 5-kt easterly winds existed on both maps. While temperatures around other parts of Arkansas and points east into Tennessee and Kentucky had rebounded above freezing, the region of interest remains still slightly below freezing. Again, the pattern continued of more widespread freezing temperatures on the no-terrain simulation map while on the actual-terrain simulation freezing temperatures remained confined to the flood plain in response to terrain elevation influence.

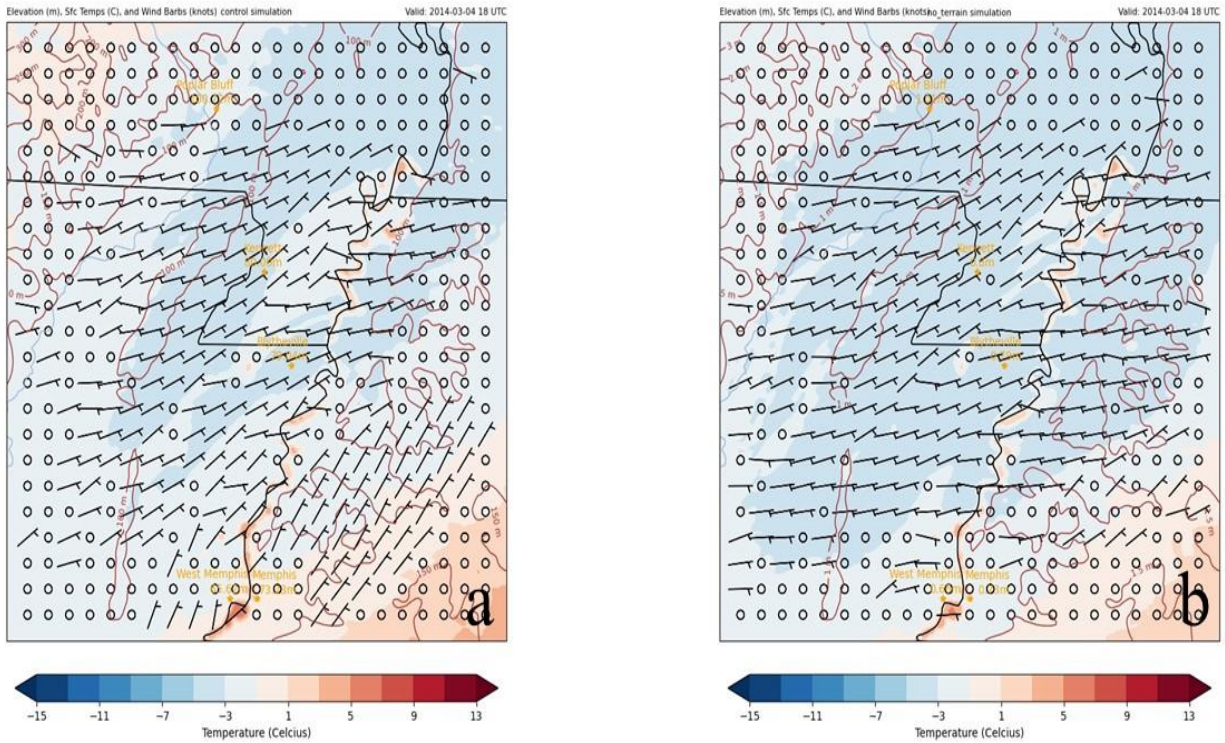

Figure 6.16 - d03 temperature maps from 1800 UTC on 04 March 2014. Each map features surface wind barbs (kts) in black, temperature shaded from blue to red from below -15°C up through 13°C. Topographic lines and values are featured on each map in dark brown.

6.2.1.5 0000 UTC 05 March 2014

The final 3 time steps that encompass the 05 March 2014 portion of this case study took place as the impact of the cold-air damming event on the roadways of the region of interest began to wane. The d02 streamline maps (Figure 6.17) as 05 March began showed more southerly change to the surface flow pattern over the northern half of the map as the high-pressure system influences this portion of the Midwest while northerly flow presided over the southern and southeastern quadrant of both simulation maps. East-southeasterly flow over the region of interest continued at this time on both simulation maps. Extremely little contrast in the maps was observed.

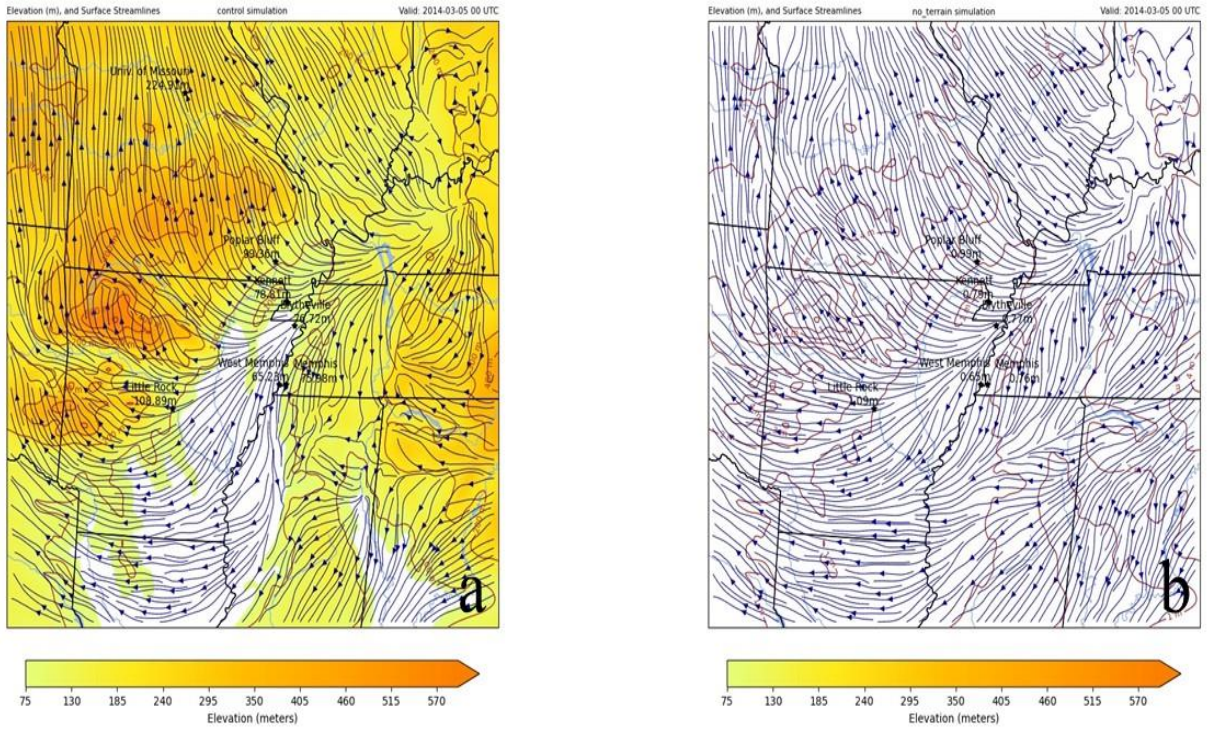

Figure 6.17 - d02 streamline maps from 0000 UTC on 05 March 2014. Map (a) is from the actual-terrain simulation run. Map (b) is from the no-terrain simulation run. Surface wind streamlines are depicted in navy blue on each map. The elevation heights are shaded from 75 m up through 570 m. Topographic lines are shaded in dark brown.

The d02 temperature maps (Figure 6.18) beginning the 05 March 2014 analysis depicted the cold pocket of air still existing at the surface over the region of interest. As the sun set around 0000 UTC on 05 March the d02 regional temperature map showed how colder temperatures within the cold dome associated with the region of interest began to regress to the below-freezing values seen during the previous night. Winds across most of the maps were calm save for 5-kt southerly winds over the Ozark Plateau to the west of the region of interest. Temperatures across the region were slightly warmer at this time than 24 hours prior with more above-freezing temperatures to the south over southern Arkansas and the Gulf Coast states.

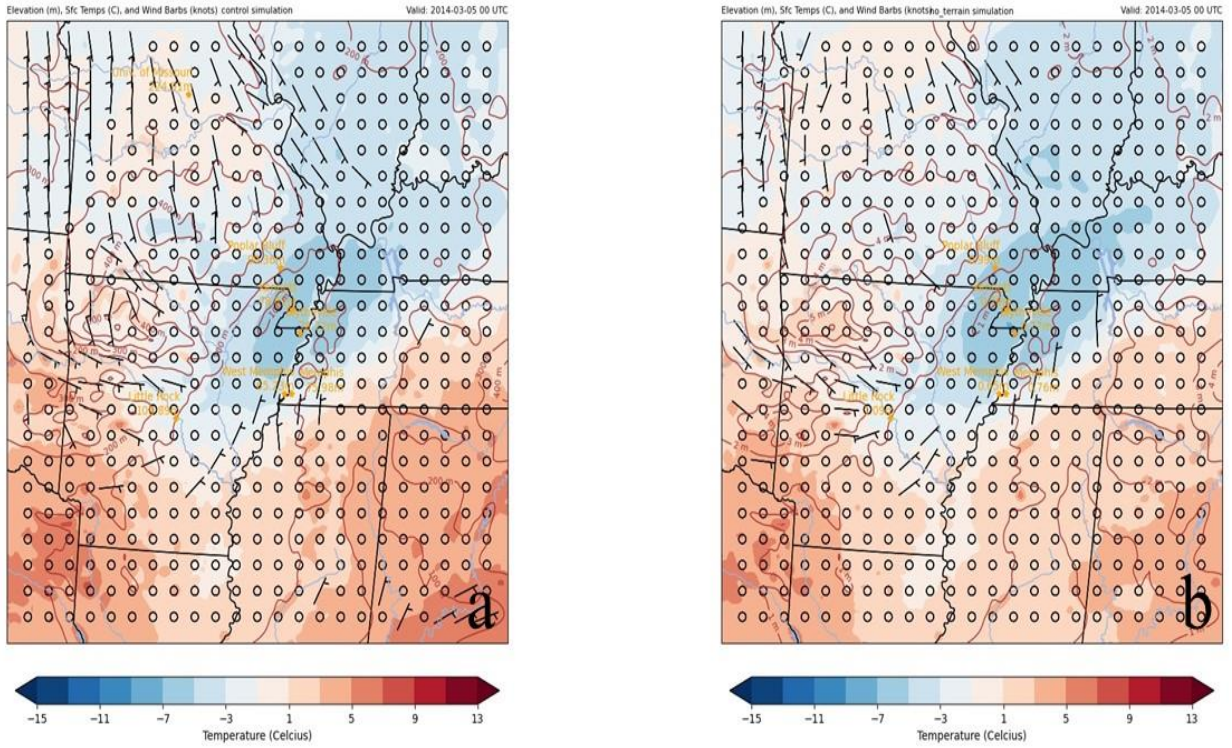

Figure 6.18 - d02 temperature maps from 0000 UTC on 05 March 2014. Each map features surface wind barbs (kts) in black, temperature shaded from blue to red from below -15°C up through 13°C. Topographic lines and values are featured on each map in dark brown.

The d03 streamline maps (Figure 6.19) from 0000 UTC on 05 March 2014 focused more on the easterly flow over the region of interest. Due to the calm flow over the area at this time little contrast was observed between the 2 simulation runs. Streamlines were very uniform over the region of interest on both simulation maps despite the differences in elevation between the actual-terrain simulation and the no-terrain simulation.

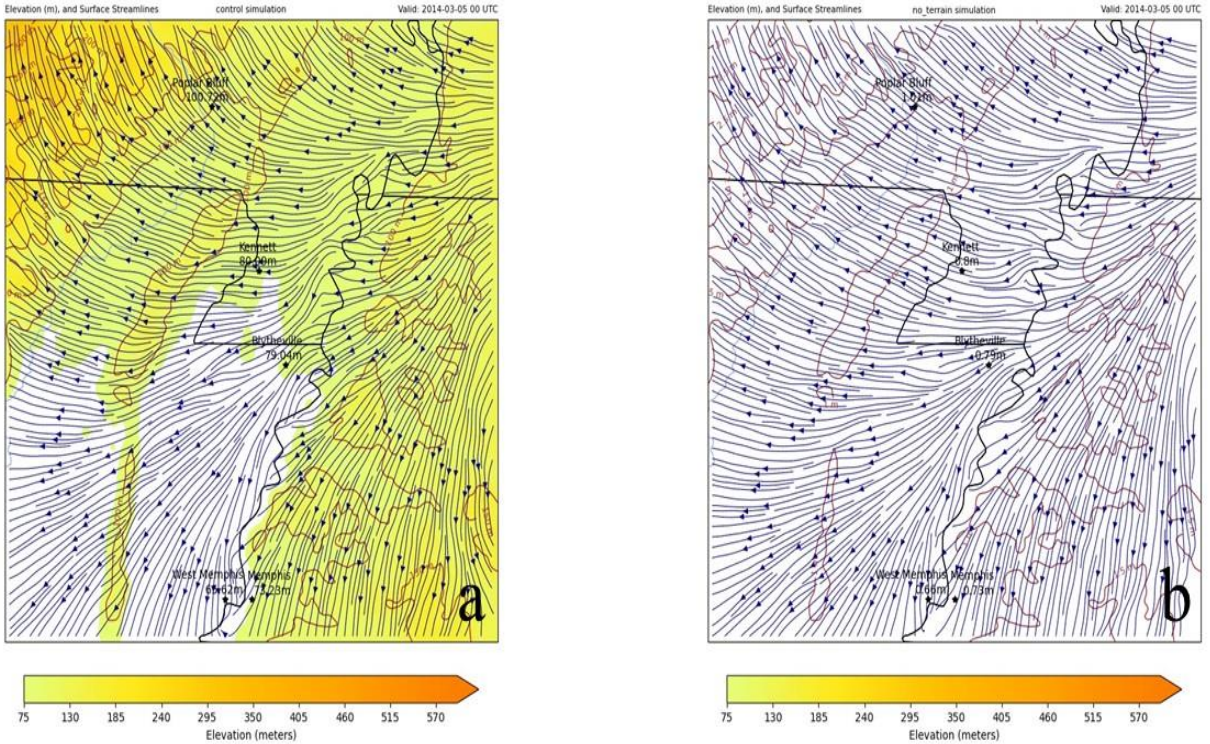

Figure 6.19 - d03 streamline maps from 0000 UTC on 05 March 2014. Map (a) is from the actual-terrain simulation runs. Map (b) is from the no-terrain simulation runs. Surface wind flow streamlines are featured in navy blue on each map. The elevation is shaded from 75 m up through 570 m. Topographic lines are featured in dark brown.

Winds on the d03 temperature maps (Figure 6.20) of 0000 UTC 05 March 2014 had mostly calmed across the region of interest save for 5-kt east-northeasterly oriented winds along the Mississippi River and closer to the Memphis stations near the Interstate 40 corridor in east central Arkansas as seen on the d03 temperature maps. A small pocket of colder temperatures existed along the state border between Missouri and Arkansas on the no-terrain simulation run. The pattern of more widespread colder temperatures on the no-terrain simulation map continued.

Figure 6.20 - d03 temperature maps from 0000 UTC on 05 March 2014. Each map features surface wind barbs (kts) in black, temperature shaded from blue to red from below -15°C up through 13°C. Topographic lines and values are featured on each map in dark brown.

6.2.1.6 0600 UTC 05 March 2014

The d02 streamlines maps, (Figure 6.21) as night persisted on 05 March 2014 showed a divergence of 10-m wind flow over the region of interest. The northwestern portion of the maps showed southerly flow while the southwestern extent of the maps was clearly more disorganized and northeasterly. Streamlines were more compact near the escarpment of the Ozark Plateau near the Poplar Bluff, Missouri station on the no-terrain simulation map (Fig. 6.21b).

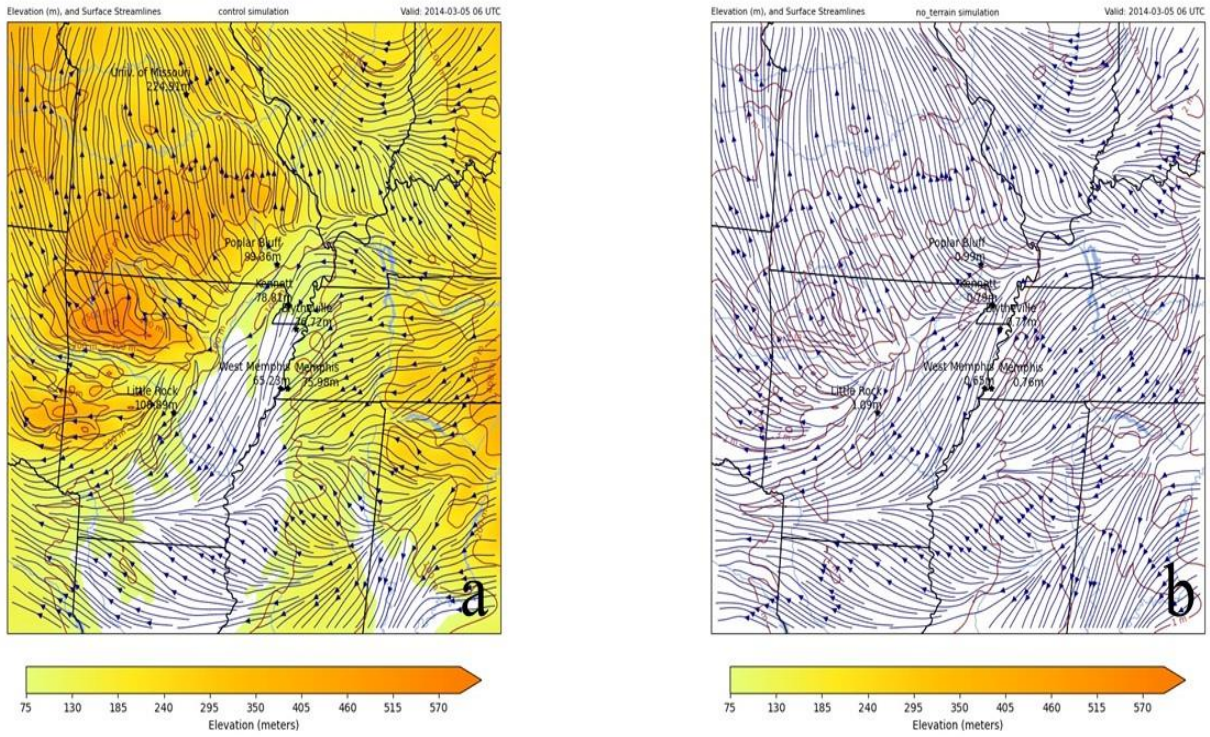

Figure 6.21 - d02 streamline maps from 0600 UTC on 05 March 2014. Map (a) is from the actual-terrain simulation run. Map (b) is from the no-terrain simulation run. Surface wind streamlines are depicted in navy blue on each map. The elevation heights are shaded from 75 m up through 570 m. Topographic lines are shaded in dark brown.

The regional d02 temperature maps (Figure 6.22) highlighted the cold dome situated over the region of interest at 0600 UTC on 05 March 2014. The region of interest was now surrounded by warmer temperatures even to the north over Missouri and Illinois. Both simulation maps contained the coldest temperatures directly over the Blytheville, Arkansas (KHKA) station as the no-terrain simulation run (Fig. 6.22b) continued to feature slightly colder temperatures over a wider area of the map. On that no-terrain simulation map the colder temperatures extended up into Missouri, Illinois, and extreme western Kentucky.

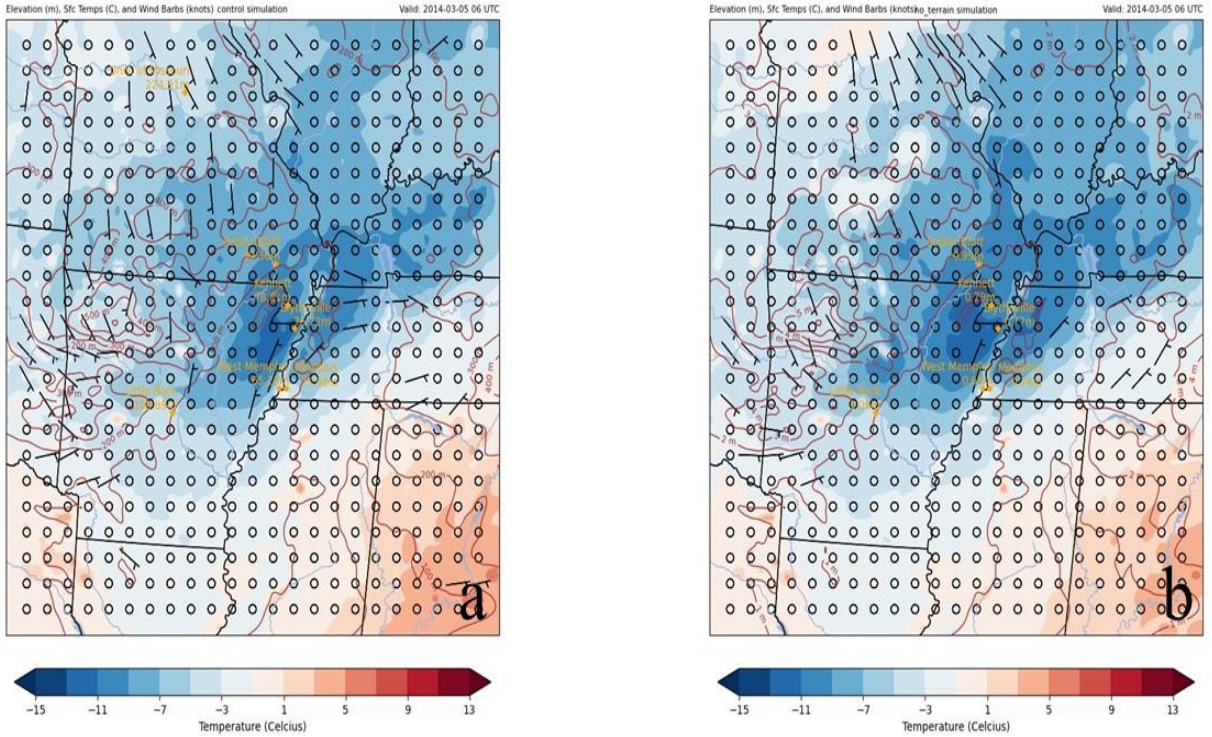

Figure 6.22 - d02 temperature maps from 0600 UTC on 05 March 2014. Each map features surface wind barbs (kts) in black, temperature shaded from blue to red from below -15°C up through 13°C. Topographic lines and values are featured on each map in dark brown.

By 0600 UTC of 05 March the deflection points in the flow pattern existed directly over the region of interest as indicated on the d03 streamline maps (Figure 6.23) for that time step. A large contrast was found between the actual-terrain and no-terrain simulation maps at this time. The actual-terrain simulation map (Fig, 6.23a) featured deflection of the 10-m wind flow from easterly to north-northeasterly as the flow collided with both the Ozark Plateau and the ridge embedded in the eastern Arkansas flood plain. The no-terrain simulation run (Fig. 6.23b), however, continued its easterly flow easily over those features which were nonexistent during the simulation.

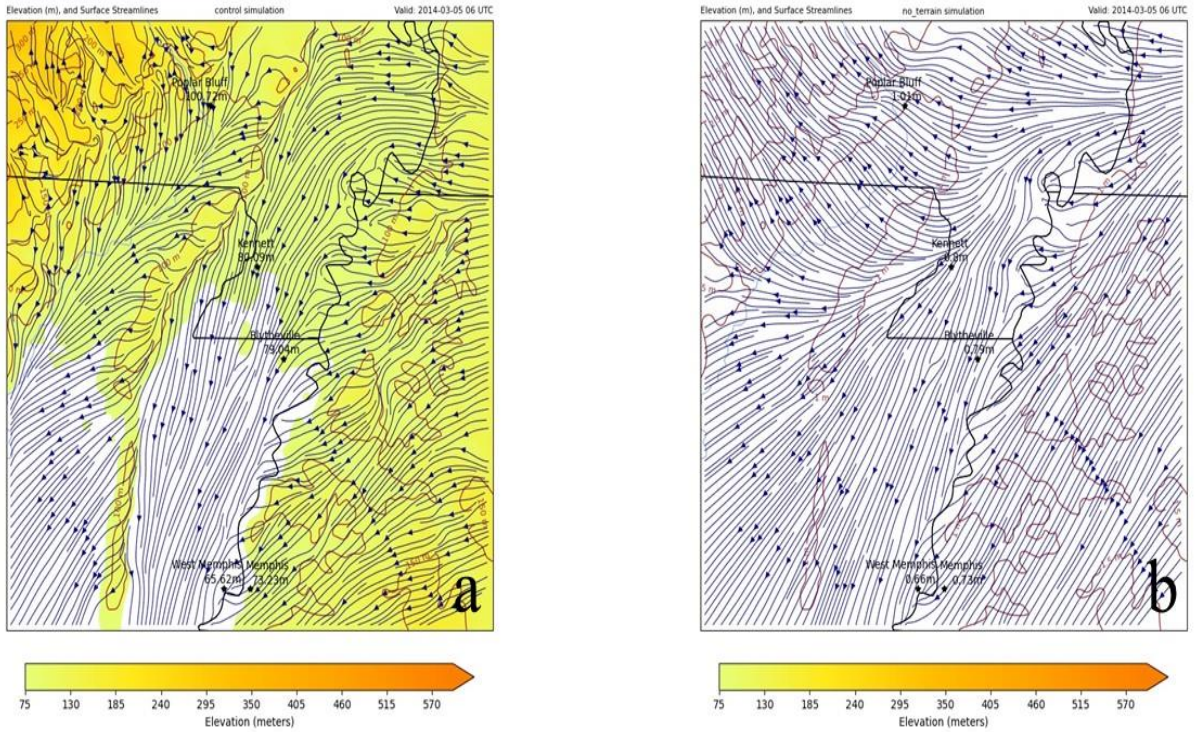

Figure 6.23 - d03 streamline maps from 0600 UTC on 05 March 2014. Map (a) is from the actual-terrain simulation runs. Map (b) is from the no-terrain simulation runs. Surface wind flow streamlines are featured in navy blue on each map. The elevation is shaded from 75 m up through 570 m. Topographic lines are featured in dark brown.

The area influenced by freezing temperatures was significantly smaller, according to the d03 temperature maps (Figure 6.24) for 0600 UTC, than seen on the previous 0600 UTC map from 04 March. Judging solely from these d03 temperature maps, one would assume that these freezing temperatures encompass a larger region of colder temperatures. Regarding the regional temperature map (Figure 6.22), it was understood that these freezing temperatures were anomalous as the region surrounding continued to rebound from the passage of the mid-latitude cyclone now 48 hours prior. In keeping with that sentiment, even the freezing temperatures on these d03 temperature maps were warmer than previously experienced the night before on 04 March. That these freezing temperatures existed still over the region of interest (specifically channeled through the flood plain on the actual-terrain run map (Fig. 6.24a) at this time lends to evidence for a cold-air damming event.

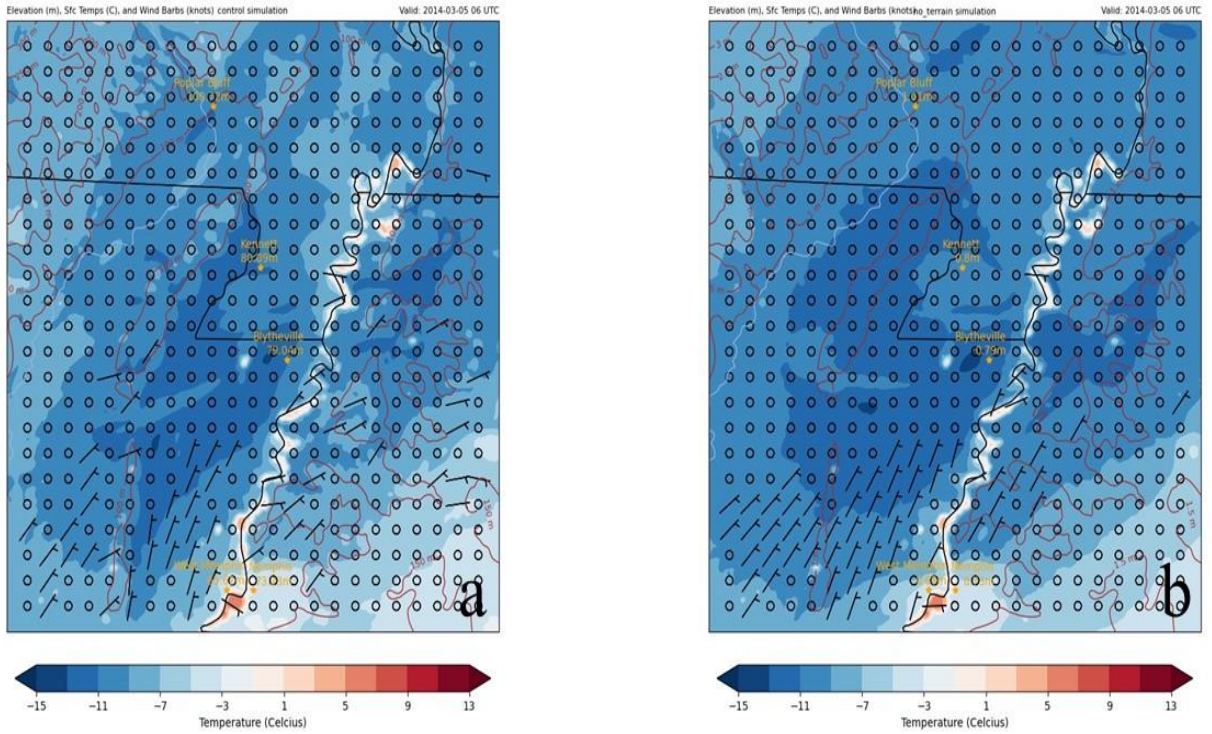

Figure 6.24 - d03 temperature maps from 0600 UTC on 05 March 2014. Each map features surface wind barbs (kts) in black, temperature shaded from blue to red from below -15°C up through 13°C. Topographic lines and values are featured on each map in dark brown.

6.2.1.7 1200 UTC 05 March 2014

The actual-terrain versus no-terrain comparison concluded at 1200 UTC on 05 March 2014. Regional streamline maps (Figure 6.25) showed deflection along the escarpment of the Ozark Plateau in northern Arkansas and southern Missouri which acted as a dividing line between southerly flow to the north over Missouri and north-northeasterly flow to the south over eastern Arkansas and Louisiana.

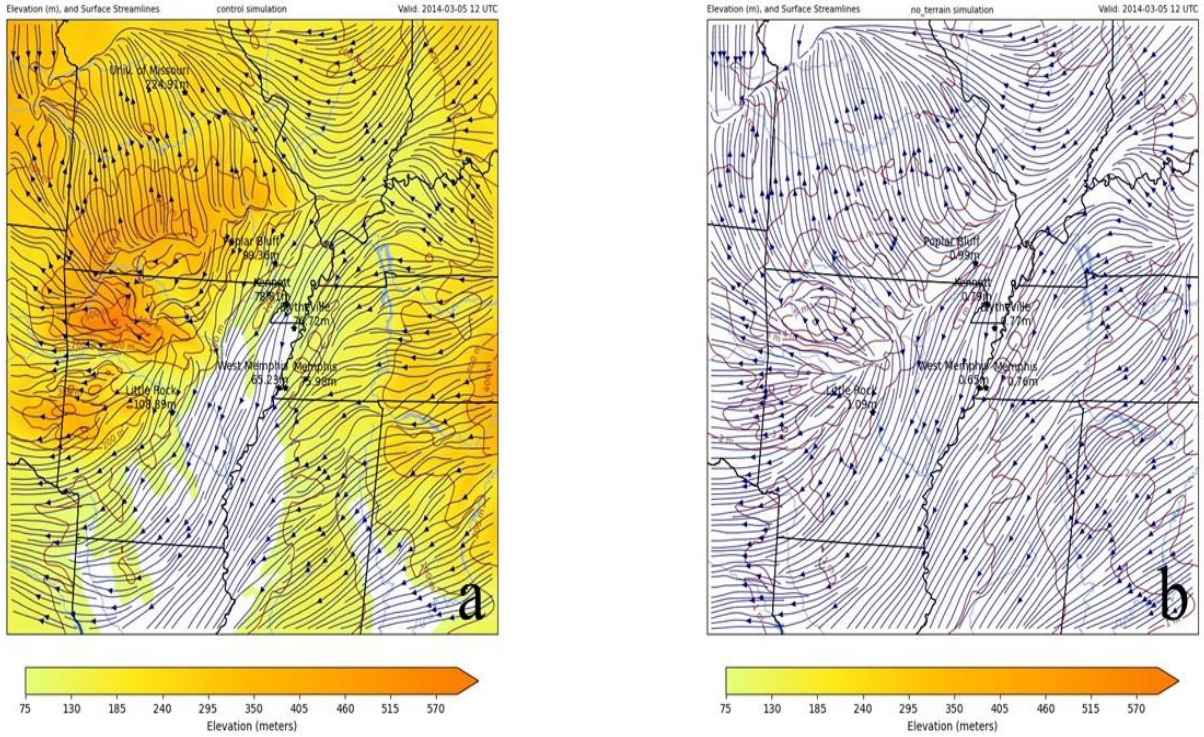

Figure 6.25 - d02 streamline maps from 1200 UTC on 05 March 2014. Map (a) is from the actual-terrain simulation run. Map (b) is from the no-terrain simulation run. Surface wind streamlines are depicted in navy blue on each map. The elevation heights are shaded from 75 m up through 570 m. Topographic lines are shaded in dark brown.

By 1200 UTC the d02 regional temperature maps (Figure 6.26) showed the coldest temperature values were placed between the Blytheville, Arkansas station and embedded ridge just to the west. On the regional maps the surface cold dome up against the Plateau was evident on the actual-terrain simulation map (Fig. 6.25a). Weak 5-kt winds were found mainly over the southern extent of the region of interest and into western Tennessee.

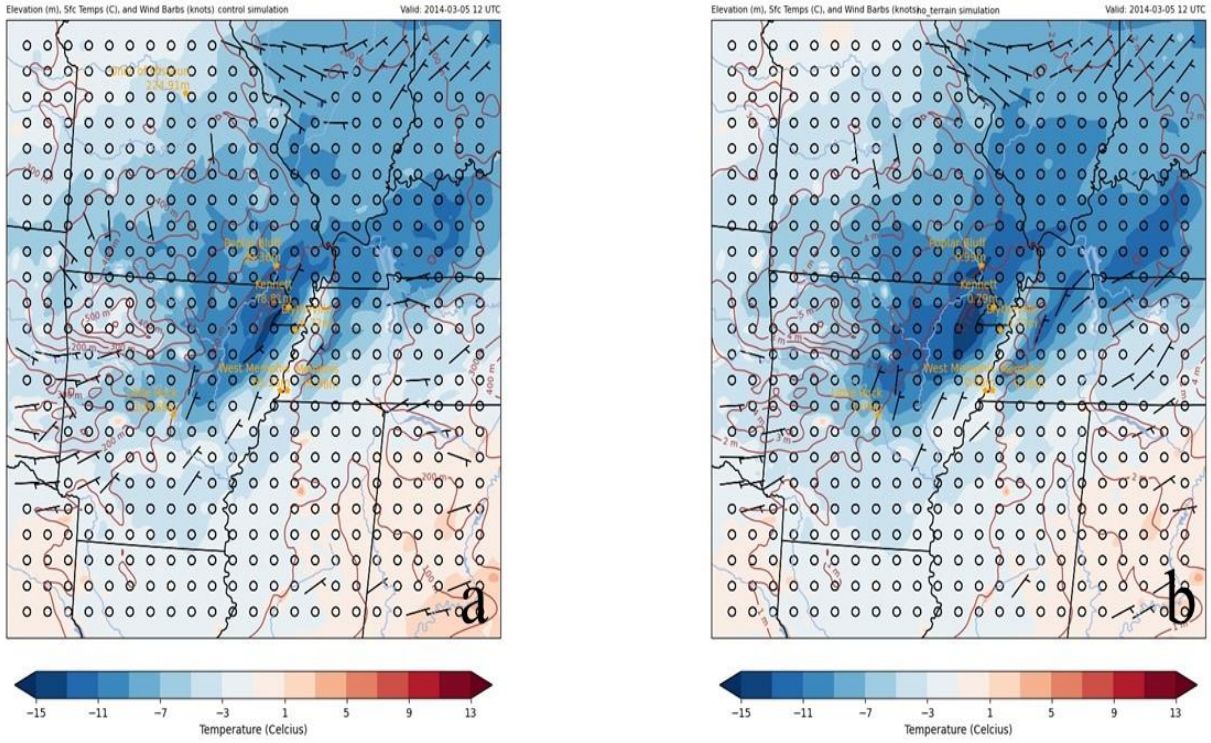

Figure 6.26 - d02 temperature maps from 1200 UTC on 05 March 2014. Each map features surface wind barbs (kts) in black, temperature shaded from blue to red from below -15°C up through 13°C. Topographic lines and values are featured on each map in dark brown.

The no-terrain simulation d03 streamline map (Fig 6.27b) depicted the changeover from the southerly flow to the north to the northeasterly flow to the southeast as the shift in wind direction was evident over where the Ozark Plateau would be (northwest corner of the map) normally. On the actual-terrain simulation map (6.27a) the entirety of the map was northeasterly suggesting the changeover was shifted slightly north by the presence of the Plateau. Deviation again existed on this map where the embedded ridge on the flood plain continued to help direct surface flow around its elevation. This deviation was not apparent on the no-terrain simulation map where streamlines were more organized and uniform across the region of interest.

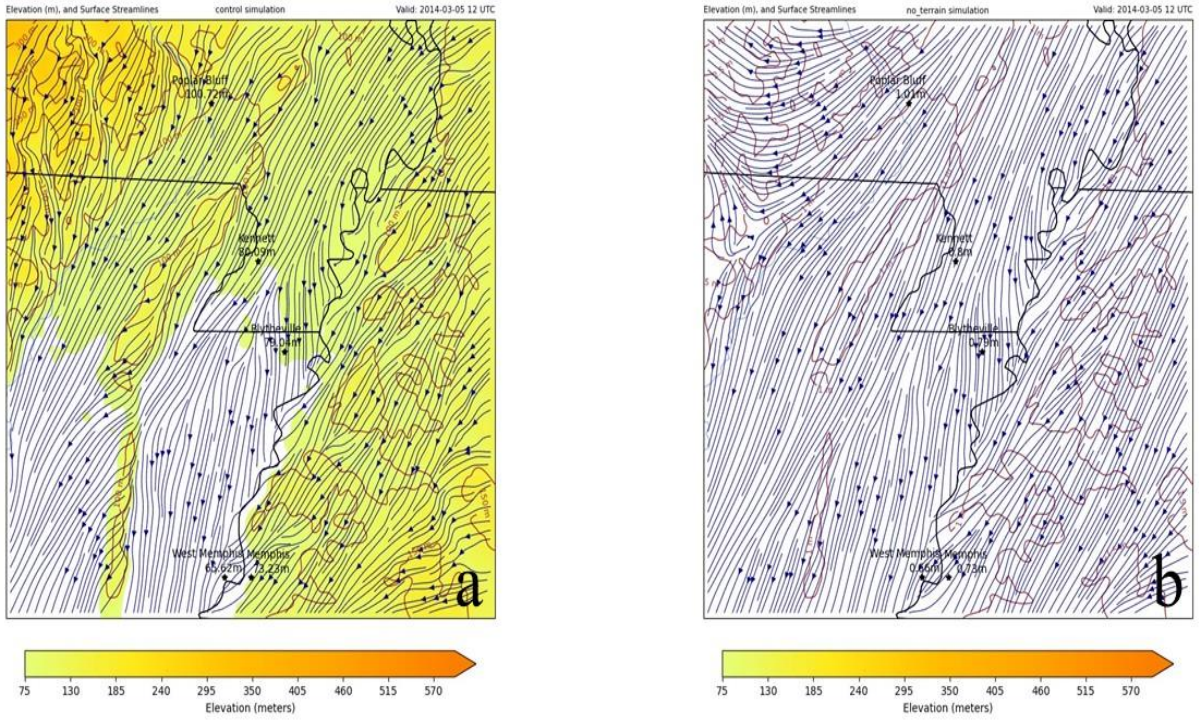

Figure 6.27 - d03 streamline maps from 1200 UTC on 05 March 2014. Map (a) is from the actual-terrain simulation runs. Map (b) is from the no-terrain simulation runs. Surface wind flow streamlines are featured in navy blue on each map. The elevation is shaded from 75 m up through 570 m. Topographic lines are featured in dark brown.

Calm conditions and weak 5-kt flow depicted by wind barbs on the d03 temperature map (Figure 6.28) showed that the flow was weak enough that the smaller ridge seemed to be trapping the coldest air against its southeastern flank as the 10-m wind field bent around the ridge and calm conditions persisted downstream on the actual-terrain simulation map (Fig. 6.28a). The area of coldest temperatures continued to decrease on both maps signaling the erosion of the cold dome of surface air as the cold-air damming event came to an end.

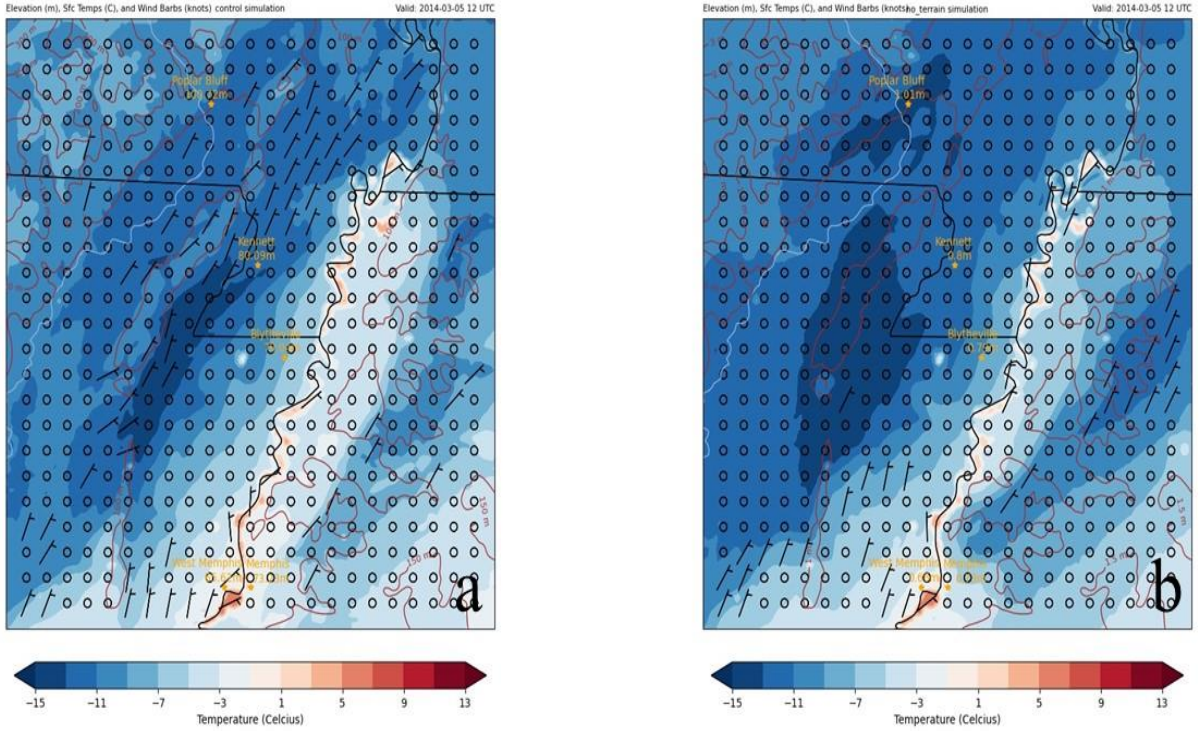

Figure 6.28 - d03 temperature maps from 1200 UTC on 05 March 2014. Each map features surface wind barbs (kts) in black, temperature shaded from blue to red from below -15°C up through 13°C. Topographic lines and values are featured on each map in dark brown.

6.2.2 Actual-Terrain versus Half-Terrain Comparison

Focus shifted to the comparison between the actual-terrain simulation runs and the half-terrain simulation runs. For the half-terrain simulation runs the elevation values within the domains were multiplied by 0.5 effectively cutting the elevation in half. Differences between the 2 simulation runs were more subtle than other comparisons as the actual-terrain and half-terrain simulations contained the 2 closest values for elevation of the 3 comparisons explained here. Analysis of the same time steps evaluated during the actual-terrain-no-terrain comparison (Chapter 6, Section 6.2.1) from the 04 March 2014 are again evaluated here.

6.2.2.1 0000 UTC 04 March 2014

Post-frontal regime 10-m wind streamlines viewed on the 0000 UTC d02 streamline maps (Figure 6.29) dominated the region as the date turned to 04 March 2014. This was like what was viewed in the actual-terrain versus no-terrain simulation comparison. Influence from the parent anticyclone was observed in the region to the north over northeastern Missouri and Illinois where easterly flow presided. Northeasterly flow over the region of interest helped to push cold, moist surface air into the flood plain of eastern Arkansas.

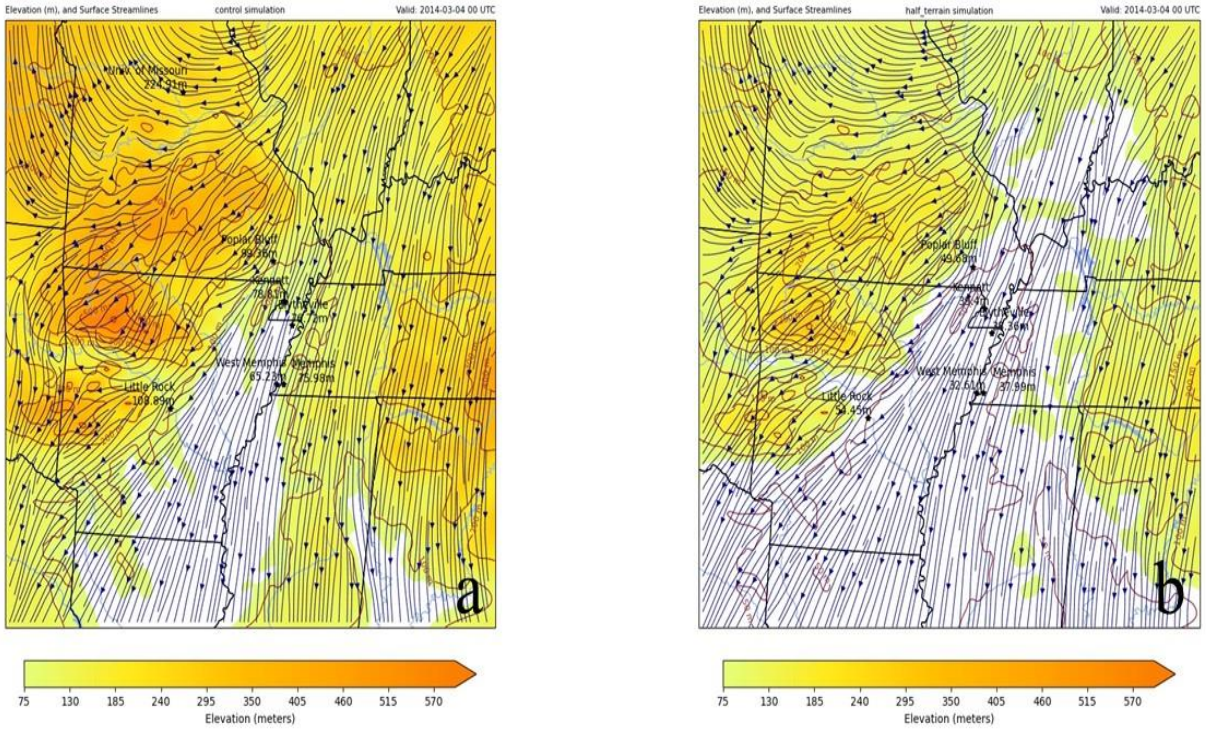

Figure 6.29 - d02 streamline maps from 0000 UTC on 04 March 2014. Map (a) is from the actual-terrain simulation run. Map (b) is from the half-terrain simulation run. Surface wind streamlines are depicted in navy blue on each map. The elevation heights are shaded from 75 m up through 570 m. Topographic lines are shaded in dark brown.

Regional d02 temperature maps (Figure 6.30) from the initial 0000 UTC time step on 04 March 2014 showed how winds within the surface flow of the region were relatively weak with only 5-kt winds as their strongest wind speed components. In certain areas of the maps (including to the north where the parent anticyclonic flow was viewed in the streamline maps of Figure 6.29) calm conditions were expressed by the model simulation runs. Warmer above freezing temperatures existed in the southern extent of the regional maps, while subfreezing temperatures pushed into the region from the north behind the previous days mid-latitude cyclone. Colder temperatures were seen in the region of interest as the northeasterly flow identified previously helped to push cold air into the flood plain. Thus far, the regional maps showed very little contrast between the actual-terrain simulation and the half-terrain simulation runs.

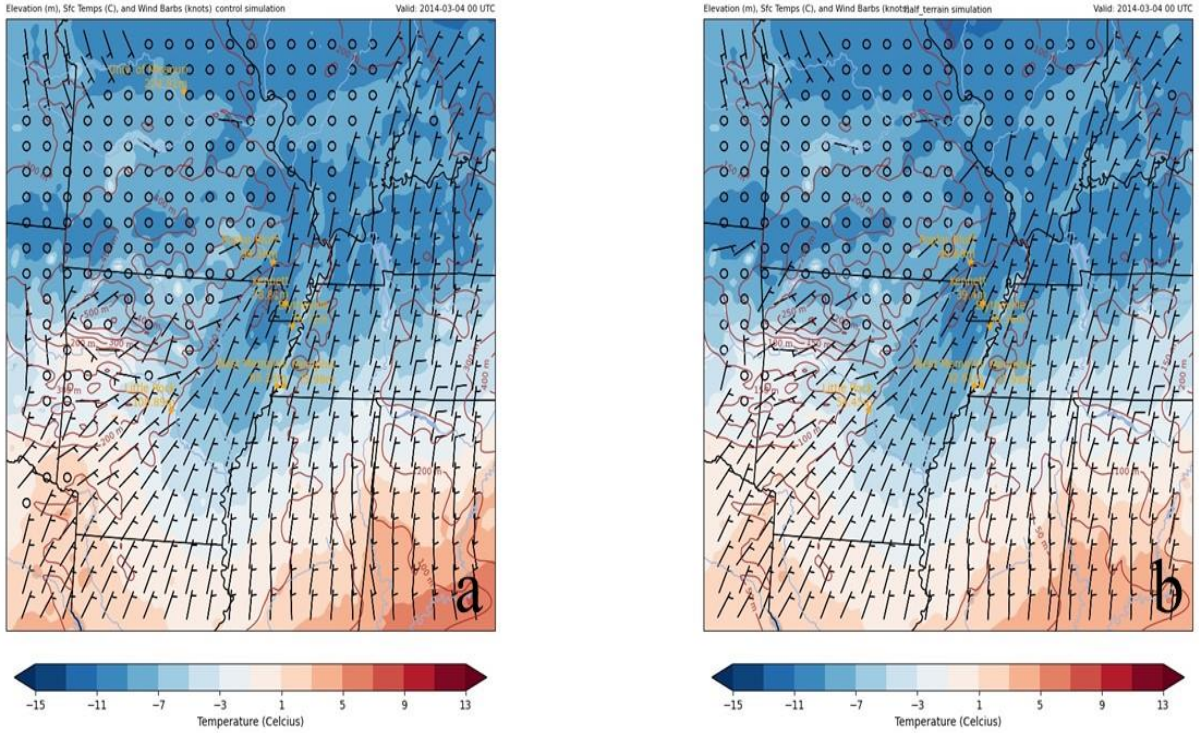

Figure 6.30 - d02 temperature maps from 0000 UTC on 04 March 2014. Each map features surface wind barbs (kts) in black, temperature shaded from blue to red from below -15°C up through 13°C. Topographic lines and values are featured on each map in dark brown.

Focused d03 region of interest streamline maps (Figure 6.31) showed terrain shading in the half-terrain simulation runs (Fig. 6.31b). The northeasterly surface flow observed in the d02 regional map from the same time step (Figure 6.29) dominated these maps with little contrast between the actual-terrain and half-terrain simulation runs. Compared to the no-terrain simulation the streamlines were less uniform especially in the areas adjacent and downstream of the embedded ridge within the flood plain though little difference was noticed between the 2 maps of Figure 6.31. This was most likely due to the lack of wind speed observed in the d02 temperature maps (Figure 6.30) in which wind barbs are plotted and only 5-kt winds were observed in this area. Lack of speed in the surface flow would potentially decrease any deviation seen in the streamline plots of these maps.

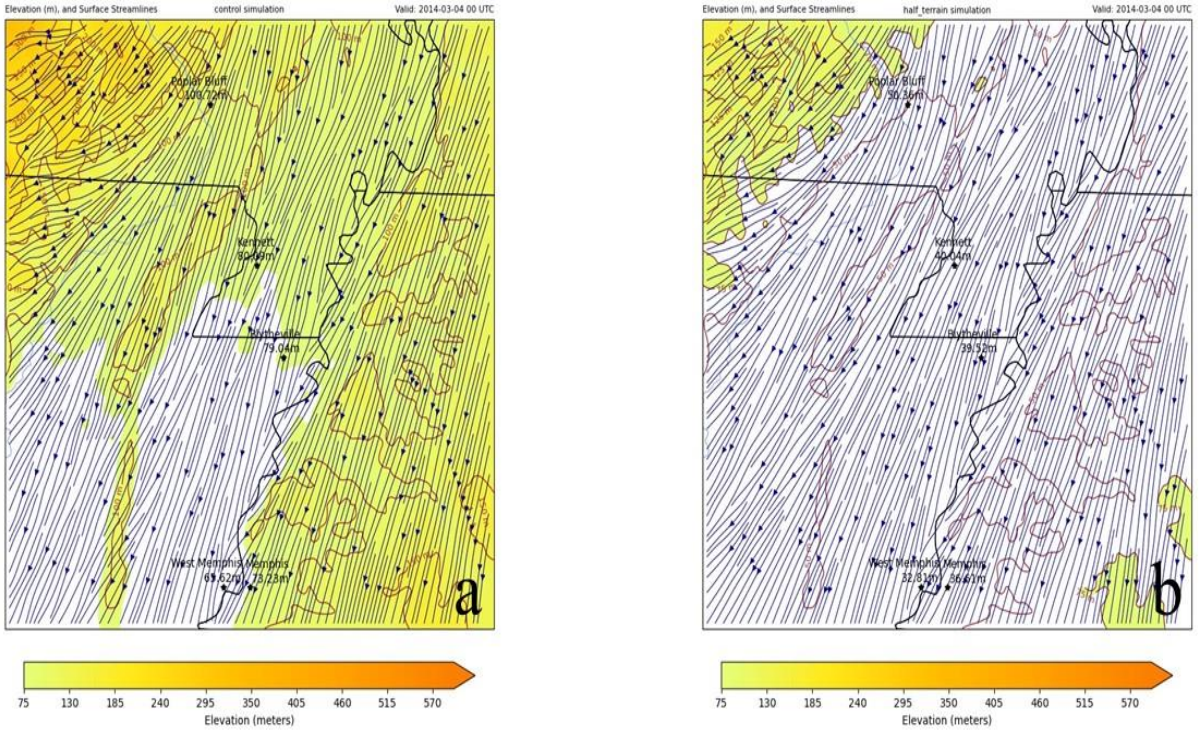

Figure 6.31 - d03 streamline maps from 0000 UTC on 04 March 2014. Map (a) is from the actual-terrain simulation runs. Map (b) is from the half-terrain simulation runs. Surface wind flow streamlines are featured in navy blue on each map. The elevation is shaded from 75 m up through 570 m. Topographic lines are featured in dark brown.

Temperature maps from the same d03 focused region of interest (Figure 6.32) showed the 5-kt winds previously analyzed on regional d02 temperature maps (Figure 6.30) from the same time step. Here the contrast was easily seen in the temperature field. The “channeling effect” of the Ozark Plateau was again observed on the actual-terrain simulation run (Fig. 6.32a). The half-terrain simulation run (Fig. 6.32b) showed more widespread freezing temperatures and colder temperatures locally than its actual-terrain simulation counterpart. Reviewing the actual-terrain-no-terrain comparison, the freezing temperatures in the no-terrain simulations were far more widespread in the d03 temperature analysis from the same time step (Figure 6.4). In the half-terrain simulation, there was more channeling of the freezing temperature down into the flood plain, though not to the extent of what was observed on the actual-terrain simulation run. This channeling view on the half-terrain simulation run in response to damming at the northeastern point of the embedded ridges again adds to the evidence for terrain elevation influence on these cold-air damming events.

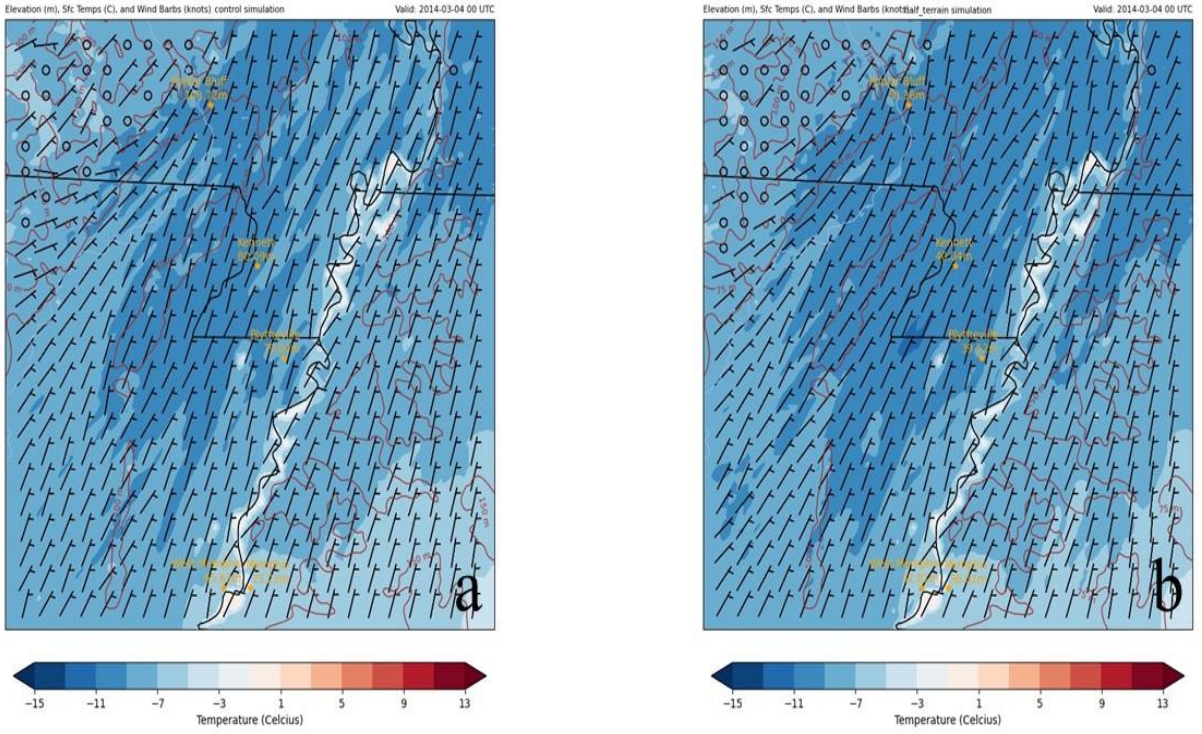

Figure 6.32 - d03 temperature maps from 0000 UTC on 04 March 2014. Each map features surface wind barbs (kts) in black, temperature shaded from blue to red from below -15°C up through 13°C. Topographic lines and values are featured on each map in dark brown.

6.2.2.2 0600 UTC 04 March 2014

Analysis of the actual-terrain and half-terrain simulations continued into the overnight hours of 04 March 2014. A col point in the surface flow streamlines had developed on both maps in the d02 regional streamline comparison (Figure 6.33) to the north of the region of interest over southeastern Missouri. Easterly flow associated with the parent anticyclone continued to slowly migrate to the south pushing the post-frontal wind field slowly away from the area. South of the col point northeasterly surface flow continued over the region of interest.

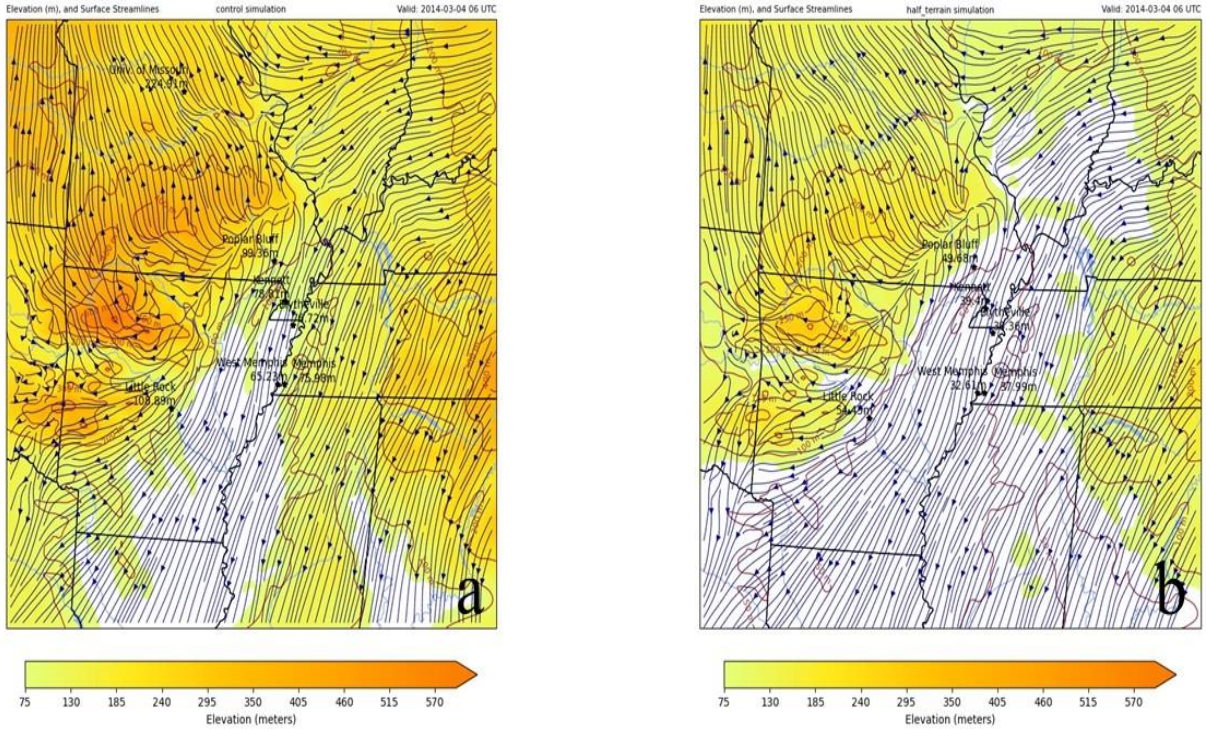

Figure 6.33 - d02 streamline maps from 0600 UTC on 04 March 2014. Map (a) is from the actual-terrain simulation run. Map (b) is from the half-terrain simulation run. Surface wind streamlines are depicted in navy blue on each map. The elevation heights are shaded from 75 m up through 570 m. Topographic lines are shaded in dark brown.

The regional d02 temperature maps (Figure 6.34), like the previous comparison, showed the effect of diurnal processes on the temperature field now that the sun had fallen below the horizon for several hours. The temperature gradient was easily seen on both simulation maps of the temperature comparison as the temperature fell significantly from south to north. The coldest temperatures were found in the region of interest and stretched to the east and west in a narrow band across the half-terrain simulation (Fig. 6.34b). The actual-terrain simulation (Fig. 6.34a) did not feature the same band of coldest temperatures but did keep the coldest surface air entrenched in the flood plain of eastern Arkansas. The wind field on both maps was unchanged from the previous time step with weak 5-kt northeasterly winds in the region of interest and calmer conditions over much of the region.

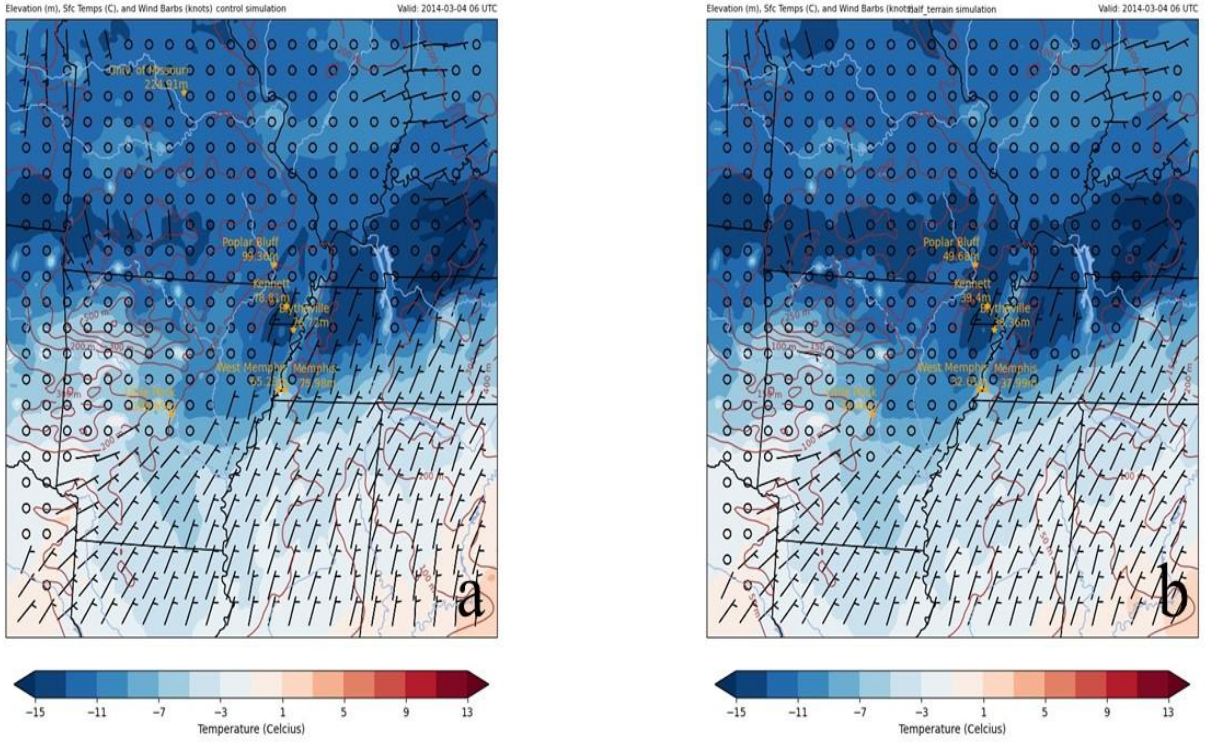

Figure 6.34 - d02 temperature maps from 0600 UTC on 04 March 2014. Each map features surface wind barbs (kts) in black, temperature shaded from blue to red from below -15°C up through 13°C. Topographic lines and values are featured on each map in dark brown.

A closer focus on the d03 streamline maps (Figure 6.35) highlighted the northeasterly surface flow seen on the previous regional streamline map. There was more deviation around the embedded ridge within the flood plain on the actual-terrain simulation map (Fig. 6.35a) than what was observed on the half-terrain simulation map (Fig. 6.35b). On the half-terrain simulation there was deviation, but not as pronounced as what was observed on its actual-terrain simulation counterpart.

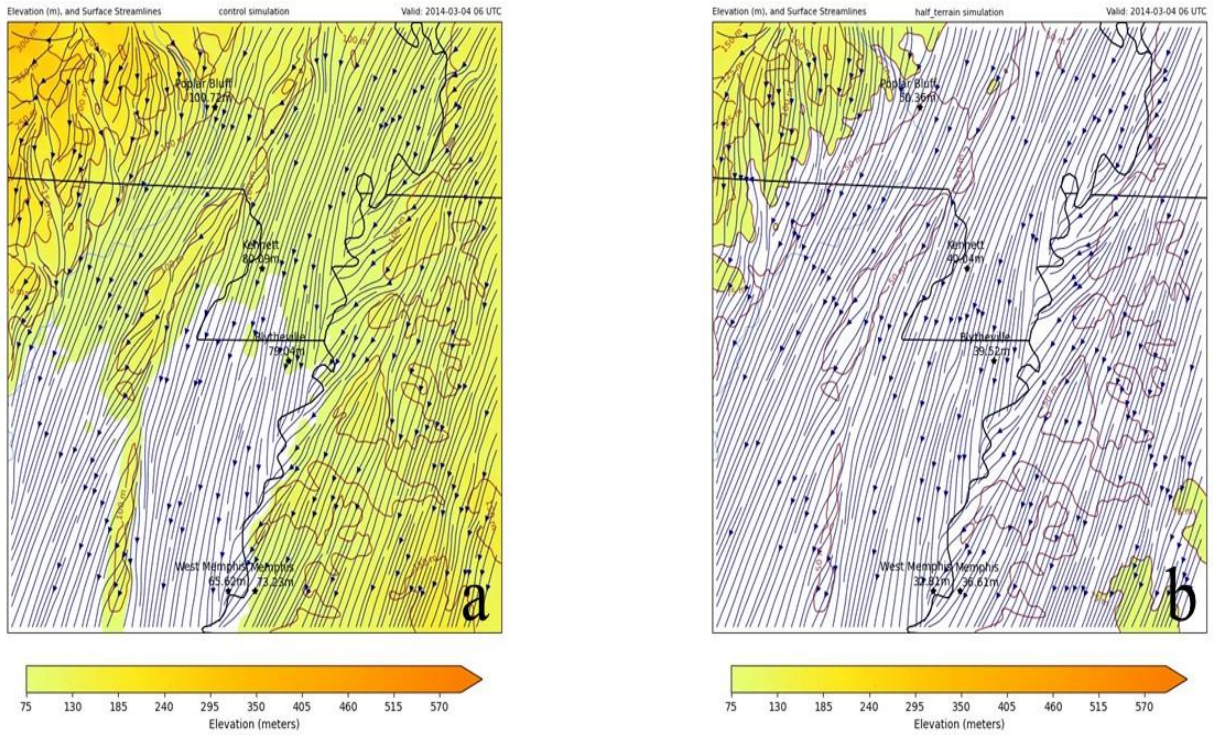

Figure 6.35 - d03 streamline maps from 0600 UTC on 04 March 2014. Map (a) is from the actual-terrain simulation runs. Map (b) is from the half-terrain simulation runs. Surface wind flow streamlines are featured in navy blue on each map. The elevation is shaded from 75 m up through 570 m. Topographic lines are featured in dark brown.

The actual-terrain simulation d03 temperature map (Fig 6.36a) at 0600 UTC on 04 March 2014 featured the coldest surface air entrenched in the flood plain over the bootheel of Missouri and down into northeastern Arkansas between the embedded ridge west of the Blytheville, Arkansas station and the Mississippi River. The half-terrain simulation map showed the coldest temperatures in that area as well but extended the coldest temperatures much further north into southeastern Missouri. East of the Mississippi River 5-kn northeasterly winds were present, while to the west of the river only the area between the Plateau and the river contained the same northeasterly winds. Other areas on both simulation maps were experiencing calm conditions.

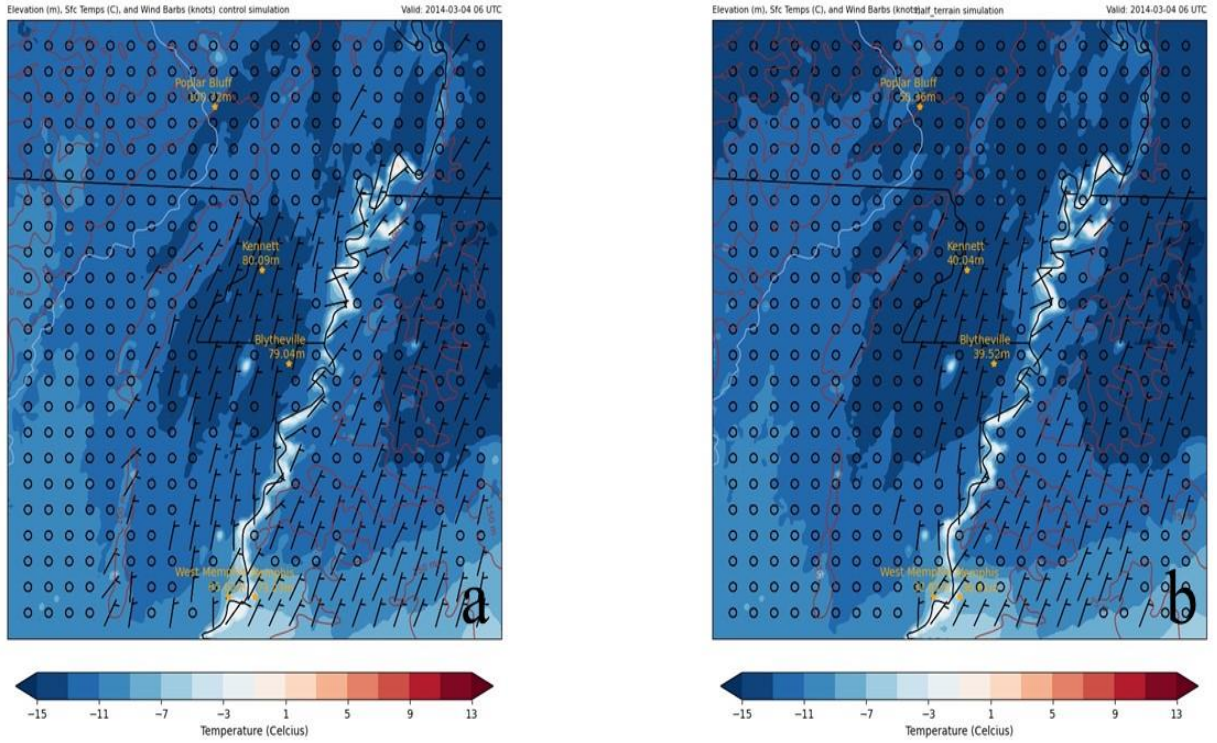

Figure 6.36 - d03 temperature maps from 0600 UTC on 04 March 2014. Each map features surface wind barbs (kts) in black, temperature shaded from blue to red from below -15°C up through 13°C. Topographic lines and values are featured on each map in dark brown.

6.2.2.3 1200 UTC 04 March 2014

As the sun rose at 1200 UTC on 04 March 2014 the d02 streamline maps (Figure 6.37) from that time step showed the col point in the streamline flow had shifted to the east over Illinois. The influence of the parent anticyclone shifted to the south as the northeasterly flow over the region of interest continued. The diverging line between the southerly flow to the north and northerly flow to the south had set up over the Ozark Plateau in southern Missouri.

Figure 6.37 - d02 streamline maps from 1200 UTC on 04 March 2014. Map (a) is from the actual-terrain simulation run. Map (b) is from the half-terrain simulation run. Surface wind streamlines are depicted in navy blue on each map. The elevation heights are shaded from 75 m up through 570 m. Topographic lines are shaded in dark brown.

Coldest temperatures on the d02 temperature maps (Figure 6.38) were again observed at 1200 UTC time step due to diurnal processes just before sunrise. More widespread freezing temperatures were again observed on the half-terrain simulation map (Fig. 6.38b) with warmer conditions to the south. Both maps featured 5-kt northeasterly winds in the southeastern half of the regional maps and southerly 5-kt winds over central Missouri with calm conditions over the Ozark Plateau. The calm northeasterly flow over the region of interest helped to continue pushing cold surface air into the area causing the freezing temperatures to channel into the flood plain from the north-northeast.

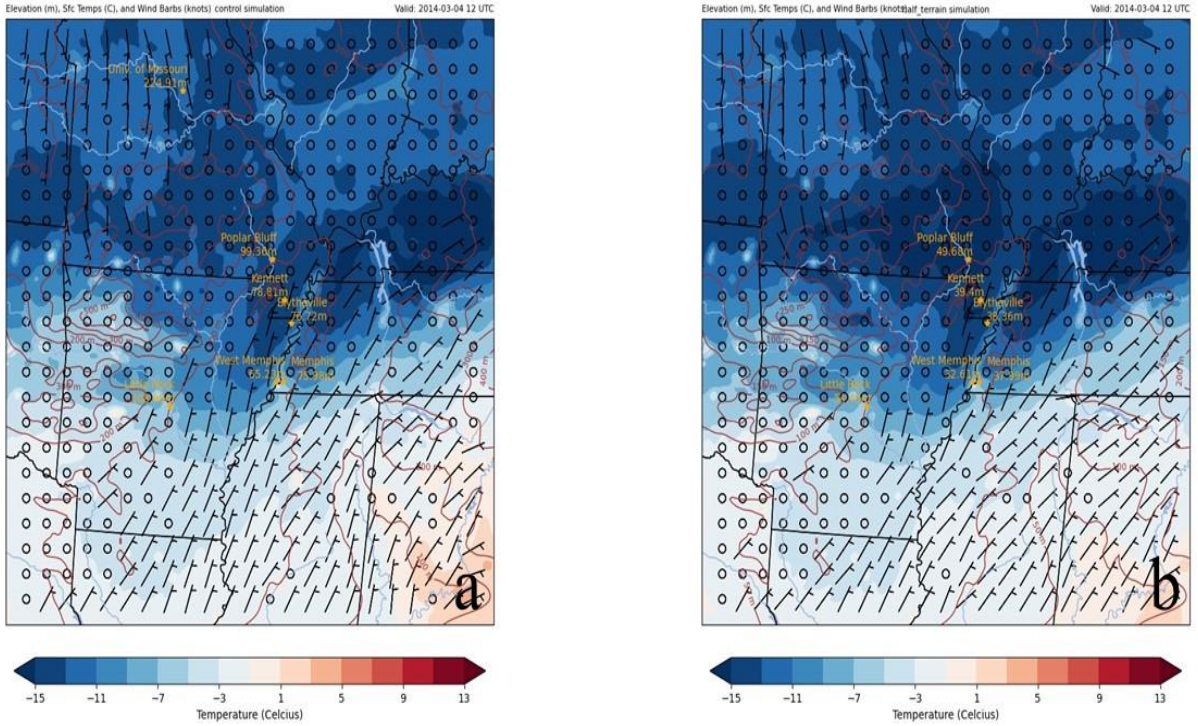

Figure 6.38 - d02 temperature maps from 1200 UTC on 04 March 2014. Each map features surface wind barbs (kts) in black, temperature shaded from blue to red from below -15°C up through 13°C. Topographic lines and values are featured on each map in dark brown.

While 10-m wind streamlines observed on the d03 region of interest maps (Figure 6.39) were for the most part northeasterly through the area, the influence of the parent anticyclone was observed in the northeastern quadrant of both simulation maps. Easterly flow had begun to slowly make its way into the region of interest and promoted terrain-orthogonal flow in the region of interest as day broke on 04 March 2014. The same pattern of deviation over the ridge just west of Blytheville, Arkansas continued on the actual-terrain simulation map (6.39a) with only slight deviation observed on the half-terrain simulation map (6.39b).

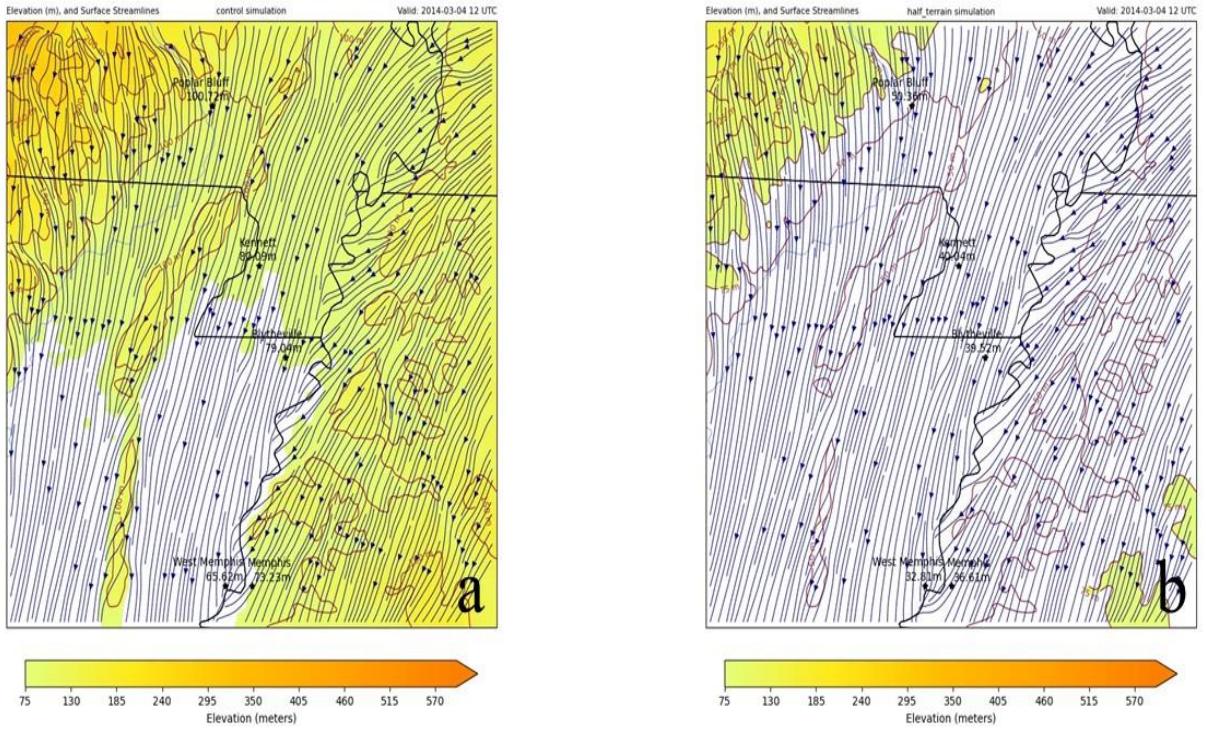

Figure 6.39 - d03 streamline maps from 1200 UTC on 04 March 2014. Map (a) is from the actual-terrain simulation runs. Map (b) is from the half-terrain simulation runs. Surface wind flow streamlines are featured in navy blue on each map. The elevation is shaded from 75 m up through 570 m. Topographic lines are featured in dark brown.

Winds on the d03 temperature maps (Figure 6.40) also indicated the beginning of the shift to a more easterly course for 10-m winds in the region of interest as the parent anticyclone pushed its southern flank into the Midsouth. The coldest temperatures observed in the area resided just west of the Blytheville, Arkansas and Kennett, Missouri stations on the half-terrain simulation (Fig. 6.40b). Like what had been observed previously, there was some channeling of the cold air into the flood plain on the half-terrain simulation map, but more so on the actual-terrain simulation map (Fig. 6.40a) indicating the influence of terrain elevation with larger values.

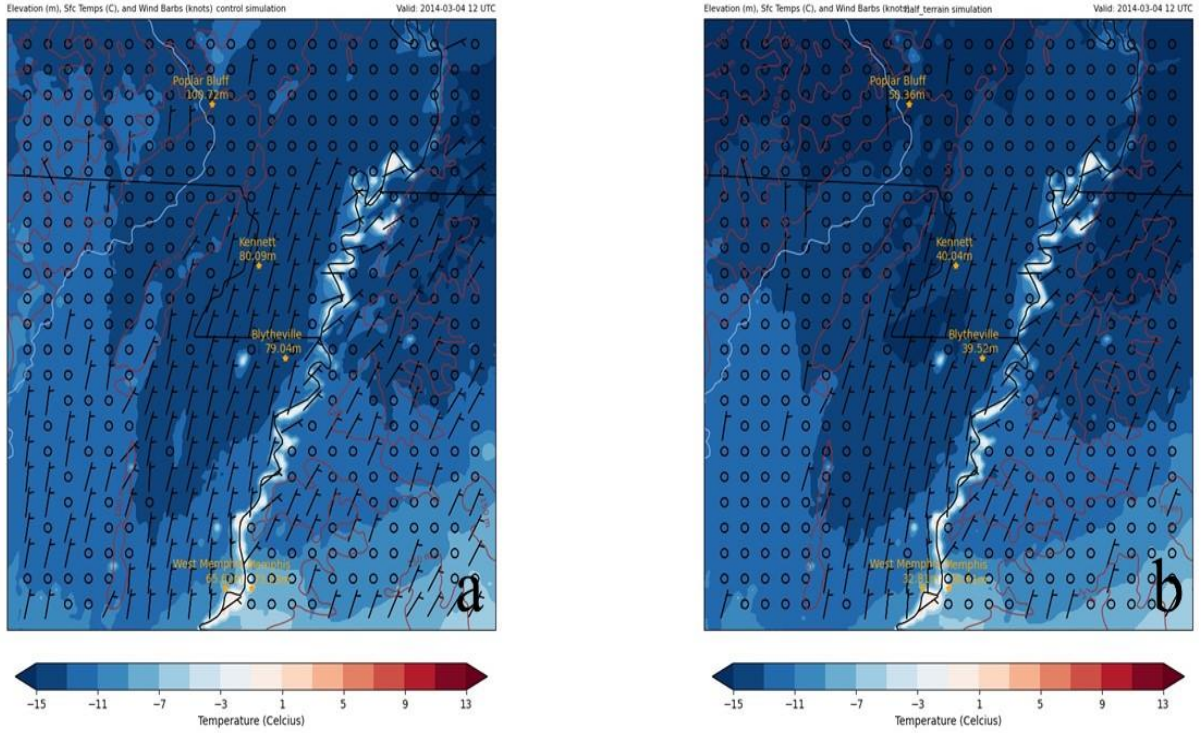

Figure 6.40 - d03 temperature maps from 1200 UTC on 04 March 2014. Each map features surface wind barbs (kts) in black, temperature shaded from blue to red from below -15°C up through 13°C. Topographic lines and values are featured on each map in dark brown.

6.2.2.4 1800 UTC 04 March 2014

The 6-hour time progression showed the most aggressive shift in wind direction as viewed on the d02 regional streamlines maps (Figure 6.41) at 1800 UTC on 04 March 2014. By midday, easterly flow presided over the eastern half of the regional maps including the region of interest in eastern Arkansas. The southwestern edge of the high-pressure center to the northeast was easily identified on both simulation maps as the easterly flow over the region of interest quickly turned southerly as streamlines accelerated over the Ozark Plateau.

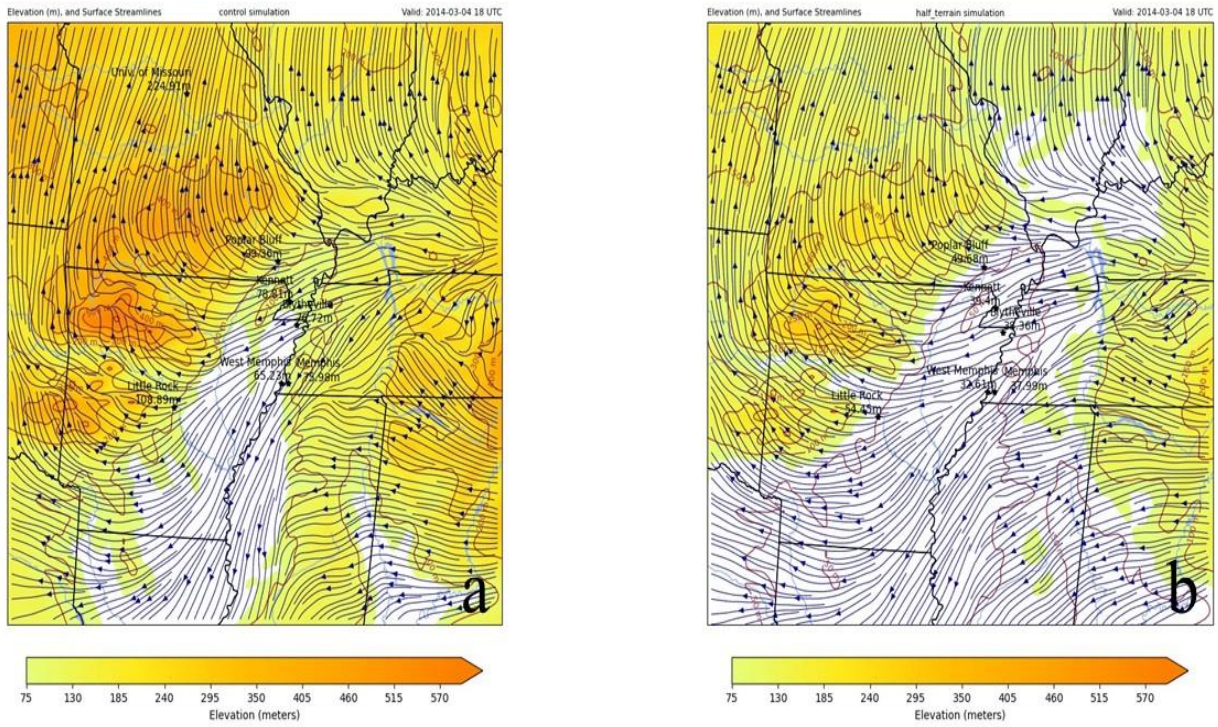

Figure 6.41 - d02 streamline maps from 1800 UTC on 04 March 2014. Map (a) is from the actual-terrain simulation run. Map (b) is from the half-terrain simulation run. Surface wind streamlines are depicted in navy blue on each map. The elevation heights are shaded from 75 m up through 570 m. Topographic lines are shaded in dark brown.

The d02 temperature maps (Figure 6.42) of the 1800 UTC 04 March 2014 time step depicted a significant warming of temperatures in the region including western Arkansas and central Tennessee. However, along that same latitude in northeastern Arkansas temperatures remained just below freezing in the region of interest. Little contrast was observed between the simulation maps save for some differences in temperature values in both warm and cold temperature extremes within the temperature field. Calm conditions were experienced over much of the region save for the region of interest where weak 5-kt easterly flow was observed over area around the Blytheville, Arkansas station. This was the strongest evidence thus far for cold-air damming as the weak surface flow was being deterred by the Ozark Plateau as observed on both simulation maps.

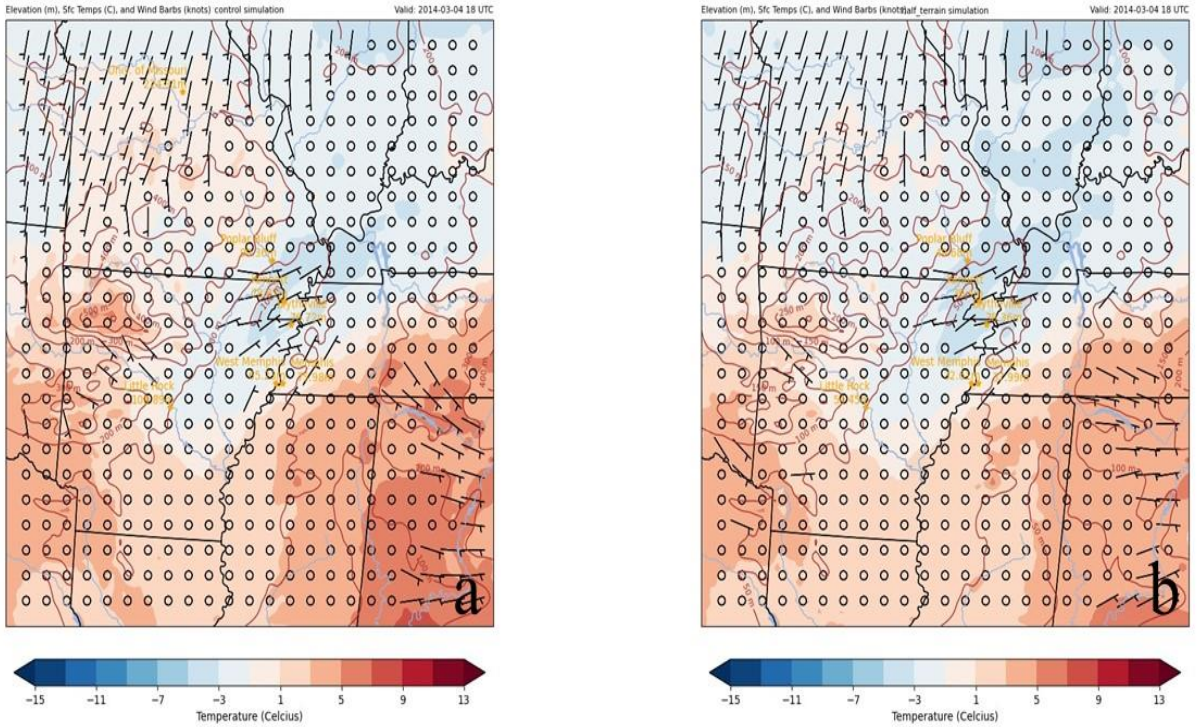

Figure 6.42 - d02 temperature maps from 1800 UTC on 04 March 2014. Each map features surface wind barbs (kts) in black, temperature shaded from blue to red from below -15°C up through 13°C. Topographic lines and values are featured on each map in dark brown.

The shift to a mainly easterly flow over the region of interest was evident on both simulation maps of the d03 streamline maps (Figure 6.43) from 1800 UTC on 04 March 2014. Little contrast between the simulation runs was viewed on each map even with the directional shift in the surface flow streamlines. The easterly shift seemed to have decreased deviation in the streamlines across the embedded ridge on both simulation maps. The southern flank of the parent anticyclone was also evident as the streamlines turn to a more southeasterly course as the 10-m wind flow oriented towards the escarpment of the Ozark Plateau.

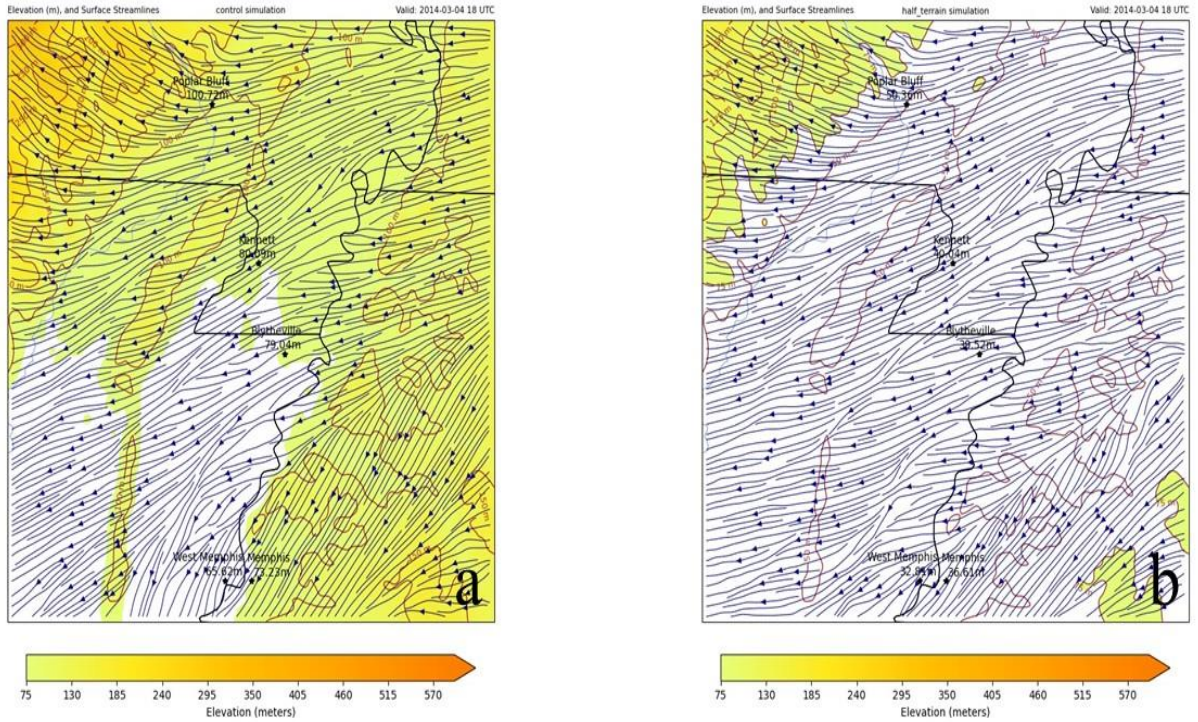

Figure 6.43 - d03 streamline maps from 1800 UTC on 04 March 2014. Map (a) is from the actual-terrain simulation runs. Map (b) is from the half-terrain simulation runs. Surface wind flow streamlines are featured in navy blue on each map. The elevation is shaded from 75 m up through 570 m. Topographic lines are featured in dark brown.

The pattern of channeled below-freezing temperatures on the d03 temperature actual-terrain simulation map (6.44a) continued at 1800 UTC on 04 March 2014. Again, the below-freezing temperatures on the half-terrain simulation were much more spread out further north into Missouri and Illinois (Fig. 6.44b). Winds were consistent on both simulation maps with weak easterly flow observed over the region bolstering the cold-air damming theory. Even on the half-terrain simulation map the coldest air did not infiltrate the Plateau even when the elevation was half of its true value.

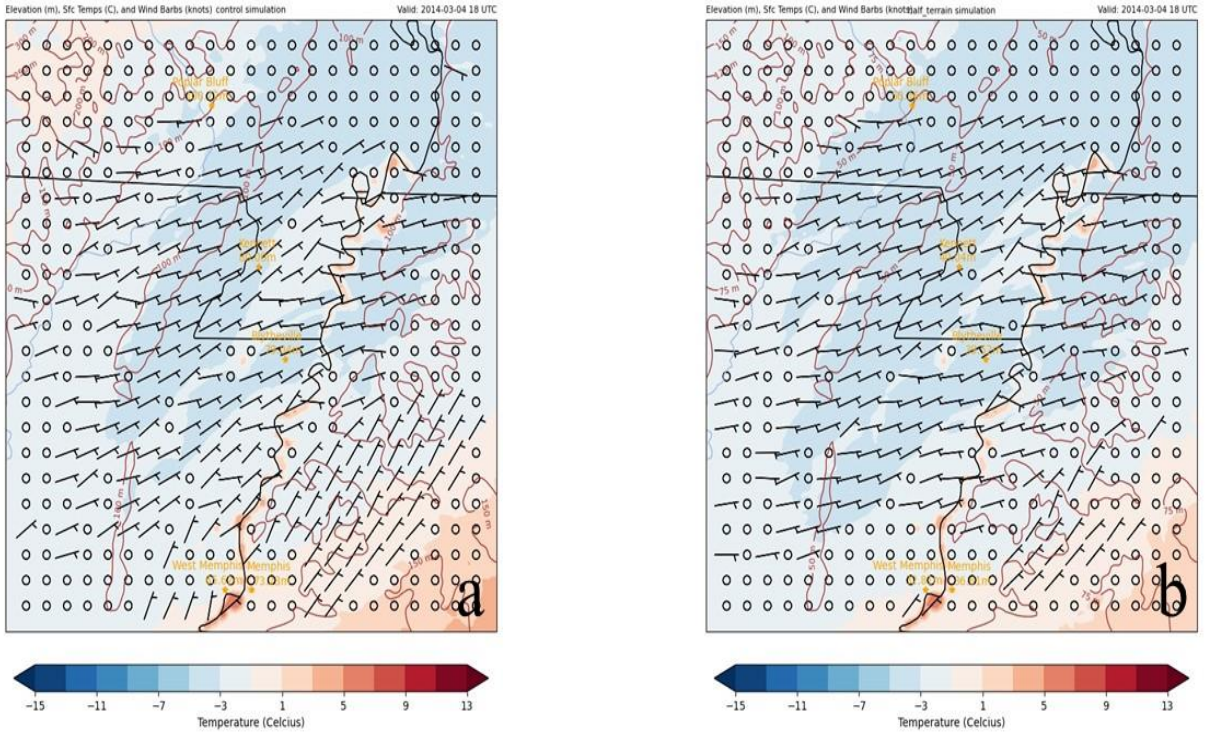

Figure 6.44 - d03 temperature maps from 1800 UTC on 04 March 2014. Each map features surface wind barbs (kts) in black, temperature shaded from blue to red from below -15°C up through 13°C. Topographic lines and values are featured on each map in dark brown.

6.2.2.5 0000 UTC 05 March 2014

As the sun set and the date transitioned to 05 March, the d02 regional streamline maps (Figure 6.45) continued terrain-orthogonal flow as the parent anticyclones southern flank dominated surface flow streamlines over much of both simulation maps. In the region of interest, the directional shift continued as a more southeasterly flow was observed. Any surface cold air within the flood plain of eastern Arkansas was being forced up against the escarpment of the Ozark Plateau.

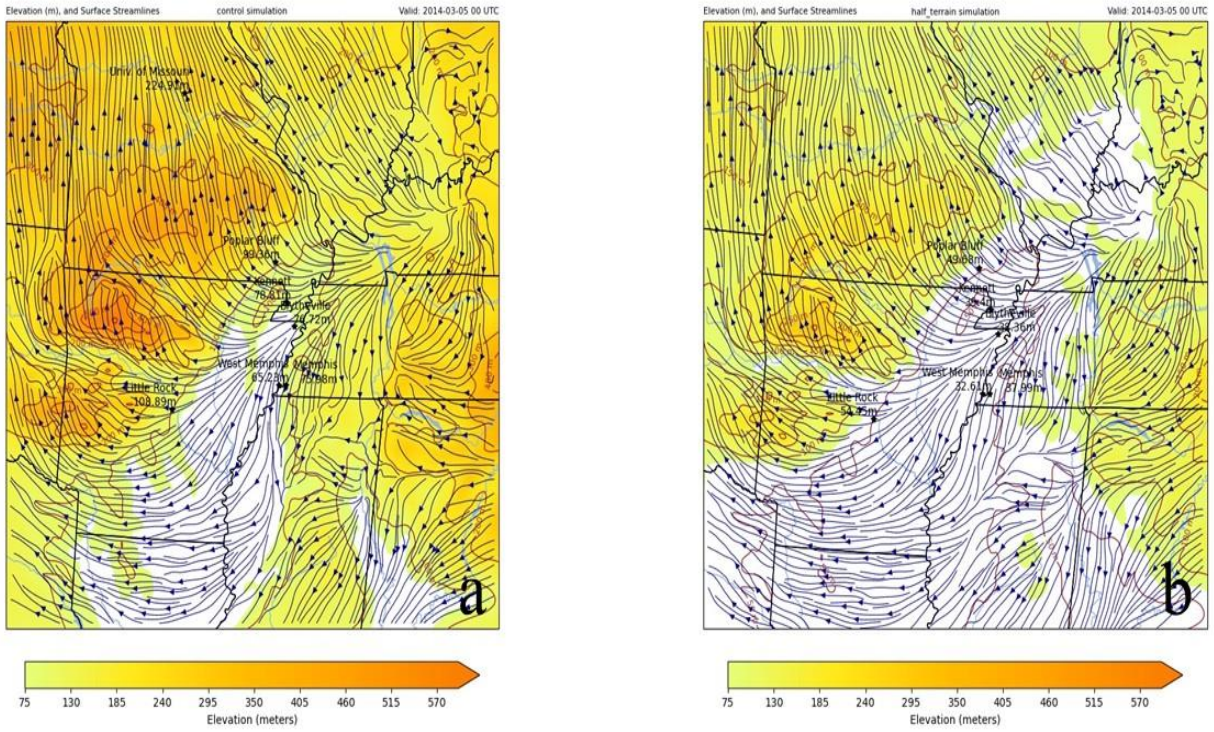

Figure 6.45 - d02 streamline maps from 0000 UTC on 05 March 2014. Map (a) is from the actual-terrain simulation run. Map (b) is from the half-terrain simulation run. Surface wind streamlines are depicted in navy blue on each map. The elevation heights are shaded from 75 m up through 570 m. Topographic lines are shaded in dark brown.

The temperature field and its gradients on the 0000 UTC 05 March 2014 d02 temperature maps (Figure 6.46) were similar comparing the actual-terrain and half-terrain simulation maps. Warmer temperatures in the southern extent of both maps transitioned to colder air further north with a distinct cold dome of surface air directly over the region of interest. The wind field was calmer on the half-terrain simulation (Fig. 6.46b) with fewer 5-kt wind barbs observed and much of the region under calm conditions. The actual-terrain simulation (Fig. 6.46a) contained a few more 5-kt wind barbs, specifically over eastern Missouri and northwestern Arkansas.

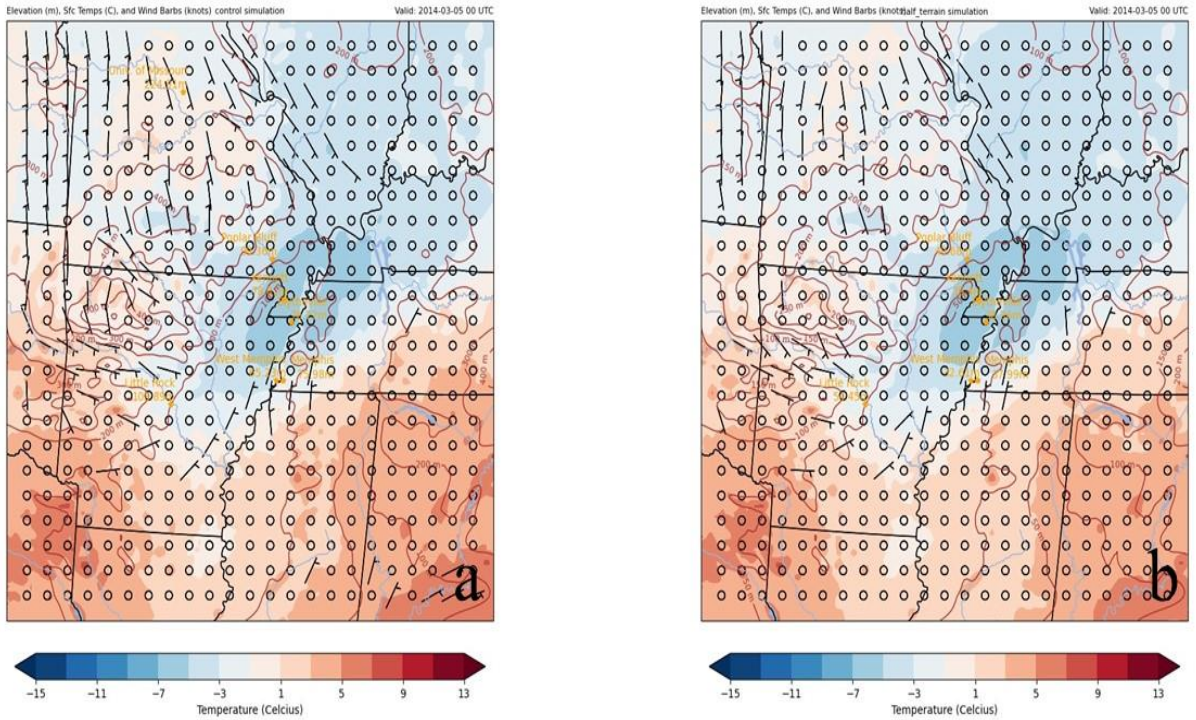

Figure 6.46 - d02 temperature maps from 0000 UTC on 05 March 2014. Each map features surface wind barbs (kts) in black, temperature shaded from blue to red from below -15°C up through 13°C. Topographic lines and values are featured on each map in dark brown.

A closer focus on streamlines in the region of interest highlighted the directional shift to a more southeasterly surface flow in the d03 streamlines maps (Figure 6.47). Surface flow on both simulation maps was perpendicular to the southeastern flank of the Ozark Plateau. The only minor differences in deviation over the embedded ridges in the flood plain could be found in the contrast between the actual-terrain simulation streamlines over the ridge, (Fig. 6.47a) and its half-terrain simulation counterpart (Fig. 6.47b).

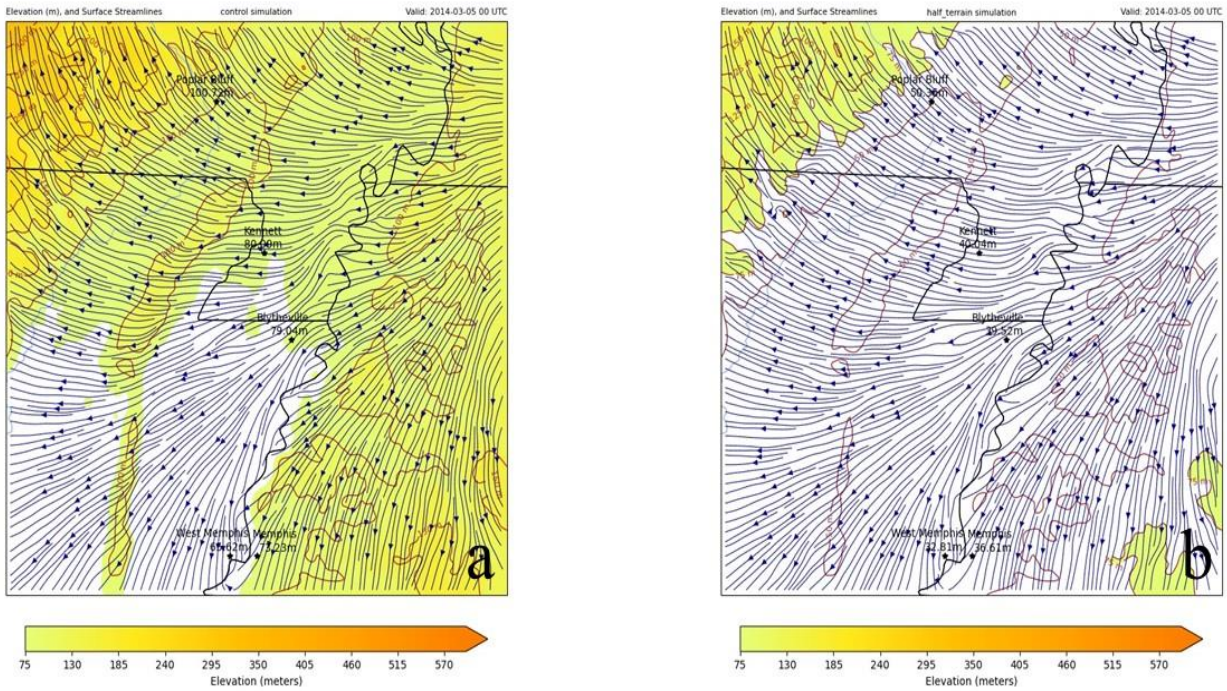

Figure 6.47 - d03 streamline maps from 0000 UTC on 05 March 2014. Map (a) is from the actual-terrain simulation runs. Map (b) is from the half-terrain simulation runs. Surface wind flow streamlines are featured in navy blue on each map. The elevation is shaded from 75 m up through 570 m. Topographic lines are featured in dark brown.

While some channeling of colder temperatures into the flood plain was occurring on the d03 temperature maps (Figure 6.48) for this time step, the lack of wind speed through the region of interest was the difference between 0000 UTC on 05 March 2014 and previous analyzed time steps. Predominantly calm conditions over the region of interest helped to limit the channeling effect on the cold temperatures seen previously, allowing the cold pool of surface air to spread out within the flood plain. The escarpment of Plateau continued to act as a barrier (especially considering the orthogonal streamline flow seen previously) even though the temperature field on both simulation maps contained little contrast between the actual-terrain and half-terrain simulations.

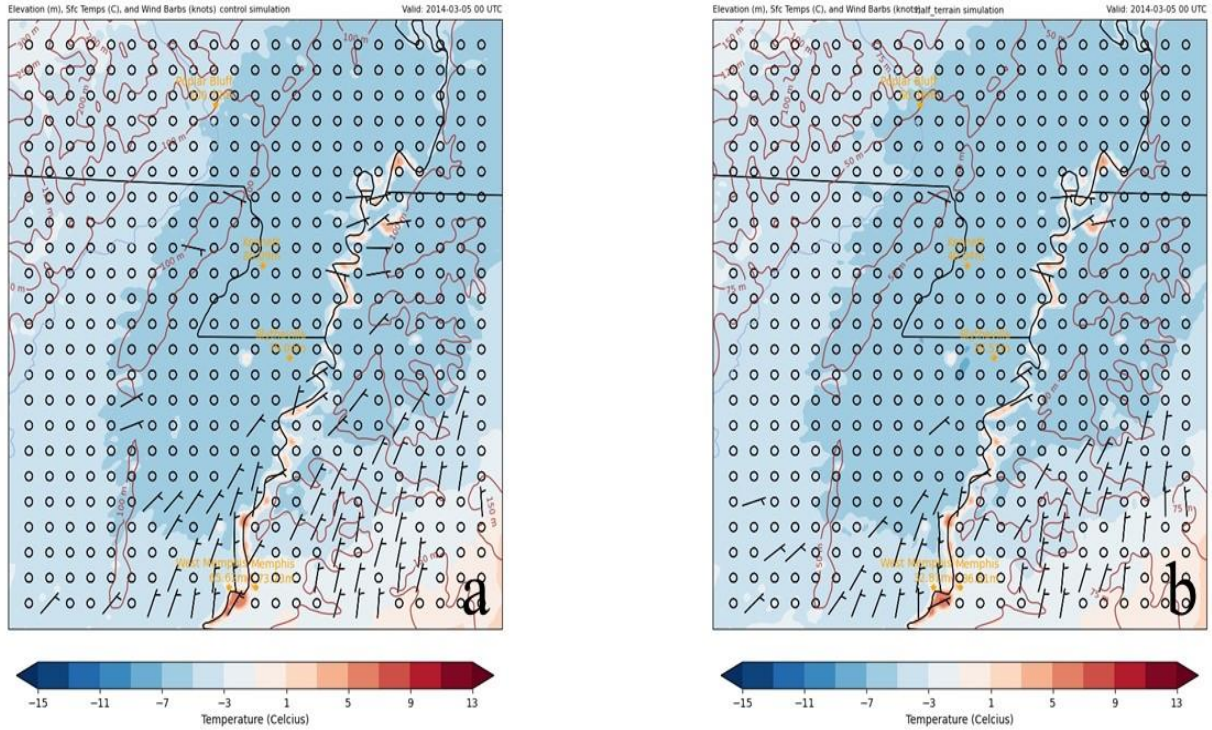

Figure 6.48 - d03 temperature maps from 0000 UTC on 05 March 2014. Each map features surface wind barbs (kts) in black, temperature shaded from blue to red from below -15°C up through 13°C. Topographic lines and values are featured on each map in dark brown.

6.2.2.6 0600 UTC 05 March 2014

Analysis continued into the second night of the actual-terrain versus half-terrain comparison. The d02 regional streamline maps (Figure 6.49) from 0600 UTC on 05 March 2014 resolved a bisecting 10-m wind flow pattern over the region of interest along the escarpment of the Ozark Plateau just to the northeast of the flood plain. Streamlines to the north over the Plateau remained southerly while on the other side of the divergent line the surface flow over the region of interest returned to a northeasterly course. This was most likely due to a weak wind field across the region though at this point this was an inference and needed further analysis of maps from this time step.

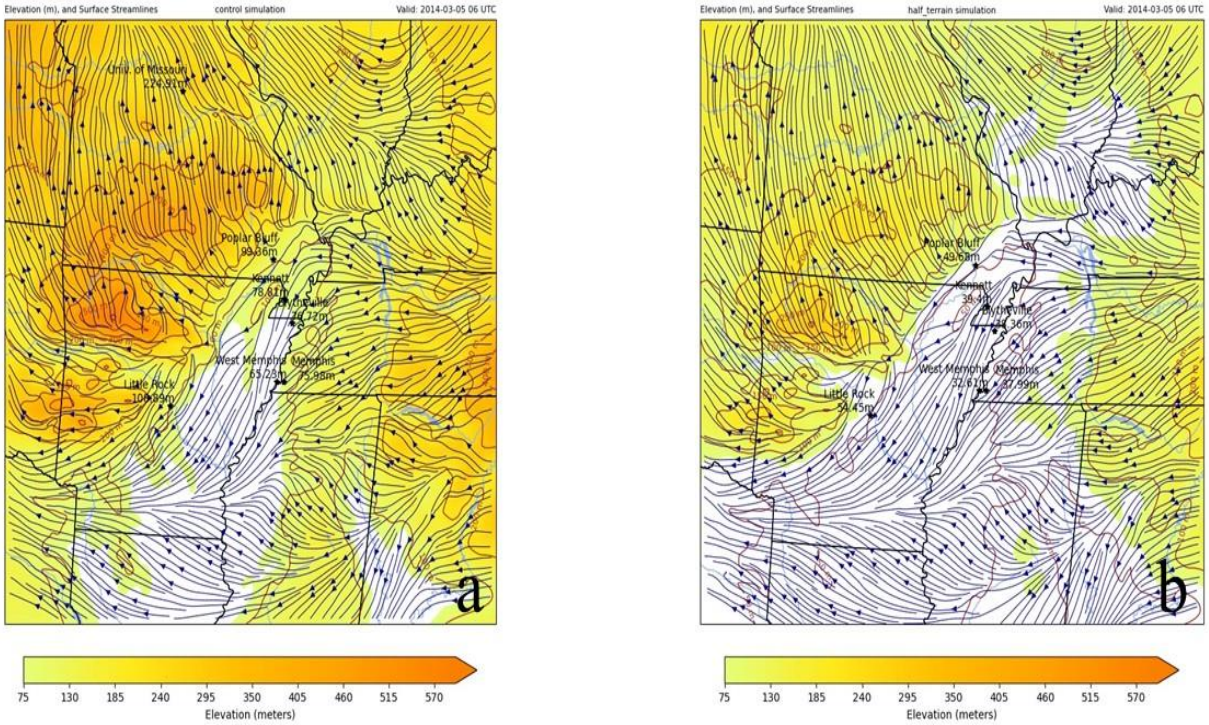

Figure 6.49 - d02 streamline maps from 0600 UTC on 05 March 2014. Map (a) is from the actual-terrain simulation run. Map (b) is from the half-terrain simulation run. Surface wind streamlines are depicted in navy blue on each map. The elevation heights are shaded from 75 m up through 570 m. Topographic lines are shaded in dark brown.

The d02 regional temperature maps (Figure 6.50) from this time step did not regress back to the temperatures observed the previous night. This was consistent with the previous comparative analysis. The wind field was calm across the region save for some weak 5-kt winds near the Mississippi River and to the north over the Ozark Plateau in Missouri. The cold pool of air over the region of interest remained on both simulation maps with a little more widespread cold temperatures extending further east into Kentucky and Tennessee on the half-terrain simulation map (Fig. 6.50b).

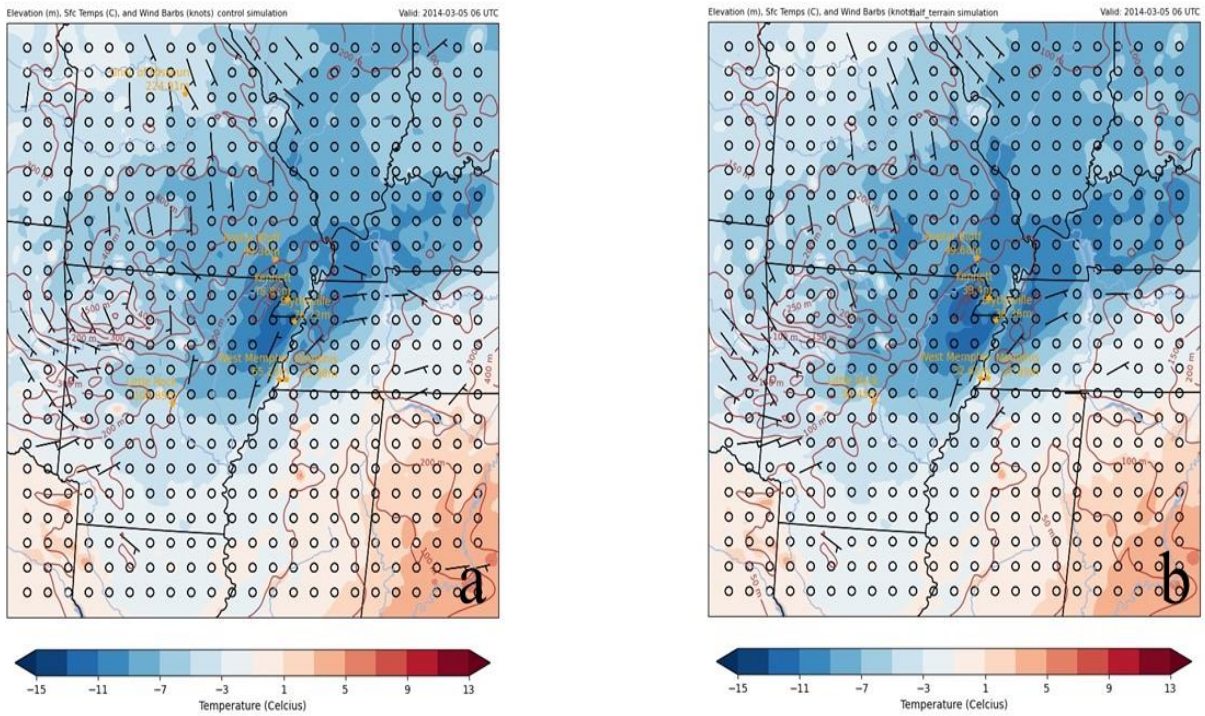

Figure 6.50 - d02 temperature maps from 0600 UTC on 05 March 2014. Each map features surface wind barbs (kts) in black, temperature shaded from blue to red from below -15°C up through 13°C. Topographic lines and values are featured on each map in dark brown.

The focused d03 streamline maps (Figure 6.51) showed the presence of a convergence line and a divergence line in the surface flow streamline pattern within the flood plain. The WRF model resolved the converging line running parallel to the escarpment of the Ozark Plateau just to the east. Here the northerly flow over the Plateau converged with east-northeasterly flow just west of the embedded ridge. This was observed on both actual-terrain and half-terrain simulation maps with little contrast. The diverging line was placed by the model just east of the embedded ridge where flow over the ridge was more easterly while to the east of the line the streamlines turned more northerly. The flow was less organized over the embedded ridge on the actual-terrain simulation map (Fig. 6.51a). Streamlines over the half-terrain simulated ridge are more organized and uniform as they traverse over the elevation. This contrast between the 2 simulation maps was yet another indication of terrain elevation influence.

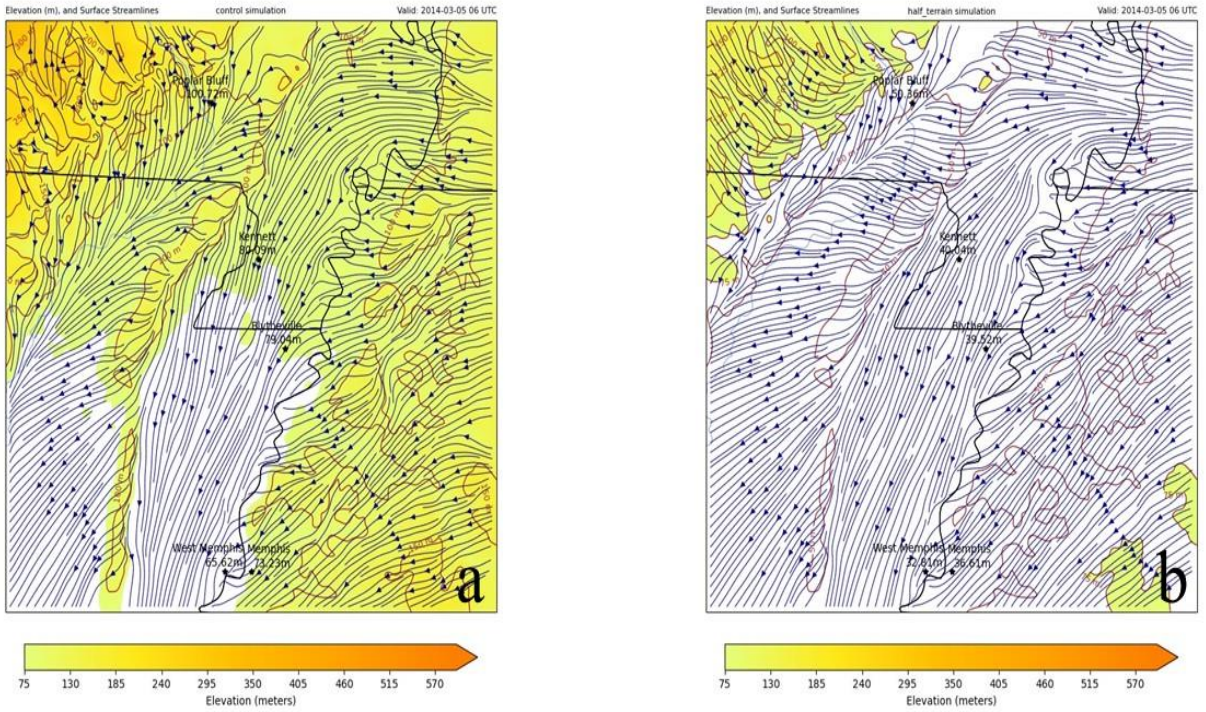

Figure 6.51 - d03 streamline maps from 0600 UTC on 05 March 2014. Map (a) is from the actual-terrain simulation runs. Map (b) is from the half-terrain simulation runs. Surface wind flow streamlines are featured in navy blue on each map. The elevation is shaded from 75 m up through 570 m. Topographic lines are featured in dark brown.

Calm conditions over the region of interest on the d03 temperature maps (Figure 6.52) where the converging and diverging lines resided on the d03 streamline maps (Figure 6.53) inferred a more variable 10-m wind flow than what was resolved on the streamline maps. Due to calm wind conditions in the stable surface layer the model may have had trouble resolving actual realistic streamline flow. The coldest temperatures on each map resided in northeastern Arkansas just east of the embedded ridge on the actual-terrain simulation. (Fig. 6.52a) Cold temperatures also were found across the ridge and into the flood plain between the ridge and the Plateau on the half-terrain simulation map (Fig. 6.52b).

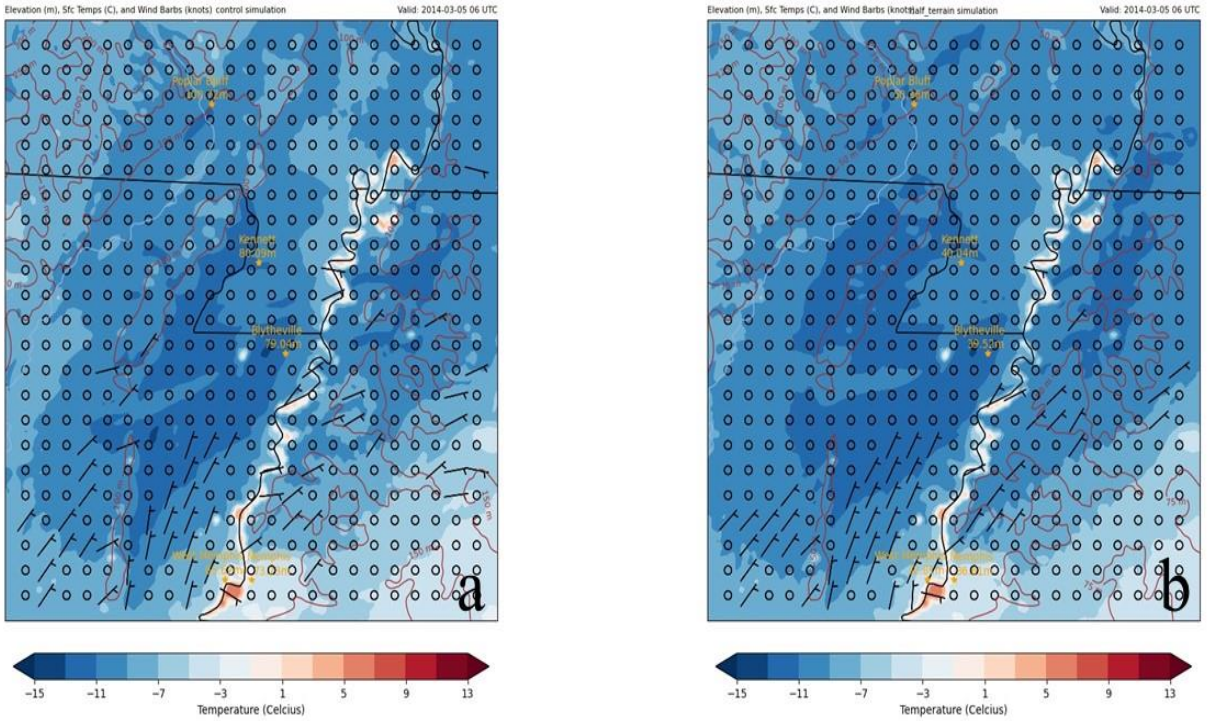

Figure 6.52 - d03 temperature maps from 0600 UTC on 05 March 2014. Each map features surface wind barbs (kts) in black, temperature shaded from blue to red from below -15°C up through 13°C. Topographic lines and values are featured on each map in dark brown.

6.2.2.7 1200 UTC 05 March 2014

Comparison of the actual-terrain versus half-terrain simulations terminated at the 1200 UTC 05 March 2014 time step. At this point the d02 regional streamline maps (Figure 6.53) continued to resolve a divergent surface flow pattern running parallel to the Ozark Plateau escarpment with northerly flow to the southeast and southerly flow over the Plateau to the northwest of the divergence line. From previous analysis, this divergent line may have been a result of the WRF model having difficulty resolving the calm wind conditions over the region, but further analysis was needed to confirm this theory.

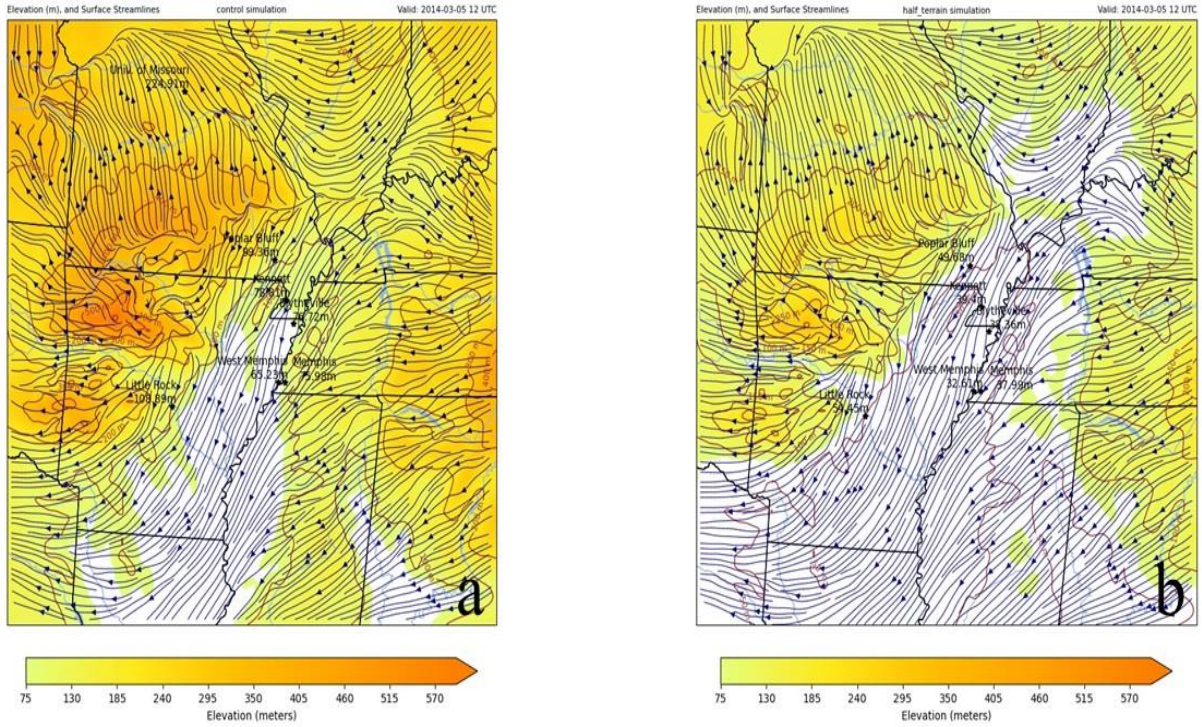

Figure 6.53 - d02 streamline maps from 1200 UTC on 05 March 2014. Map (a) is from the actual-terrain simulation run. Map (b) is from the half-terrain simulation run. Surface wind streamlines are depicted in navy blue on each map. The elevation heights are shaded from 75 m up through 570 m. Topographic lines are shaded in dark brown.

The coldest temperatures of the second night occurred on the d02 temperature maps of 1200 UTC on 05 March 2014 (Figure 6.54) due to diurnal processes, though the affected area was significantly smaller than the previous night. The area of coldest temperatures was slightly larger on the half-terrain simulation map (6.54b), though there was little contrast in the temperature field between the simulation maps. Save for a few northeasterly 5-kt winds the region remained under calm wind conditions.

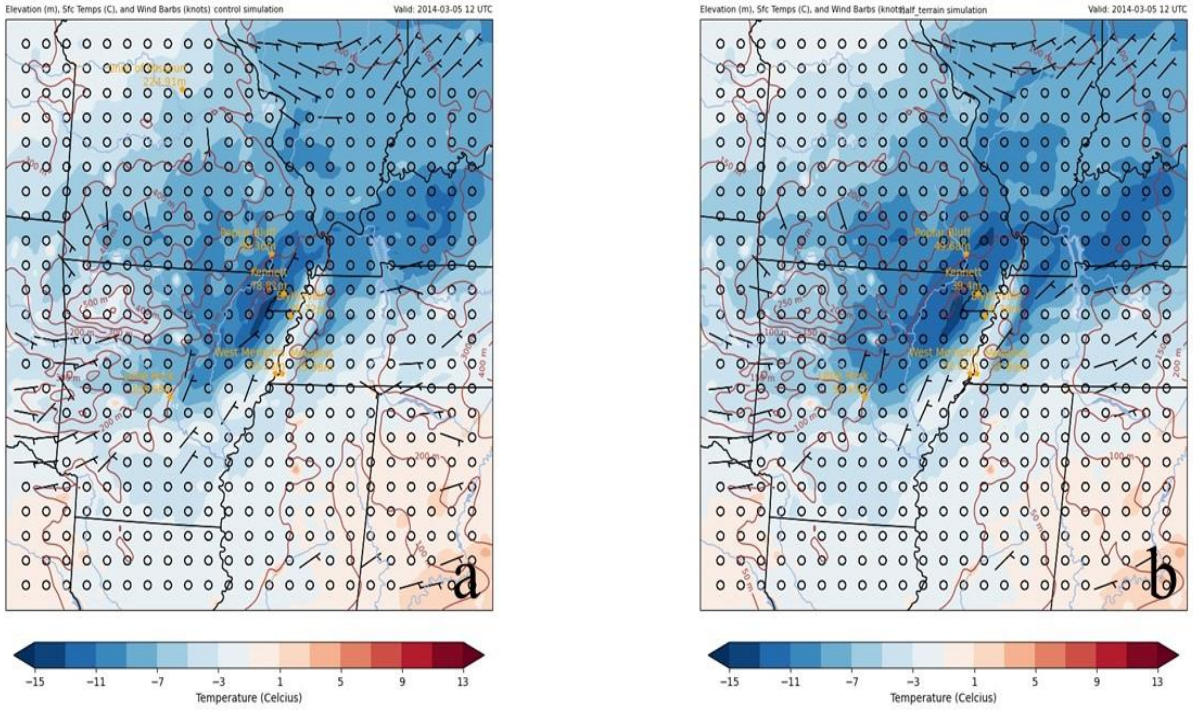

Figure 6.54 - d02 temperature maps from 1200 UTC on 05 March 2014. Each map features surface wind barbs (kts) in black, temperature shaded from blue to red from below -15°C up through 13°C. Topographic lines and values are featured on each map in dark brown.

The d03 streamline maps (Figure 6.55) of the final time step reverted to northeasterly flow over the region of interest as the area of the d03 map resided to the southeast of the diverging line seen on the previous d02 regional streamline map of the same time step (Figure 6.53). The actual-terrain simulation map resumed its deviation of streamlines around the embedded ridge (Fig. 6.55a) while the half-terrain simulation (Fig. 6.55b) showed little to no deviation over the embedded ridge at this time.

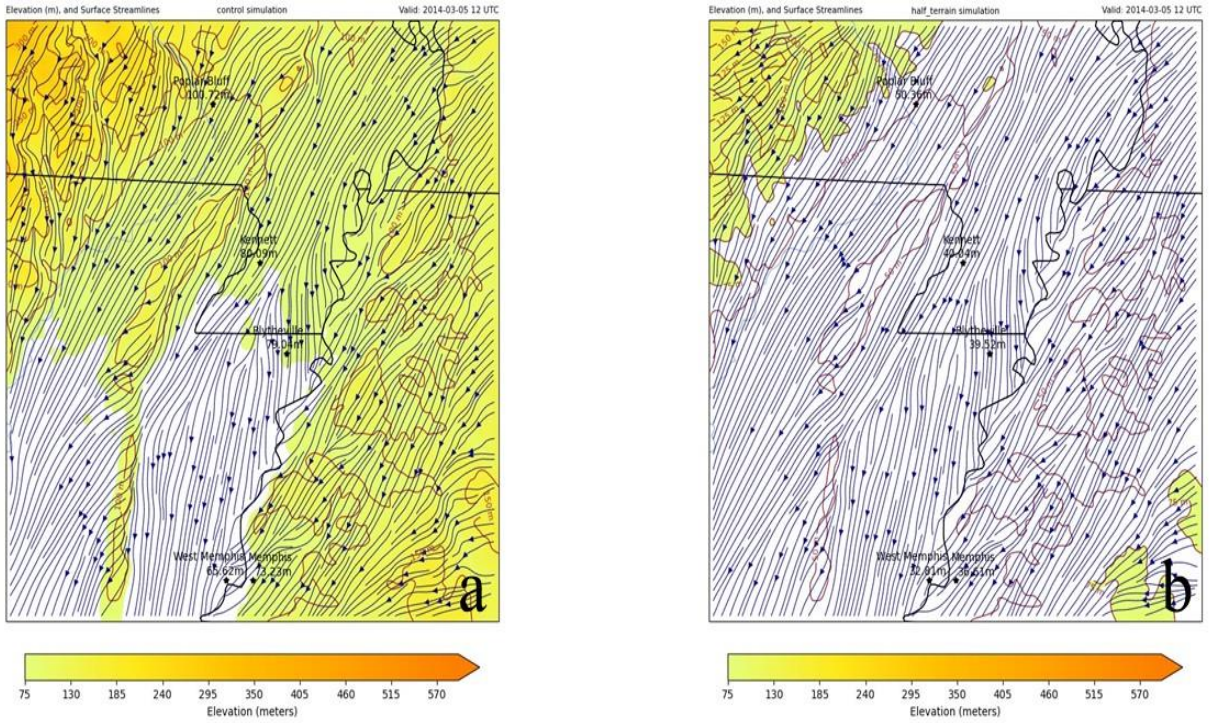

Figure 6.55 - d03 streamline maps from 1200 UTC on 05 March 2014. Map (a) is from the actual-terrain simulation runs. Map (b) is from the half-terrain simulation runs. Surface wind flow streamlines are featured in navy blue on each map. The elevation is shaded from 75 m up through 570 m. Topographic lines are featured in dark brown.

A small region of northeasterly 5-kt winds that existed on the d03 temperature actual-terrain simulation map (Fig. 6.56a) around the embedded ridge west of the Blytheville, Arkansas station was not seen on the half-terrain simulation map (Fig. 6.56b) at the same time. Calm conditions were much more prevalent on the half-terrain map. The smaller areas of cold temperatures were still in place 6 hours later on each map with little contrast in the temperature field. With winds no longer terrain-orthogonal the cold air damming event had come to an end.

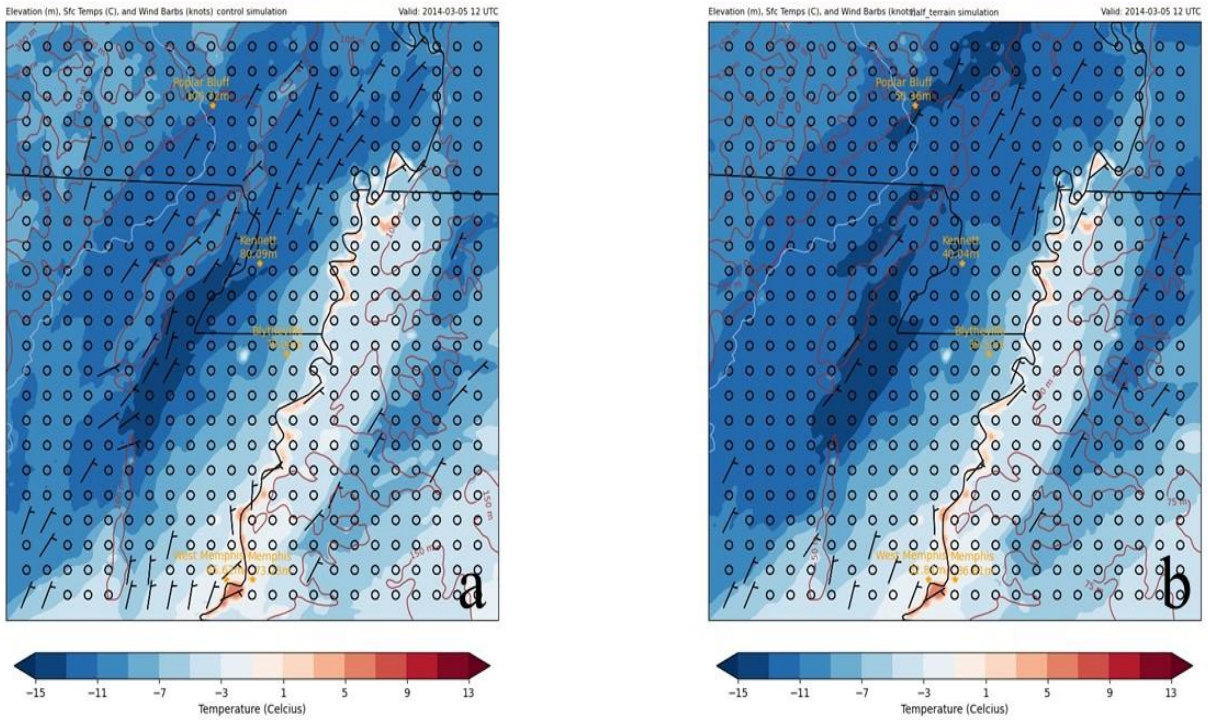

Figure 6.56 - d03 temperature maps from 1200 UTC on 05 March 2014. Each map features surface wind barbs (kts) in black, temperature shaded from blue to red from below -15°C up through 13°C. Topographic lines and values are featured on each map in dark brown.

6.2.3 Actual-Terrain versus Double-Terrain Comparison

The final comparison for the March 2014 case study examined the comparison between the double-terrain simulation in which elevation values were doubled to the actual-terrain simulation which acts as a baseline control for all the comparisons performed thus far. The analysis took place between 0000 UTC on 04 March 2014 and 1200 UTC 05 March 2014 when impacts from the cold-air damming event were experienced.

6.2.3.1 0000 UTC 04 March 2014

Comparison of the double-terrain and actual-terrain simulation runs began at the onset of 04 March 2014 matching the 2 previous comparisons. The d02 streamline maps of 0000 UTC 04 (Figure 6.57) March showed significant differences between the actual-terrain and double-terrain simulation runs. Apart from the contrast in shading of elevation values between the actual-terrain simulation run (Fig. 6.57a) and the double-terrain run (Fig. 6.57b), the double-terrain simulation map featured a stark difference in streamlines over the Ozark Plateau versus those over the Mississippi River flood plain. The northeasterly flow over the flood plain resolved very smooth, well organized, uniform surface flow streamlines on the double-terrain simulation map. Flow over the Plateau showed a more easterly component, and the streamlines were disorganized as the model accounted for streamlines deviating around significantly higher elevation values than previously seen.

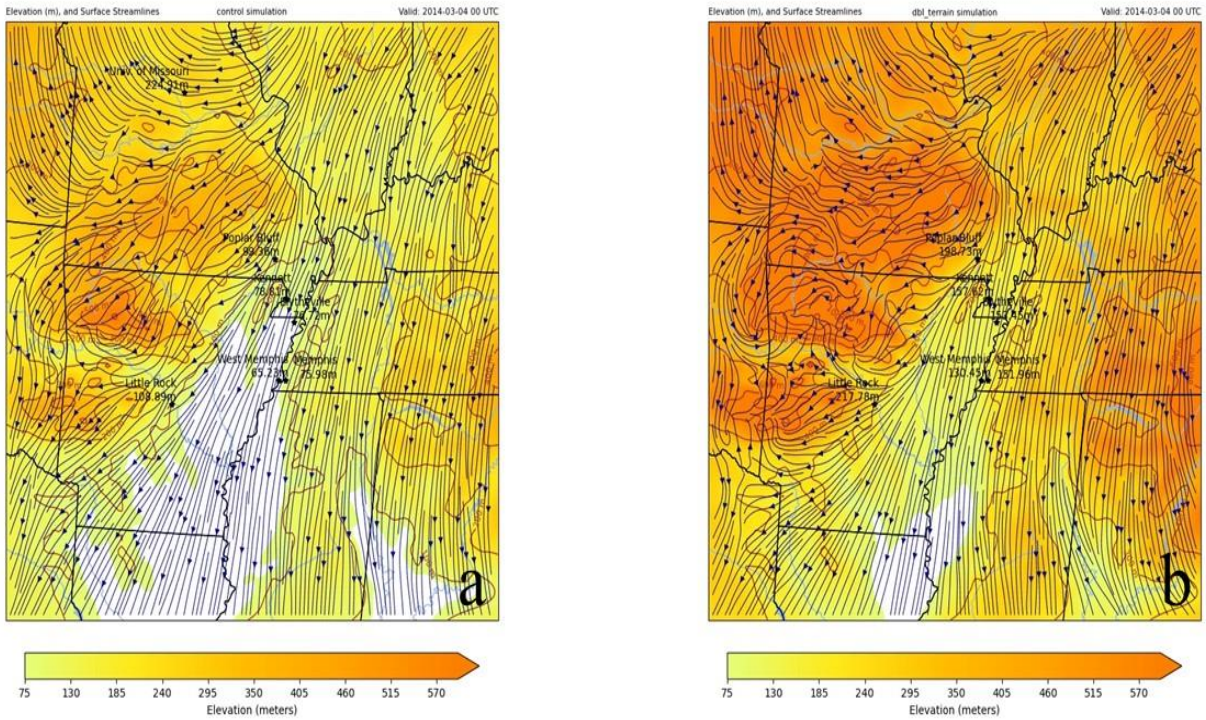

Figure 6.57 - d02 streamline maps from 0000 UTC on 04 March 2014. Map (a) is from the actual-terrain simulation run. Map (b) is from the double-terrain simulation run. Surface wind streamlines are depicted in navy blue on each map. The elevation heights are shaded from 75 m up through 570 m. Topographic lines are shaded in dark brown.

The d02 temperature maps (Figure 6.58) from this time step were more similar than their streamline counterparts. Both maps featured northeasterly 5-kt winds over the eastern Arkansas flood plain. Stronger winds were found on the actual-terrain simulation map (Fig. 6.58a) than the double-terrain specifically over the Ozark Plateau in western Arkansas. The coldest surface air was observed over northeastern Arkansas though at this time step the actual-terrain simulation resolved more widespread cold air than its comparative counterpart.

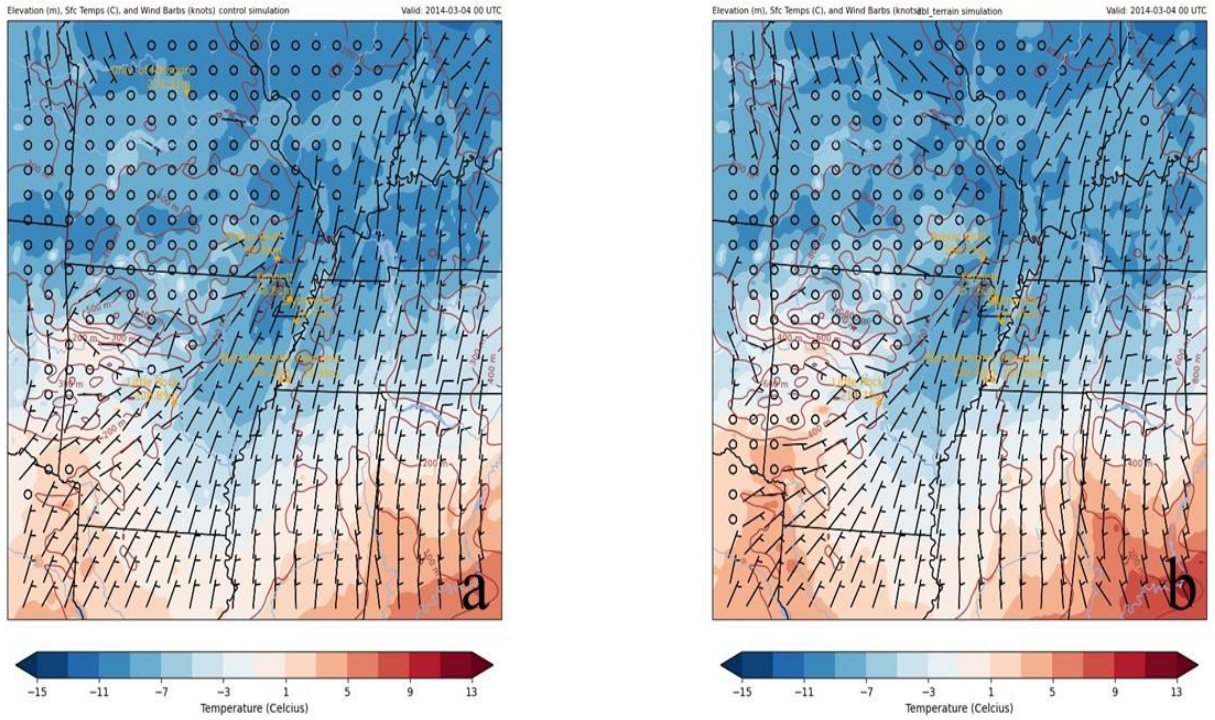

Figure 6.58 - d02 temperature maps from 0000 UTC on 04 March 2014. Each map features surface wind barbs (kts) in black, temperature shaded from blue to red from below -15°C up through 13°C. Topographic lines and values are featured on each map in dark brown.

The contrast in the streamline fields was observed on the d03 streamline maps (Figure 6.59) of 0000 UTC on 04 March. Significant differences were seen over the Ozark Plateau and the escarpment just at the edge of the flood plain and the elevation increase in the northwestern quadrant of both maps. Northeasterly streamlines shifted dramatically to a more southerly course as they turned into the Plateau itself on the double-terrain simulation map. This was unique to the double-terrain simulation run and showcased effects of exaggerated terrain elevation values.

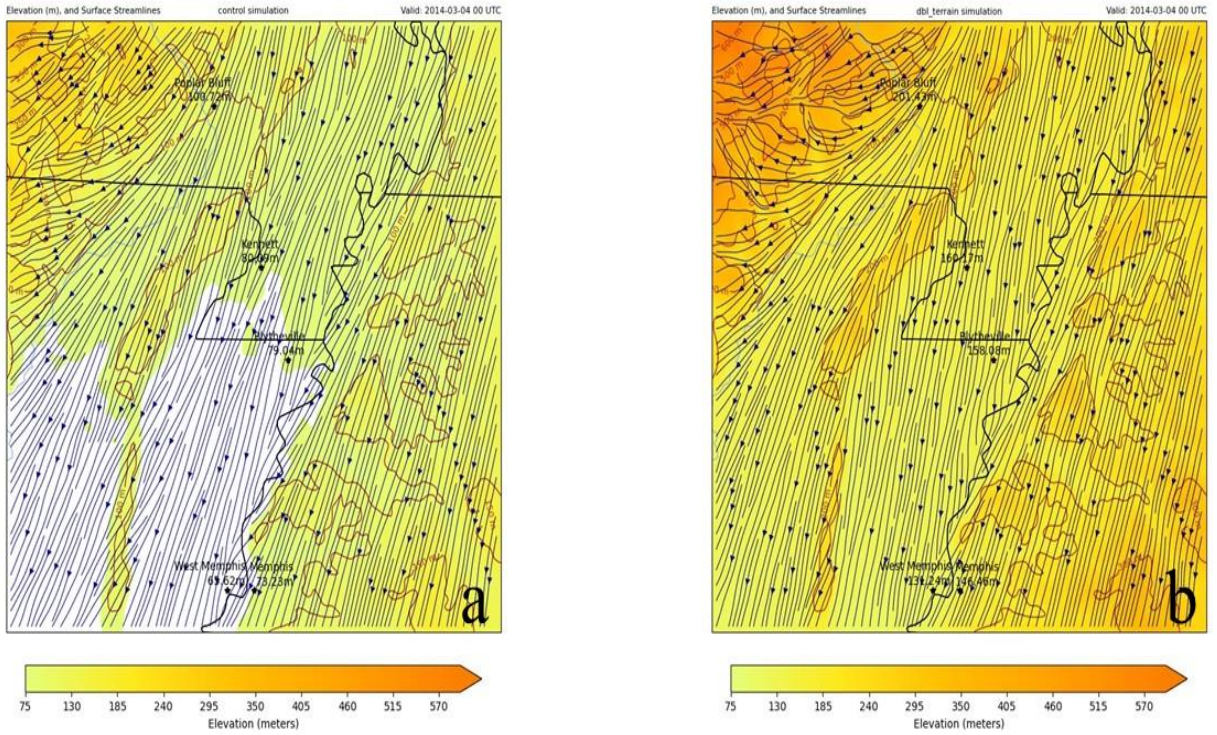

Figure 6.59 - d03 streamline maps from 0000 UTC on 04 March 2014. Map (a) is from the actual-terrain simulation runs. Map (b) is from the double-terrain simulation runs. Surface wind flow streamlines are featured in navy blue on each map. The elevation is shaded from 75 m up through 570 m. Topographic lines are featured in dark brown.

The 10-m wind fields observed on the d03 temperature maps (Fig. 6.60) were similar featuring the 5-kt northeasterly winds barbs also viewed on the d02 temperature maps (Figure 6.58). The biggest difference between simulation runs was the smaller area of coldest temperature values found on the double-terrain simulation map (Fig. 6.60b) compared to the larger area found on the actual-terrain map. On the double-terrain simulation map the “channeling effect” seen in previous comparisons was maximized by the largest elevation values viewed thus far. The coldest temperature values were seen around the embedded ridge and up against the Ozark Plateau in the northwestern portion of the map.

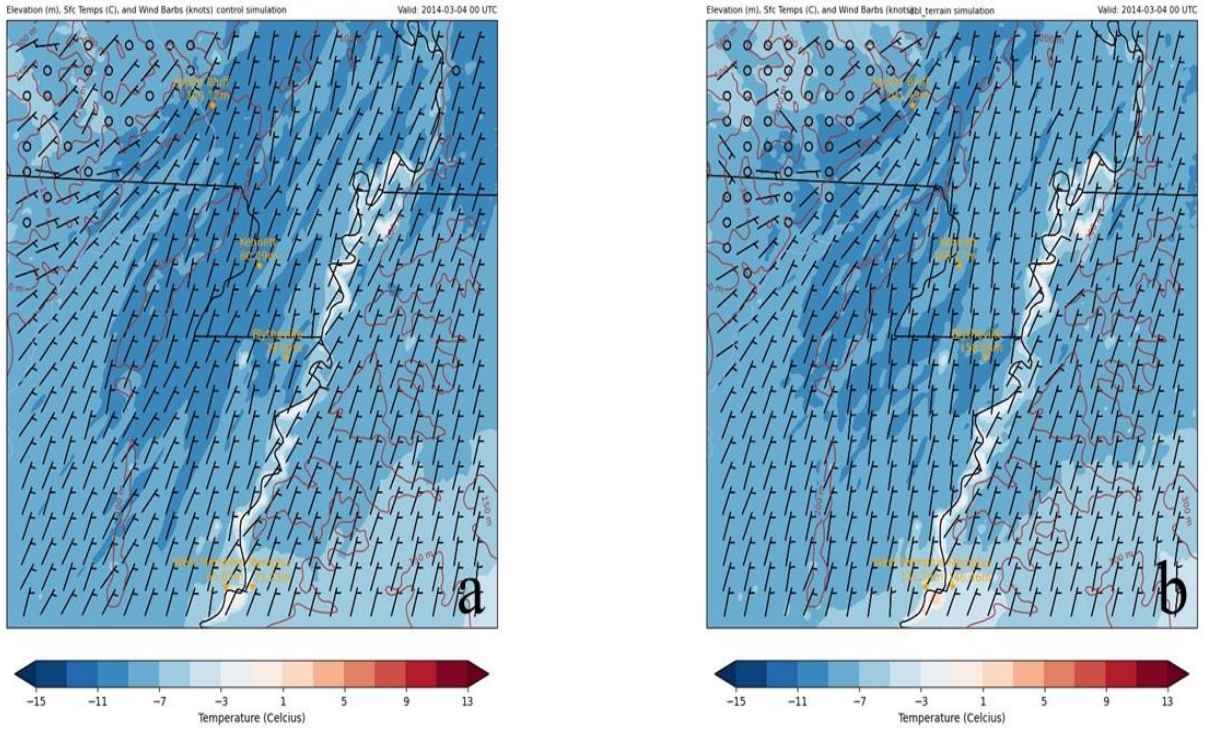

Figure 6.60 - d03 temperature maps from 0000 UTC on 04 March 2014. Each map features surface wind barbs (kts) in black, temperature shaded from blue to red from below -15°C up through 13°C. Topographic lines and values are featured on each map in dark brown.

6.2.3.2 0600 UTC 04 March 2014

As day turned to night little change was observed 6 hours later over the d02 streamline maps (Figure 6.61) of 0600 UTC of 04 March. The deviation of northeasterly surface flow through the flood plain to southerly flow over the Ozark Plateau had shifted slightly north on the double-terrain simulation map (Fig. 6.61b). This kept northeasterly surface flow over the flood plain and the escarpment of the Plateau. The streamlines had shifted slightly to a more northerly course observed on the double-terrain simulation.

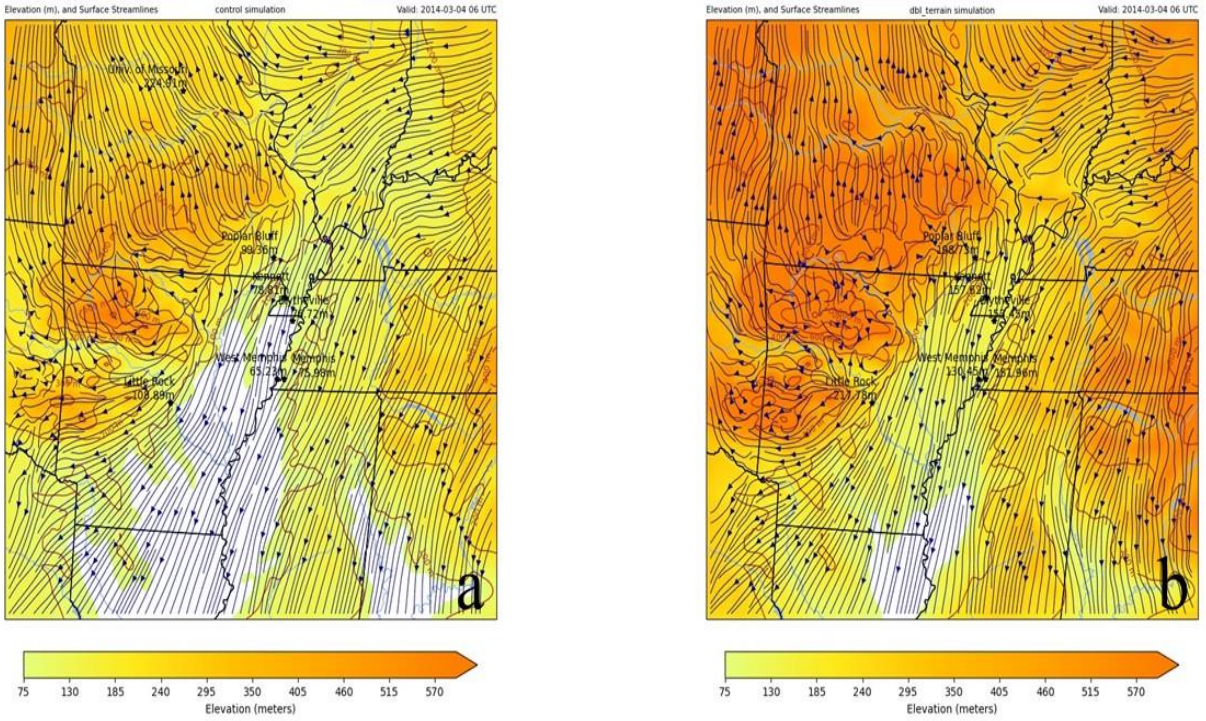

Figure 6.61 - d02 streamline maps from 0600 UTC on 04 March 2014. Map (a) is from the actual-terrain simulation run. Map (b) is from the double-terrain simulation run. Surface wind streamlines are depicted in navy blue on each map. The elevation heights are shaded from 75 m up through 570 m. Topographic lines are shaded in dark brown.

The effects of diurnal processes were seen on the d02 regional temperature maps (Figure 6.62). Southerly 5-kt winds over Missouri were observed on the double-terrain simulation map (Fig. 6.62b) but less so on its actual-terrain simulation counterpart (Fig. 6.62a). The temperature fields were again similar and significantly colder than 6 hours previous, though the coldest temperatures on the double-terrain simulation are confined to mainly east of the Mississippi River with only a few local areas of colder temperatures in extreme southeastern Missouri and northeastern Arkansas. North-northeasterly 10-m winds were observed over the flood plain in eastern Arkansas on both simulation maps.

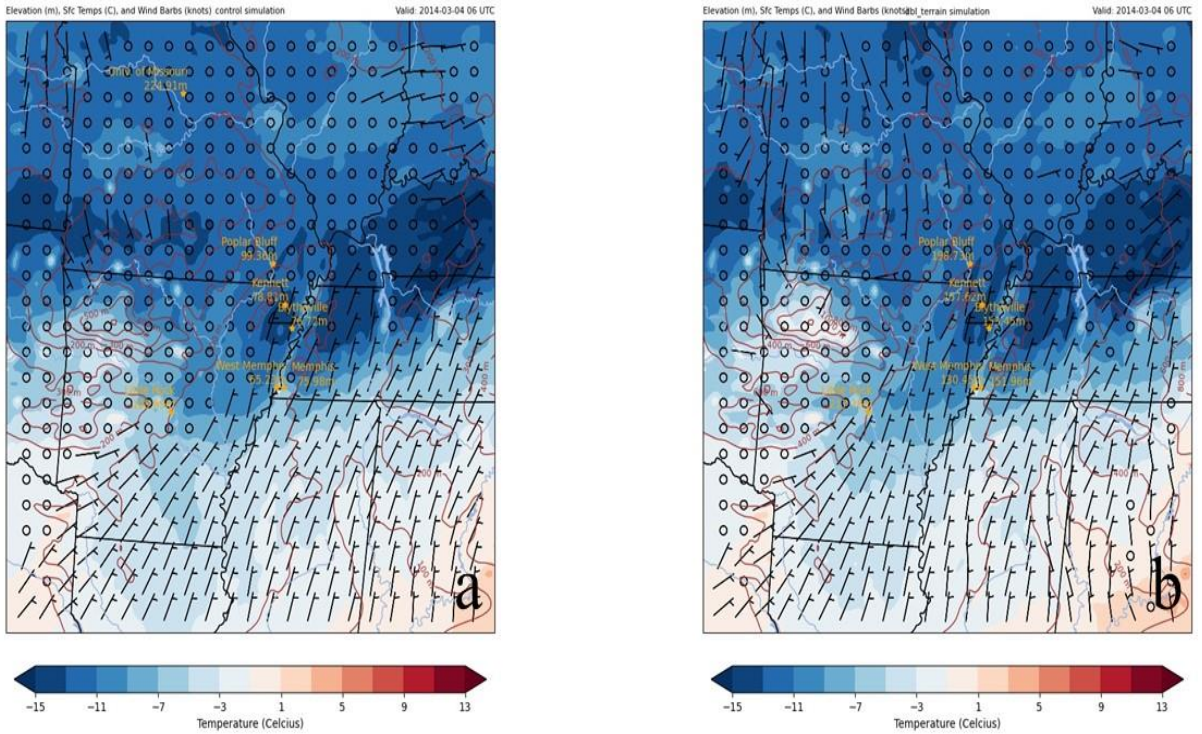

Figure 6.62 - d02 temperature maps from 0600 UTC on 04 March 2014. Each map features surface wind barbs (kts) in black, temperature shaded from blue to red from below -15°C up through 13°C. Topographic lines and values are featured on each map in dark brown.

The focused d03 streamline maps (Figure 6.63) of the 0600 UTC 04 March time step reinforced the observations from the d02 regional streamline maps (Figure 6.61) in which the divergent line where northeasterly flow shifted to southerly over the Plateau had indeed shifted north of the escarpment away from the flood plain. All streamlines on both simulation maps of the d03 streamline simulations were oriented in the northeasterly direction seen mainly in the flood plain of simulated maps. Strong deviation over the embedded ridges of the double-terrain simulation (Fig. 6.63a) was observed. The disorganized nature of the 10-m wind streamlines over the Ozark Plateau contrasted with the uniform consistent nature of the streamlines within the flatter flood plain locations on both simulation maps.

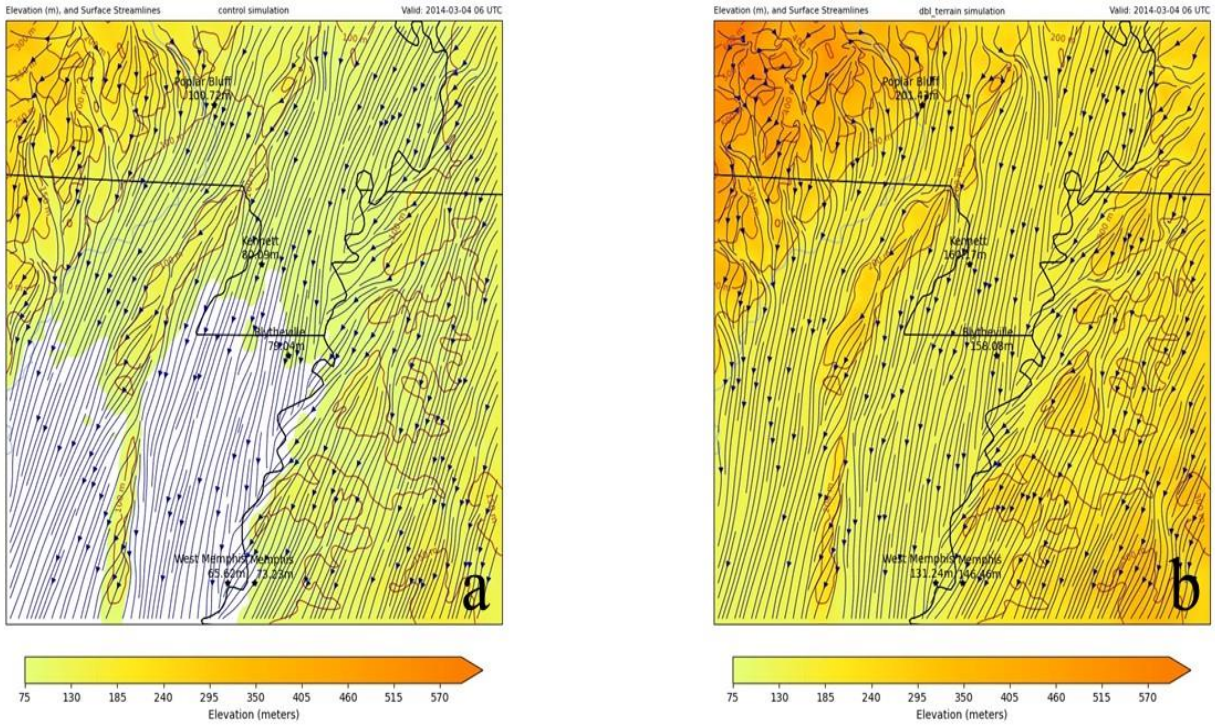

Figure 6.63 - d03 streamline maps from 0600 UTC on 04 March 2014. Map (a) is from the actual-terrain simulation runs. Map (b) is from the double-terrain simulation runs. Surface wind flow streamlines are featured in navy blue on each map. The elevation is shaded from 75 m up through 570 m. Topographic lines are featured in dark brown.

The temperature fields observed on the d03 temperature maps (Figure 6.64) of this time step featured the coldest areas of 2-m temperature trapped up against the terrain features of each simulation map. Both the embedded ridge of the flood plain and the escarpment of the Ozark Plateau were helping to channel the coldest air into the flatter flood plain terrain around these raised elevation values on each simulation map. The coldest air on the actual-terrain simulation (Fig. 6.64a) was a bit more widespread than its double-terrain counterpart (Fig. 6.64b). On the double-terrain simulation, the areas of coldest temperature were collocated with 5-kt northeasterly winds. This indicated that the slow surface flow was continuing to push cold air from the snowpack to the northeast into the flood plain further south.

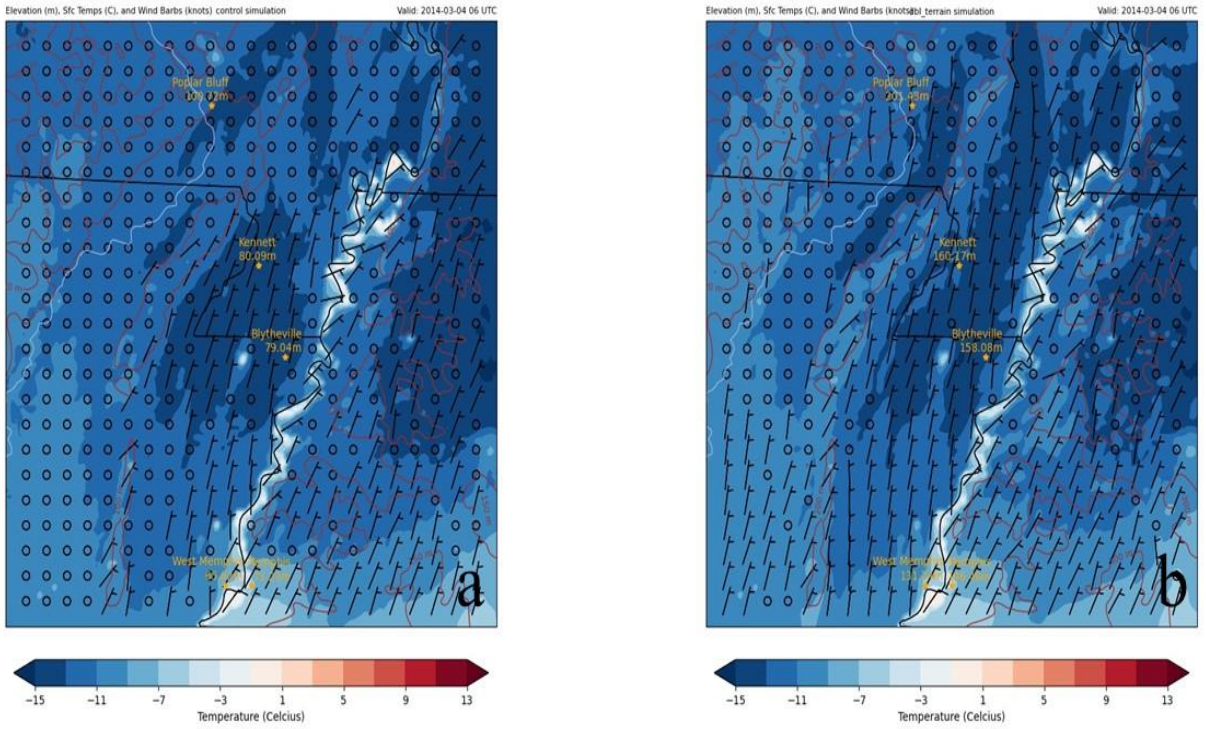

Figure 6.64 - d03 temperature maps from 0600 UTC on 04 March 2014. Each map features surface wind barbs (kts) in black, temperature shaded from blue to red from below -15°C up through 13°C. Topographic lines and values are featured on each map in dark brown.

6.2.3.3 1200 UTC 04 March 2014

By the 1200 UTC time step of 04 March 2014, the d02 streamline maps (Figure 6.65) began to show the surface flow associated with the parent anticyclone to the northeast pushing into the region as the sun rose on 04 March. Though the surface flow in the region of interest continued to be northeasterly there existed a slight shift to the east in 10-m wind streamlines over southeast Missouri and western Kentucky. Little contrast was viewed from a regional scale on the streamline maps at this time. Disorganized surface flow over the Plateau was evident next to the smooth streamlines observed over the flood plain portions of these regional streamline maps.

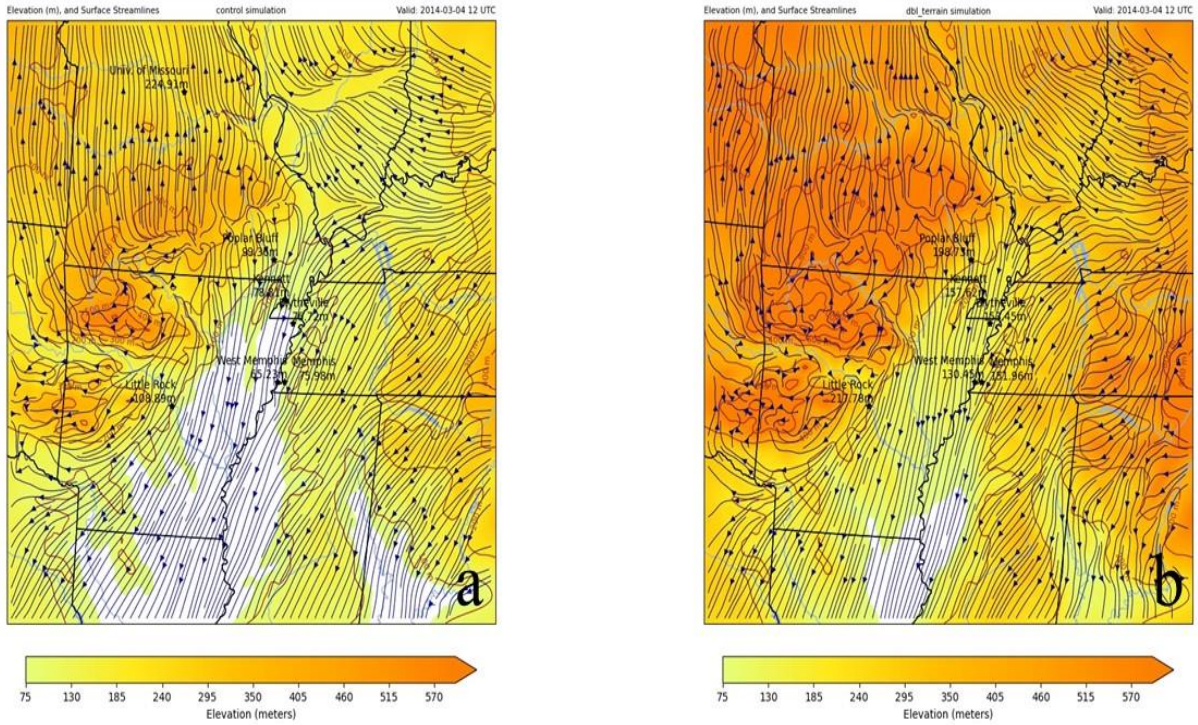

Figure 6.65 - d02 streamline maps from 1200 UTC on 04 March 2014. Map (a) is from the actual-terrain simulation run. Map (b) is from the double-terrain simulation run. Surface wind streamlines are depicted in navy blue on each map. The elevation heights are shaded from 75 m up through 570 m. Topographic lines are shaded in dark brown.

The temperature fields of the 1200 UTC 04 March 2014 time steps resolved a sharp temperature gradient on both d02 regional temperature maps (Figure 6.66). Warmer temperatures to the south gave way to the coldest temperatures experienced thus far on each simulation map. The coldest air was much more widespread on the actual-terrain simulation map (Fig, 6.66a) where a broad belt of cold air was observed east to west from southeastern Kansas through Kentucky. The double-terrain map only featured the coldest surface air from the region of interest in extreme northeastern Arkansas. Despite the differences in temperature field the cold dome over the region of interest was evident on both simulation maps. A band of calm wind conditions bisects the wind field on each simulation map with southerly winds over Missouri and northeasterly flow to the southeast over eastern Arkansas and Mississippi. The more widespread area of colder temperatures on the actual-terrain map fit the pattern seen in previous comparisons.

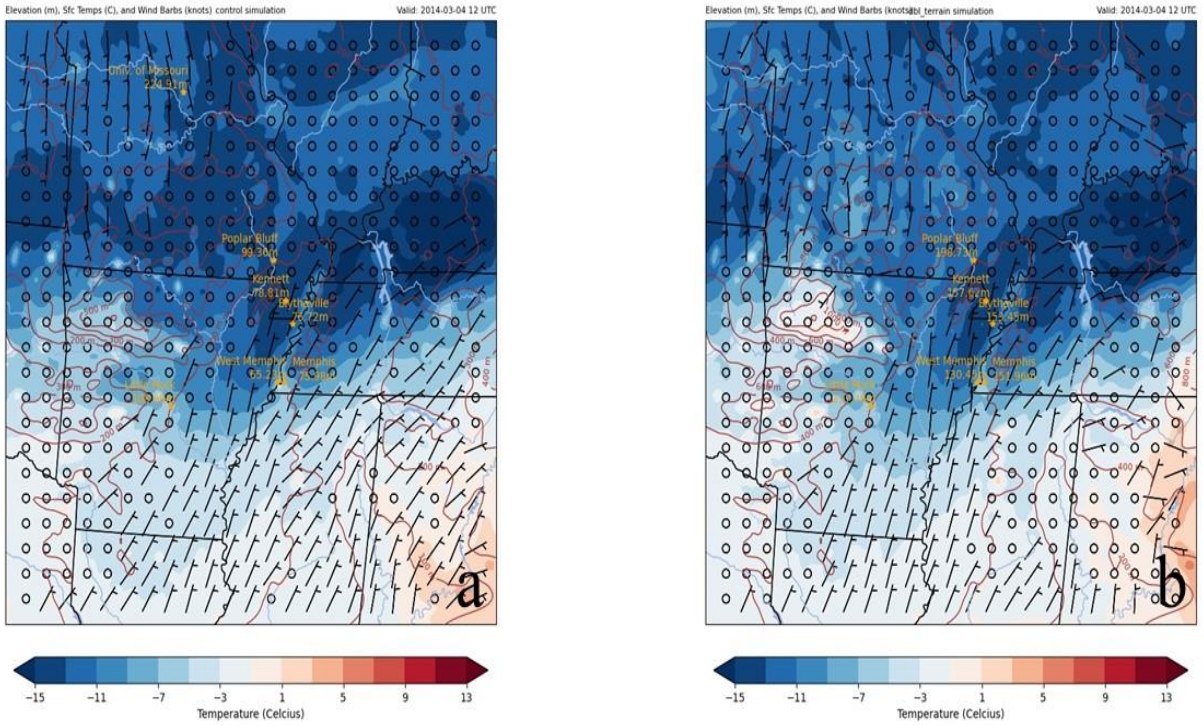

Figure 6.66 - d02 temperature maps from 1200 UTC on 04 March 2014. Each map features surface wind barbs (kts) in black, temperature shaded from blue to red from below -15°C up through 13°C. Topographic lines and values are featured on each map in dark brown.

Northeasterly surface flow was observed on both maps of the d03 streamline simulations (Figure 6.67) at 1200 UTC. The streamlines over and around the embedded ridges were observed to not cross over the ridges of the flood plain on the double-terrain simulation (Fig. 6.67b). Every streamline that originated around the ridge was deflected away with the only streamlines originating on the ridges observed on the ridge. Those that did originate on the ridge quickly move to the south off the ridge. This same behavior was not observed on the actual-terrain simulation where a few streamlines did cross the ridge. This lack of deviation on the actual-terrain simulation was yet another piece of evidence for terrain influence during these cold-air damming events. The influence of the anticyclone to the northeast could be seen on the d03 streamline maps as well with easterly flow pushing into the region of interest from the northeast.

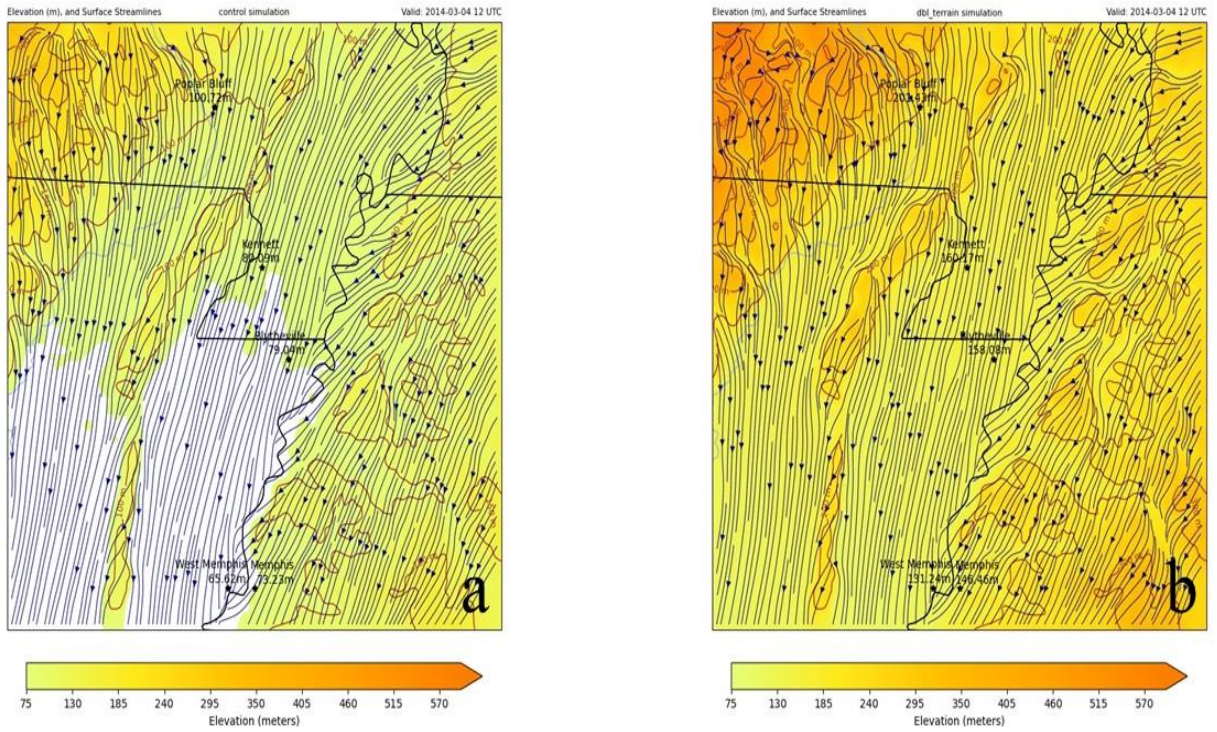

Figure 6.67 - d03 streamline maps from 1200 UTC on 04 March 2014. Map (a) is from the actual-terrain simulation runs. Map (b) is from the double-terrain simulation runs. Surface wind flow streamlines are featured in navy blue on each map. The elevation is shaded from 75 m up through 570 m. Topographic lines are featured in dark brown.

The d03 temperature simulations (Figure 6.68) as day broke featured more widespread cold surface air in the region of interest than 6 hours previous. A small local area of coldest surface air on the double-terrain simulation map (Fig. 6.68b) existed just to the northeast of the Blytheville, Arkansas station which was not present on the actual-terrain simulation (Fig. 6.68a). Despite this observation, the channeling of cold air on the double-terrain simulation kept the coldest surface air contained within the flood plain and less spread out than what was observed on the actual-terrain simulation. Northeasterly surface flow in the wind barb field was viewed on both simulation maps within the region of interest with more easterly winds shown to the northeast over Kentucky.

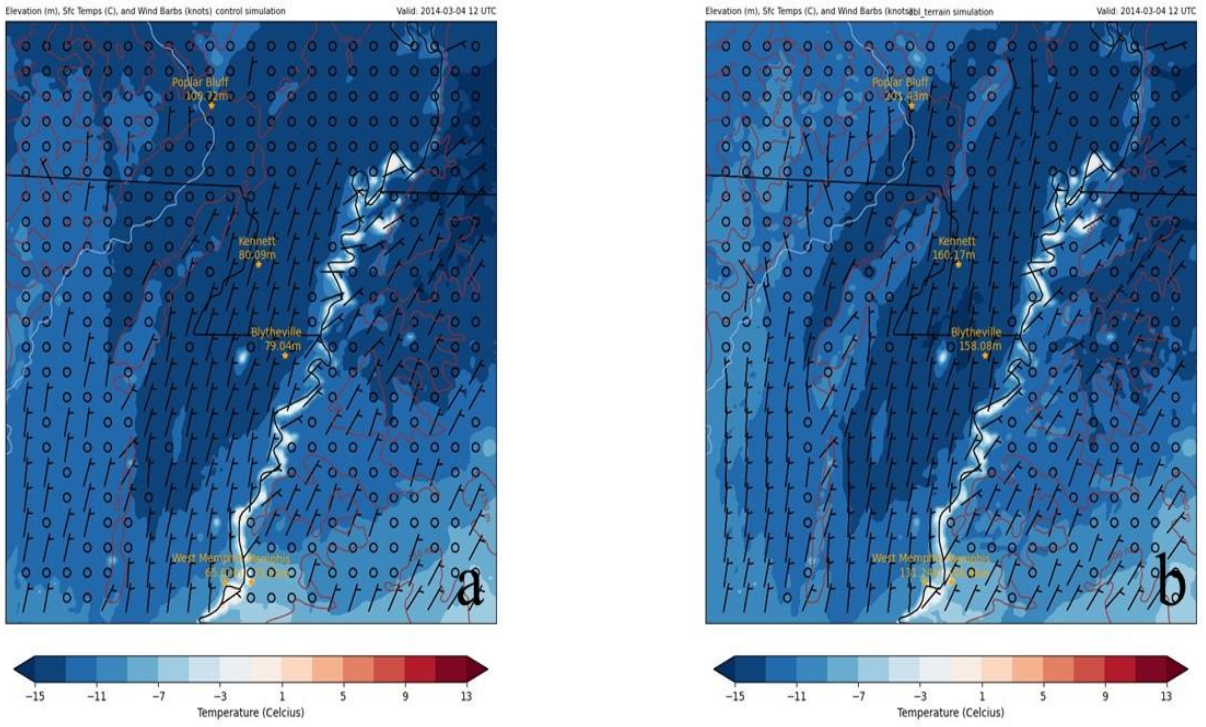

Figure 6.68 - d03 temperature maps from 1200 UTC on 04 March 2014. Each map features surface wind barbs (kts) in black, temperature shaded from blue to red from below -15°C up through 13°C. Topographic lines and values are featured on each map in dark brown.

6.2.3.4 1800 UTC 04 March 2014

The easterly shift in surface flow wind direction over the region of interest continued 6 hours later on the 1800 UTC d02 regional streamline maps (Figure 6.69). On a regional scale, little contrast was seen in the streamline field. The flow was east-northeasterly over the flood plain of eastern Arkansas but veered southerly just north of the escarpment of the Ozark Plateau. The southwestern flank of the parent anticyclone to the northeast was observed on both simulation maps. This surface flow setup being terrain-orthogonal to the southeastern flank of the Plateau is favorable for cold-air damming.

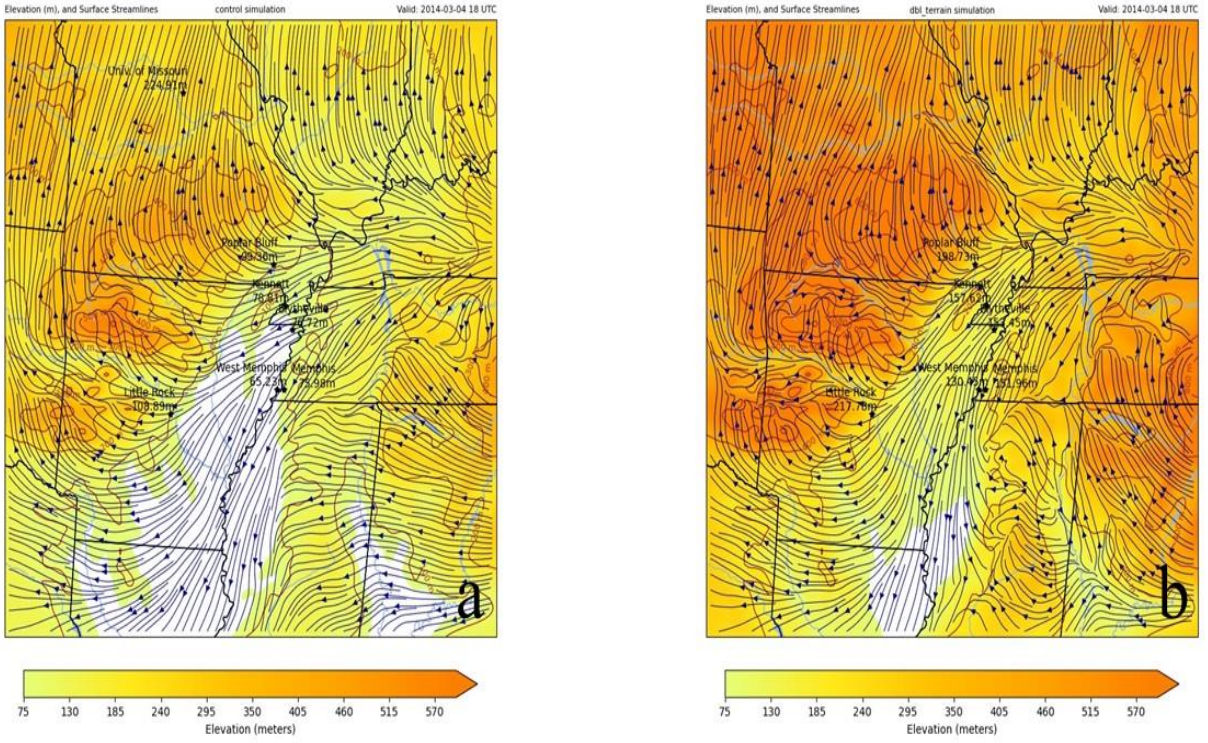

Figure 6.69 - d02 streamline maps from 1800 UTC on 04 March 2014. Map (a) is from the actual-terrain simulation run. Map (b) is from the double-terrain simulation run. Surface wind streamlines are depicted in navy blue on each map. The elevation heights are shaded from 75 m up through 570 m. Topographic lines are shaded in dark brown.

Despite the significant temperature increase observed on the majority of the d02 regional temperature maps (Figure 6.70), the cold pool over the region of interest in northeastern Arkansas was still present at 1800 UTC on 04 March 2014. Significant differences existed in the 10-m wind field for each simulation map. The actual-terrain simulation (Fig. 6.70a) contained a much more easterly component to the winds found over northeastern Arkansas. The double-terrain simulation (Fig. 6.70b) maintained the northeasterly directional component seen in earlier time steps. The increase in temperature was significantly more on the double-terrain simulation than its actual-terrain counterpart. Specifically, the higher elevations in western Arkansas on the double-terrain map were 4-6°C warmer than observed on the actual-terrain simulation map. This was due to the model's accounting for diurnal processes and solar radiation on higher elevations.

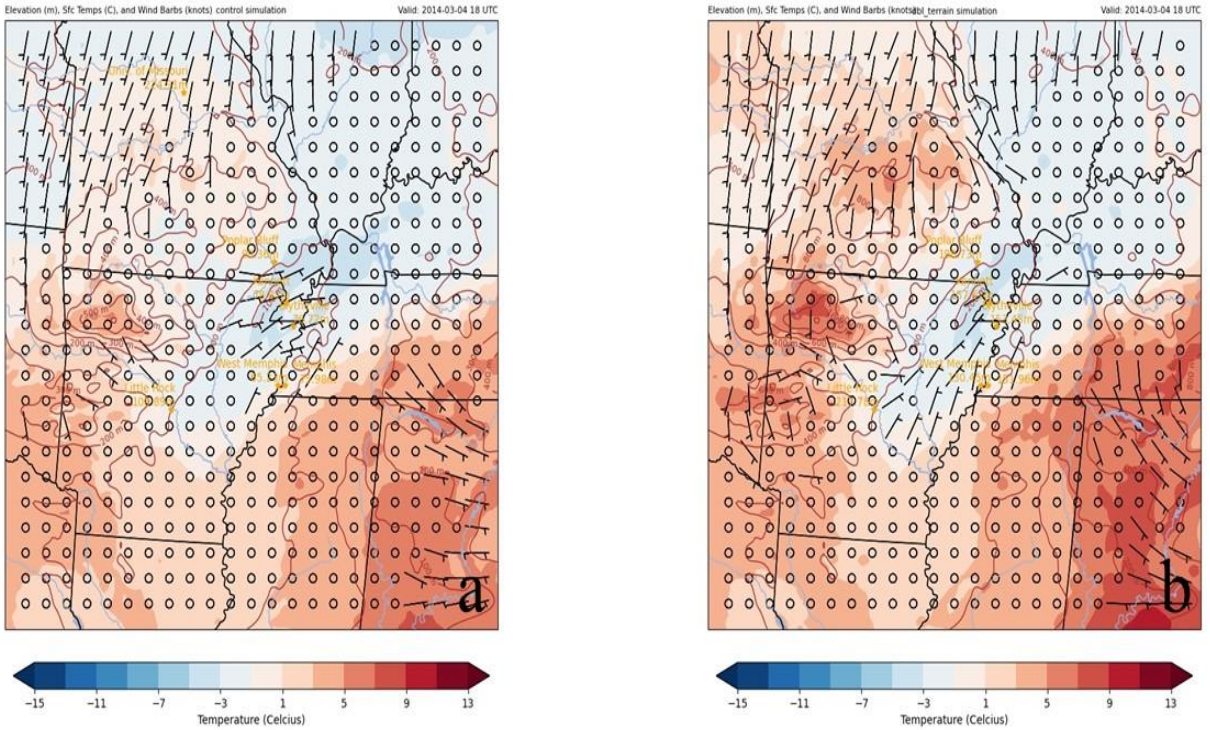

Figure 6.70 - d02 temperature maps from 1800 UTC on 04 March 2014. Each map features surface wind barbs (kts) in black, temperature shaded from blue to red from below -15°C up through 13°C. Topographic lines and values are featured on each map in dark brown.

The terrain-orthogonal surface flow was evident on both simulation maps when focused in on the d03 streamline maps (Figure 6.71) of this time step. Surface flow turned directly into the escarpment of the Plateau in the northwestern portion of both simulation maps. The actual-terrain simulation map (Fig. 6.71a) did indicate a more easterly component than its double-terrain counterpart as viewed on the regional d02 streamline maps (Figure 6.69). Despite the directional difference both maps contained streamlines flowing over the embedded ridge within the flood plain.

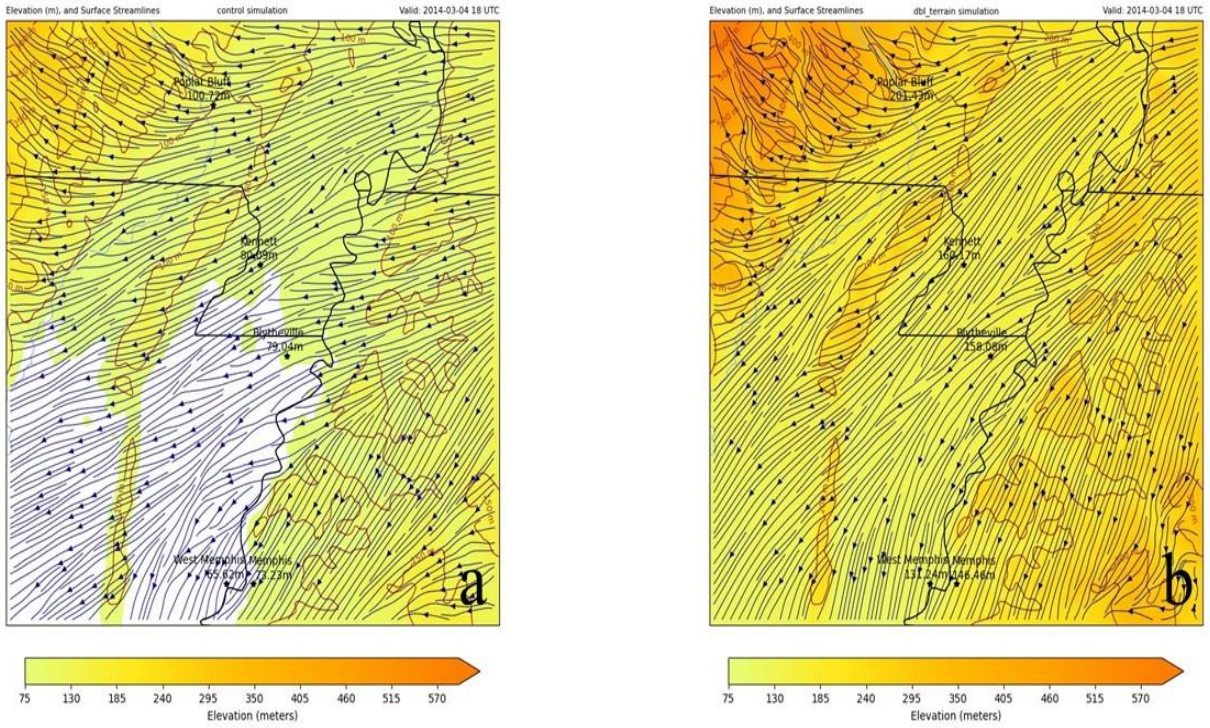

Figure 6.71 - d03 streamline maps from 1800 UTC on 04 March 2014. Map (a) is from the actual-terrain simulation runs. Map (b) is from the double-terrain simulation runs. Surface wind flow streamlines are featured in navy blue on each map. The elevation is shaded from 75 m up through 570 m. Topographic lines are featured in dark brown.

The focused d03 temperature maps (Figure 6.72) resolved the directional difference in the 10-m wind fields on both surface maps as the actual-terrain simulation contained a more easterly directional component and the double-terrain simulation maintained a northeasterly flow. Despite these maps being the warmest when pertaining to the temperature field, below-freezing temperatures still dominated the region of interest. The cold pool was smaller due to the "channeling effect" pattern that continued as elevations were altered to higher values. The below-freezing temperatures were more widespread to the northeast on the actual-terrain simulation (Fig. 6.72a) than the double-terrain simulation map. This series of maps from the 1800 UTC time step of 04 March was perhaps some of the clearest evidence for cold-air damming with this event. The simulations showed that the elevation heights of the double-terrain simulation reduced cold-air damming due to the northeasterly channeling of 10-m winds through the flatter elevations of the flood plain where 10-m winds were able to maintain an easterly directional component in the actual-terrain simulation in the same location at that time.

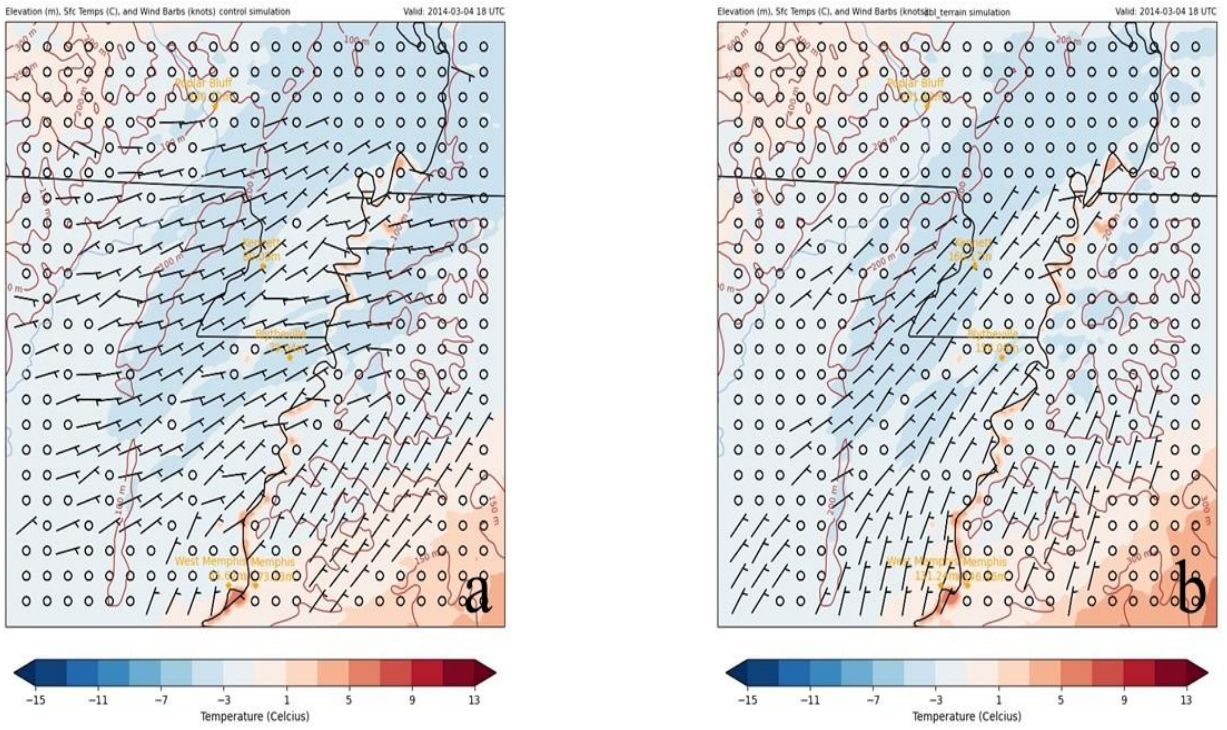

Figure 6.72 - d03 temperature maps from 1800 UTC on 04 March 2014. Each map features surface wind barbs (kts) in black, temperature shaded from blue to red from below -15°C up through 13°C. Topographic lines and values are featured on each map in dark brown.

6.2.3.5 0000 UTC 05 March 2014

The first time step of 05 March 2014 continued the directional shift to an easterly course over the region of interest on the d02 regional streamline maps (Figure 6.73). Little contrast separated the 2 simulation maps in which the surface flow diverged over the flood plain of eastern Arkansas with the more western streamlines veering more southerly closer to the Ozark Plateau, and the more eastern streamlines remaining more east-northeasterly deeper into the flood plain of Arkansas.

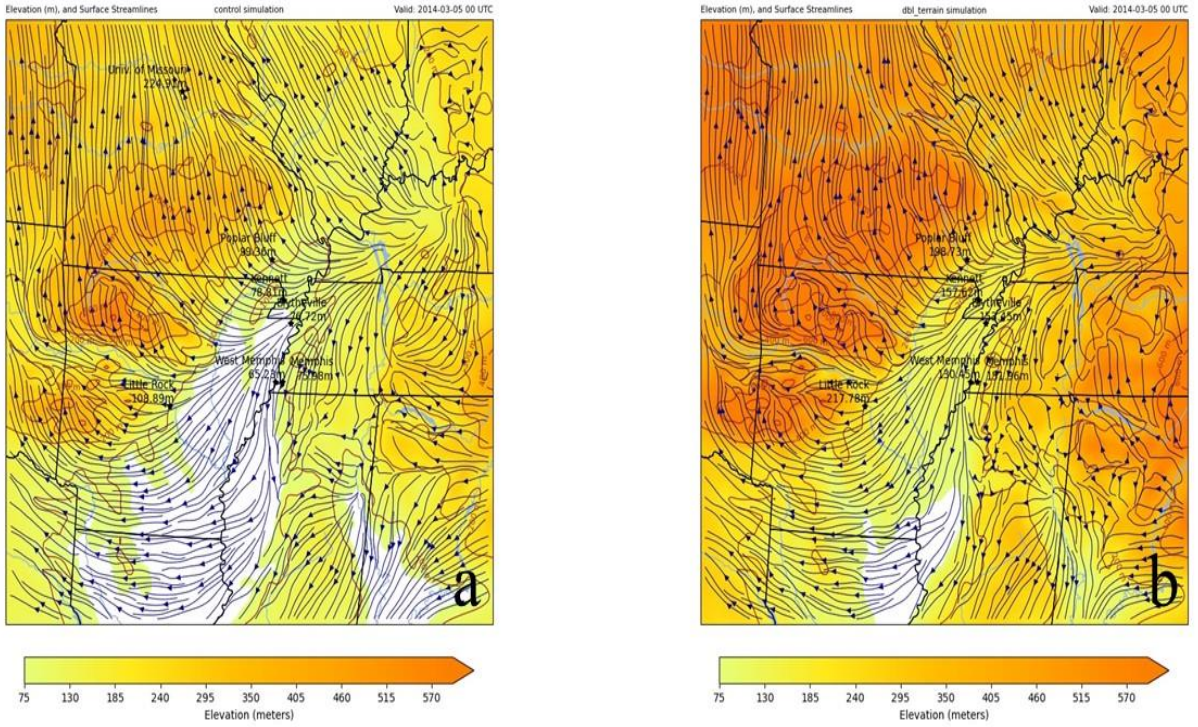

Figure 6.73 - d02 streamline maps from 0000 UTC on 05 March 2014. Map (a) is from the actual-terrain simulation run. Map (b) is from the double-terrain simulation run. Surface wind streamlines are depicted in navy blue on each map. The elevation heights are shaded from 75 m up through 570 m. Topographic lines are shaded in dark brown.

The most prominent appearance of the cold pool located over the region of interest was observed on the 0000 UTC 05 March d02 regional temperature maps (Figure 6.74). Here the effect of diurnal processes was seen on both simulation maps with most of the maps well above freezing save for the region of interest in which below-freezing temperatures remained. Weak northeasterly winds remained on each simulation map as 10-m winds calmed over much of the region including the area of interest in eastern Arkansas.

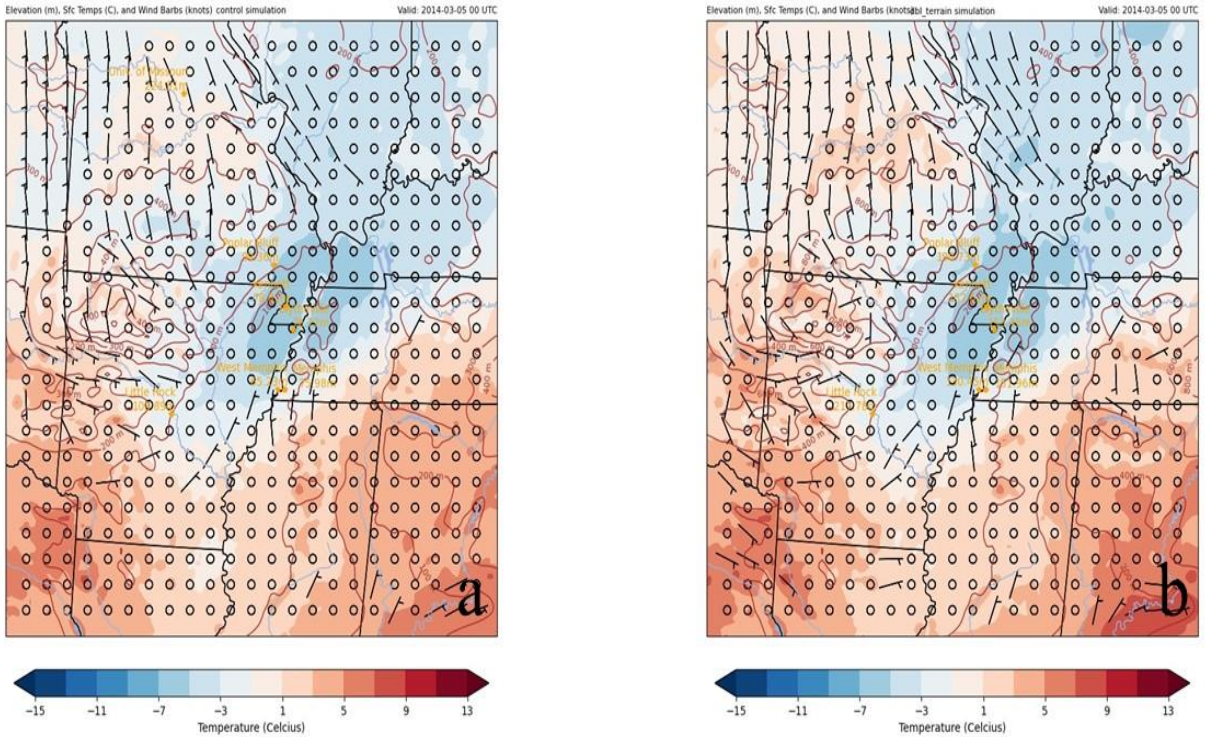

Figure 6.74 - d02 temperature maps from 0000 UTC on 05 March 2014. Each map features surface wind barbs (kts) in black, temperature shaded from blue to red from below -15°C up through 13°C. Topographic lines and values are featured on each map in dark brown.

A lack of contrast was observed between the 2 d03 streamline maps (Figure 6.75) of 0000 UTC time step. Southeasterly flow up against the escarpment of the Ozark Plateau to the northwest gave way to easterly flow over the Blytheville, Arkansas station. To the south the surface flow remained more northeasterly further away from the parent high pressure system to the northeast. Deviation of streamlines over the embedded ridges existed on both simulation maps. The channeling around the embedded ridges and disruption of streamlines is more exaggerated on the double-terrain simulation (Fig. 6.75b) due to the larger elevation height values.

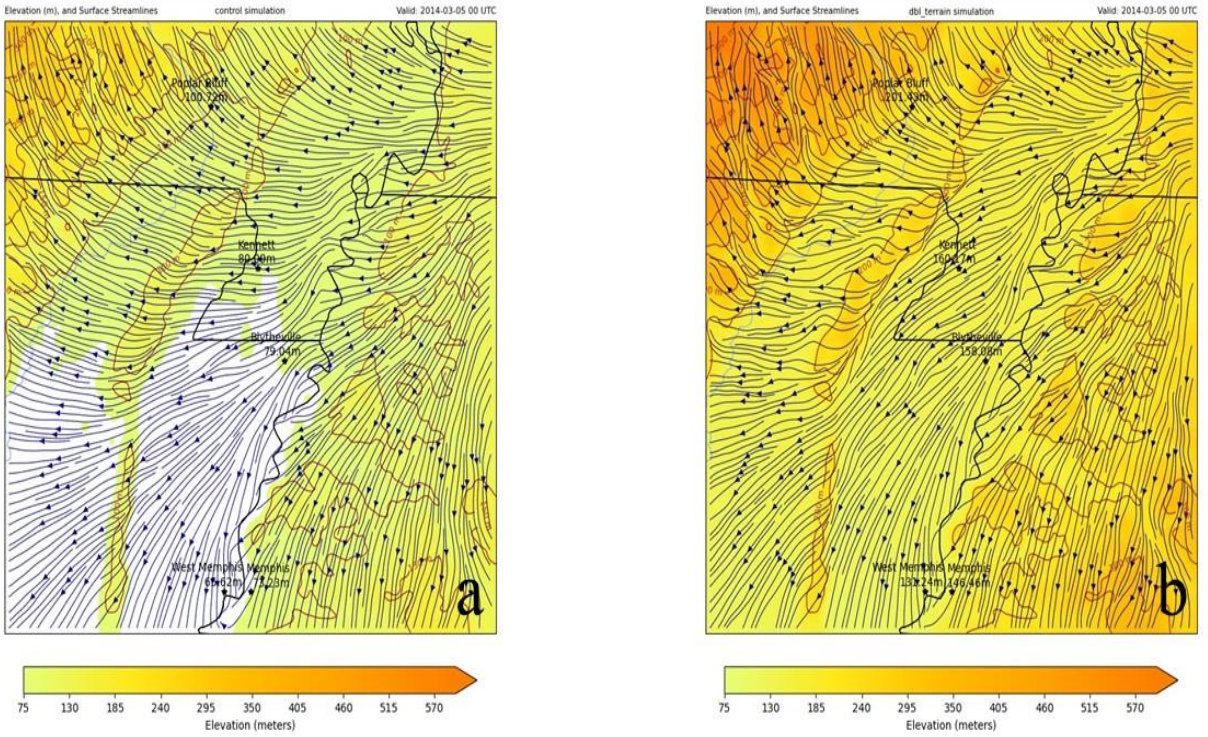

Figure 6.75 - d03 streamline maps from 0000 UTC on 05 March 2014. Map (a) is from the actual-terrain simulation runs. Map (b) is from the double-terrain simulation runs. Surface wind flow streamlines are featured in navy blue on each map. The elevation is shaded from 75 m up through 570 m. Topographic lines are featured in dark brown.

The d03 temperature maps (Figure 6.76) of 0000 UTC 05 March contained temperature fields that had little contrast including the widespread nature of the cold pool on simulation map. The lack of wind speed in the region of interest seemed to reduce the effects of local topography on said temperature fields. Therefore, the coldest temperatures spread out across the flatter elevations of the flood plain on both simulation maps with only the escarpment barricading further expansion of cold surface air. 10-m winds were equally lacking contrast with only easterly 10-m winds observed over the embedded ridges as calm conditions continued to be viewed over the region of interest.

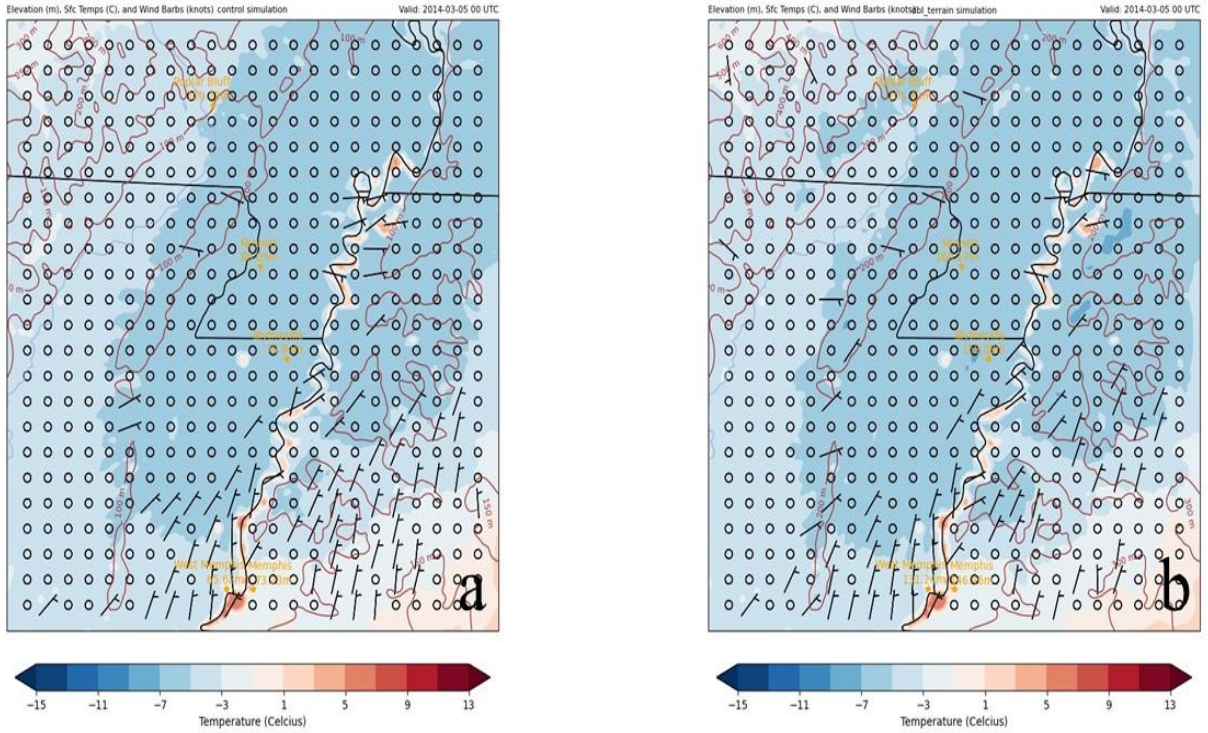

Figure 6.76 - d03 temperature maps from 0000 UTC on 05 March 2014. Each map features surface wind barbs (kts) in black, temperature shaded from blue to red from below -15°C up through 13°C. Topographic lines and values are featured on each map in dark brown.

6.2.3.6 0600 UTC 05 March 2014

The 0600 UTC 05 March 2014 time step signaled the beginning of the end for the cold-air damming event in previous comparisons and held true again when analyzing the d02 regional streamline maps (Figure 6.77). The diverging line that denoted where streamlines either traveled in a southerly fashion up into the Plateau or continued a northeasterly track had moved north as the parent anticyclone began to lose its influence on the region. 10-m wind flow became less terrain-orthogonal which inhibited the cold-air damming event to persist. The diverging line was in a more favorable position on the actual-terrain simulation map (6.77a) than on the double-terrain map (6.77b) in which the line was clearly north of the escarpment and pushing streamlines flowing from the Ozark Plateau to the north.

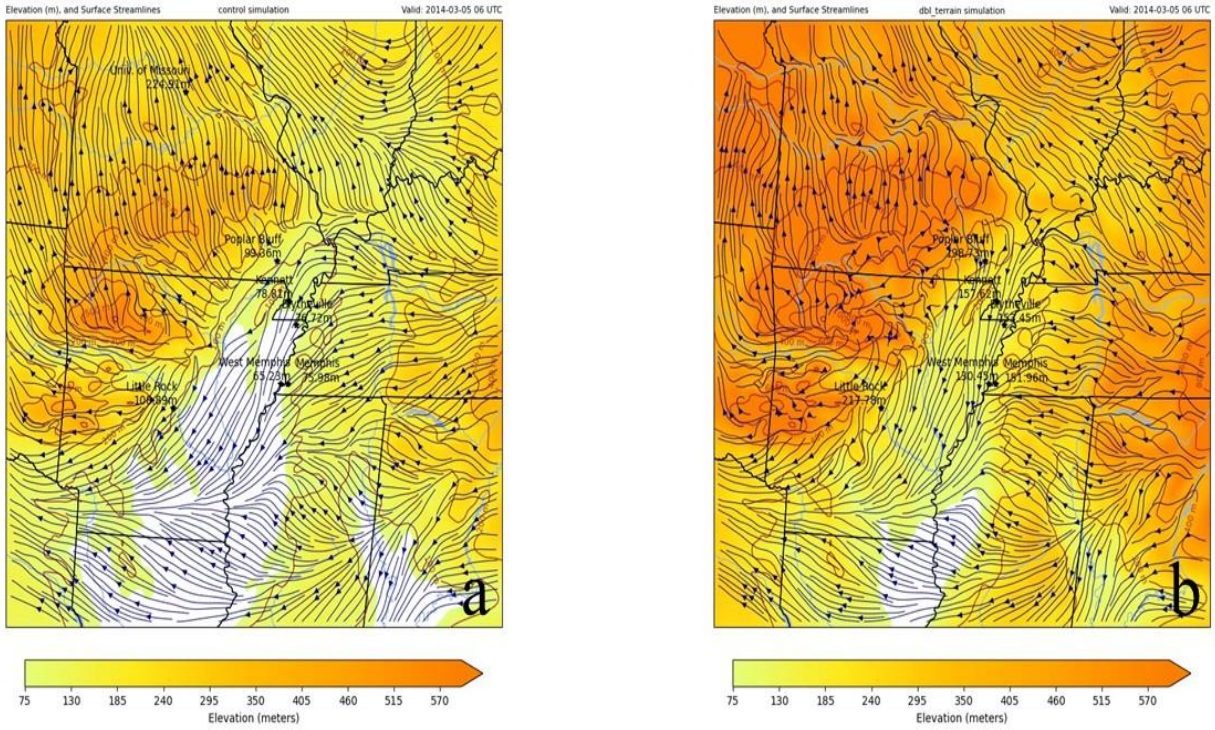

Figure 6.77 - d02 streamline maps from 0600 UTC on 05 March 2014. Map (a) is from the actual-terrain simulation run. Map(b) is from the double-terrain simulation run. Surface wind streamlines are depicted in navy blue on each map. The elevation heights are shaded from 75 m up through 570 m. Topographic lines are shaded in dark brown.

Regression of the temperature fields back to below freezing on both simulation maps of the 0600 UTC 05 March d02 temperature maps (Figure 6.78) was expected due to diurnal processes over the course of the second night. Temperatures were not as cold as the previous night, but the cold pool was still evident over the region of interest in northeastern Arkansas. Weak 5-kt winds seen over eastern Arkansas repeated what was observed on the previous streamline maps (Figure 6.77), in which wind direction turned back to a northeasterly flow signaling the end of the cold air damming event.

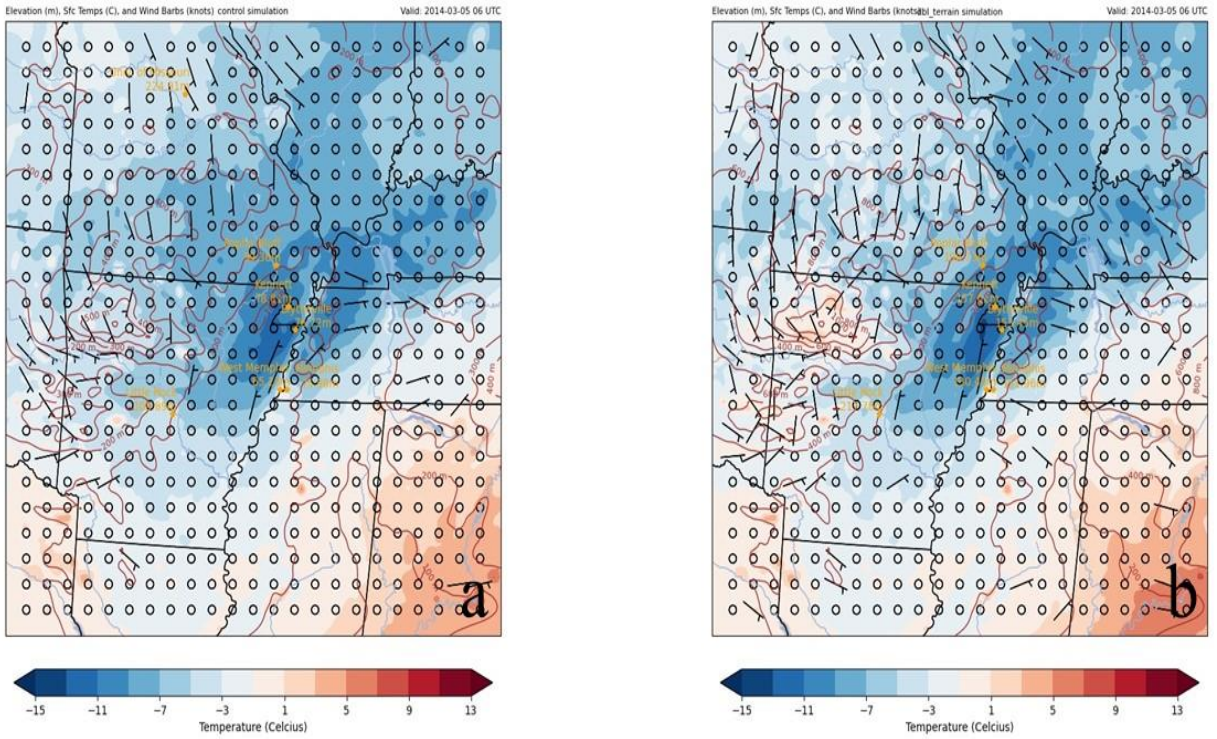

Figure 6.78 - d02 temperature maps from 0600 UTC on 05 March 2014. Each map features surface wind barbs (kts) in black, temperature shaded from blue to red from below -15°C up through 13°C. Topographic lines and values are featured on each map in dark brown.

Focused d03 streamline maps (Figure 6.79) from the 0600 UTC 05 March time step showed surface flow now in a northerly direction flowing down off the escarpment of the Ozark Plateau into the flatter flood plains of the region of interest. The double-terrain simulation map (Fig. 6.79b) resolved that most streamlines were deflected around or away from the embedded ridges of the flood plain. The actual-terrain simulation (Fig. 6.79a) showed some deviation of streamlines as well, but many more do cross over the ridges. At this point, surface flow was no longer supporting the cold-air damming event.

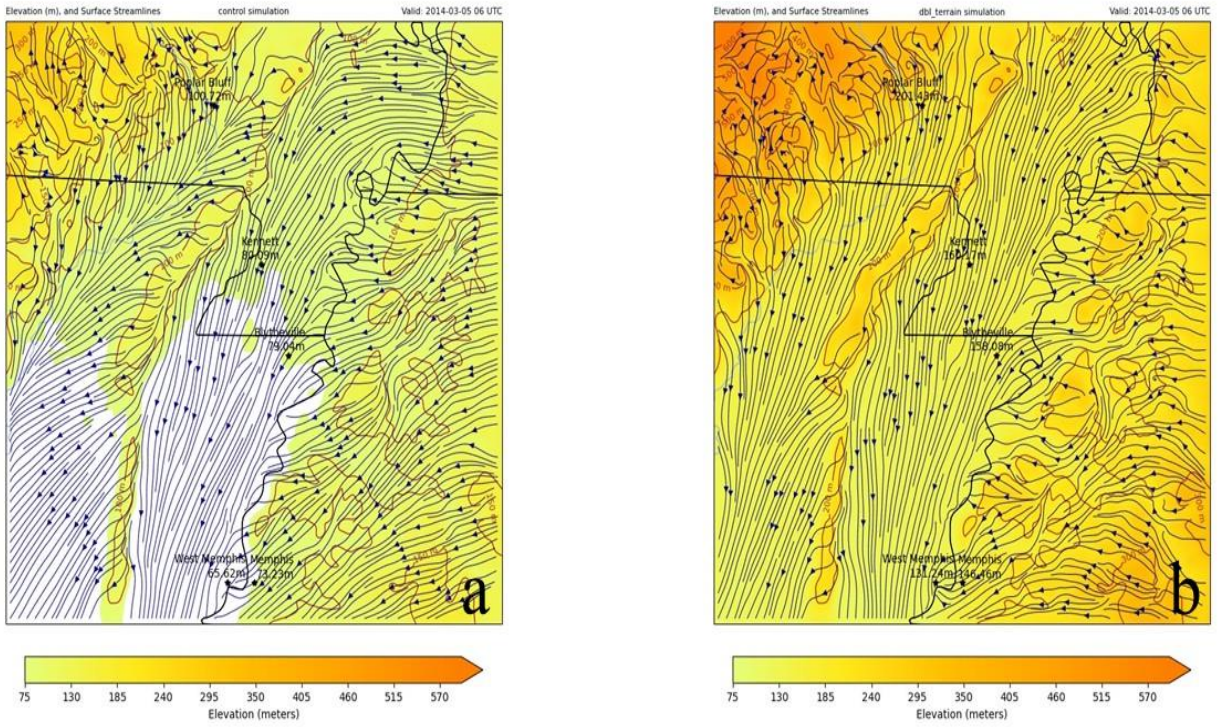

Figure 6.79 - d03 streamline maps from 0600 UTC on 05 March 2014. Map (a) is from the actual-terrain simulation runs. Map (b) is from the double-terrain simulation runs. Surface wind flow streamlines are featured in navy blue on each map. The elevation is shaded from 75 m up through 570 m. Topographic lines are featured in dark brown.

The coldest location on the d03 temperature maps (Figure 6.80) of the 0600 UTC time step occurred on the double-terrain simulation map (Fig. 6.80b) just to the east of the embedded ridge. The temperature field on each map indicated where the ridges were located as the temperature over the ridges was a few °C warmer than the flood plain on either side. Northerly 5-kt winds on the double-terrain simulation were observed in the flood plain where calm conditions were found on the actual-terrain simulation map (Fig. 6.80a). The "channeling effect" of the coldest air into the flood plain was very pronounced on the double-terrain simulation map, but less so on the actual-terrain simulation. On that simulation map the cold air was more widespread but still blocked from westward expansion by the Plateau.

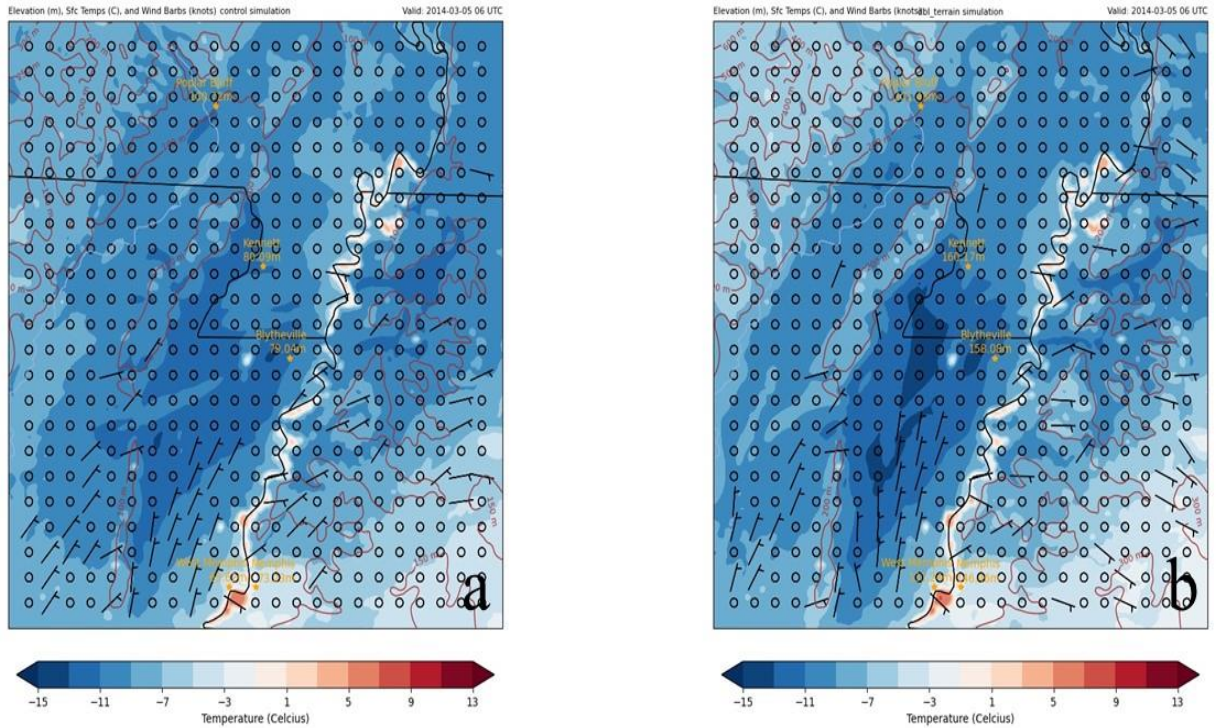

Figure 6.80 - d03 temperature maps from 0600 UTC on 05 March 2014. Each map features surface wind barbs (kts) in black, temperature shaded from blue to red from below -15°C up through 13°C. Topographic lines and values are featured on each map in dark brown.

6.2.3.7 1200 UTC 05 March 2014

The final time step of analysis at 1200 UTC 05 March 2014 resolved little evidence of the cold-air damming event in this comparison. The d02 streamline maps (Figure 6.81) showed northerly surface flow streaming down over the Ozark Plateau into the flood plain to the south. This would indicate that surface flow was no longer trapping cold air up against the escarpment of the Ozark Plateau.

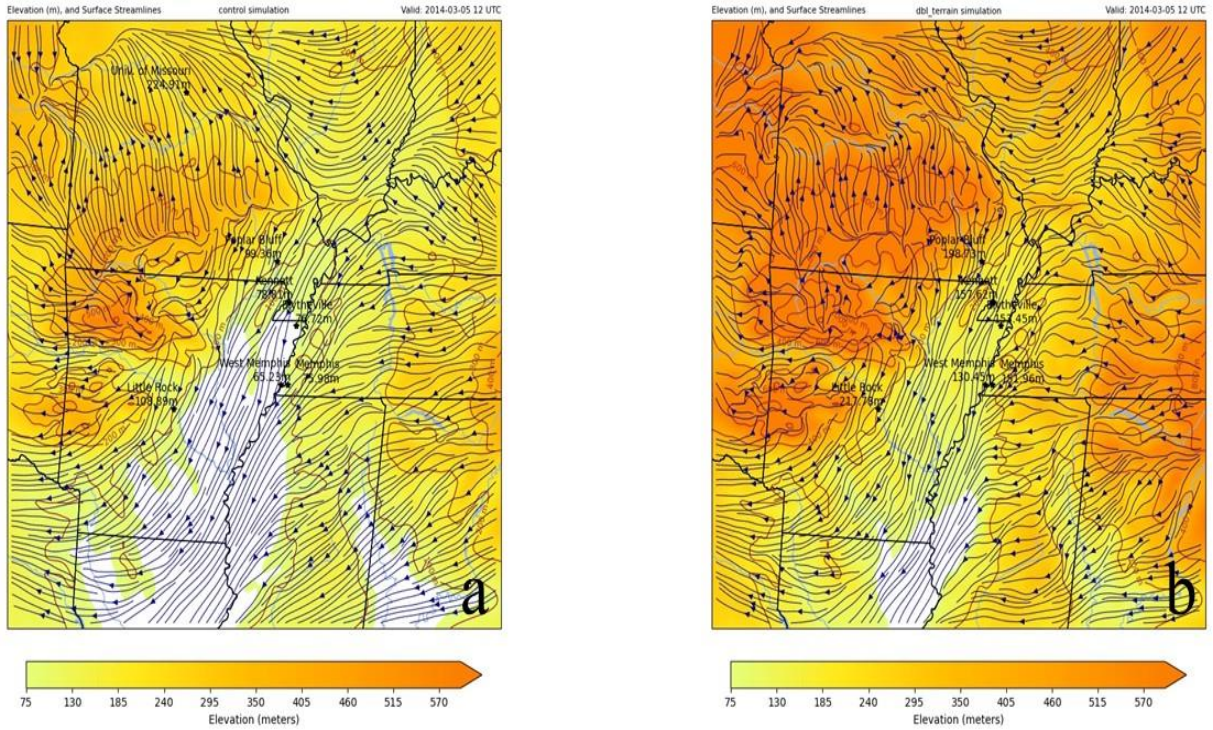

Figure 6.81 - d02 streamline maps from 1200 UTC on 05 March 2014. Map (a) is from the actual-terrain simulation run. Map (b) is from the double-terrain simulation run. Surface wind streamlines are depicted in navy blue on each map. The elevation heights are shaded from 75 m up through 570 m. Topographic lines are shaded in dark brown.

Diurnal processes helped to contribute to the coldest temperatures of the night observed on the d02 temperature maps (Figure 6.82). The cold pool pushing through the flood plain was observed on both simulation maps. The continued presence of cold air in the flood plain despite surface flow not being favorable for cold-air damming is attributed to the remaining snowpack to the north of the flood plain of eastern Arkansas. The elongated stretching of the coldest location indicated that the northerly winds were pushing the cold air deeper into the flood plain further south.

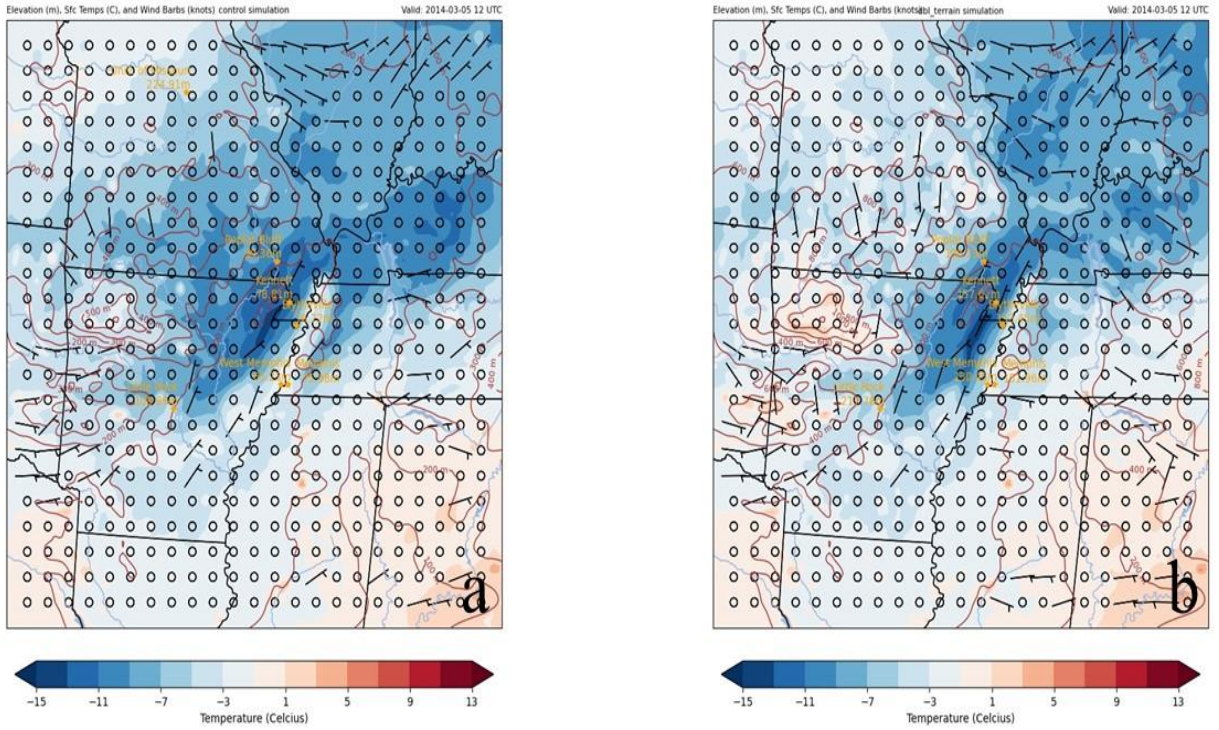

Figure 6.82 - d02 temperature maps from 1200 UTC on 05 March 2014. Each map features surface wind barbs (kts) in black, temperature shaded from blue to red from below -15°C up through 13°C. Topographic lines and values are featured on each map in dark brown.

The d03 streamline maps (Figure 6.83) focused on the region of interest reinforce what was analyzed on the d02 streamline maps (Figure 6.81) from the same time step in that surface flow was no longer conducive to cold-air damming. Little contrast between the 2 simulation maps observed here existed, though the streamlines were now crossing the embedded ridge on both simulation maps which was not seen in the previous time step.

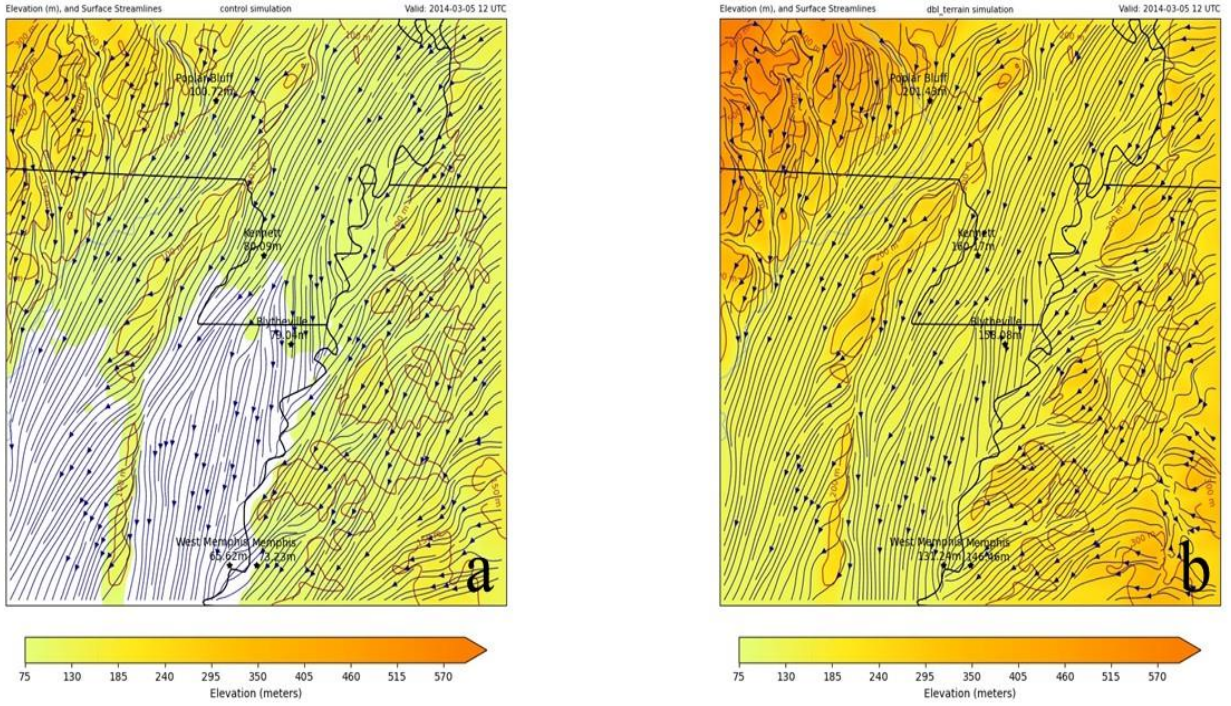

- *Figure 6.83 - d03 streamline maps from 1200 UTC on 05 March 2014. Map (a) is from the actual-terrain simulation runs. Map (b) is from the double-terrain simulation runs. Surface wind flow streamlines are featured in navy blue on each map. The elevation is shaded from 75 m up through 570 m. Topographic lines are featured in dark brown.*

The d03 temperature maps (Figure 6.84) showed the forcing of the coldest temperature areas down into the flood plain of the region of interest around the embedded ridges located on each simulation map. It is inferred that this is caused by the northerly flow (indicated on the simulation maps by the 10-m wind field) pushing the cold air down deeper into the flood plain. In previous analysis the streamlines showed the deviation of surface flow around the embedded ridges. On both simulation maps of this time step where wind barbs were observed they were oriented around the ridges.

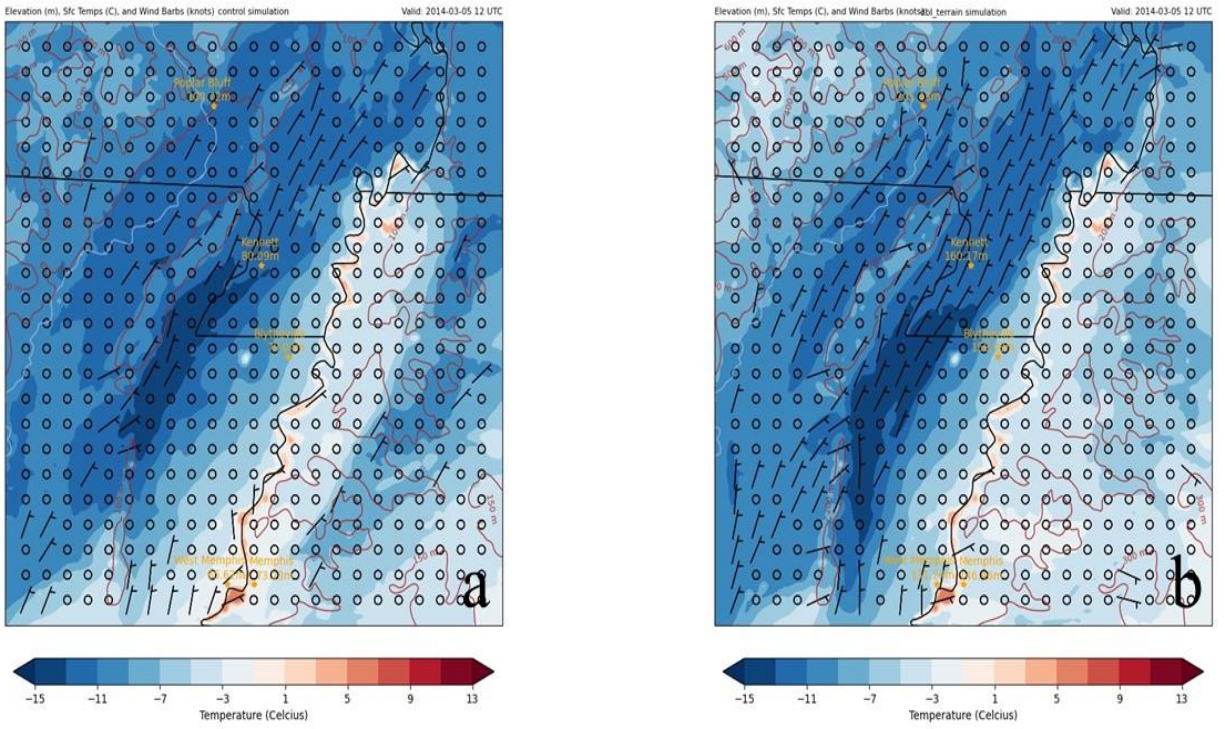

Figure 6.84 - d03 temperature maps from 1200 UTC on 05 March 2014. Each map features surface wind barbs (kts) in black, temperature shaded from blue to red from below -15°C up through 13°C. Topographic lines and values are featured on each map in dark brown.

6.2.4 04 March 2014 Results & Conclusions

The initial case study from March 2014 was chosen for the WRF modeling phase of research due to its profound impacts on the region and very pronounced features both synoptically and on the mesoscale. This proved to be true in the maps analyzed in the previous sections. What was unexpected were the various details about how and why this event came to be that came to light through the third phase of research.

The "channeling effect" mentioned multiple times in the comparative analysis of the d02 and d03 temperature maps perhaps became some of the most important visual evidence for the impact of elevation height on manipulation of the temperature field between the escarpment of the Ozark Plateau and the flood plain of the Mississippi River. The widespread nature of the coldest air on the no-terrain simulation temperature maps versus how the coldest air became confined and trapped within the flood plain as elevation height was increased through the other 3 simulation maps reinforced this evidence of elevation height influence on the temperature field. Furthermore, the "channeling" around the embedded ridges within the alluvial plain were a direct result of damming occurring at the northeastern point of each ridge. Early in the simulation the northeasterly surface flow helped to push the cold, moist air over the snowpack deeper into the flood plain further south. The d03 streamline maps, especially in the time steps before 1800 UTC on 04 March 2014, show how the streamlines are redirected or "channeled" around the ridges. While the areal region of damming was much smaller against the point of these ridges than later when directional flow shifted to a more terrain-orthogonal, in this case easterly component, the damming led to terrain-influenced channeling. This channeling was not apparent in the no-terrain simulations but did appear

in higher elevation simulations. This effect observed in the actual-terrain simulation temperature maps strongly suggested that the elevation of the Ozark Plateau helped to create a cold-air damming situation in which road surfaces become icy and impassable.

The d02 and d03 streamline maps provided insight into how 10-m wind flow could be manipulated by a sudden increase in elevation height. In particular, the embedded ridges within the flood plain just east of the escarpment of the Ozark Plateau and just west of the Blytheville, Arkansas station (KHKA) repeatedly deviated or disrupted the course of streamlines attempting to cross over the ridge. This deviation became stronger when wind speeds became calm and decreased when wind speeds increased. This disruption of the streamlines by the embedded ridges and the escarpment of the larger Plateau just to the northwest helped to slow any advective processes trying to overcome these terrain features.

Finally, the importance of the presence of the snowpack over the region of interest with larger accumulation totals to the north and northeast was evident in how the WRF model resolved this case through the times of impact. Comparative analysis began at 0000 UTC on 04 March 2014 when reports of icy conditions and stranded motorists were initiated. However, surface flow did not become terrain-orthogonal to create and maintain a cold-air damming event until early the following morning. It was the north-northeasterly flow from the parent anticyclone to the northeast that helped to advect cold, moist surface air from the larger snowpack to the northeast down into the flood plain of eastern Arkansas. Only after the directional shift of 10-m wind flow to a more easterly course in response to anticyclone migration occurred did the cold-air damming event truly happen. Model verification using observed surface conditions from both METAR

reports and meteorograms from several of the stations within the region of interest indicated that the WRF model correctly shifted the directional 10-m wind component at the correct times. Before this shift occurs, the constant funneling of cold, moist air into the region was inferred to be the impetus for hazardous conditions. The occurrence of the cold-air damming within the region prolonged the event into the following morning.

6.3 27 November 2016 Case Study

The second case study used for WRF modeling analysis took place on 27 November 2016. The point location for this cold-air damming event was the Kennett, Missouri station (KTKX) just north of the Blytheville, Arkansas station over the state border into Missouri. METAR reports of present weather conditions began at 23:55 UTC on 26 November 2016 with mist (BR) observed at that time. Mist observations turned to fog (FG) and eventually freezing fog (FZFG) by 0815 UTC as temperatures overnight fell just below freezing. Reports of freezing fog, fog, and mist continued until 1455 UTC 27 November 2016. Based on these METAR observations, analysis of WRF modeling simulations took place between 0000 UTC of 27 November 2016 and 1800 UTC on 27 November 2016.

Table 6.1 - The cold-air damming characteristics for the 27 November 2016 cold-air damming event. These conditions were analyzed in the second phase of research in which potential cases were scrutinized to determine if cold-air damming was occurring. Red indicates that the characteristic was satisfied for the presence of cold-air damming. Green indicates that the characteristic was not satisfied, and cold-air damming was not occurring.

27 November 2016 Case	**Station: KTKX**
Parameter	**Grade**
Anticyclone Placement	
Terrain Orthogonal Wind	
Sounding Inversion	
Sounding Surface Wind	
Radar Reflectivity	
Froude Number	
Surface Moisture	
Surface Temperatures	
Cloud Cover	

This case was identified during the second phase of research in which a 5-year period was analyzed for the identification of Ozark Plateau induced cold-air damming events. The 27 November 2016 event was eventually classified as a yellow case. Table 6.1 shows how the potential cold-air damming event was analyzed. The first 6 characteristics listed were all satisfied (red) indicating that cold-air damming was taking place. However, during the impactful characteristic analysis the 2-m temperature characteristic was not satisfied meaning cold-air damming while occurring did not impact surface conditions in an adverse way.

The synoptic setup for this event placed a high-pressure system centered over the region of interest at 1200 UTC on 26 November 2016 (Fig. 6.85a) and again shifted just south into northeastern Arkansas at 1800 UTC on 26 November 2016 (Fig. 6.85b).

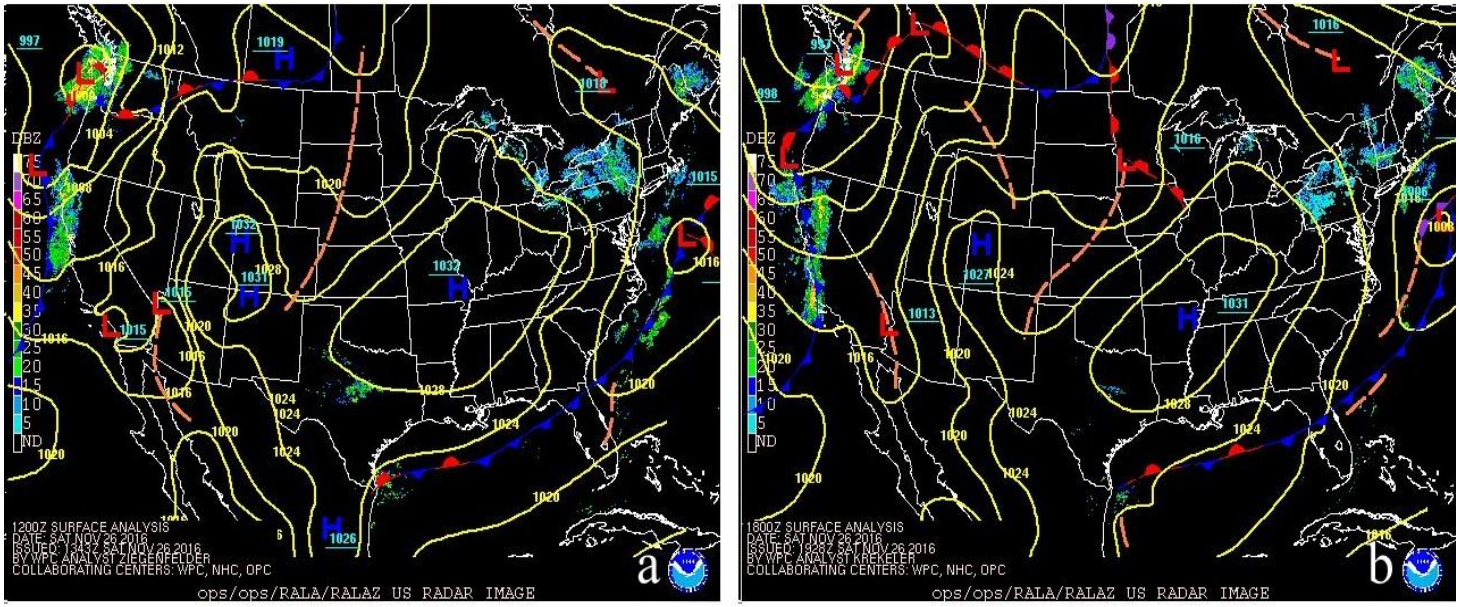

Figure 6.85 - A radar-overlayed surface pressure map from the 27 November 2016 case study. Map (a) is the surface pressure map at 1200 UTC on 26 November 2016. Map (b) is the 1800 UTC surface pressure map on 26 November 2016. The solid yellow lines are isobars with associated blue H's representing centers of high pressure and red L's symbolic of centers of low pressure. These surface maps also contain traditional frontal symbols with blue-pipped lines representing cold fronts, red-pipped lines representing warm fronts, alternating red-blue pipped lines for stationary fronts, and orange dashed lines for shortwaves. An overlaid radar composite taken from the National Weather Service's network of WSR-88D radar stations depicts areas of precipitation across the CONUS from 0 to 75 decibels (dBz). Chart courtesy of NOAA/NWS.

By 0000 UTC on 27 November 2016 (Fig. 6.86a) the surface pressure map depicted eastward transition of the anticyclone into central Tennessee/eastern Kentucky. This repositioning of the high-pressure center opened the region of interest up to the system's western flank. This resolved southerly flow and terrain-orthogonal 10-m winds over the Kennett, Missouri station. The timing of this 10-m wind flow directional shift coincided with the METAR report observing cold-air damming type conditions. This positioning of the high-pressure center continued through 0600 UTC on 27 November 2016 (Fig. 6.86b).

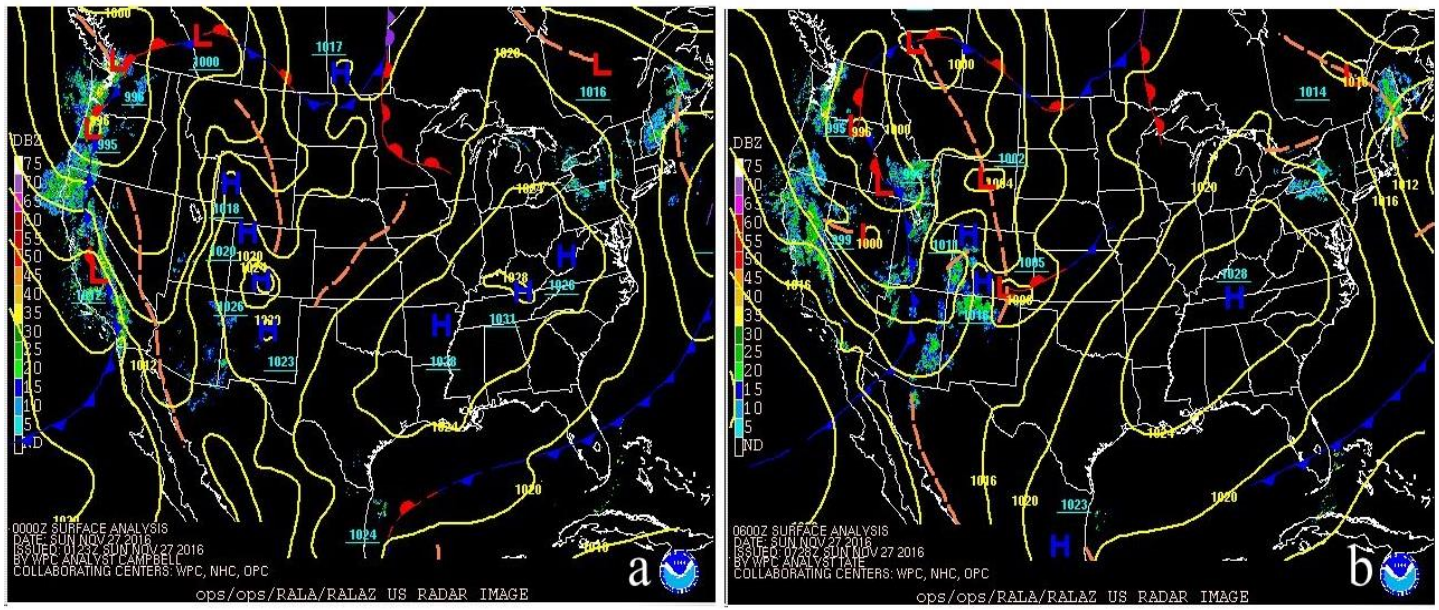

Figure 6.86 - A radar-overlayed surface pressure map from the 27 November 2016 case study. Map (a) is the surface pressure map at 0000 UTC on 27 November 2016. Map (b) is the 0600 UTC surface pressure map on 27 November 2016. The solid yellow lines are isobars with associated blue H's representing centers of high pressure and red L's symbolic of centers of low pressure. These surface maps also contain traditional frontal symbols with blue-pipped lines representing cold fronts, red-pipped lines representing warm fronts, alternating red-blue pipped lines for stationary fronts, and orange dashed lines for shortwaves. An overlaid radar composite taken from the National Weather Service's network of WSR-88D radar stations depicts areas of precipitation across the CONUS from 0 to 75 decibels (dBz). Chart courtesy of NOAA/NWS.

By 1200 UTC on 27 November 2016, the cold-air damming event occurring in the bootheel of Missouri continued. The anticyclone by this time step had begun to push to the east over the mid-Atlantic coastal areas (Fig. 6.87a). The region of interest was now being influenced by the western flank of the high-pressure center to the east as well as the eastern edge of a low-pressure system strengthening to the west over the high plains of Colorado. By 1800 UTC on 27 November 2016, approximately 3 hours after the last observed report of cold-air damming surface conditions, the anticyclone was observed over the mid-Atlantic region and the low-pressure system to the west was pushing into western Kansas.

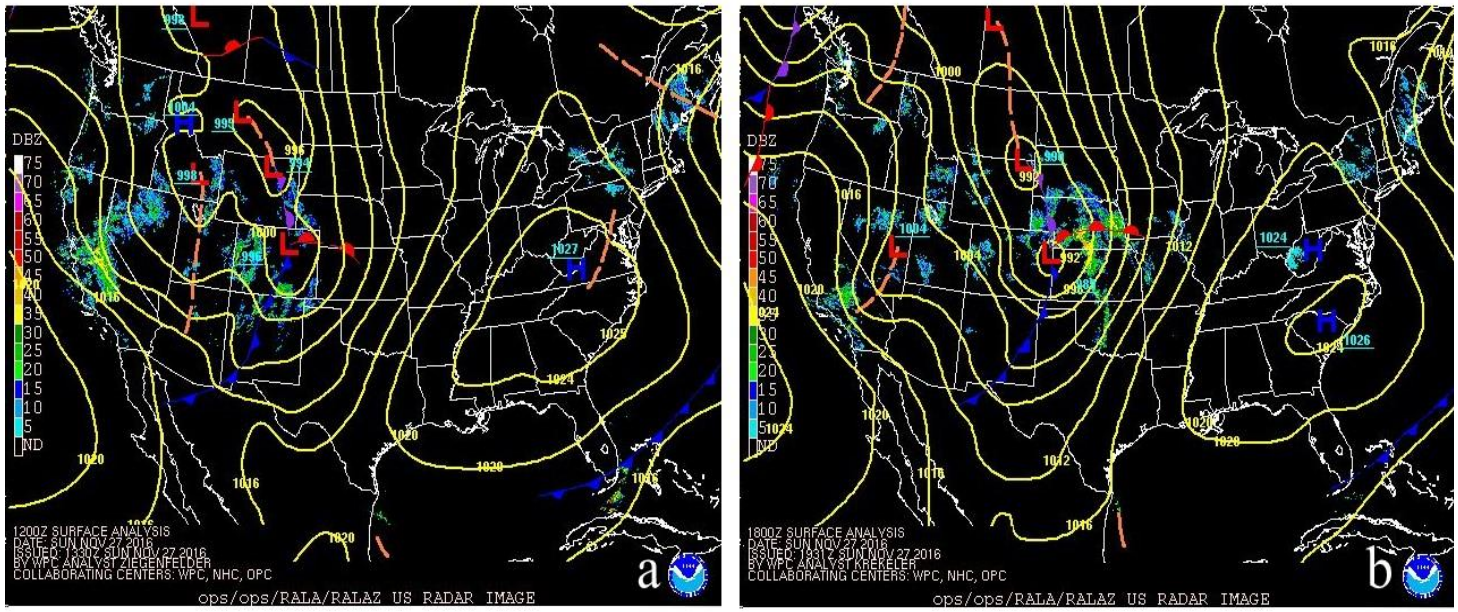

Figure 6.87 - A radar-overlayed surface pressure map from the 27 November 2016 case study. Map (a) is the surface pressure map at 1200 UTC on 27 November 2016. Map (b) is the 1800 UTC surface pressure map on 27 November 2016. The solid yellow lines are isobars with associated blue H's representing centers of high pressure and red L's symbolic of centers of low pressure. These surface maps also contain traditional frontal symbols with blue-pipped lines representing cold fronts, red-pipped lines representing warm fronts, alternating red-blue pipped lines for stationary fronts, and orange dashed lines for shortwaves. An overlaid radar composite taken from the National Weather Service's network of WSR-88D radar stations depicts areas of precipitation across the CONUS from 0 to 75 decibels (dBz). Chart courtesy of NOAA/NWS.

6.3.1 Actual-Terrain versus No-Terrain Comparison

In keeping consistent with previous WRF modeling analysis, the first comparison of the 27 November 2016 cold-air damming event was between the actual-terrain simulation and the no-terrain simulations performed on this event. The d02 and d03 domains were unchanged from the previous case study analysis as the point location station for this 27 November 2016 case study: Kennett, Missouri is located only a few miles north of the previous case studies point location: Blytheville, Arkansas. Due to the timing of METAR reports observing cold-air damming conditions from the Kennett, Missouri ASOS station, analysis time steps began at 0000 UTC on 27 November 2016 concluded at the 1800 UTC 27 November 2016 time step.

6.3.1.1 0000 UTC 27 November 2016

Analysis of this cold-air damming event began with the d02 regional streamline maps (Figure 6.88) analysis of 0000 UTC on 27 November 2016. Both the actual-terrain and no-terrain simulation maps featured a col point located just west of the West Memphis, Arkansas station over the region of interest. This col point on each map created southerly flow over the Kennett, Missouri station on each map in response to the placement of the parent anticyclone to the east over Tennessee. To the south and southeast of the col point northerly flow was found on both simulation maps. Little contrast in the streamline fields was observed at this time step.

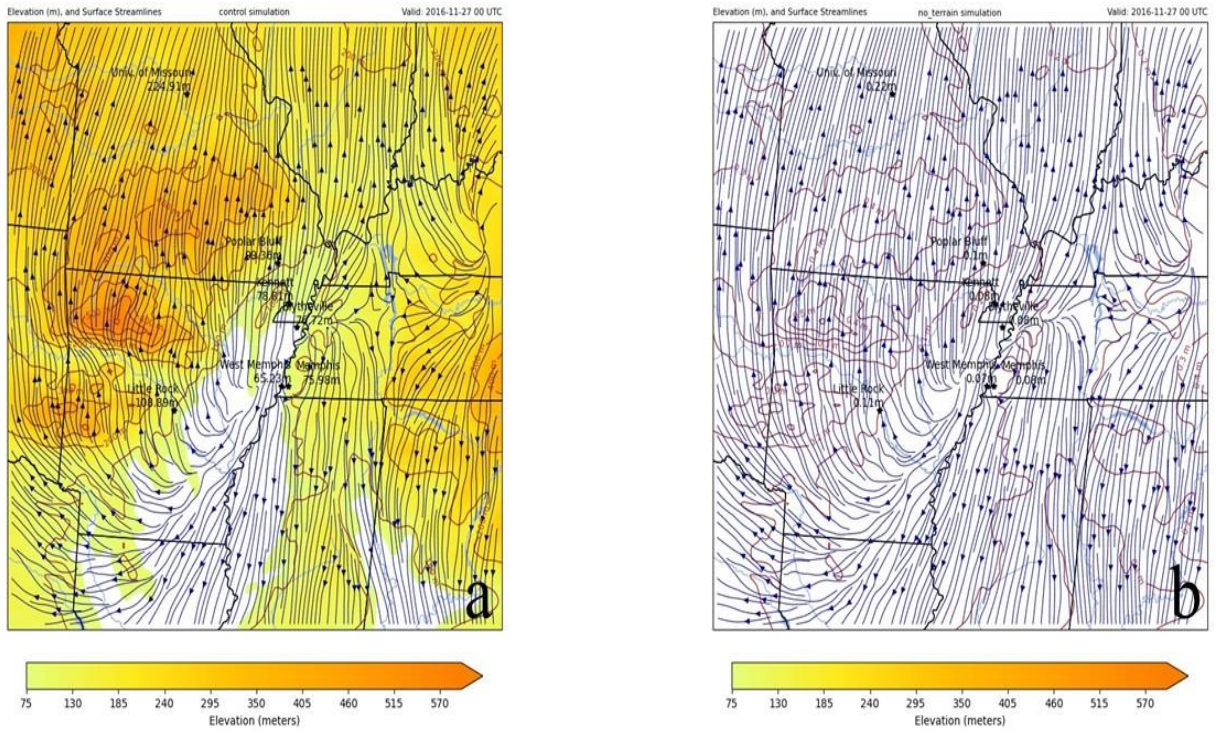

Figure 6.88 - d02 streamline maps from 0000 UTC on 27 November 2016. Map (a) is from the actual-terrain simulation run. Map (b) is from the no-terrain simulation run. Surface wind streamlines are depicted in navy blue on each map. The elevation heights are shaded from 75 m up through 570 m. Topographic lines are shaded in dark brown.

Warmer colors representing above-freezing temperatures on the d02 regional temperature maps (Figure 6.89) on both simulation maps were observed at the 0000 UTC time step. Relatively colder temperatures existed in the northeastern quadrant of the regional maps, but there was contrast in the temperature fields found on the simulation maps. On the actual-terrain simulation (Fig. 6.89a) the colder air filtered into the Ozark Plateau of southern Missouri. That was not the case on the no-terrain simulation map (Fig. 6.89b) where the colder air was mainly east of Missouri into southern Illinois and did not infiltrate further west. Little contrast was seen in the 10-m wind field of each simulation map. 5-kt southerly winds were observed in the northern portions of both simulation maps with calm conditions over the southern half of each map.

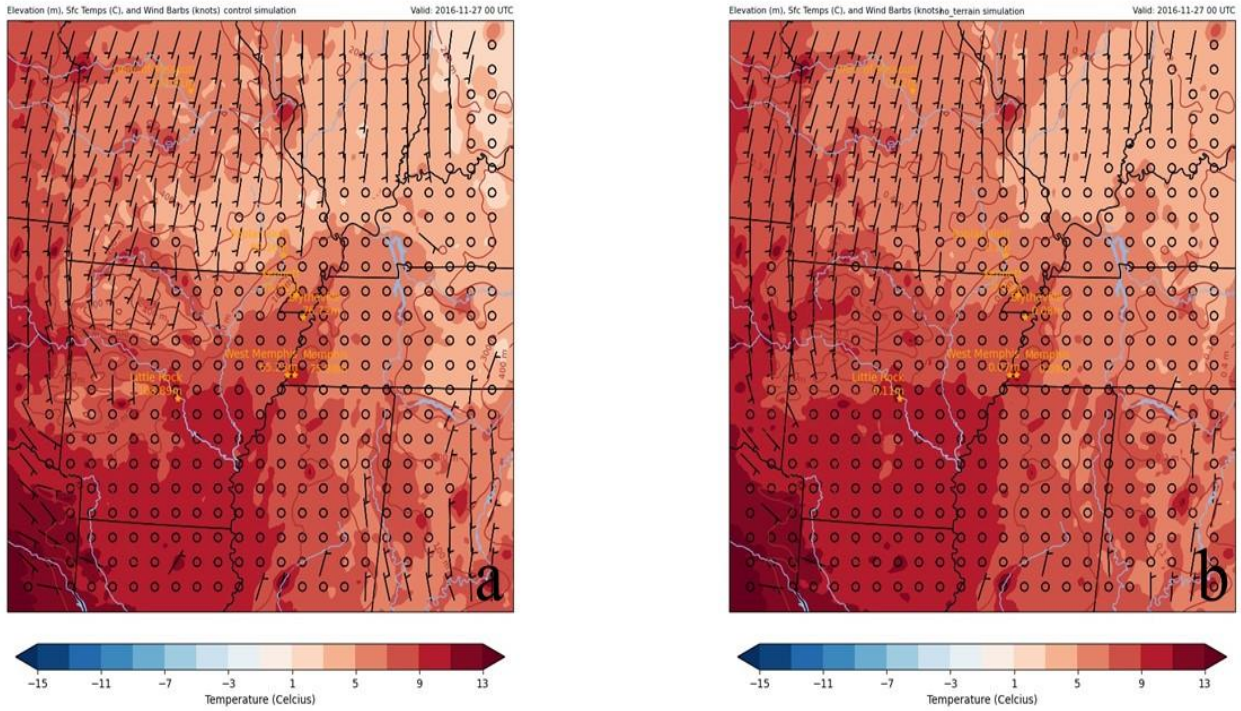

Figure 6.89 - d02 temperature maps from 0000 UTC on 27 November 2016. Each map features surface wind barbs (kts) in black, temperature shaded from blue to red from below -15°C up through 13°C. Topographic lines and values are featured on each map in dark brown.

The col point in the streamline fields of the d02 streamline maps from the 0000 UTC time step (Figure 6.88) was observed on the d03 streamline maps just to the west-northwest of the West Memphis, Arkansas station. Streamline fields were similar on both d03 streamline maps, save for some interaction with the embedded ridges found in the flood plain. Like the previous case study, the no-terrain simulation (Fig. 6.90b) featured smooth, uniform streamline flow over the ridges (or lack thereof in this simulated case). The actual-terrain simulation map (Fig. 6.90a), however, featured deviations of 10-m wind flow over and around the embedded ridges of the flood plain.

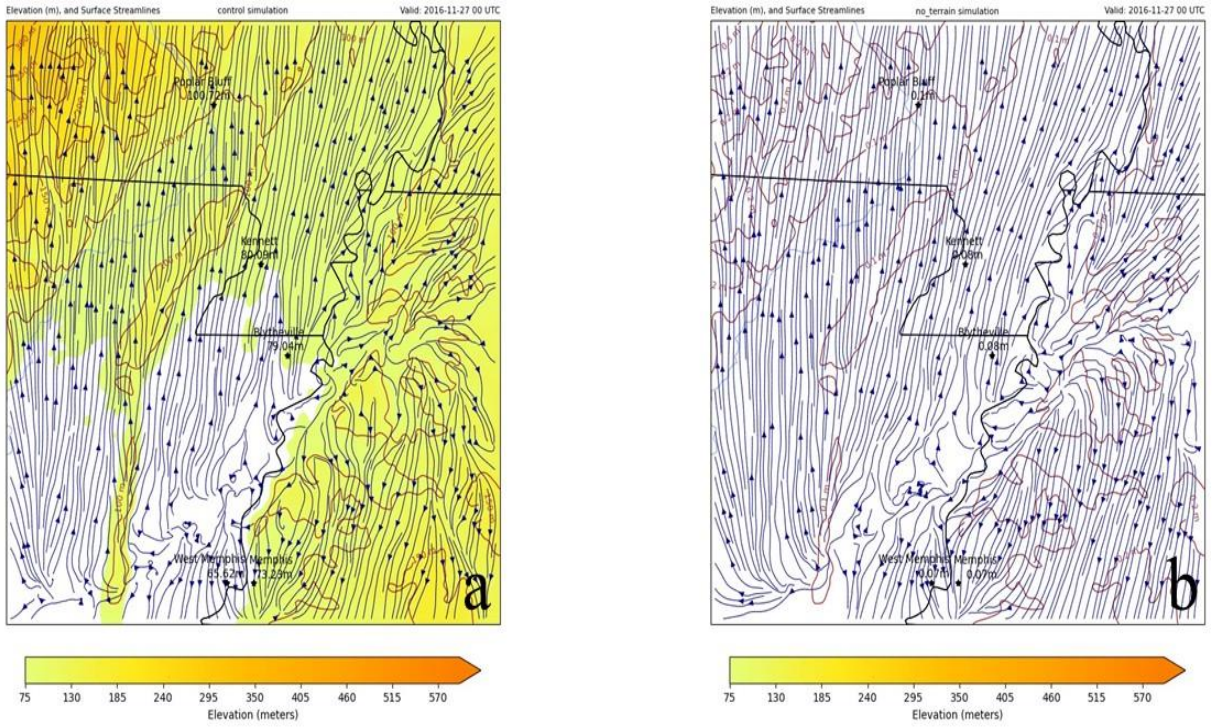

Figure 6.90 - d03 streamline maps from 0000 UTC on 27 November 2016. Map (a) is from the actual-terrain simulation runs. Map (b) is from the no-terrain simulation runs. Surface wind flow streamlines are featured in navy blue on each map. The elevation is shaded from 75 m up through 570 m. Topographic lines are featured in dark brown.

Similar temperature fields on each simulation of the d03 temperature maps (Figure 6.91), save for the extreme northwestern portion of the grid over the Plateau, were observed at 0000 UTC. On the no-terrain simulation map (Fig. 6.91b) the wind field was calm except for 3 grid points in which southerly 5-kt winds were found. The actual-terrain simulation map (Fig. 6.91a) featured more northerly winds in the northern portion of the simulated map. In that same area, the colder air seen on the regional temperature maps previously was seen again on the actual-terrain simulation d03 temperature map and not on the no-terrain simulation map.

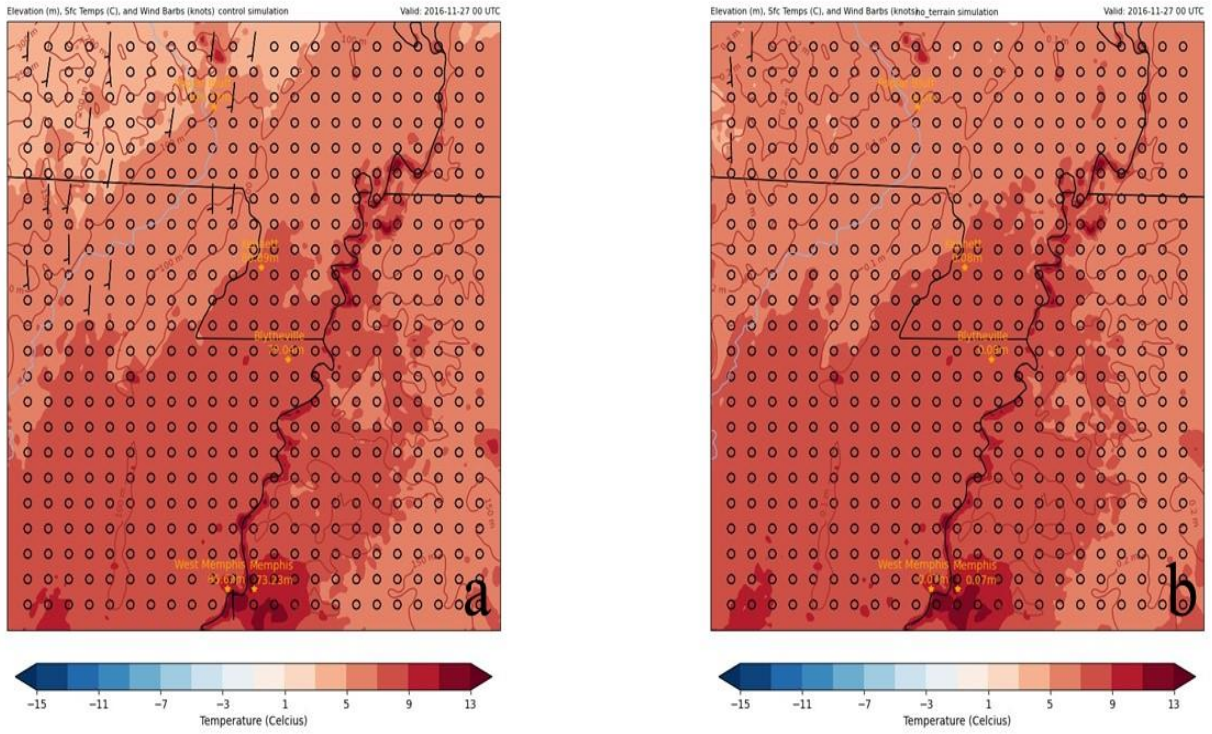

Figure 6.91 - d03 temperature maps from 0000 UTC on 27 November 2016. Each map features surface wind barbs (kts) in black, temperature shaded from blue to red from below -15°C up through 13°C. Topographic lines and values are featured on each map in dark brown.

6.3.1.2 0600 UTC 27 November 2016

As day transitioned to night the 0600 UTC time step showed a shift in streamlined surface flow on the d02 regional streamline maps (Figure 6.92). The col point viewed on the regional streamline maps 6 hours previously had shifted to the east over Tennessee. This opened the region of interest up to southerly flow throughout the flood plain on both simulation maps. Less contrast between simulations existed on the regional streamline maps as the deviation in surface flow due to elevation value differences occurred at a finer scale than what the d02 domain possessed. Both of these simulation maps highlighted the western flank of the parent anticyclone influencing the 10-m wind flow over the central and northern portions of both simulation streamline maps.

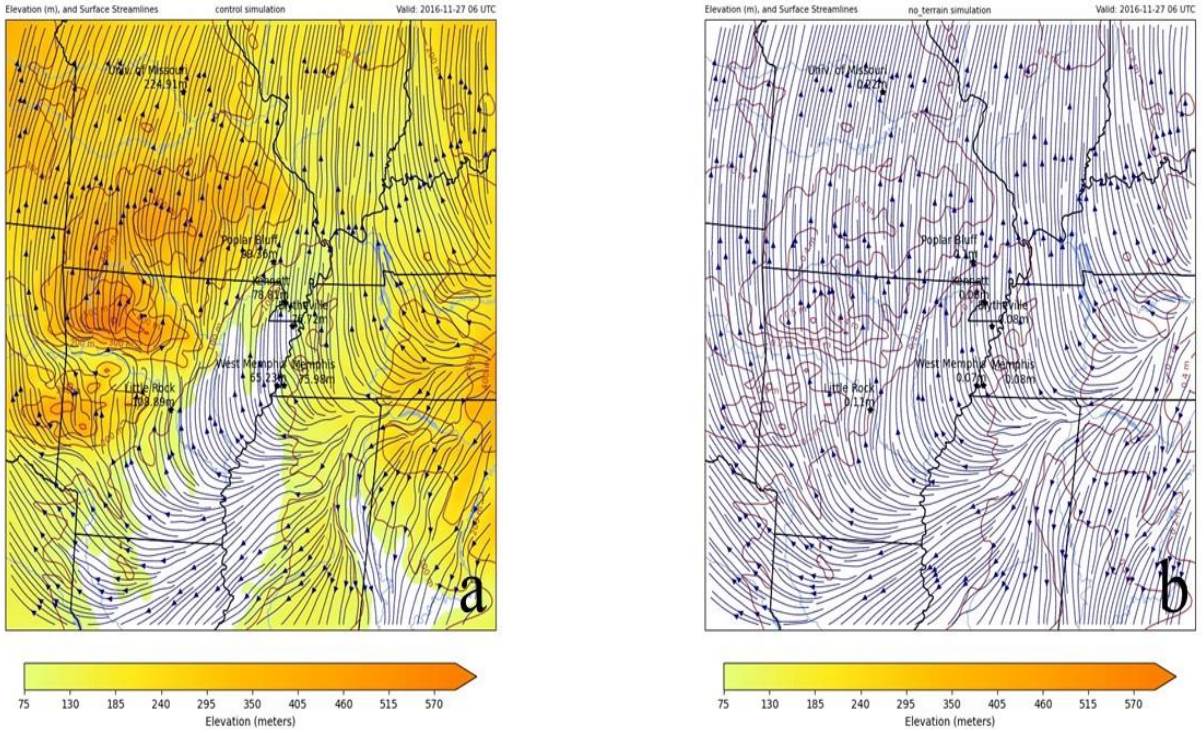

Figure 6.92 - d02 streamline maps from 0600 UTC on 27 November 2016. Map (a) is from the actual-terrain simulation run. Map (b) is from the no-terrain simulation run. Surface wind streamlines are depicted in navy blue on each map. The elevation heights are shaded from 75 m up through 570 m. Topographic lines are shaded in dark brown.

Diurnal processes helped to cool off the temperature fields observed in the d02 regional temperature maps (Figure 6.93) of 0600 UTC on 27 November 2016. Temperatures had fallen to near freezing in the eastern half of both simulated maps. Near the point location within the region of interest temperatures had fallen to around 3°C despite METAR reports expressing freezing conditions. This may have been the WRF model resolving temperatures a 1-2°C too warm, though the case study did not satisfy 2-m temperatures being below freezing in phase two of research involving the 5-year study. The elevation of the Ozark Plateau does manipulate some of the colder temperatures on the actual-terrain simulation map (Fig. 6.93a) into a more westerly direction as opposed to the lack of elevation on the no-terrain simulation (Fig. 6.93b) in which the colder temperatures filter further south into central Arkansas. The 10-m wind fields are very similar with 5-kt southerly winds over the northwestern half of the maps and calm conditions to the southeast.

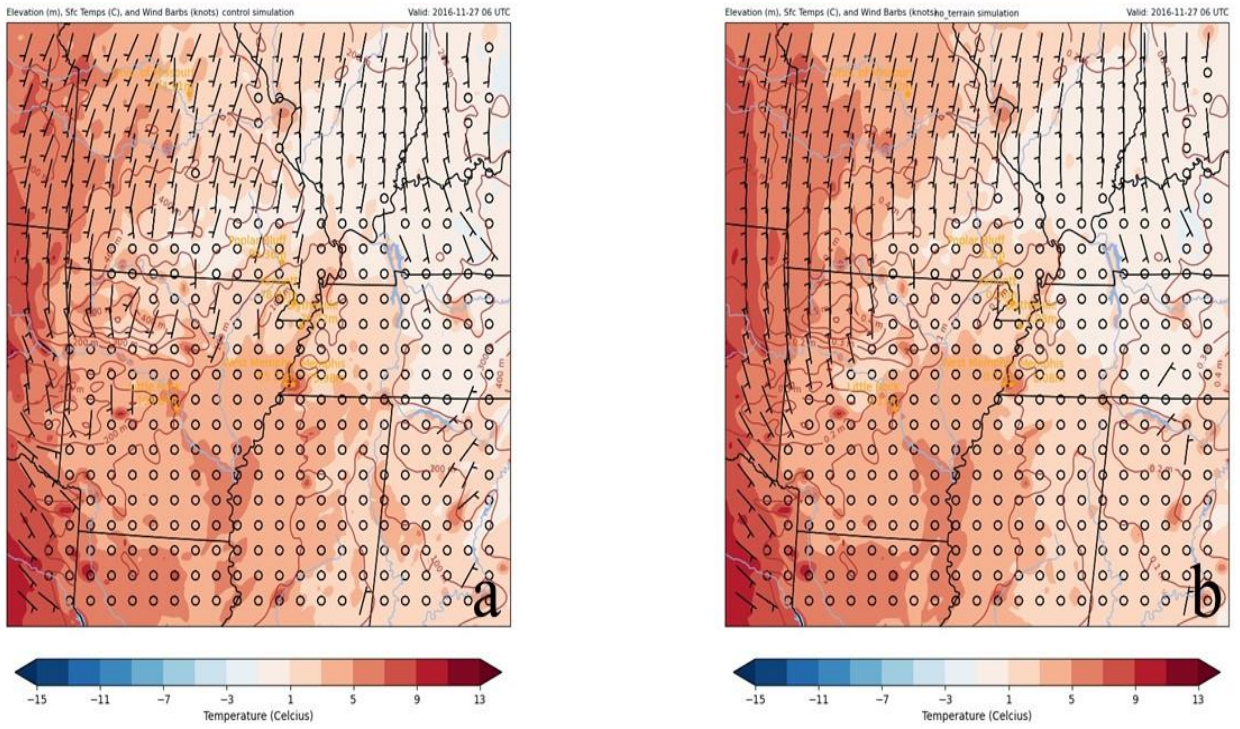

Figure 6.93 - d02 temperature maps from 0600 UTC on 27 November 2016. Each map features surface wind barbs (kts) in black, temperature shaded from blue to red from below -15°C up through 13°C. Topographic lines and values are featured on each map in dark brown.

The d03 streamline maps (Figure 6.94) of this time step showed more contrast in the 10-m wind flow than what was observed on its d02 regional counterpart from the 0600 UTC time step. Deviation existed over the embedded ridges on the actual-terrain simulation (Fig. 6.94a), specifically over the southern point of larger ridge in extreme northeastern Arkansas. Streamlines were deflected around the ridge rather than over them in a smooth, uniform way as observed on the no-terrain simulation (Fig. 6.94b). Streamlines were disrupted and deflected over the elevation of the Plateau to the northwest on the actual-terrain simulation where surface flow was more organized on the no-terrain simulation. The southerly directional component of the streamlines on both maps was favorable for cold-air damming.

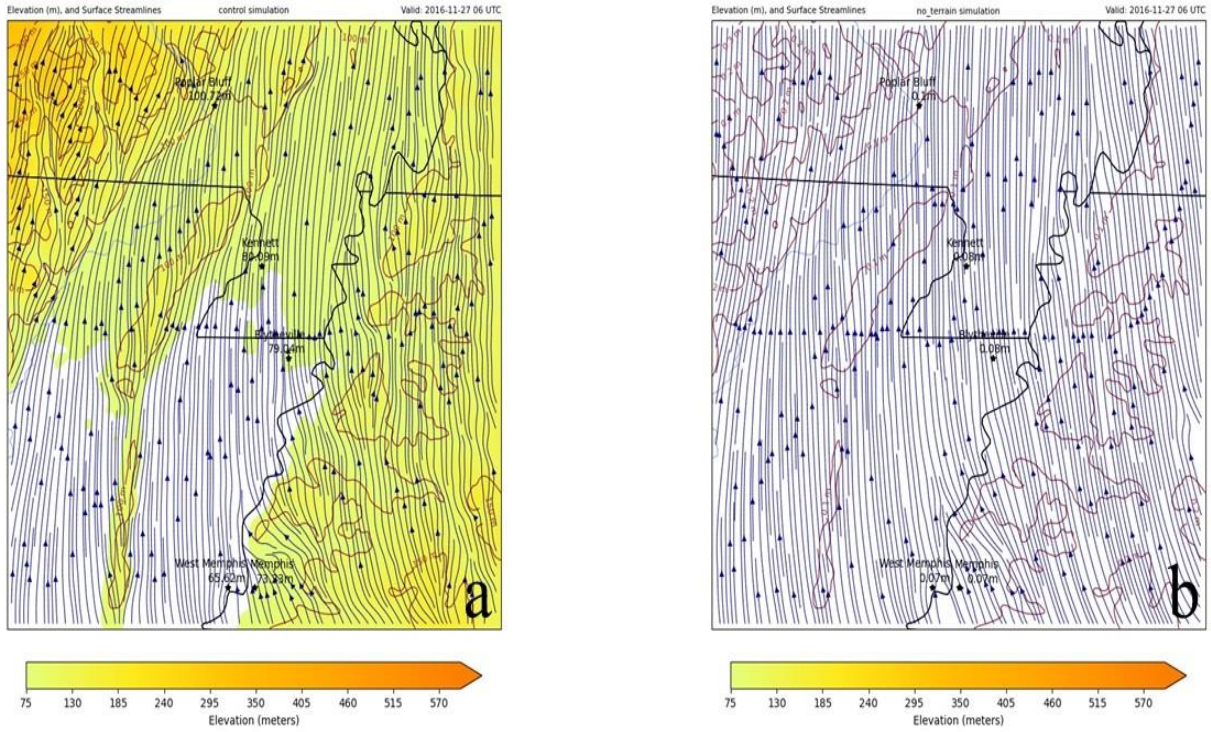

Figure 6.94 - d03 streamline maps from 0600 UTC on 27 November 2016. Map (a) is from the actual-terrain simulation runs. Map (b) is from the no-terrain simulation runs. Surface wind flow streamlines are featured in navy blue on each map. The elevation is shaded from 75 m up through 570 m. Topographic lines are featured in dark brown.

The 0600 UTC d03 temperature maps (Figure 6.95) for this comparison resolved some differences in the 10-m wind field. The 5-kt winds on the no-terrain simulation (Fig. 6.95b) were more widespread across the region of interest than its actual-terrain counterpart (Fig. 6.95a). On that actual-terrain simulation the winds near the embedded ridge showed the deflection seen previously on the d03 streamline actual-terrain simulation map (Fig. 6.94a). The temperature fields did not show much contrast on the d03 maps as was observed on the d02 maps. Both temperature fields had cooled significantly due to diurnal processes at the 0600 UTC time step.

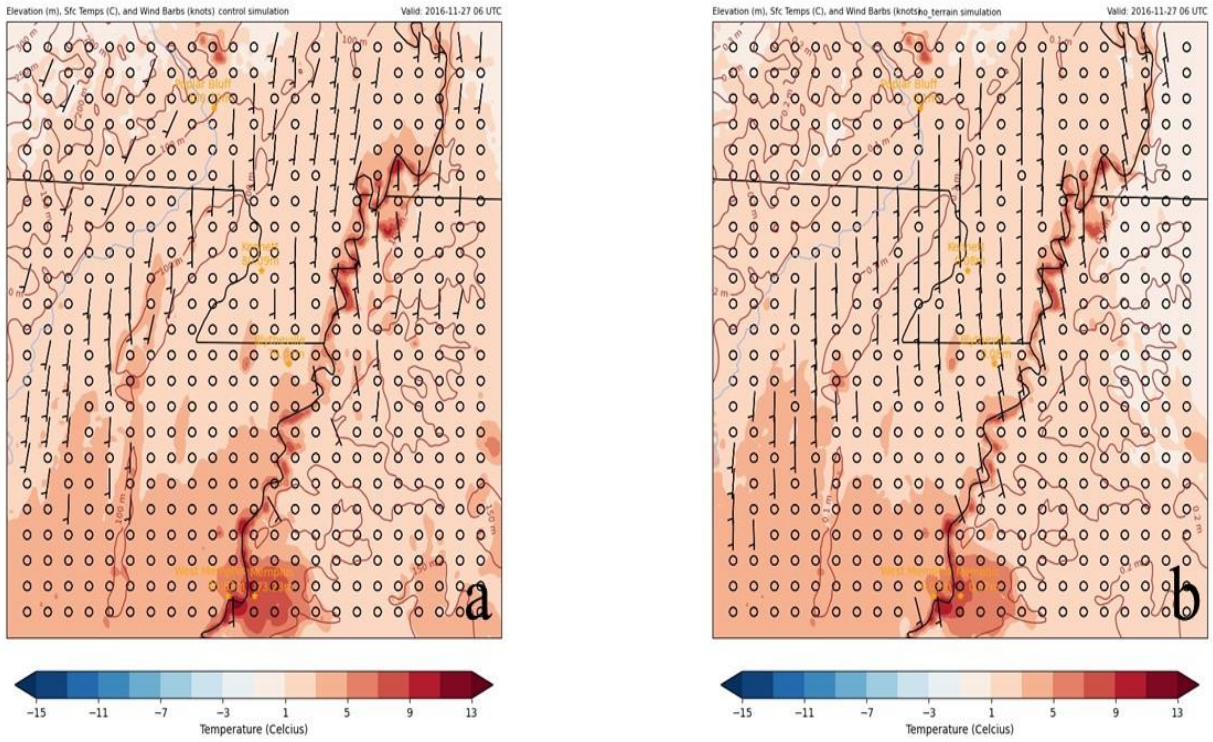

Figure 6.95 - d03 temperature maps from 0600 UTC on 27 November 2016. Each map features surface wind barbs (kts) in black, temperature shaded from blue to red from below -15°C up through 13°C. Topographic lines and values are featured on each map in dark brown.

6.3.1.3 1200 UTC 27 November 2016

Just before daybreak on 27 November the d02 regional streamline maps (Figure 6.96) showed little difference in 10-m wind flow from 6 hours previous as southerly flow continued to be observed over much of the region. This was mainly in response to the high-pressure center to the east over central Tennessee/central Kentucky moving very little overnight. The western flank of the anticyclone continued to impose its southerly influence on the region of interest. Little contrast on a regional scale between the actual-terrain and the no-terrain simulation maps was observed.

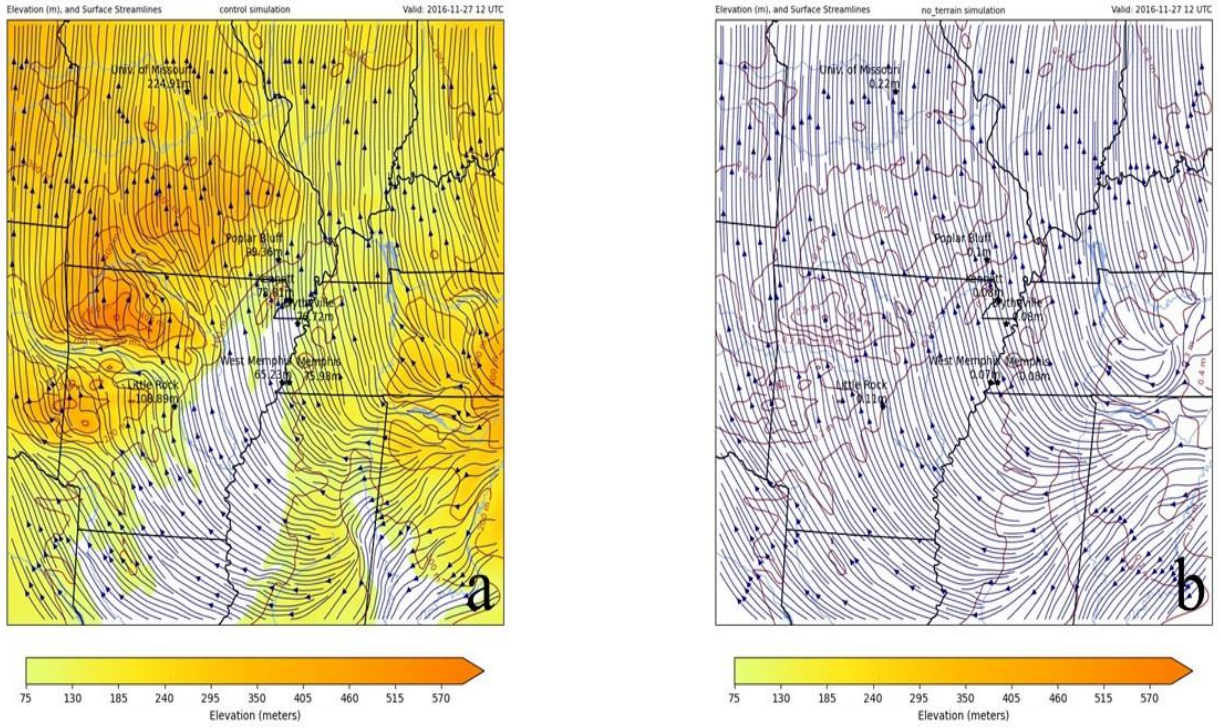

Figure 6.96 - d02 streamline maps from 1200 UTC on 27 November 2016. Map (a) is from the actual-terrain simulation run. Map (b) is from the no-terrain simulation run. Surface wind streamlines are depicted in navy blue on each map. The elevation heights are shaded from 75 m up through 570 m. Topographic lines are shaded in dark brown.

Much like the regional streamline maps, the 10-m wind field viewed on the no-terrain simulation d02 temperature map (Fig. 6.97b) was very organized and uniform where wind barbs did exist. The northwestern half of the map held 5-kt winds, and it was evident that the flow on the simulation maps was southerly. On the actual-terrain simulation (Fig. 6.97a) over the Ozark Plateau there was some directional shifting as the elevation deflected 10-m wind flow away from the mainly southerly course. Warm temperatures over the extreme western side of both simulation maps turned colder to the east with freezing to just below-freezing temperatures viewed in the region of interest over southeastern Missouri and northeastern Arkansas. Colder temperatures existed further west on the actual-terrain map which was not observed on its no-terrain simulation counterpart.

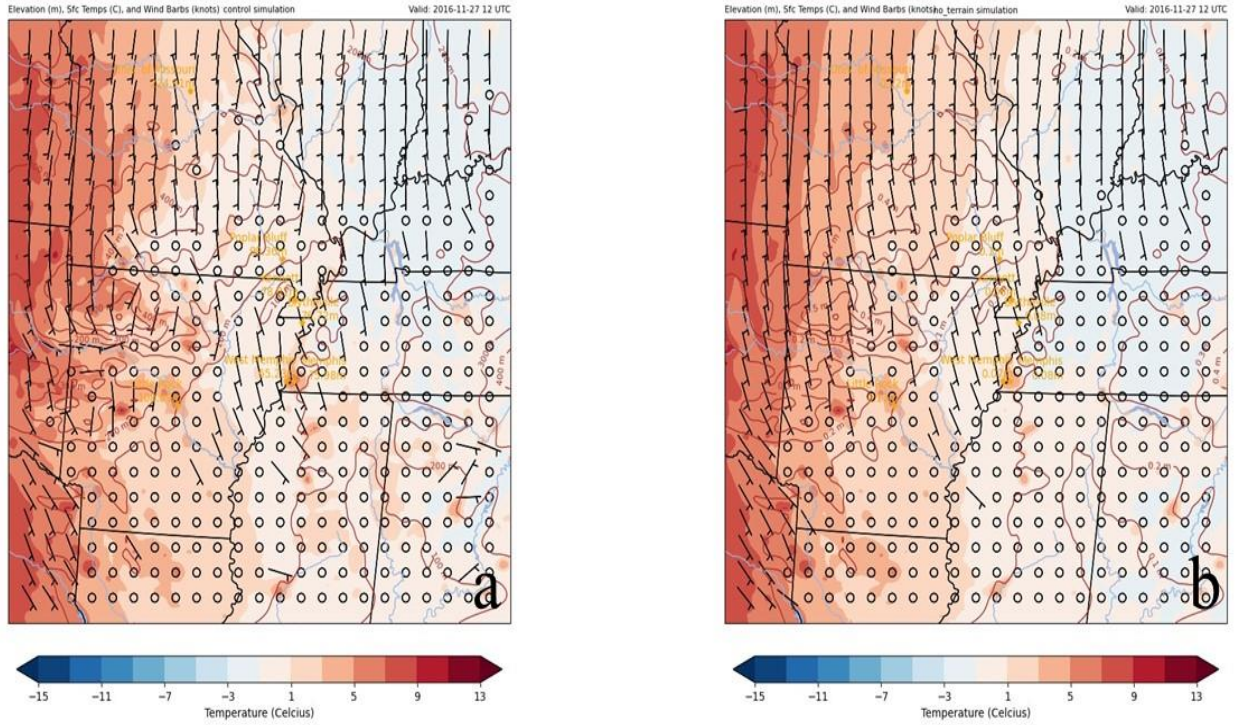

Figure 6.97 - d02 temperature maps from 1200 UTC on 27 November 2016. Each map features surface wind barbs (kts) in black, temperature shaded from blue to red from below -15°C up through 13°C. Topographic lines and values are featured on each map in dark brown.

Due to the stagnant movement of the parent anticyclone the d03 streamline maps from 1200 UTC on 27 November 2016 resolved similar observations to the d03 streamline maps from 6 hours previous. Southerly terrain-orthogonal flow was viewed over the region of interest and continued to be advantageous for cold-air damming. Deviation over the embedded ridges was observed on the actual-terrain simulation map from this time step (Fig. 6.98a). Organized wind flow over the ridges on the no-terrain simulation map continued into the morning hours.

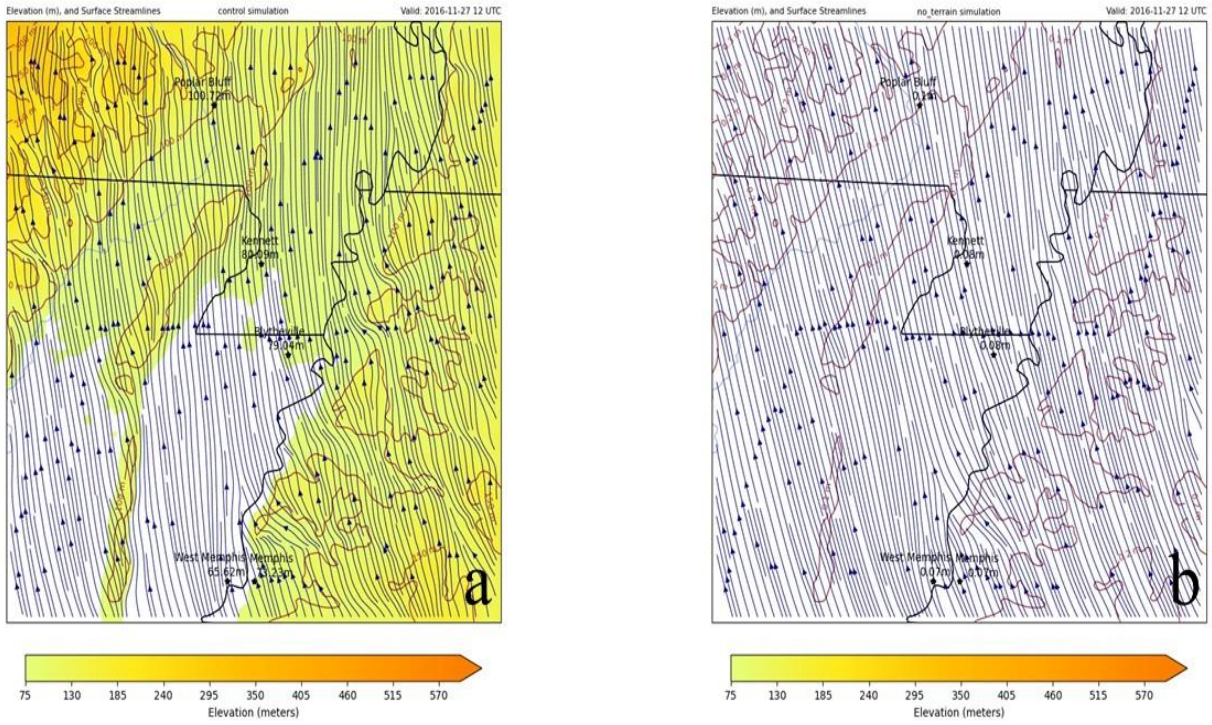

Figure 6.98 - d03 streamline maps from 1200 UTC on 27 November 2016. Map (a) is from the actual-terrain simulation runs. Map (b) is from the no-terrain simulation runs. Surface wind flow streamlines are featured in navy blue on each map. The elevation is shaded from 75 m up through 570 m. Topographic lines are featured in dark brown.

The d03 temperature maps (Figure 6.99) from 1200 UTC on 27 November contained similar temperature fields for each simulation map. The warm to cold temperature gradient was observed with slightly warmer temperatures over the western edge of the maps and colder temperatures further east as viewed on the previous d02 temperature maps. The 10-m wind field contained 5-kt southerly winds on the no-terrain map which was not observed on its actual-terrain simulation counterpart. On the actual-terrain simulation map more calm conditions, especially on the eastern side of the embedded ridge, were observed. This may have been a result of elevation influence occurring as it was not evident on the no-terrain simulation map.

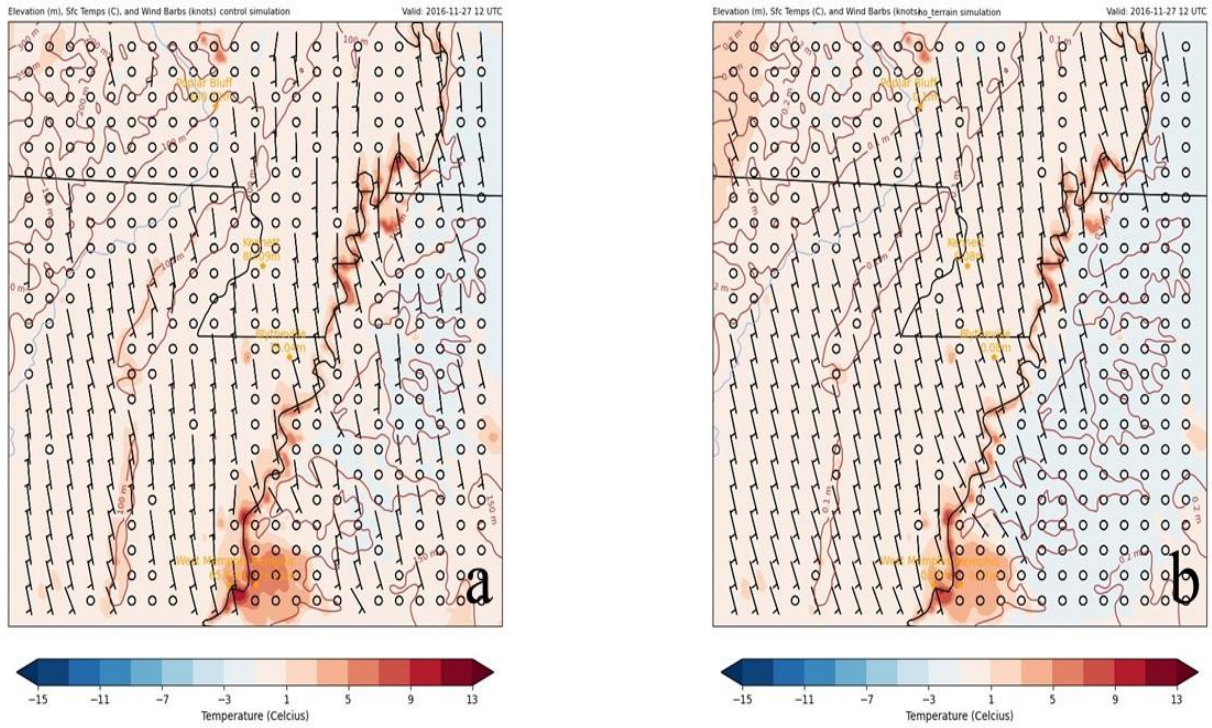

Figure 6.99 - d03 temperature maps from 1200 UTC on 27 November 2016. Each map features surface wind barbs (kts) in black, temperature shaded from blue to red from below -15°C up through 13°C. Topographic lines and values are featured on each map in dark brown.

6.3.1.4 1800 UTC 27 November 2016

By 1800 UTC the identification evidence for cold-air damming had ended approximately 3 hours prior with the final METAR report of freezing conditions from the Kennett, Missouri (KTKX) ASOS station having occurred at 1455 UTC on 27 November. Southerly flow dominated the d02 regional streamline maps (Figure 6.100), bringing warmer air into the region. This combined with the diurnal process of daytime heating ceased freezing conditions at the point location and effectively ended the cold-air damming event. Little contrast was observed between the actual-terrain and no-terrain simulation maps at this time.

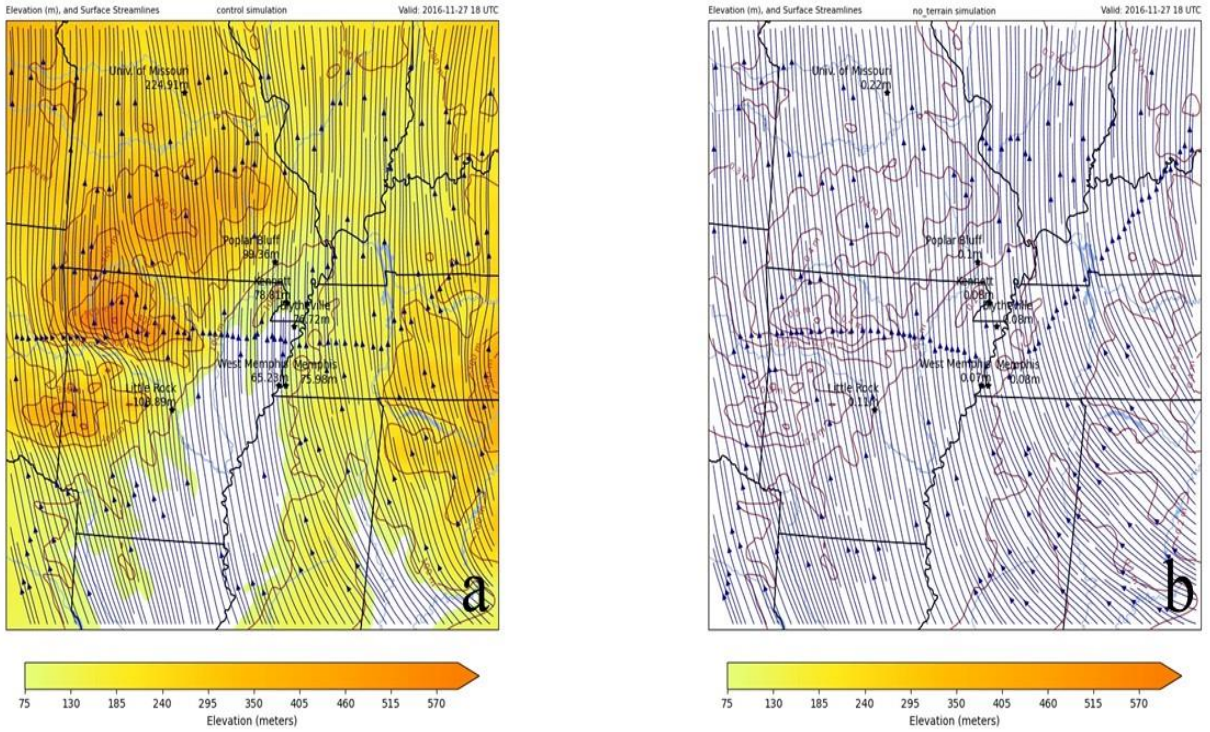

Figure 6.100 - d02 streamline maps from 1800 UTC on 27 November 2016. Map (a) is from the actual-terrain simulation run. Map (b) is from the no-terrain simulation run. Surface wind streamlines are depicted in navy blue on each map. The elevation heights are shaded from 75 m up through 570 m. Topographic lines are shaded in dark brown.

Significantly warmer temperatures were resolved on the d02 regional temperature maps (Figure 6.101) of 1800 UTC on 27 November. The southerly flow found on the regional streamline maps had pushed temperatures in the southern region to values above 13°C and was visible in the 10-m wind fields of both simulation maps. Slightly cooler temperatures existed over the Ozark Plateau on the actual-terrain simulation (Fig. 6.101a), but the warming trend was viewed in the region of interest which was inferred to have ended the cold-air damming event.

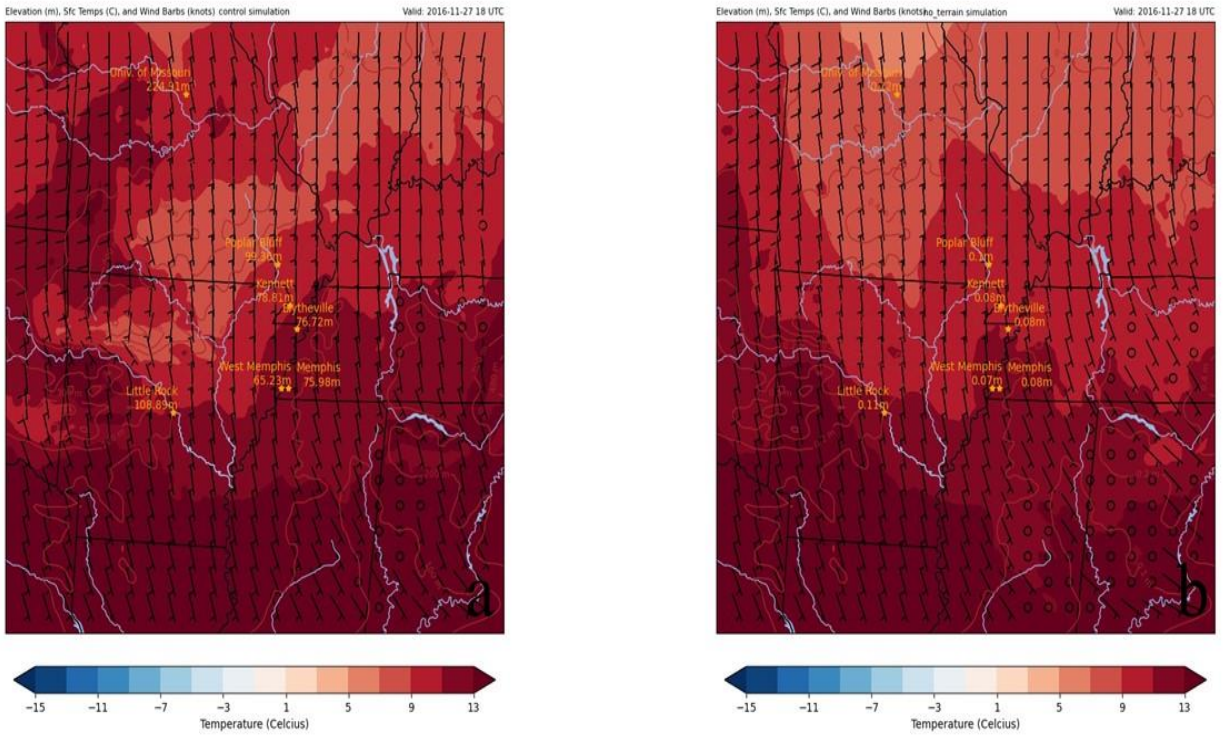

Figure 6.101 - d02 temperature maps from 1800 UTC on 27 November 2016. Each map features surface wind barbs (kts) in black, temperature shaded from blue to red from below -15°C up through 13°C. Topographic lines and values are featured on each map in dark brown.

Similar streamlined flow on both simulation maps of the d03 streamline maps (Figure 6.102) from 1800 UTC on 27 November 2016 was most likely due to the increased wind speeds over the region of interest seen on the previous d02 regional temperature map (Figure 6.100). This increase had eliminated any deviation around the embedded ridges of the flood plain normally seen on the actual-terrain simulation d03 streamline maps of previous time steps.

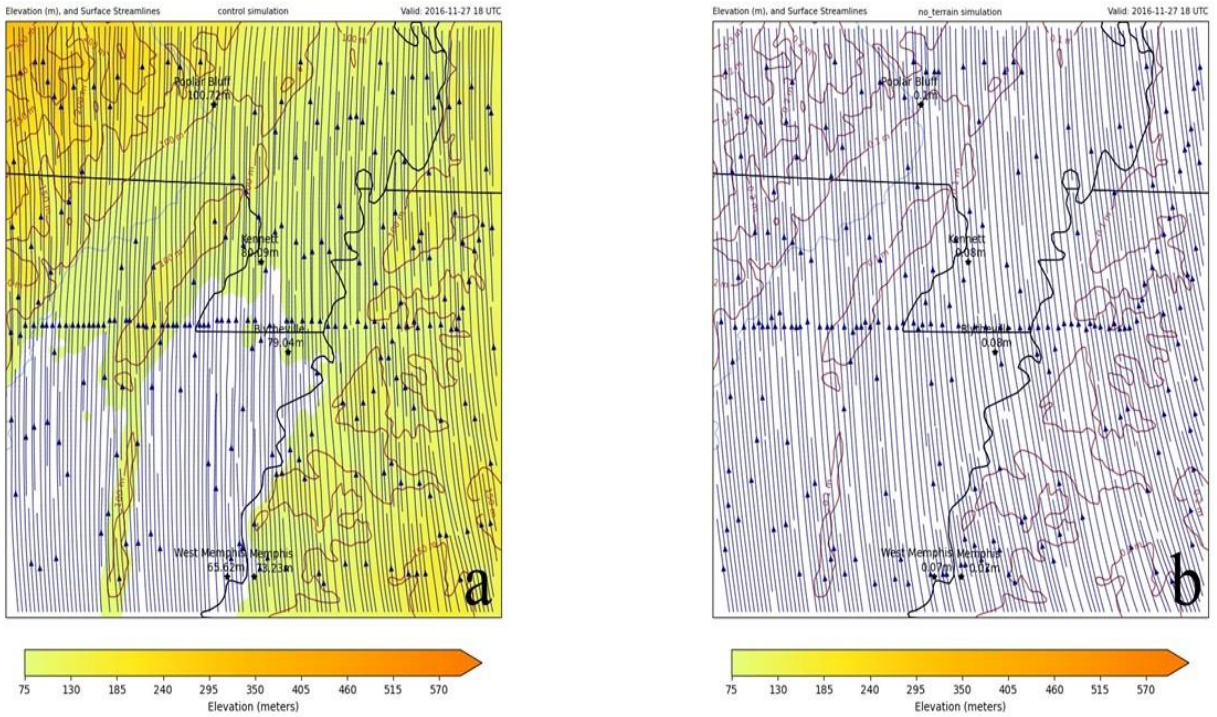

Figure 6.102 - d03 streamline maps from 1800 UTC on 27 November 2016. Map (a) is from the actual-terrain simulation runs. Map (b) is from the no-terrain simulation runs. Surface wind flow streamlines are featured in navy blue on each map. The elevation is shaded from 75 m up through 570 m. Topographic lines are featured in dark brown.

The d03 temperature maps (Figure 6.103) resolved a significant warmup in the temperature fields of both simulation maps. The 10-m wind fields of each map are similar with southerly 5-kt winds observed on both simulation maps. Temperature values between 9-11°C at the Kennett, Missouri station in southeastern Missouri signaled that the cold-air damming event had ended.

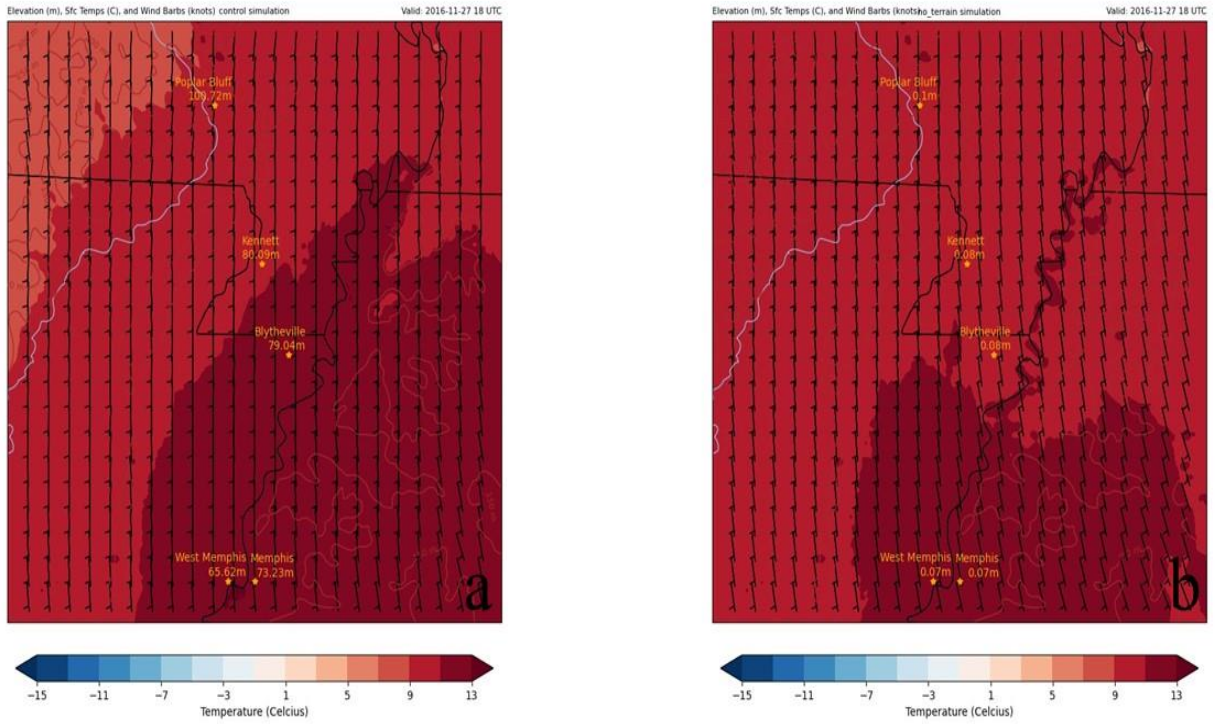

Figure 6.103 - d03 temperature maps from 1800 UTC on 27 November 2016. Each map features surface wind barbs (kts) in black, temperature shaded from blue to red from below -15°C up through 13°C. Topographic lines and values are featured on each map in dark brown.

6.3.2 Actual-Terrain versus Half-Terrain Comparison

Elevation heights were altered to half of their original values and the analysis of the 27 November 2016 case study continued with a comparison between the actual-terrain simulation and the half-terrain simulation runs. This was consistent with the procedures of analysis performed on the previous case study and the time steps analyzed here were the same as those of the actual-terrain versus no-terrain comparison. Elevation height values in the half-terrain simulation were multiplied by a value of 0.5.

6.3.2.1 0000 UTC 27 November 2016

The col point viewed in the previous comparative analysis associated with the d02 regional streamline maps (Figure 6.104) of 0000 UTC had shifted slightly east into eastern Tennessee on the half-terrain simulation map (Fig. 6.104b). The simulation maps were similar to the previous comparison: southerly flow to the north of the col point which included the region of interest and northerly flow over the southern half of the regional streamline maps.

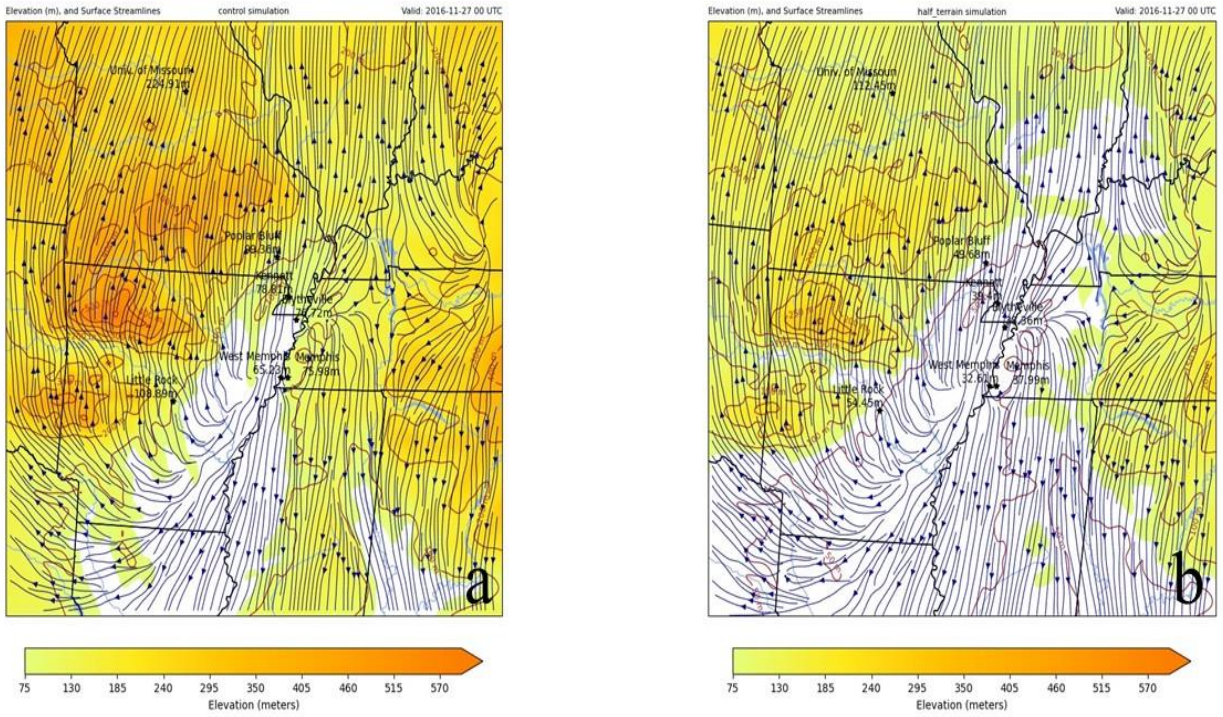

Figure 6.104 - d02 streamline maps from 0000 UTC on 27 November 2016. Map (a) is from the actual-terrain simulation run. Map (b) is from the half-terrain simulation run. Surface wind streamlines are depicted in navy blue on each map. The elevation heights are shaded from 75 m up through 570 m. Topographic lines are shaded in dark brown.

The d02 temperature maps (Figure 6.105) of the 0000 UTC time step showed little contrast as the actual-terrain and the half-terrain simulations contained elevation height values that were closer together than any of the other simulation runs. Therefore, the 10-m wind fields on both simulation maps observed calm conditions over most of the southern extent of each map and 5-kt southerly wind flow over the north and northwest portions of each map. The contrast seen in the previous analysis of regional temperature fields at this time was absent for the actual-terrain versus half-terrain analysis where cooler temperatures infiltrating southeastern Missouri on the actual-terrain simulation (Fig. 6.105a) had also done so on the half-terrain simulation (Fig. 6.105b) albeit in a smaller area.

Figure 6.105 - d02 temperature maps from 0000 UTC on 27 November 2016. Each map features surface wind barbs (kts) in black, temperature shaded from blue to red from below -15°C up through 13°C. Topographic lines and values are featured on each map in dark brown.

Closer focus on the region of interest in the d03 streamline maps (Figure 6.106) showed that the col point that looked shifted to the east on the half-terrain d02 streamline simulation (Fig. 6.104b) was much less defined on the half-terrain d03 streamline simulation (Fig. 6.106b). Deviation over the embedded ridges contrasted with the streamlines in the half-terrain simulation which flowed uniformly over the ridge and deviated around or terminated at the edge of the ridges in the actual-terrain simulation.

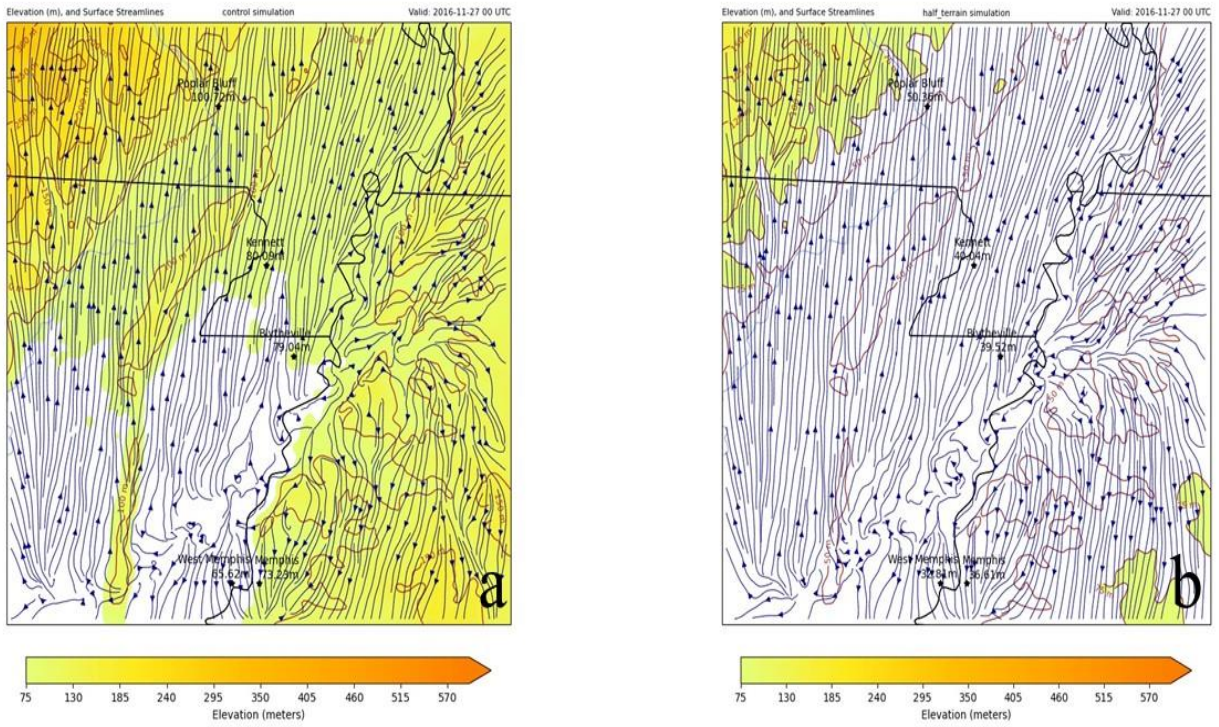

Figure 6.106 - d03 streamline maps from 0000 UTC on 27 November 2016. Map (a) is from the actual-terrain simulation runs. Map (b) is from the half-terrain simulation runs. Surface wind flow streamlines are featured in navy blue on each map. The elevation is shaded from 75 m up through 570 m. Topographic lines are featured in dark brown.

Calm conditions on the half-terrain simulation of the d03 temperature maps (Fig. 6.107b) at 0000 UTC were different than the southerly 5-kt wind field observed on the actual-terrain simulation (Fig. 6.107a) over the northwestern extent of the region of interest including the escarpment of the Ozark Plateau. Here the only difference in the temperature fields of these simulation maps was seen over the Plateau, as well as, where colder temperatures on the actual-terrain map were somewhat reduced in areal coverage on the half-terrain simulation map. Otherwise, the temperature fields were similar at this time step.

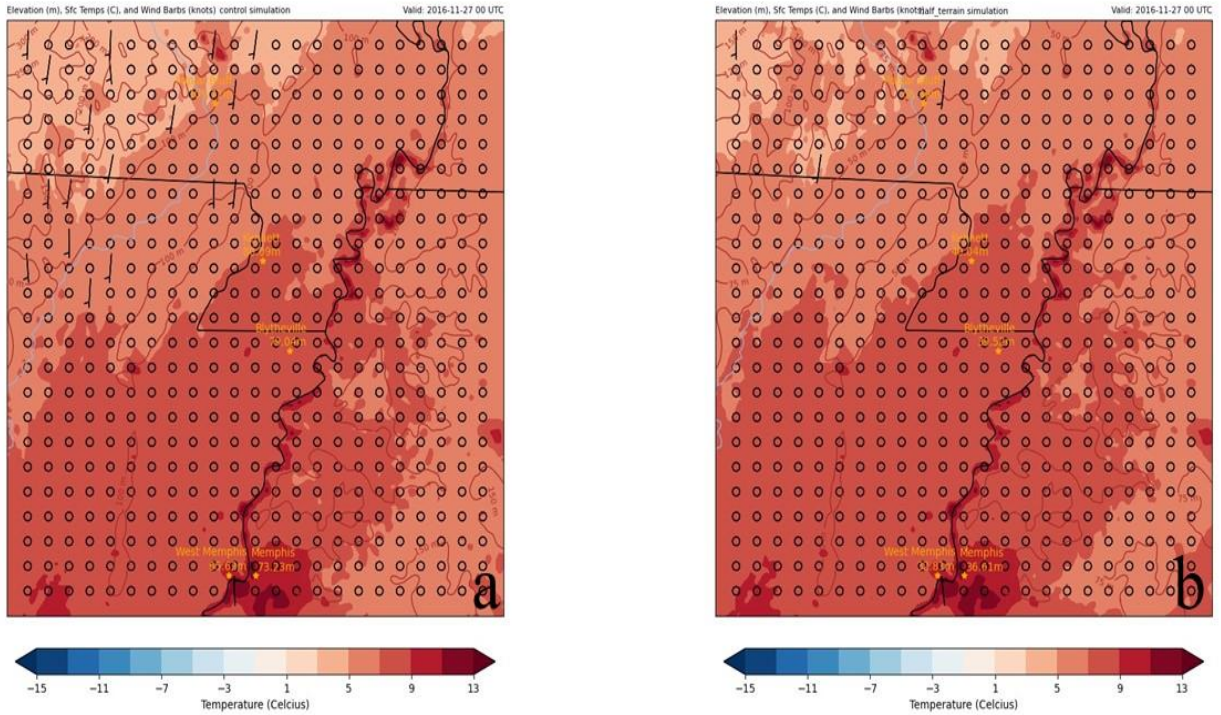

Figure 6.107 - d03 temperature maps from 0000 UTC on 27 November 2016. Each map features surface wind barbs (kts) in black, temperature shaded from blue to red from below -15°C up through 13°C. Topographic lines and values are featured on each map in dark brown.

6.3.2.2 0600 UTC 27 November 2016

Regional d02 streamline maps (Figure 6.108) 6 hours later at 0600 UTC on 27 November 2016 featured deviation of streamlines over the elevation of the Ozark Plateau on the actual-terrain simulation (Fig. 6.108a), but a more organized 10-m wind flow in the same areas on the half-terrain simulation (Fig. 6.108b). The col point on both simulation maps had pushed eastward into Tennessee in response to the eastward migration of the parent anticyclone observed in the synoptic overview. Southerly flow over the region of interest continued on both simulation maps into the overnight hours of 27 November.

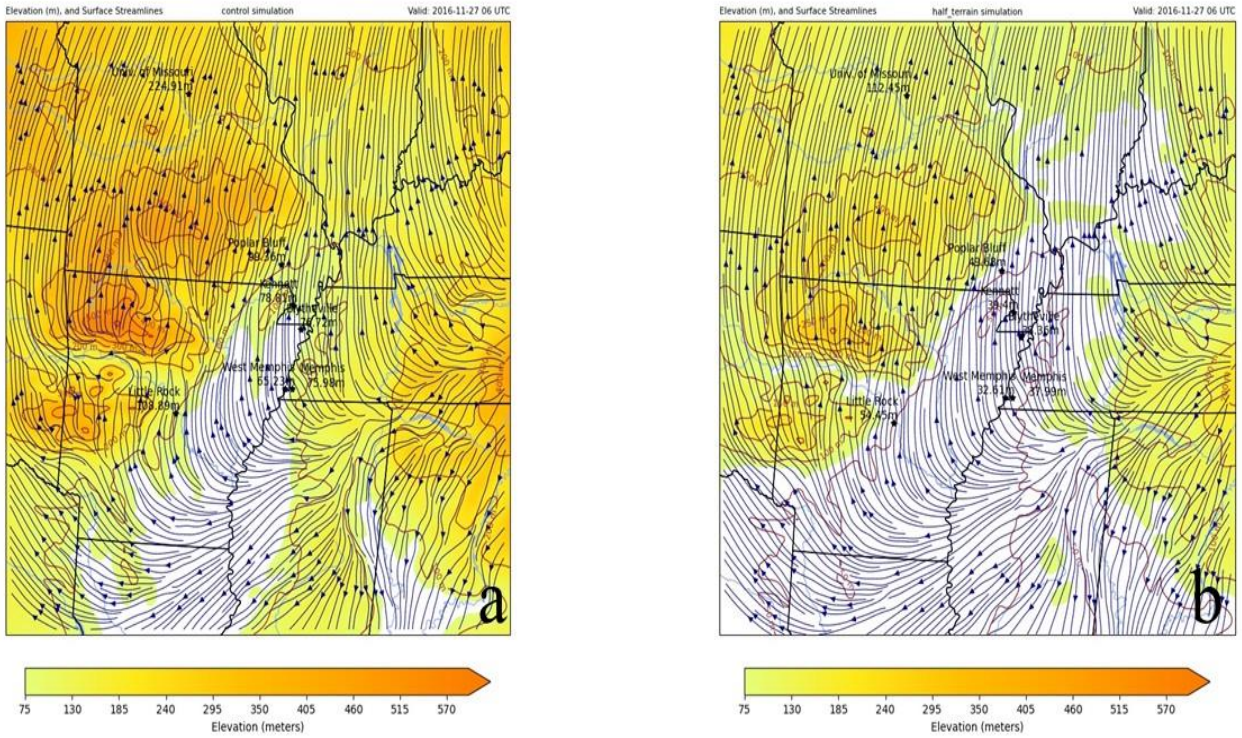

Figure 6.108 - d02 streamline maps from 0600 UTC on 27 November 2016. Map (a) is from the actual-terrain simulation run. Map (b) is from the half-terrain simulation run. Surface wind streamlines are depicted in navy blue on each map. The elevation heights are shaded from 75 m up through 570 m. Topographic lines are shaded in dark brown.

Temperature decreases in response to radiational cooling on the d02 regional temperature maps (Figure 6.109) despite the southerly flow were found on both simulation maps at 0600 UTC. The maps were bisected by calm conditions in the 10-m wind field to the southeast and 5-kt southerly winds to the northwest. As viewed in the previous analysis a temperature gradient existed from west to east with colder temperatures to the east of the Mississippi River. Over the region of interest temperatures had fallen back to 1-3°C on both simulation maps. Very little contrast on a regional scale was observed at this time step.

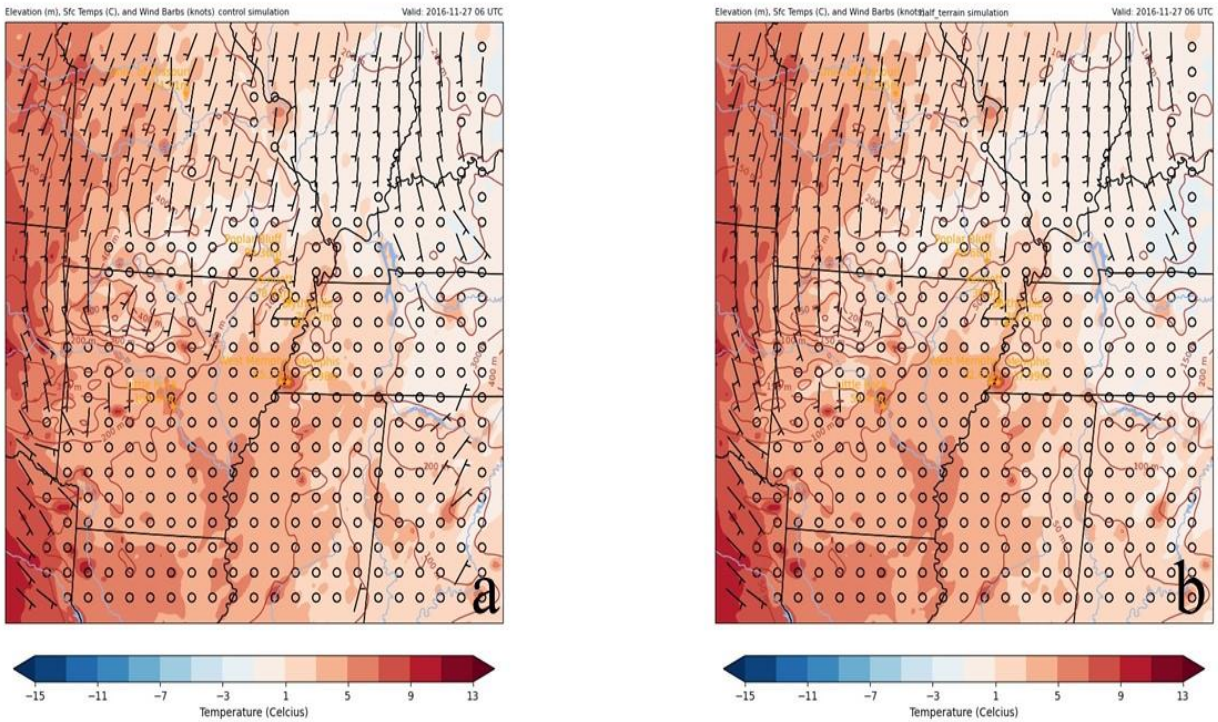

Figure 6.109 - d02 temperature maps from 0600 UTC on 27 November 2016. Each map features surface wind barbs (kts) in black, temperature shaded from blue to red from below -15°C up through 13°C. Topographic lines and values are featured on each map in dark brown.

The southerly flow over the region of interest in the d03 streamline maps (Figure 6.110), in response to the western flank of the parent anticyclone to the east, was found on both simulation maps overnight on 27 November 2016. The only contrast in the surface flow streamline field was observed on the actual-terrain simulation (Fig. 6.110a) where some deviation over the embedded ridge was occurring where streamlines were not deviated on the half-terrain simulation (Fig. 6.110b).

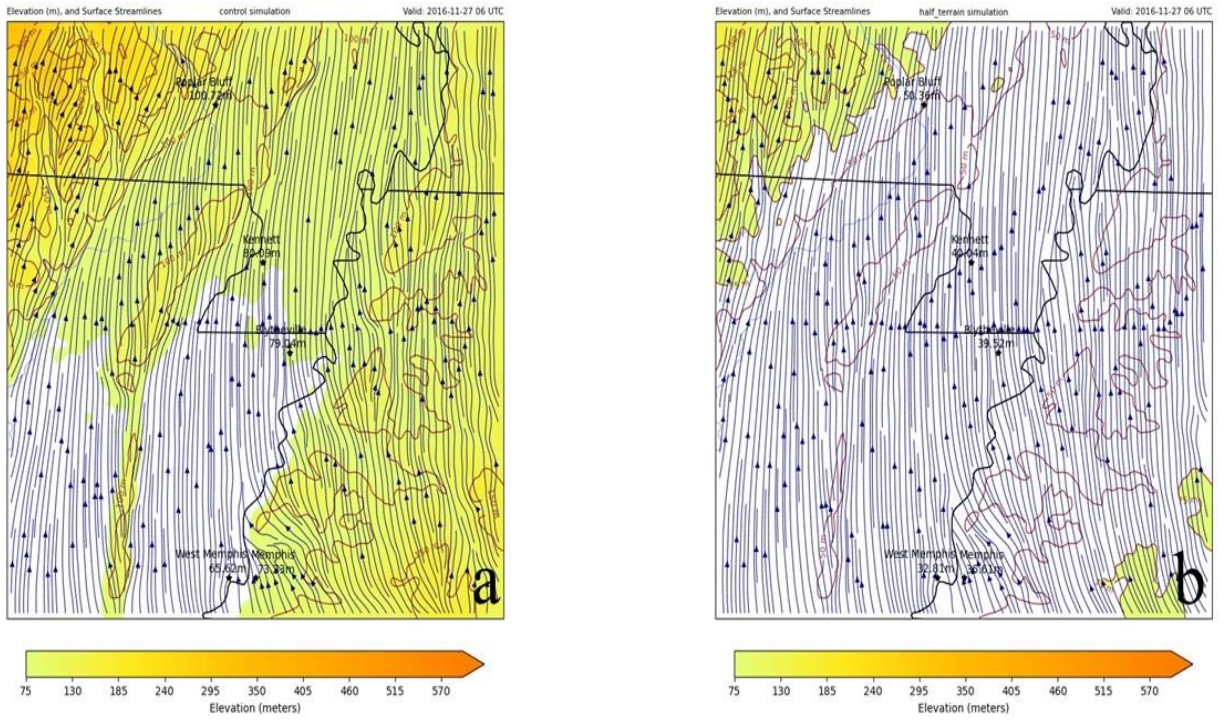

Figure 6.110 - d03 streamline maps from 0600 UTC on 27 November 2016. Map (a) is from the actual-terrain simulation runs. Map (b) is from the half-terrain simulation runs. Surface wind flow streamlines are featured in navy blue on each map. The elevation is shaded from 75 m up through 570 m. Topographic lines are featured in dark brown.

A calm 10-m wind field on the actual-terrain simulation of the d03 temperature maps (Fig. 6.111a) at 0600 UTC on 27 November contrasted from its half-terrain counterpart where more 5-kt southerly winds were observed over the region of interest. On the actual-terrain simulation the area between the embedded ridge and the escarpment of the Plateau featured calm winds with 5-kt winds over and to the southwest of the ridge. Temperature fields were similar despite elevation height differences on the simulated maps. Lack of significant wind speed may have limited the effect of channeling colder air into the flood plain at this time.

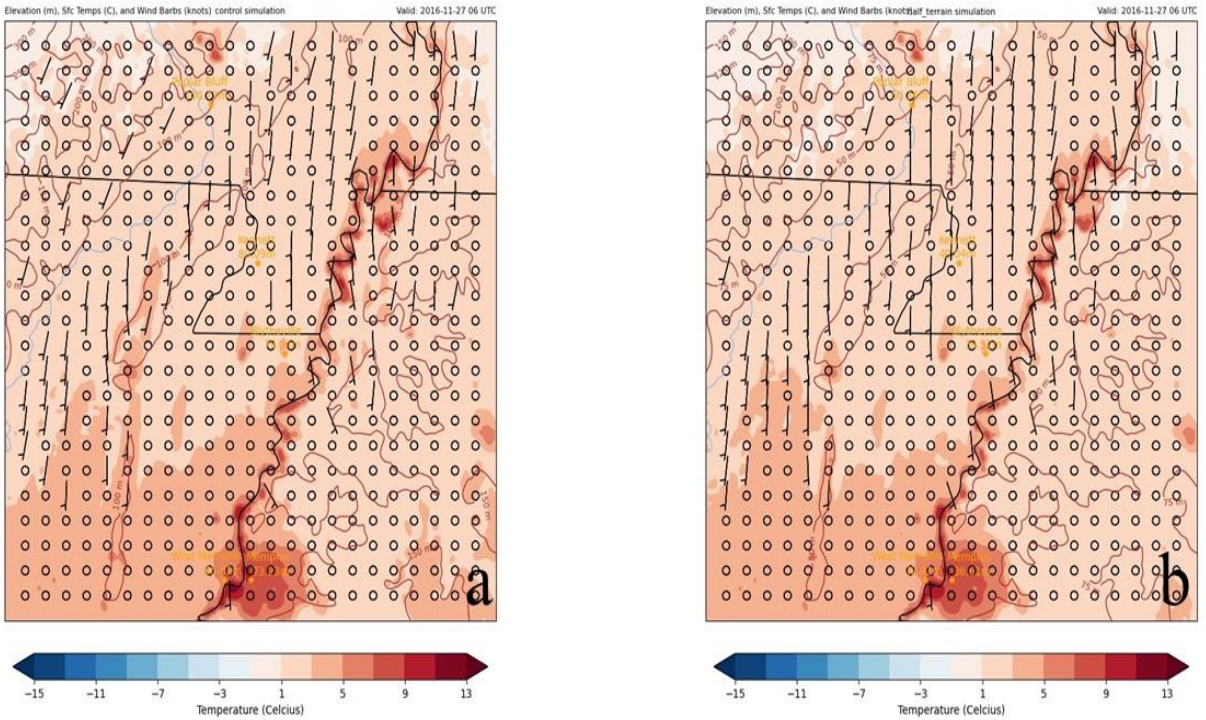

Figure 6.111 - d03 temperature maps from 0600 UTC on 27 November 2016. Each map features surface wind barbs (kts) in black, temperature shaded from blue to red from below -15°C up through 13°C. Topographic lines and values are featured on each map in dark brown.

6.3.2.3 1200 UTC 27 November 2016

The parent anticyclone continued to track to the east 6 hours later at 1200 UTC on 27 November yet the d02 regional streamline maps (Figure 6.112) of this comparison still depicted the western flank influencing 10-m wind flow over the region. The only northerly directional components observed on the simulation maps occurred in the extreme southeastern corner of each simulation while all other areas experienced the southerly flow of the western edge of the high-pressure system. Regionally, there was little contrast between the simulations save for some directional steering of 10-m wind flow in the river basins contained within the Ozark Plateau on the actual-terrain simulation (Fig. 6.112a). The half-terrain d02 streamline simulation (Fig. 6.112b) did not possess elevation height values capable of this same effect.

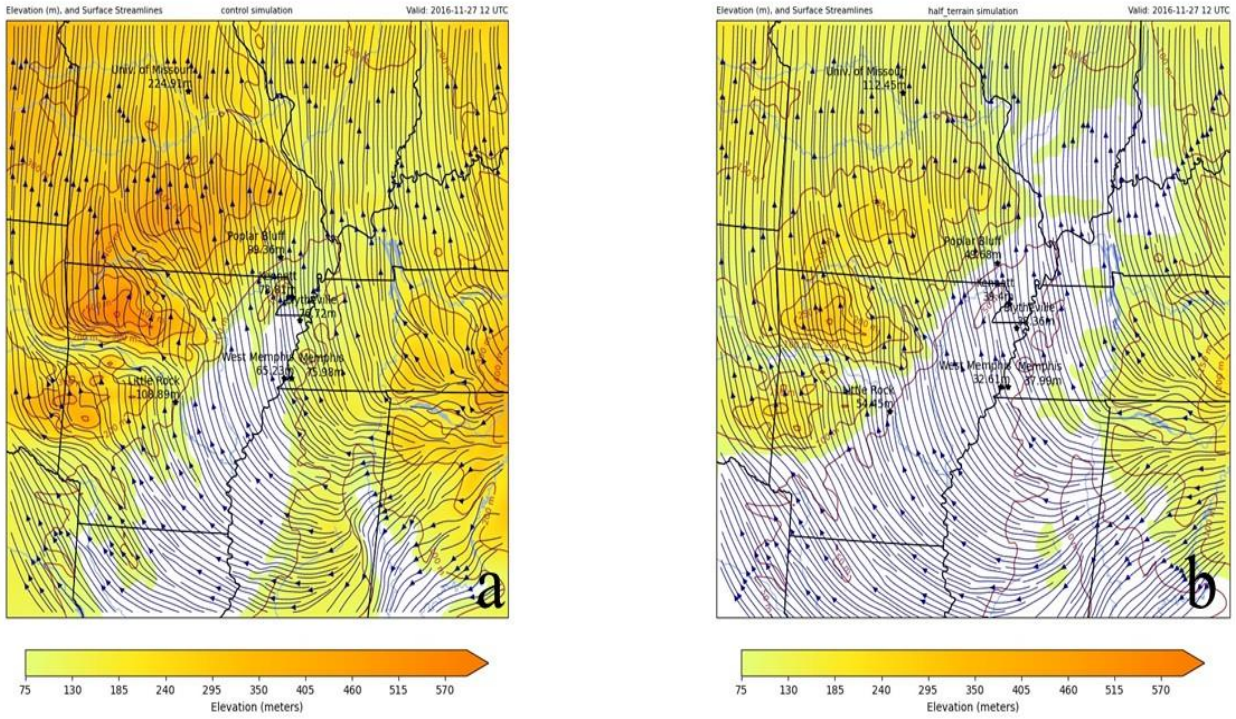

Figure 6.112 - d02 streamline maps from 1200 UTC on 27 November 2016. Map (a) is from the actual-terrain simulation run. Map (b) is from the half-terrain simulation run. Surface wind streamlines are depicted in navy blue on each map. The elevation heights are shaded from 75 m up through 570 m. Topographic lines are shaded in dark brown.

The temperature gradient over the d02 regional temperature maps (Figure 6.113) at daybreak was the strongest of the analysis on both simulation maps. Certainly, the coldest temperatures of the analysis were observed due to radiational cooling despite the southerly flow shown by the 10-m wind field of both simulation maps.

Figure 6.113 - d02 temperature maps from 1200 UTC on 27 November 2016. Each map features surface wind barbs (kts) in black, temperature shaded from blue to red from below -15°C up through 13°C. Topographic lines and values are featured on each map in dark brown.

Closer inspection of the region of interest on the d03 streamline maps (Figure 6.114) of 1200 UTC 27 November time step showed the deviation in streamlined surface flow around and over the embedded ridges on the actual-terrain simulation (Fig. 6.114a) differing from the organized, unimpeded flow over the ridges on the half-terrain simulation map (Fig. 6.114b). Otherwise, southerly streamlined surface flow continued over the region of interest under the influence of the parent anticyclone to the east. The terrain-orthogonal surface flow was conducive to trapping any cold air flowing through the flood plain up against the escarpment of the Ozark Plateau at this time.

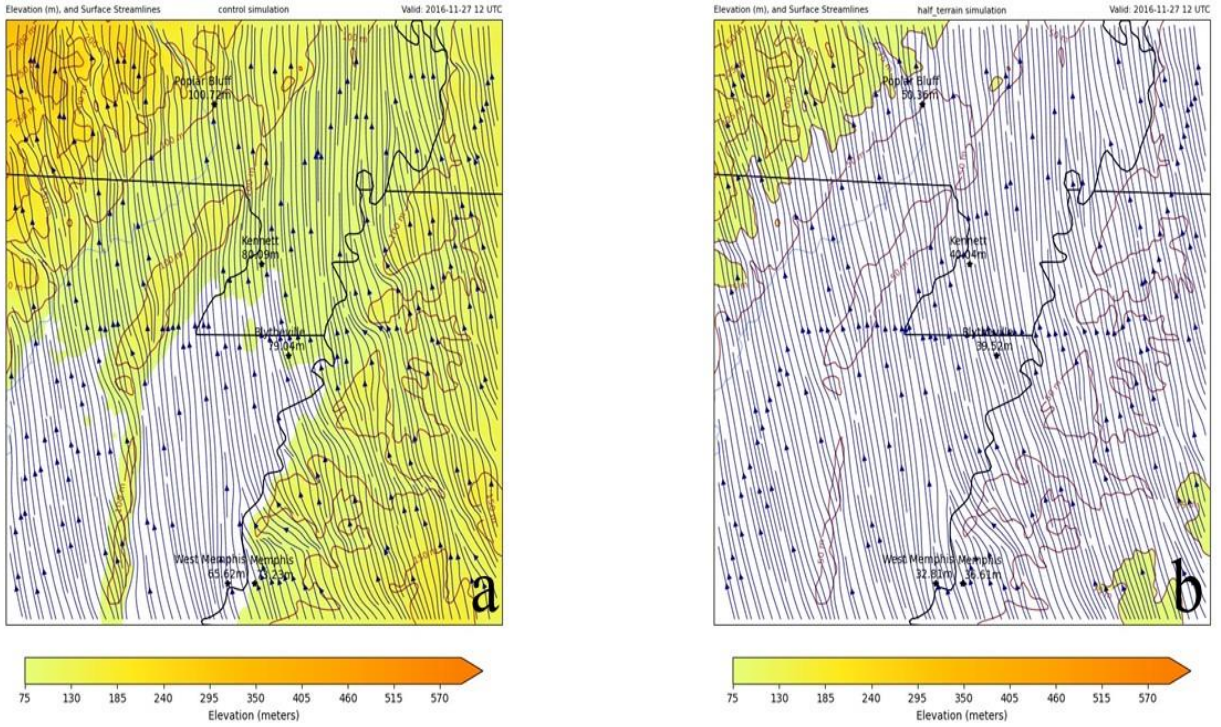

Figure 6.114 - d03 streamline maps from 1200 UTC on 27 November 2016. Map (a) is from the actual-terrain simulation runs. Map (b) is from the half-terrain simulation runs. Surface wind flow streamlines are featured in navy blue on each map. The elevation is shaded from 75 m up through 570 m. Topographic lines are featured in dark brown.

The 10-m wind fields of the d03 temperature maps (Figure 6.115) were similar through the region of interest with both simulation maps resolving calm conditions just to the east of the embedded ridges and 5-kt southerly winds through much of the flood plain. While the temperature field of both maps resolved temperatures at or just below freezing in the region of interest, the lack of change in temperatures between the Plateau and the flatter flood plain was significant. Terrain-orthogonal surface flow should dictate a temperature change between these elevation differences (and had done so in previous case study analyses) especially on the actual-terrain simulation, yet the temperature gradient seemed to be uninfluenced by the terrain-orthogonal nature of the 10-m wind field. A hypothesis about this lack of change questioned if the colder temperatures over the Ozark Plateau were due to diurnal processes and the colder temperatures in the flood plain were forced into the plain from the east-southeast where colder temperatures existed to the east of the Mississippi River. This 2-source possibility seemed the most logical for the lack of temperature change in the temperature field as the sun rose on 27 November.

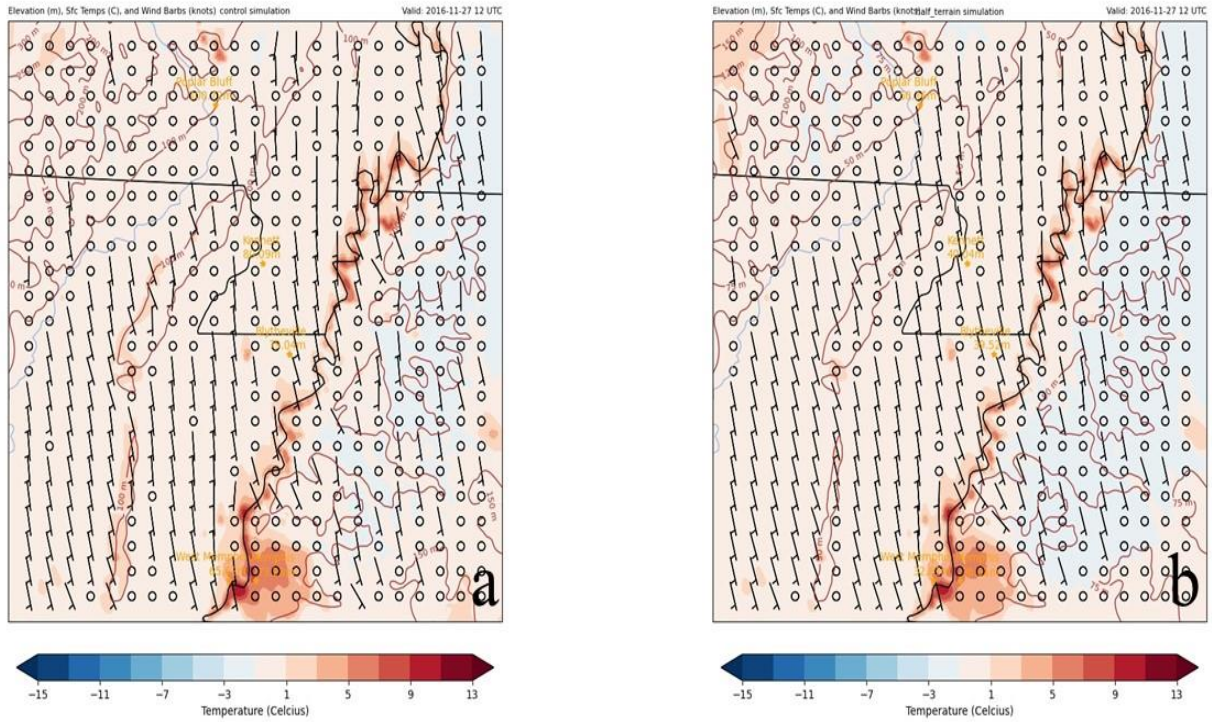

Figure 6.115 - d03 temperature maps from 1200 UTC on 27 November 2016. Each map features surface wind barbs (kts) in black, temperature shaded from blue to red from below -15°C up through 13°C. Topographic lines and values are featured on each map in dark brown.

6.3.2.4 1800 UTC 27 November 2016

By 1800 UTC 27 November 2016 the d02 regional streamline maps (Figure 6.116) showed complete southerly surface flow across the region. Some deviation around the elevation values of the Ozark Plateau on the actual-terrain simulation map (Fig. 6.116a) existed, but otherwise the streamline patterns on these simulation maps were similar.

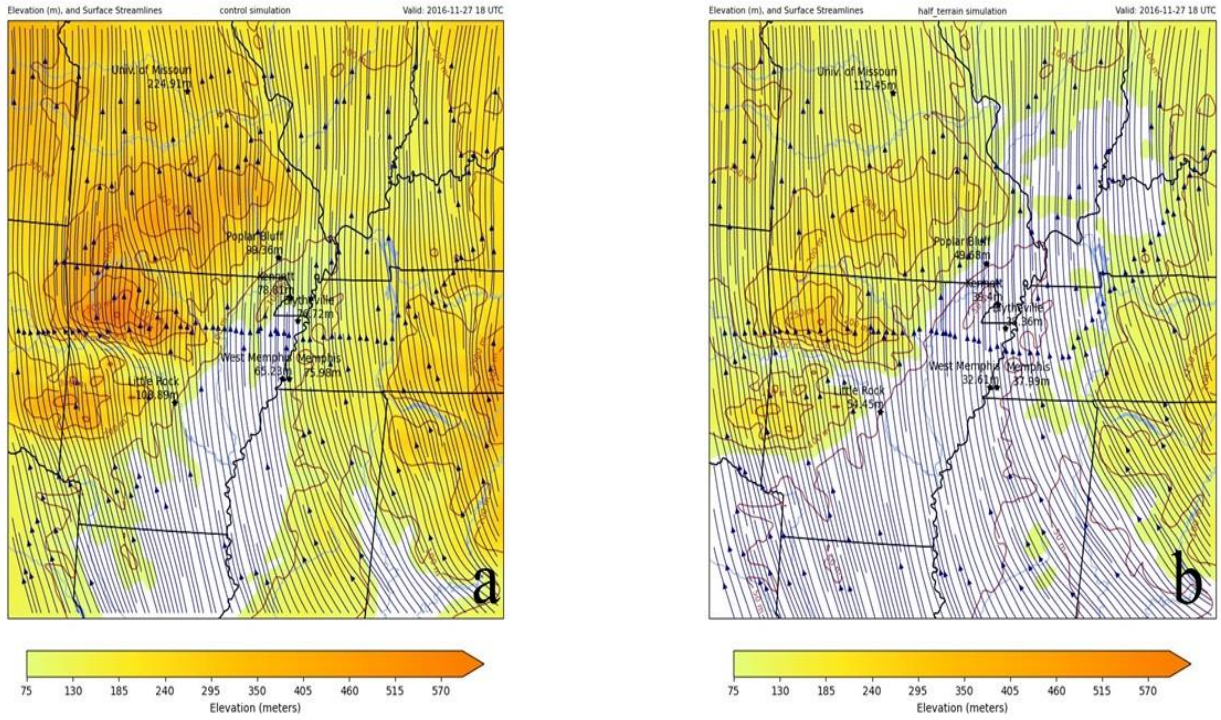

Figure 6.116 - d02 streamline maps from 1800 UTC on 27 November 2016. Map (a) is from the actual-terrain simulation run. Map (b) is from the half-terrain simulation run. Surface wind streamlines are depicted in navy blue on each map. The elevation heights are shaded from 75 m up through 570 m. Topographic lines are shaded in dark brown.

Southerly flow previously viewed on the d02 regional streamline maps (Figure 6.116) and again in the 10-m wind fields of both d02 temperature maps (Figure 6.117) helped to warm up the temperature fields of both simulation maps by 1800 UTC on 27 November. Just as observed in the previous comparison, the temperatures within the region of interest had risen to values between 11 and 13°C. The last METAR observation of cold-air damming type conditions occurred approximately 3 hours previously. The cold-air damming event for this case study had ended.

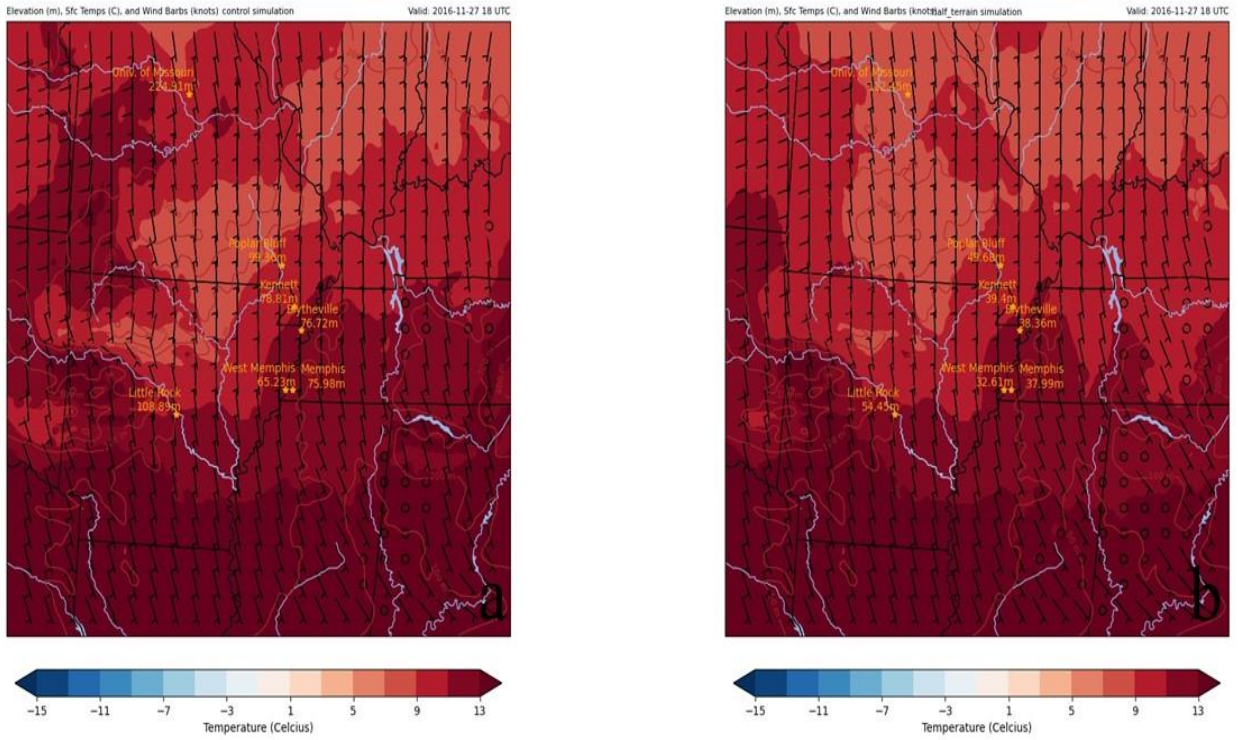

Figure 6.117 - d02 temperature maps from 1800 UTC on 27 November 2016. Each map features surface wind barbs (kts) in black, temperature shaded from blue to red from below -15°C up through 13°C. Topographic lines and values are featured on each map in dark brown.

Similar streamline surface flow lines on each simulation of the d03 streamline maps (Figure 6.118) at 1800 UTC on 27 November occurred in response to a slightly stronger wind speed in the surface flow. This resolved the lack of deviation over the embedded ridges and the escarpment of the Ozark Plateau on the actual-terrain simulation map (Fig. 6.118a).

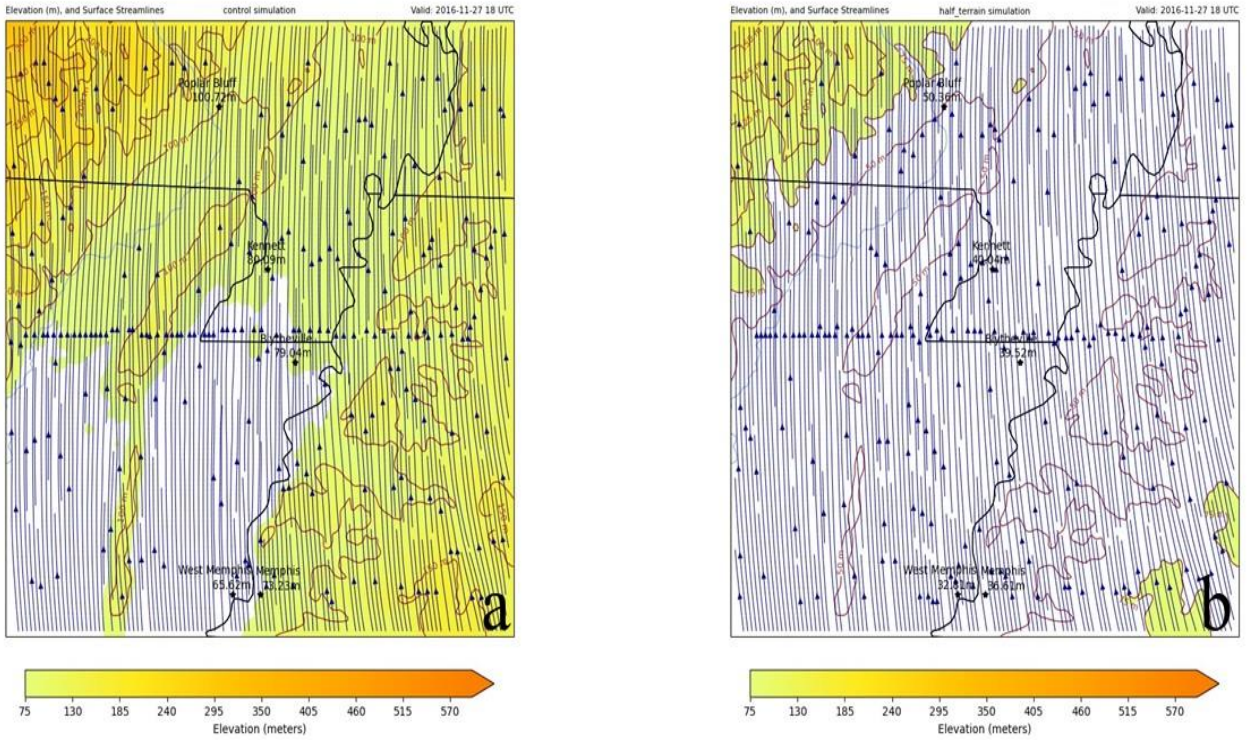

Figure 6.118 - d03 streamline maps from 1800 UTC on 27 November 2016. Map (a) is from the actual-terrain simulation runs. Map (b) is from the half-terrain simulation runs. Surface wind flow streamlines are featured in navy blue on each map. The elevation is shaded from 75 m up through 570 m. Topographic lines are featured in dark brown.

Little contrast was found in the analysis of the d03 temperature simulation maps (Figure 6.119) of 1800 UTC on 27 November save for the impedance of warm-air advection that occurred on the actual-terrain simulation (Fig. 6.119a). The temperature fields contrasted at the escarpment of the Plateau as the warmer air of the temperature field on the actual-terrain simulation was kept from riding over the elevation height values located in the northwestern corner of the map. This was evidenced by the relatively colder air to the north of the escarpment. This was not the case on the half-terrain simulation (Fig. 6.119b) where the warmer air had infiltrated the lesser elevation height values in the same location.

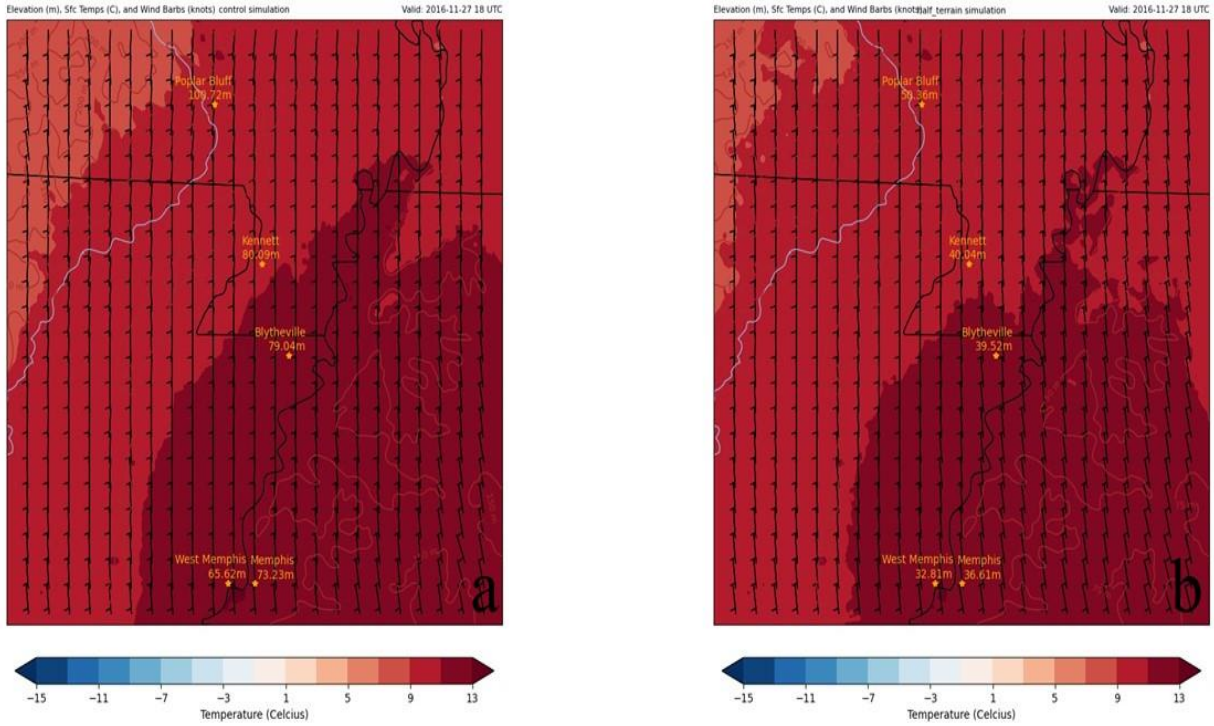

Figure 6.119 - d03 temperature maps from 1800 UTC on 27 November 2016. Each map features surface wind barbs (kts) in black, temperature shaded from blue to red from below -15°C up through 13°C. Topographic lines and values are featured on each map in dark brown.

6.3.3 Actual-Terrain versus Double-Terrain Comparison

Comparative analysis of the 27 November 2016 case study concluded with comparative analysis between actual-terrain simulations and double-terrain simulations in which elevation height values were multiplied by 2.0. This was consistent with previous analysis performed and included time steps between 0000 UTC and 1800 UTC on 27 November 2019.

6.3.3.1 0000 UTC 27 November 2019

The d02 regional streamline double-terrain simulation (Fig. 6.120b) resolved an unorganized pattern of streamlines around and over the elevation of the Ozark Plateau at 0000 UTC on 27 November 2016. While southerly flow to the north of the col point previously seen and observed on these maps once again could be found on the double-terrain simulation map over the region of interest, there was significant deviation in the streamline fields as 10-m wind flow attempted to navigate the extreme elevation height values found on the map. This was not observed on the actual-terrain simulation (Fig. 6.120a) where some deviation was occurring in response to elevation height values, but the streamline surface flow was more organized while traversing the Plateau.

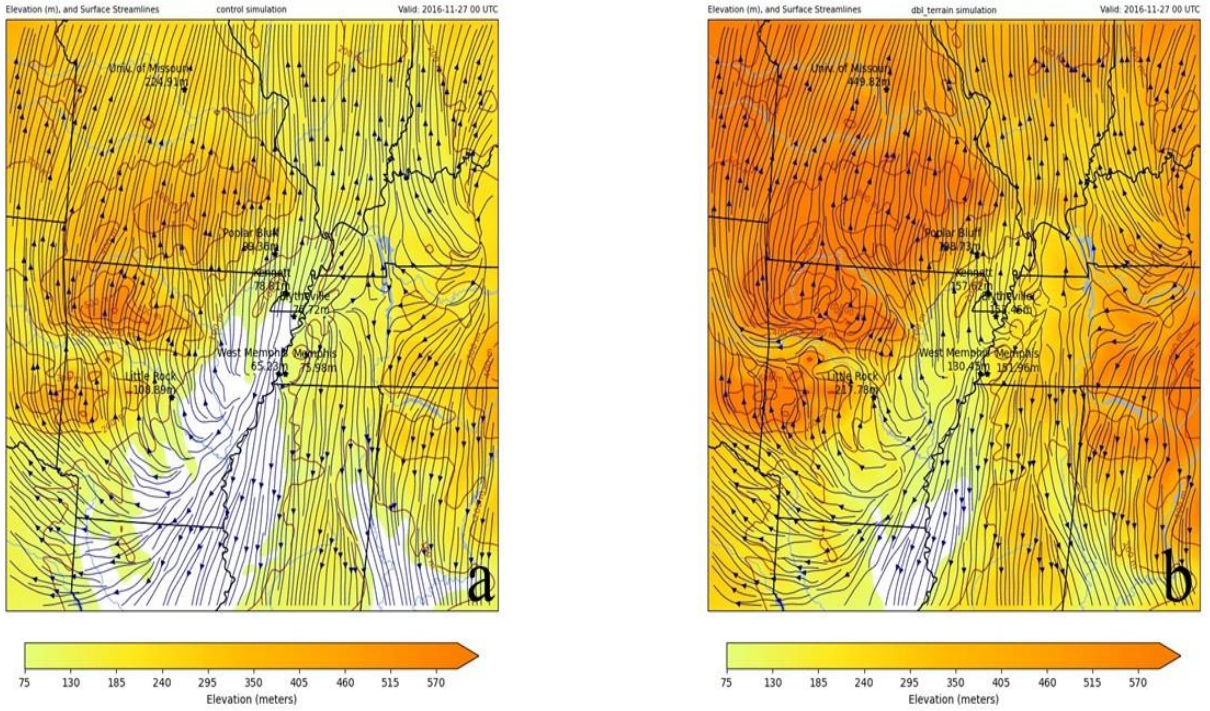

Figure 6.120 - d02 streamline maps from 0000 UTC on 27 November 2016. Map (a) is from the actual-terrain simulation run. Map (b) is from the double-terrain simulation run. Surface wind streamlines are depicted in navy blue on each map. The elevation heights are shaded from 75 m up through 570 m. Topographic lines are shaded in dark brown.

Colder air near the top of elevation heights on the d02 regional temperature maps (Figure 6.121) could be observed on each simulation map at 0000 UTC. It was inferred that the cooler temperatures resolved in these locations were a result of simply high enough altitude to mitigate the effects of daytime heating and, to a degree, the southerly flow associated with the high-pressure center propagating over the region of interest. The temperatures observed on the double-terrain map (Fig. 6.121b) were approximately 3-5°C cooler in highest elevation height locations.

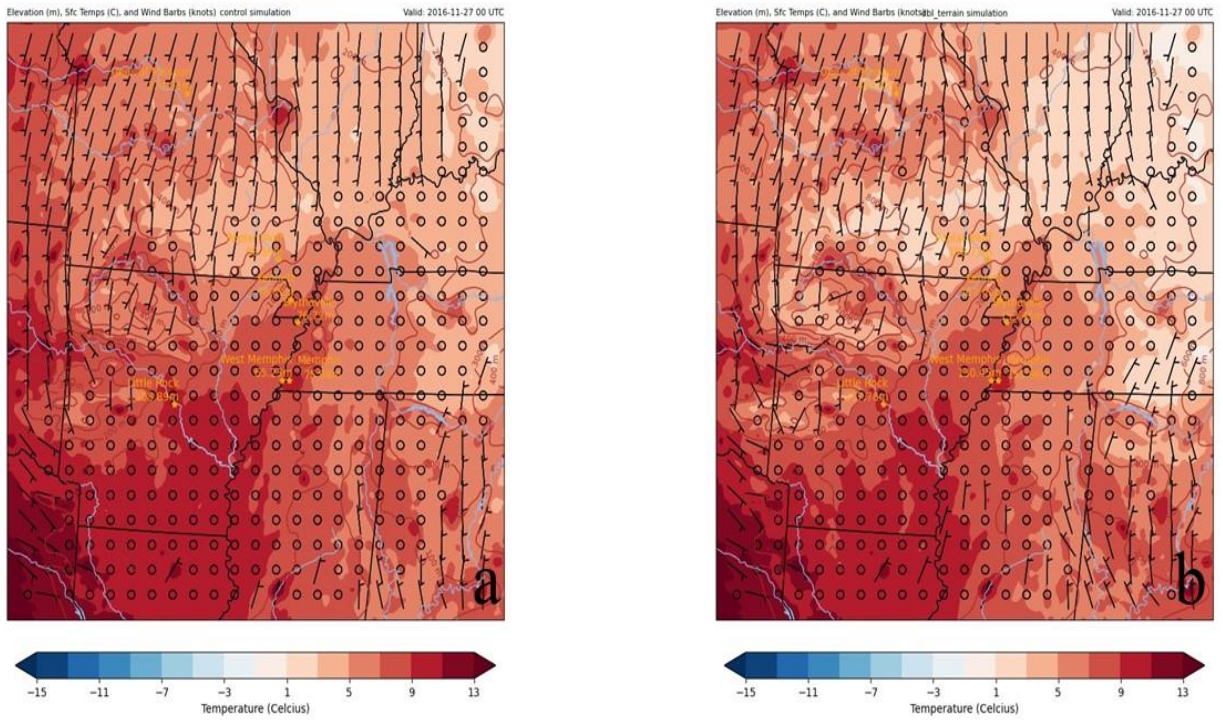

Figure 6.121 - d02 temperature maps from 0000 UTC on 27 November 2016. Each map features surface wind barbs (kts) in black, temperature shaded from blue to red from below -15°C up through 13°C. Topographic lines and values are featured on each map in dark brown.

The d03 streamline maps (Figure 6.122) of this time step resolved significant contrast in the surface flow streamline field. The double-terrain simulation was highlighted by streamlines being completely diverted around the embedded ridges of the flood plain. North of the col point all streamlines were southerly, but those that originated to the east of the ridge on the double-terrain simulation map were directed parallel to the eastern edge of the ridge. Only streamlines that originated on the ridges were able to progress westward. This was significant evidence of the elevation's manipulation of surface flow. Deviation of streamlines around the ridges existed on the actual-terrain simulation (Fig. 6.122a), but not to the degree of what was observed on the double-terrain simulation.

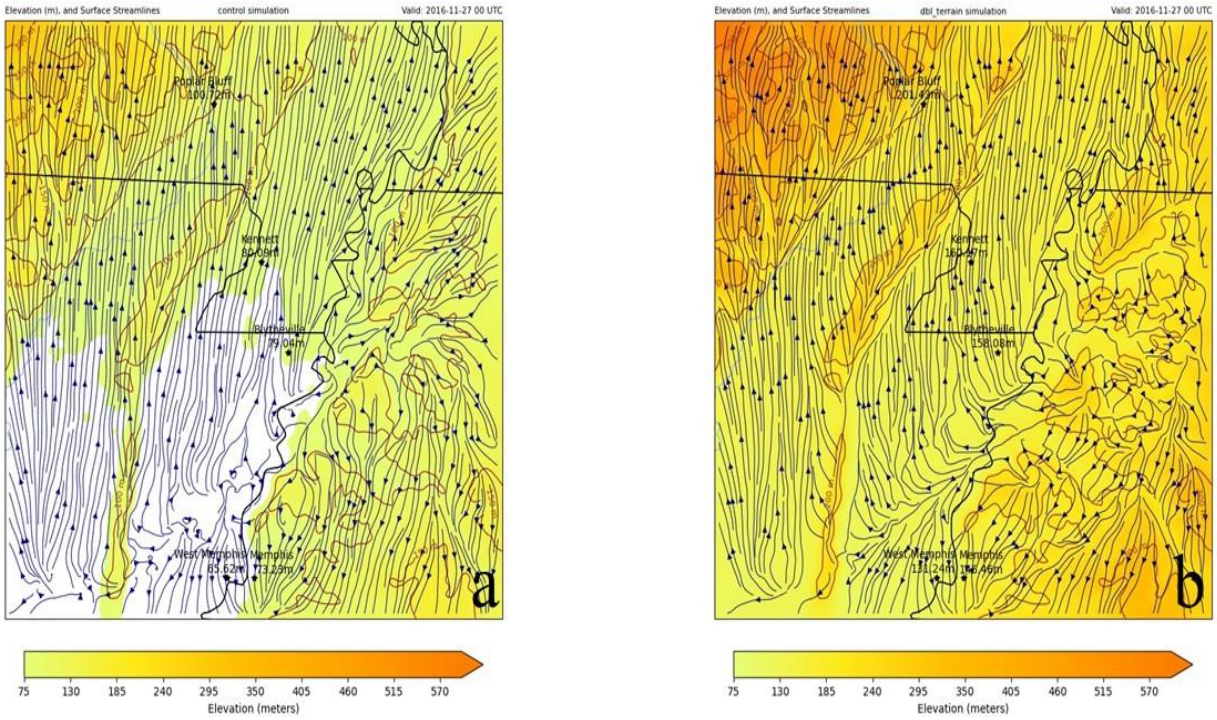

Figure 6.122 - d03 streamline maps from 0000 UTC on 27 November 2016. Map (a) is from the actual-terrain simulation runs. Map (b) is from the double-terrain simulation runs. Surface wind flow streamlines are featured in navy blue on each map. The elevation is shaded from 75 m up through 570 m. Topographic lines are featured in dark brown.

Warm air advection within the flood plain shown on the d03 temperature maps of 0000 UTC (Fig. 6.123) was inhibited by the escarpment of the Ozark Plateau. The WRF model resolved the coldest air associated with the higher elevation of the Plateau in the northwest corner of each simulation map. Calm conditions within the flood plain of each simulation map gave way to 5-kt winds over the elevation of the Plateau found further northwest. The only contrast in temperature fields on these simulated maps was the progress of warmer temperatures further north on the actual-terrain simulation (Fig. 6.123a) than what was observed on the double-terrain simulation (Fig. 6.123b).

Figure 6.123 - d03 temperature maps from 0000 UTC on 27 November 2016. Each map features surface wind barbs (kts) in black, temperature shaded from blue to red from below -15°C up through 13°C. Topographic lines and values are featured on each map in dark brown.

6.3.3.2 0600 UTC 27 November 2016

By the overnight hour of 0600 UTC on 27 November 2016 the progression of the col point associated with the center of high pressure further east was observed on both simulation maps of the d02 regional streamline maps (Figure 6.124). The double-terrain map (Fig. 6.124b) featured the deviation and diversion of streamlines around the extreme values of elevation associated with the Ozark Plateau. Southerly flow over the region of interest could be observed as the western flank of the anticyclone was now firmly in place over the region.

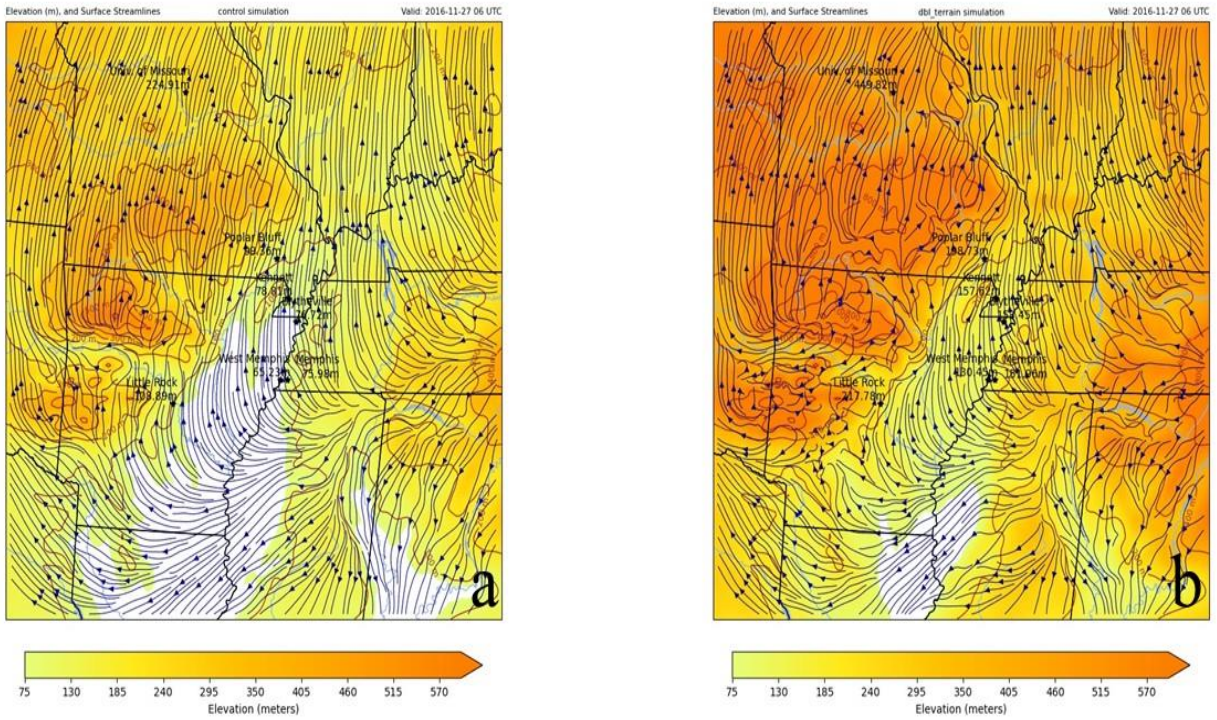

Figure 6.124 - d02 streamline maps from 0600 UTC on 27 November 2016. Map (a) is from the actual-terrain simulation run. Map (b) is from the double-terrain simulation run. Surface wind streamlines are depicted in navy blue on each map. The elevation heights are shaded from 75 m up through 570 m. Topographic lines are shaded in dark brown.

Colder surface air was observed at 0600 UTC on the d02 regional temperature maps (Figure 6.125) as a temperature gradient from west to east was viewed over the area. In the region of interest both simulation maps featured 2-m temperatures approximately 10°C cooler than 6 hours prior. Little contrast in the temperature field was seen on the simulation maps, though the 10-m wind field was disorganized on the double-terrain simulation map (Fig. 6.125b) in response to the deviation and disruption of surface flow around the elevation of the Ozark Plateau.

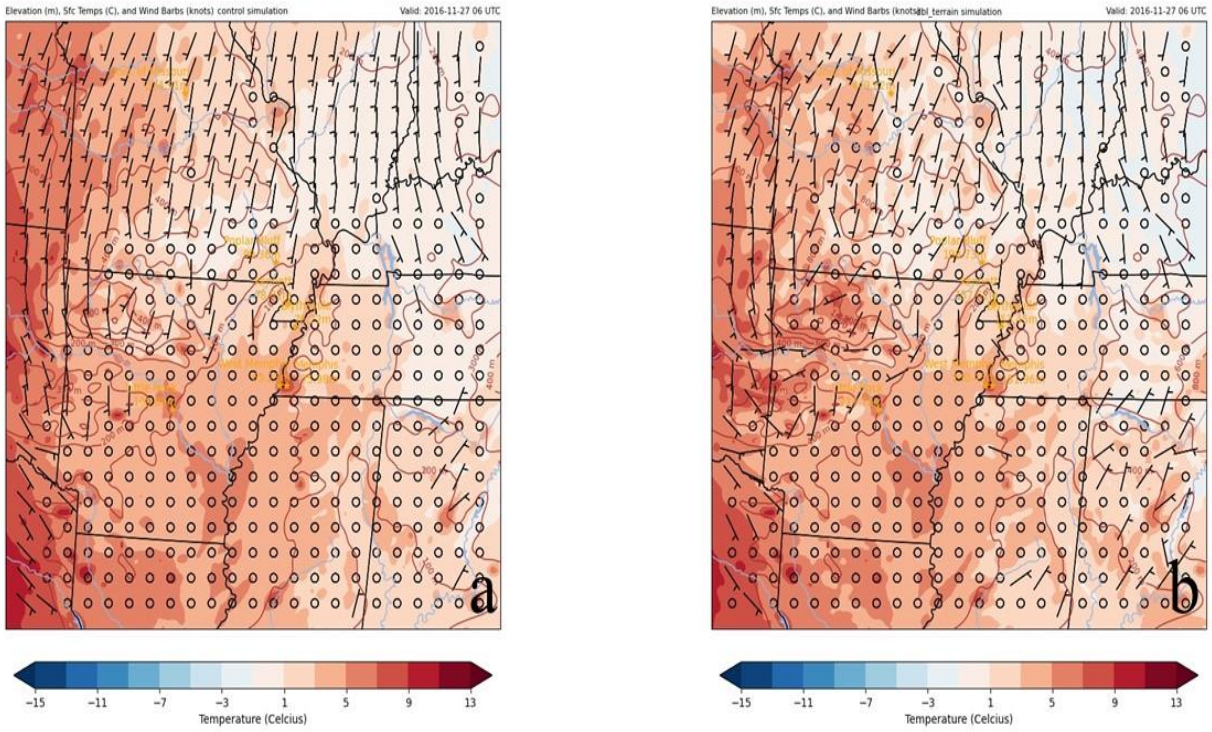

Figure 6.125 - d02 temperature maps from 0600 UTC on 27 November 2016. Each map features surface wind barbs (kts) in black, temperature shaded from blue to red from below -15°C up through 13°C. Topographic lines and values are featured on each map in dark brown.

The pattern of deflection around the embedded ridges on the double-terrain d03 streamline simulation (Fig. 6.126b) continued at 0600 UTC. The level of disruption on the double-terrain map was not matched on the actual-terrain simulation (Fig. 6.126a). As seen previously on the d02 temperature map (Figure 6.125), calmer wind conditions were associated with greater deviation of streamlines especially in and near the sudden elevation increases of the embedded ridges within the flood plain. Deviation decreased when wind speeds increased.

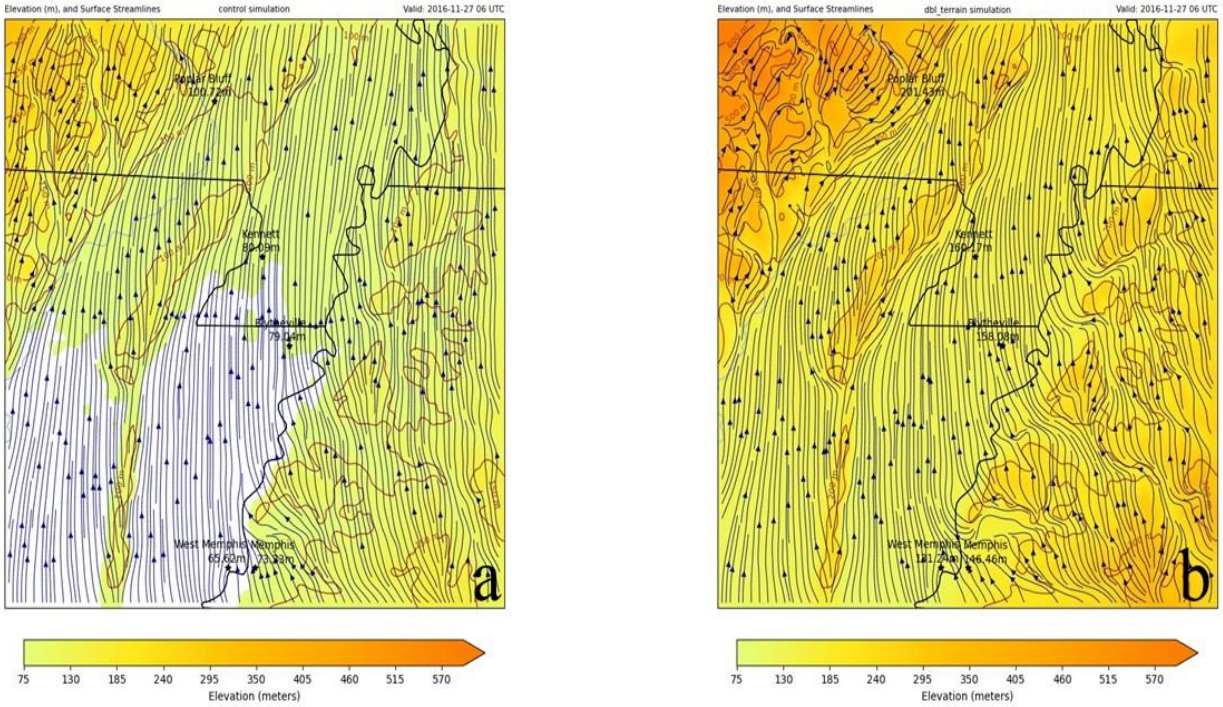

Figure 6.126 - d03 streamline maps from 0600 UTC on 27 November 2016. Map (a) is from the actual-terrain simulation runs. Map (b) is from the double-terrain simulation runs. Surface wind flow streamlines are featured in navy blue on each map. The elevation is shaded from 75 m up through 570 m. Topographic lines are featured in dark brown.

The focused d03 temperature maps (Figure 6.127) of the 0600 UTC time step were similar in terms of the temperature fields and 10-m wind fields on both the actual-terrain and double-terrain simulation maps.

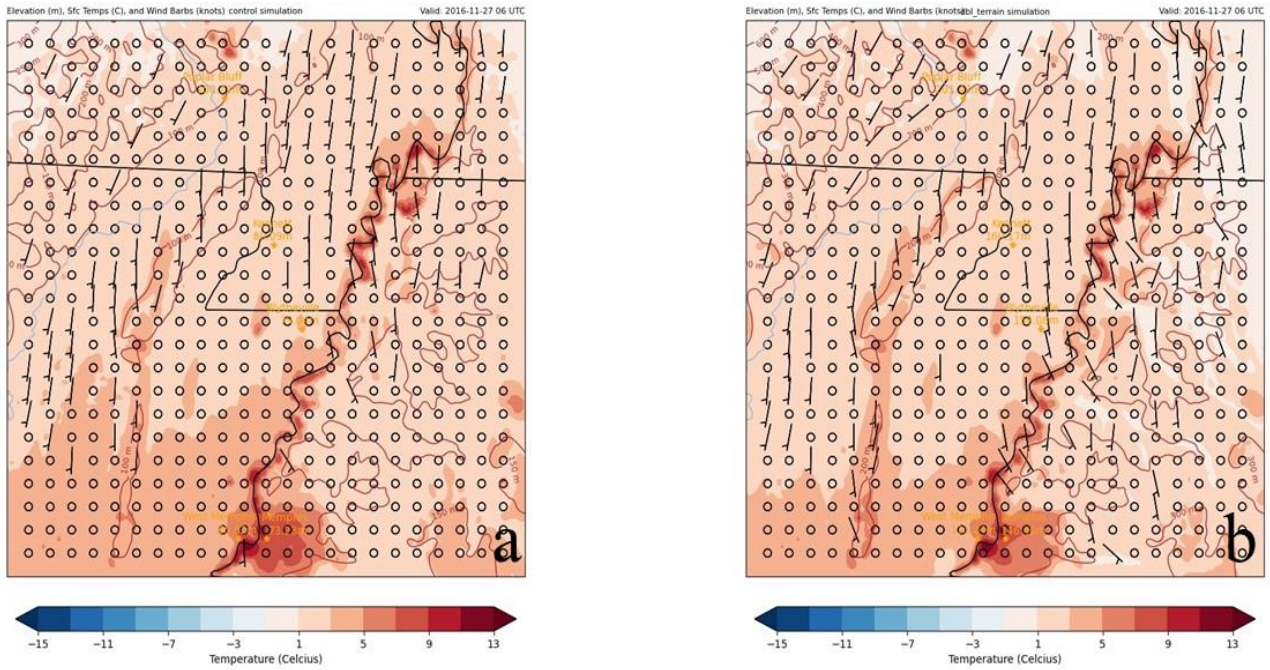

Figure 6.127 - d03 temperature maps from 0600 UTC on 27 November 2016. Each map features surface wind barbs (kts) in black, temperature shaded from blue to red from below -15°C up through 13°C. Topographic lines and values are featured on each map in dark brown.

6.3.3.3 1200 UTC 27 November 2016

Just before daybreak the western edge of the parent anticyclone was apparent on the d02 regional streamline maps (Figure 6.128) of 1200 UTC. The southerly surface flow was disrupted significantly by the extreme elevation values of the double-terrain simulation (Fig. 6.128b), as seen on previous d02 streamline maps. The actual-terrain simulation (Fig. 6.128a) resolved some deviation, but overall, more organized surface flow existed over both the region of interest and its elevations associated with the Ozark Plateau.

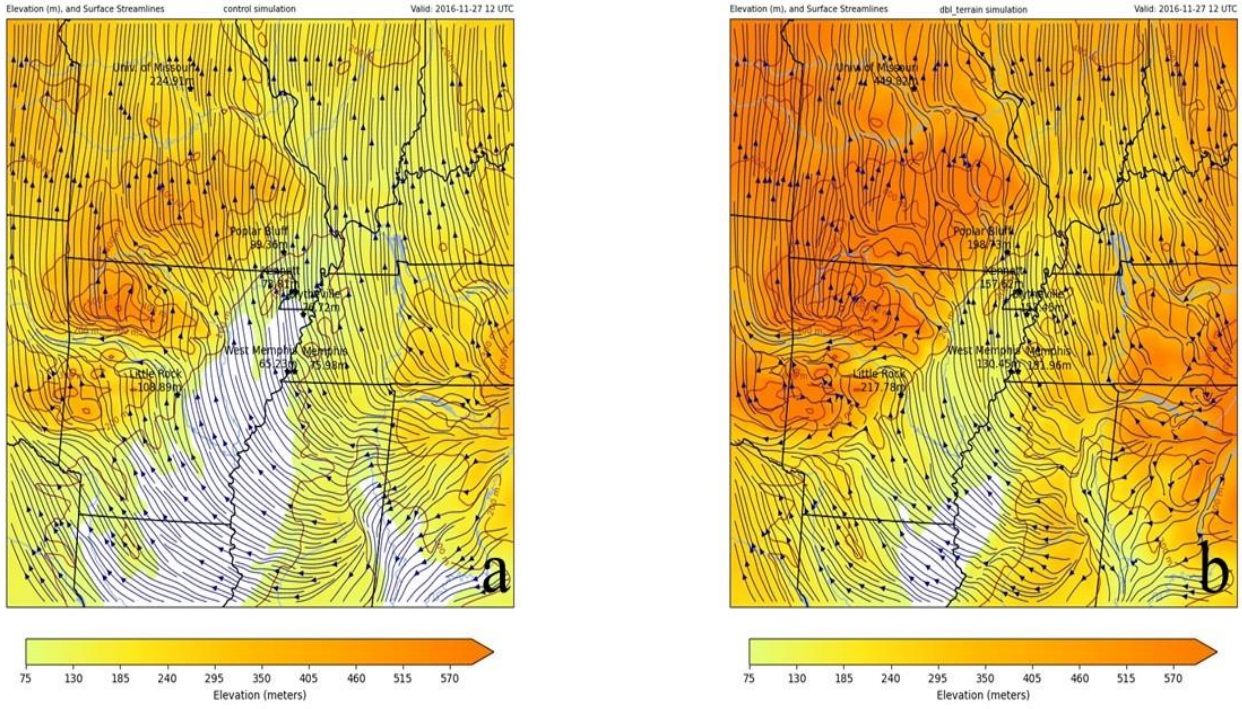

Figure 6.128 - d02 streamline maps from 1200 UTC on 27 November 2016. Map (a) is from the actual-terrain simulation run. Map (b) is from the double-terrain simulation run. Surface wind streamlines are depicted in navy blue on each map. The elevation heights are shaded from 75 m up through 570 m. Topographic lines are shaded in dark brown.

The temperature gradient that set up over the 0600 UTC time step continued 6 hours later just before sunrise with freezing to just below-freezing temperatures observed on both simulation maps in the d02 regional temperature maps (Figure 6.129). Wind speeds in the region of interest began to increase from calm to 5 knots on both simulation maps.

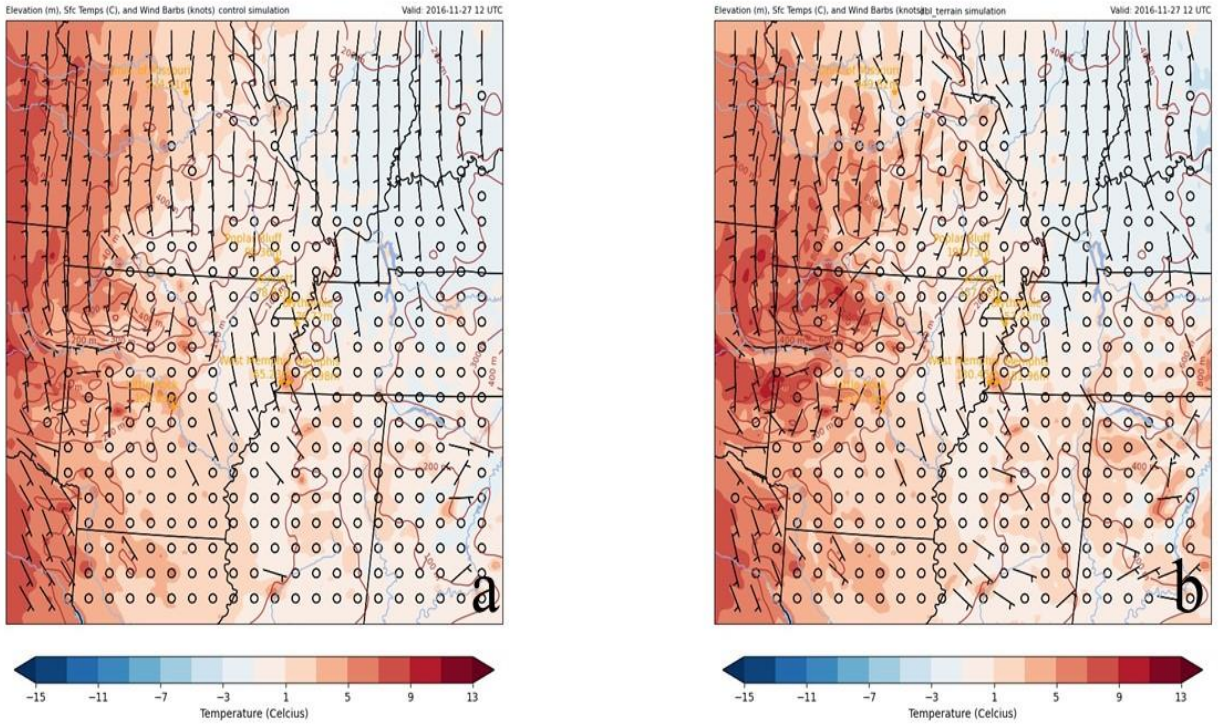

Figure 6.129 - d02 temperature maps from 1200 UTC on 27 November 2016. Each map features surface wind barbs (kts) in black, temperature shaded from blue to red from below -15°C up through 13°C. Topographic lines and values are featured on each map in dark brown.

An increase in wind speed led to a decrease in deflection of streamlines. This was evident on the d03 streamline maps (Figure 6.130) of 1200 UTC. Where previously the embedded ridges of the double-terrain simulation map caused streamlines to be completely redirected around the ridges, with increased wind speeds over the area the streamline now traversed over the ridges with only slight deviation. Increased wind speeds led to little contrast between the 2 simulation maps despite the large difference in elevation height values.

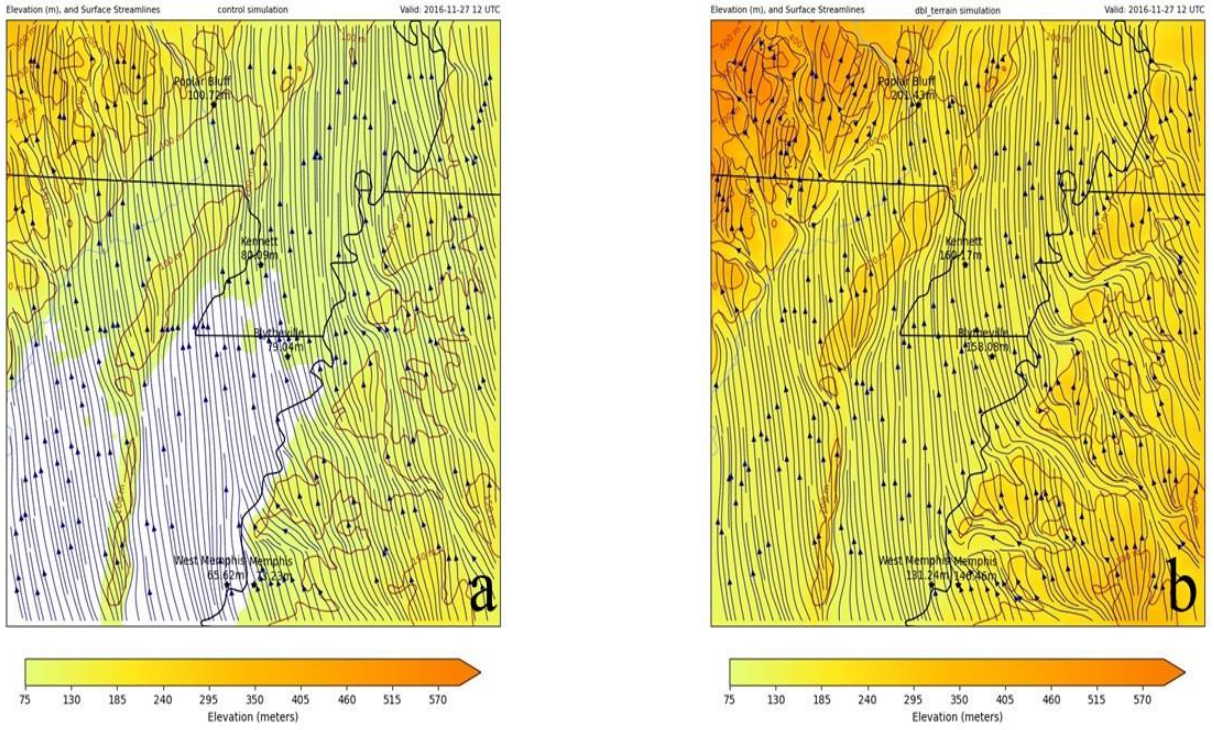

Figure 6.130 - d03 streamline maps from 1200 UTC on 27 November 2016. Map (a) is from the actual-terrain simulation runs. Map (b) is from the double-terrain simulation runs. Surface wind flow streamlines are featured in navy blue on each map. The elevation is shaded from 75 m up through 570 m. Topographic lines are featured in dark brown.

Increased wind speeds in the region of interest were observed on the d03 temperature maps (Figure 6.131) at 1200 UTC. The coldest temperatures of the analysis were resolved at this time step on both simulation maps with little contrast between the temperature fields.

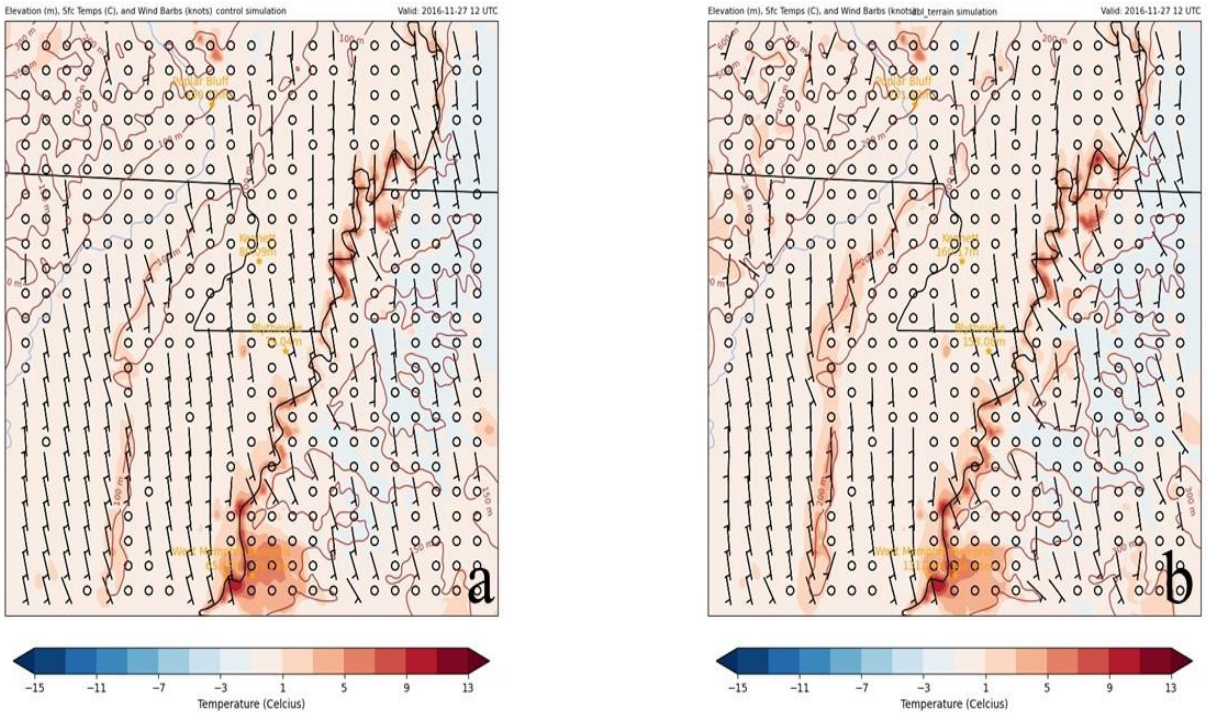

Figure 6.131 - d03 temperature maps from 1200 UTC on 27 November 2016. Each map features surface wind barbs (kts) in black, temperature shaded from blue to red from below -15°C up through 13°C. Topographic lines and values are featured on each map in dark brown.

6.3.3.4 1800 UTC 27 November 2016

As comparative analysis came to an end, increased wind speeds continued to decrease streamline deviation even on a regional scale. The d02 regional streamline maps (Figure 6.132) of 1800 UTC depicted this with organized flow over the elevation height values of the Plateau on both simulation maps. The encroaching low-pressure system as seen in the synoptic overview opened its warm sector up to the region with southerly flow aided by both the parent anticyclone to the east and the oncoming low-pressure system to the west. The cold-air damming event ended, and, in its place, significantly warmer temperatures were observed in the region of interest on both simulation maps.

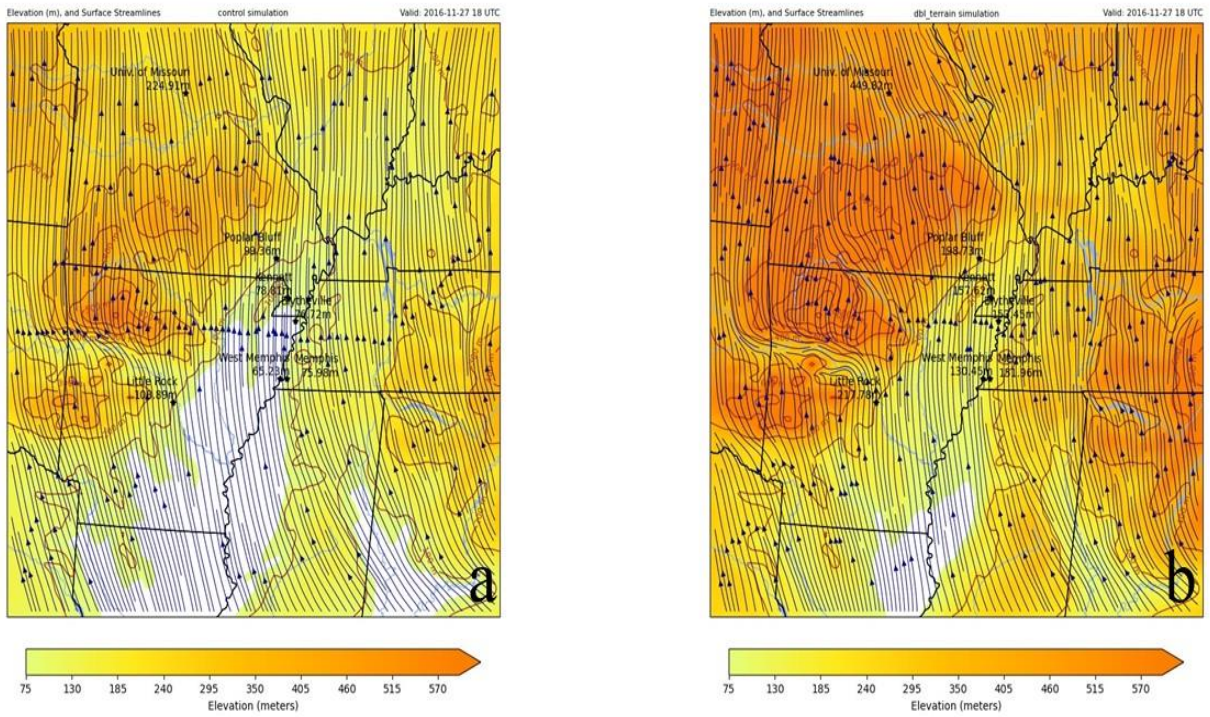

Figure 6.132 - d02 streamline maps from 1800 UTC on 27 November 2016. Map (a) is from the actual-terrain simulation run. Map (b) is from the double-terrain simulation run. Surface wind streamlines are depicted in navy blue on each map. The elevation heights are shaded from 75 m up through 570 m. Topographic lines are shaded in dark brown.

Southerly flow was depicted in the 10-m wind fields of both d02 regional temperature maps (Figure 6.133) strengthened by the pressure systems to the west and east of the region. The temperature fields warmed significantly on both simulation maps as warm air advected into the region from the south abruptly ending the cold-air damming event in the region of interest.

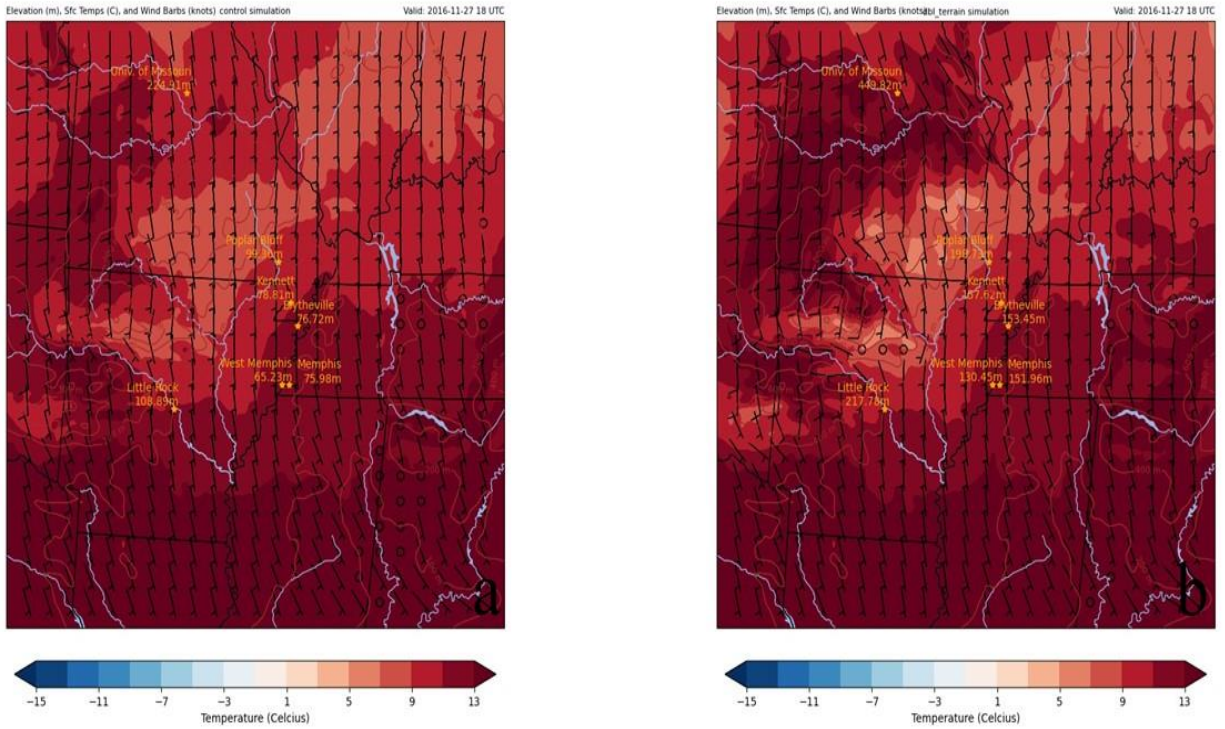

Figure 6.133 - d02 temperature maps from 1800 UTC on 27 November 2016. Each map features surface wind barbs (kts) in black, temperature shaded from blue to red from below -15°C up through 13°C. Topographic lines and values are featured on each map in dark brown.

Similar streamline fields were observed on both simulations of the d03 streamline maps (Figure 6.134) of 1800 UTC as wind speeds had ceased any deviations in flow patterns. As viewed on the regional temperature maps (Figure 6.133) the temperature fields warmed significantly due to this increased southerly wind speed.

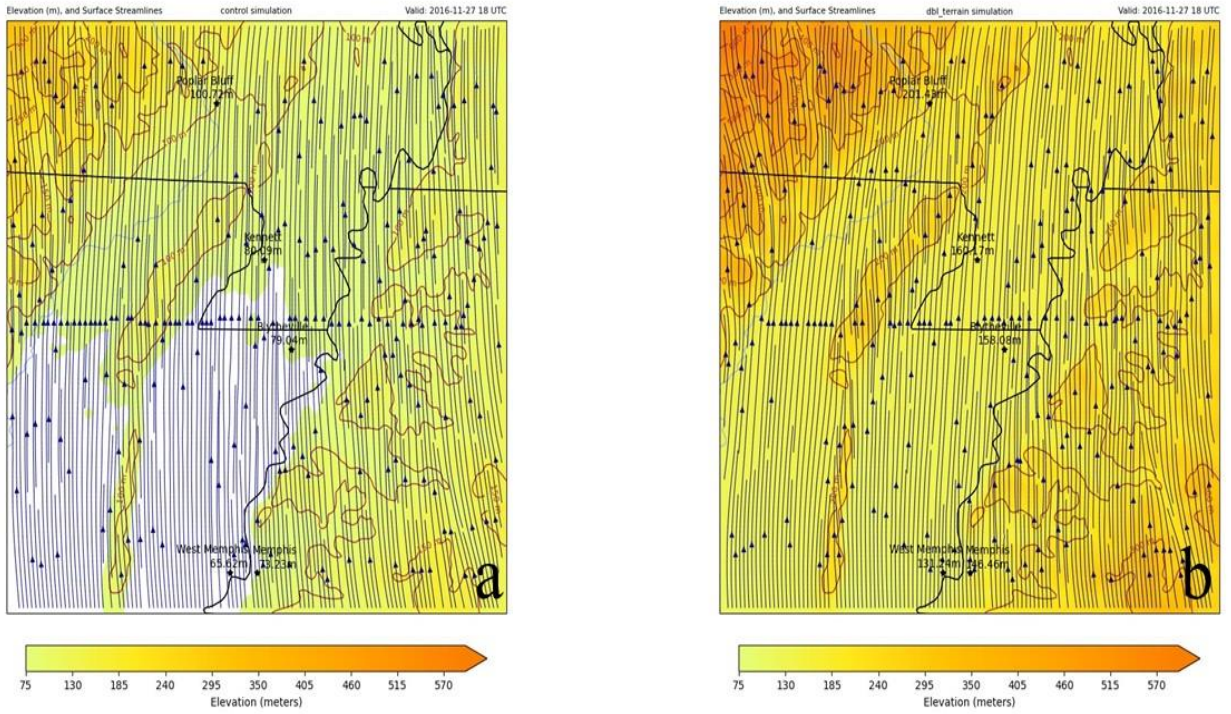

Figure 6.134 - d03 streamline maps from 1800 UTC on 27 November 2016. Map (a) is from the actual-terrain simulation runs. Map (b) is from the double-terrain simulation runs. Surface wind flow streamlines are featured in navy blue on each map. The elevation is shaded from 75 m up through 570 m. Topographic lines are featured in dark brown.

The difference in temperature field values on the d03 temperature maps (Figure 6.135) of 1800 UTC could be observed on each simulation map. The warmer temperatures extended further northwest on the actual-terrain map (Fig. 6.135a) where elevation heights were not as large as those in the same location on the double-terrain simulation map, which keeps the warmer temperatures to the south of the escarpment. Higher elevation height values of the Plateau helped inhibit the effects of warm-air advection to the north of the Ozark Plateau. The 10-m wind fields were similar on the simulation maps with 5-kt southerly flow observed over the entirety of the region of interest.

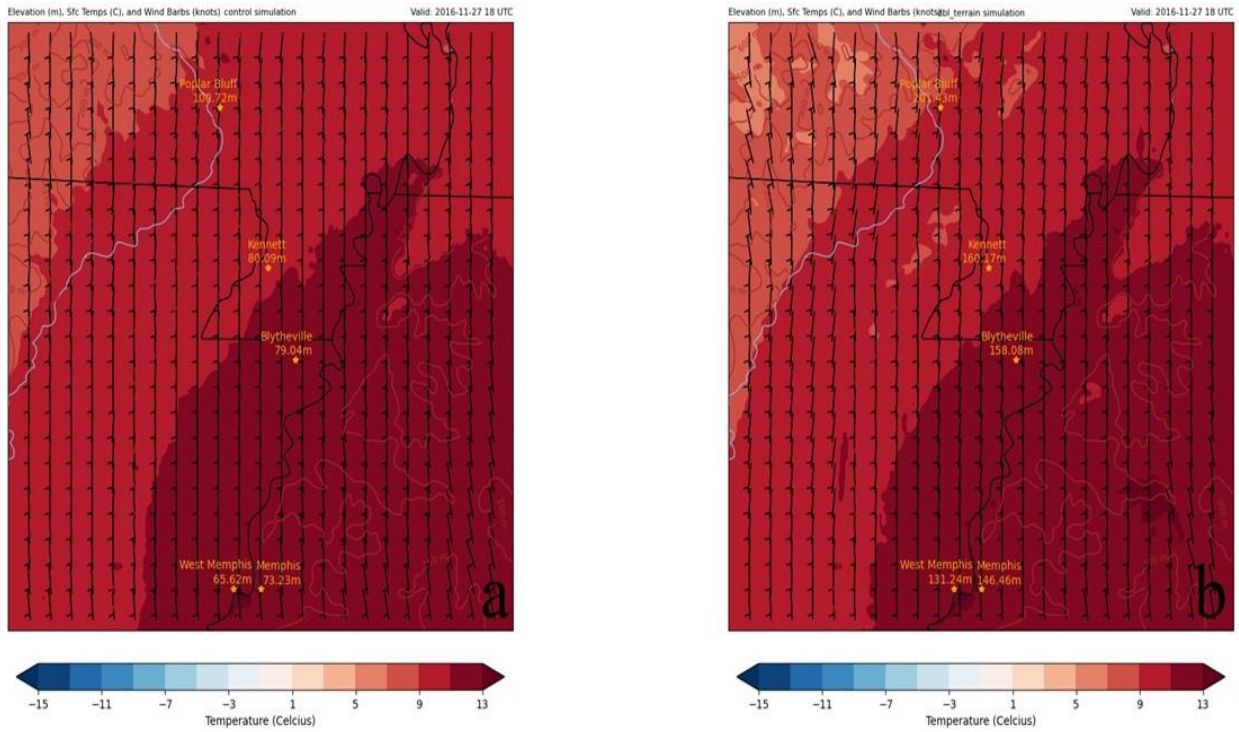

Figure 6.135 - d03 temperature maps from 1800 UTC on 27 November 2016. Each map features surface wind barbs (kts) in black, temperature shaded from blue to red from below -15°C up through 13°C. Topographic lines and values are featured on each map in dark brown.

6.3.4 27 November 2016 Results & Conclusions

The second phase of research involving the 5-year study to determine frequency and intensity of cold-air damming events in the region of interest provided this 27 November 2016 case for WRF modeling study. As detailed previously (Chapter 6, Section 6.3), this case ultimately was designated as a "yellow case" due to satisfying all the cold-air damming characteristics and conditions, but not all of the impactful cold-air damming characteristics. Results of comparative analysis argued that this case study is closer to a "red" case in which all characteristics were satisfied than its original yellow designation.

Comparative analysis, particularly at the 0600 and 1200 UTC time steps of 27 November 2016, resolved freezing and just below-freezing temperatures over the station selected as the point location for this case study: Kennett, Missouri (KTKX).

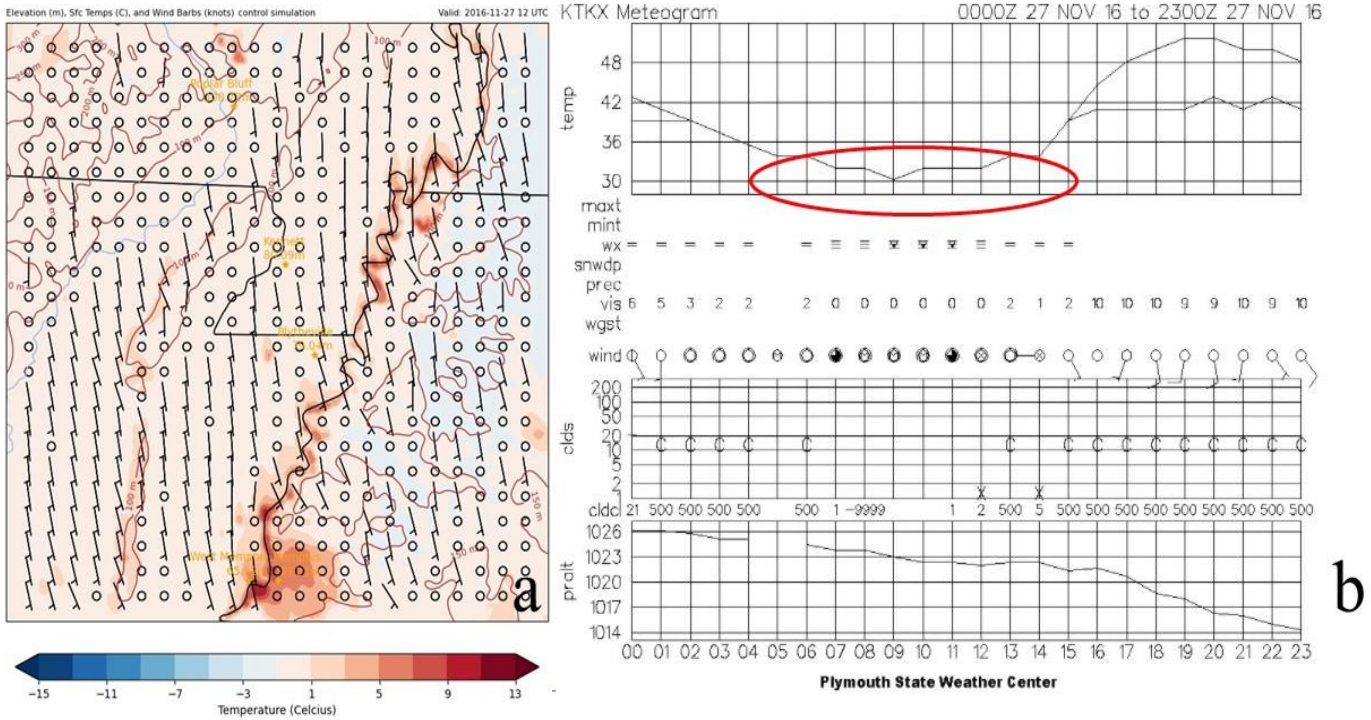

Figure 6.136 – WRF model verification using observed surface conditions from a meteorogram from the Kennett, MO station (KTKX). Map (a) is the d03 actual-terrain simulation temperature map from 1200 UTC on 27 November 2016. Map (b) is the meteorogram from KTKX with the observed temperature from 0400 to 1500 UTC on 27 November 2016 highlighted. The red box on map (a) highlights the inferred temperature range occurring at the KTKX station at this time step. Meteorogram and surface data provided by Plymouth State Weather Center data archive (https://vortex.plymouth.edu/).

Figure 6.136 provided an example of WRF model verification in which the inferred temperature range at around 0°C on the actual-terrain simulation d03 temperature map from 1200 UTC matched up with the observed 2-m temperatures (red oval) in the early morning hours of 27 November 2016 at the Kennett, Missouri station. Despite the warm 2-m temperatures observed on many of the simulation maps, the WRF model accurately resolved the freezing temperatures over the region of interest to create the conditions observed by the ASOS station located in Kennett, Missouri.

An unintended consequence of the WRF modeling analysis is the "2-source" hypothesis discussed previously in the comparative analysis. At critical time steps the temperature field did not show what was observed in the previous case study (Chapter 6, Section 6.2) in which channeling of colder surface air into the flood plain of the region of interest was occurring. During the coldest time steps of this case study (0600 and 1200 UTC on 27 November 2016) the elevation of the Ozark Plateau and the flood plain to the southeast experienced similar 2-m temperatures. This was unusual considering the 10-m wind speed at these time steps was calm over the region of interest and certainly not strong enough to push cold, dense air up onto the Plateau. What was inferred was that the colder temperatures observed on the Plateau were due to radiational cooling at altitude during the overnight hours of 27 November. This colder air was considered to not be from the direction of surface flow (southerly) at these times and was not considered part of the same cooler temperature field found to the south over the flood plain.

6.4 WRF Modeling Numerical Analysis Using the Froude Number

The final piece of analysis using the WRF model involved a numerical analysis and the Froude number to evaluate surface flow strength. The Froude number has been an

integral part of all 3 phases of research understanding cold-air damming in the Ozarks region. For the third phase of research involving WRF modeling, the Froude number was utilized to understand the strength of surface flow of the second domain (regional scale) and the third domain (innermost scale). The second domain with a larger spatial resolution was utilized more so as a quality check on the finer spatial resolution of the innermost third domain. For this phase of research, the 10-m wind flow was treated as a streaming flow over the second and third domains. Therefore, the singular Froude number for each domain was used to evaluate if the stream flow of the 10-m wind was sub- or supercritical. Values between the domains differed not only because of the spatial resolution, but also because the number of grid points increased from d02 to d03. The second domain (d02) employed 181 grid points, while the innermost domain (d03) used 231 grid points within a smaller area. Despite the finer spatial resolution and larger number of grid points in the innermost domain, the modeled elevation height values decreased because much of d03 encompasses the flatter elevations of the Mississippi River alluvial plain.

Table 6.2 - Elevation height values used for Froude number calculation for each terrain altered simulation per domain.

Elevation Height Values		
Simulation	**Domain 2**	**Domain 3**
No-Terrain	0.64 m	.32 m
Half-Terrain	324 m	162 m
Actual-Terrain	647 m	323 m
Double-Terrain	1294 m	647 m

To perform this analysis a singular Froude number was calculated for each domain at each time step of research for each case study. Using the equation detailed in Chapter 3, Section 3.2, averaged values of 10-m wind speed (U) and Brunt-Väisälä frequency (N) were calculated based on variables from each grid point within d02 and d03. For the height variable (h) the elevation of the Ozark Plateau was manipulated based on which simulation was analyzed. For example, the value for h associated with the double-terrain simulation will take the highest maximum value of double-terrain manipulated elevation height associated with the Ozark Plateau. Table 6.2 contains elevation height values used for each simulation in both domains.

6.4.1 Froude Number Analysis for 04 March 2014 Case Study

Froude number evaluation for the 04 March 2014 case study began at 1200 UTC on 03 March 2014 shortly after passage of the mid-latitude cyclone and terminated at 1200 UTC on 05 March 2014 after the cold-air damming event concluded. This time step evaluation was the same for both the d02 and d03 domains. Table 6.2 depicts the Froude number results for the second regional domain (d02).

Table 6.3 - Froude number values for the second regional domain (d02) of the 04 March 2014 case study. These Fr values coincide with the four "benchmark" simulations: no-terrain, half-terrain, actual-terrain, and double-terrain. Green shaded cells represent Froude numbers larger than 1.20 and indicate that surface flow is unimpeded. Yellow shaded cells represent Froude numbers between 1.05 and 1.20 and indicate that surface flow is somewhat impeded.

Domain 2	Froude Number								
Time Step	12UTC 3/3/14	18UTC 3/3/14	00UTC 3/4/14	06UTC 3/4/14	12UTC 3/4/14	18UTC 3/4/14	00UTC 3/5/14	06UTC 3/5/14	12UTC 3/5/14
No-Terrain	65.16	61.25	40.98	25.13	17.18	4.72	7.96	9.13	15.79
Half-Terrain	1.22	1.16	0.79	0.49	0.31	0.06	0.13	0.17	0.31
Actual-Terrain	0.56	0.54	0.37	0.23	0.14	0.01	0.06	0.08	0.15
Double-Terrain	0.21	0.23	0.16	0.09	0.05	0.01	0.01	0.03	0.07
			Fr < 1.05		1.05 ≤ Fr ≤ 1.20		Fr > 1.20		

As expected, the no-terrain simulation yielded very large Froude number values. The half-terrain simulation resulted in much smaller Froude numbers, with time steps during the cold air damming event being favorable for cold-air damming as the Fr number indicated surface flow being completely impeded. The actual-terrain simulation observed complete impedance of surface flow throughout this cold-air damming event. This was important evidence in support of a sustained cold-air damming event for this case study. The double-terrain resolved extremely low Froude numbers before, during, and after the cold-air damming event.

Table 6.4 - Froude number values for the third innermost domain (d03) of the 04 March 2014 case study. These Fr values coincide with the four "benchmark" simulations: no-terrain, half-terrain, actual-terrain, and double-terrain. Green shaded cells represent Froude numbers larger than 1.20 and indicate that surface flow is unimpeded. Yellow shaded cells represent Froude numbers between 1.05 and 1.20 and indicate that surface flow is somewhat impeded. Red shaded cells represent Froude numbers below 1.05 and indicate that surface flow is completely impeded.

Domain 3	Froude Number								
Time Step	12UTC 3/3/14	18UTC 3/3/14	00UTC 3/4/14	06UTC 3/4/14	12UTC 3/4/14	18UTC 3/4/14	00UTC 3/5/14	06UTC 3/5/14	12UTC 3/5/14
No-Terrain	168.11	147.10	88.96	42.77	44.85	50.35	33.93	29.30	39.49
Half-Terrain	3.40	2.93	1.84	0.90	0.88	0.99	0.66	0.61	0.83
Actual-Terrain	1.71	1.47	0.93	0.47	0.45	0.51	0.34	0.30	0.40
Double-Terrain	0.84	0.76	0.45	0.26	0.23	0.24	0.16	0.14	0.18
			Fr < 1.05		1.05 ≤ Fr ≤ 1.20		Fr > 1.20		

Table 6.4 shows the Froude number values for the innermost d03 domain. Results here were significantly different than those of the d02 numerical analysis. The no-terrain simulation featured very large values for the Froude number, but changes occurred when the half-terrain simulation were evaluated. In the regional d02 domain favorable Froude number values were observed later in the time steps with a gradual impedance of surface flow during the impact hours of the cold-air damming event for the half-terrain simulation. This was not the case for the d03 evaluation where the Froude number remained large enough to indicate surface flow was unimpeded through the 0600 UTC 04 March time step. Most half-terrain simulation impact time steps, however, did produce favorable Froude numbers for cold-air damming. The actual-terrain simulation featured a favorable Froude number during impactful time steps ranging from 0.3 up to 0.93 supporting a cold-air damming event. To contextualize these results Bates et al, (1987) reported Froude number results between 0.3 and 0.4 for a cold-air damming event in

Table 6.5 - Froude number values for the second regional domain (d02) of the 27 November 2016 case study. These Fr values coincide with the four "benchmark" simulations: no-terrain, half-terrain, actual-terrain, and double-terrain. Green shaded cells represent Froude numbers larger than 1.20 and indicate that surface flow is unimpeded. Yellow shaded cells represent Froude numbers between 1.05 and 1.20 and indicate that surface flow is somewhat impeded. Red shaded cells represent Froude numbers below 1.05 and indicate that surface flow is completely impeded.

Domain 2	**Froude Number**						
Time Step	**06UTC 11/26/16**	**12UTC 11/26/16**	**18UTC 11/26/16**	**00UTC 11/27/16**	**06UTC 11/27/16**	**12UTC 11/27/16**	**18UTC 11/27/16**
No-Terrain	110.32	57.48	57.10	81.29	108.00	121.95	302.16
Half-Terrain	0.21	0.12	0.14	0.18	0.23	0.25	0.67
Actual-Terrain	0.11	0.06	0.07	0.10	0.12	0.12	0.36
Double-Terrain	0.05	0.03	0.03	0.04	0.05	0.06	0.19
		Fr < 1.05		**1.05 ≤ Fr ≤ 1.20**		**Fr > 1.20**	

January of 1980 that impacted the Pennsylvania portion of the Appalachian Mountains. The double-terrain simulation produced favorable Froude number values and maintained that designation throughout the simulation.

The number of favorable Froude number values during the cold-air damming time steps for both the d02 and d03 evaluations favored the evidence of a significant cold-air damming event in this region impacting the area.

6.4.2 Froude Number Analysis for 27 November 2016 Case Study

The Froude number evaluation was again performed on the second case study of this WRF modeling research. Here the same domains were evaluated between 0600 UTC on 26 November 2016 and 0000 UTC on 28 November 2016. This time period included the 4 time steps of the cold-air damming event (0000 UTC 27 November 2016 through

Table 6.6 - Froude number values for the third innermost domain (d03) of the 04 March 2014 case study. These Fr values coincide with the four "benchmark" simulations: no-terrain, half-terrain, actual-terrain, and double-terrain. Green shaded cells represent Froude numbers larger than 1.20 and indicate that surface flow is unimpeded. Yellow shaded cells represent Froude numbers between 1.05 and 1.20 and indicate that surface flow is somewhat impeded. Red shaded cells represent Froude numbers below 1.05 and indicate that surface flow is completely impeded.

Domain 3	Froude Number						
Time Step	06UTC 11/26/16	12UTC 11/26/16	18UTC 11/26/16	00UTC 11/27/16	06UTC 11/27/16	12UTC 11/27/16	18UTC 11/27/16
No-Terrain	430.91	387.47	36.55	154.10	303.37	215.59	686.14
Half-Terrain	0.89	0.81	0.07	0.37	0.66	0.48	1.52
Actual-Terrain	0.46	0.40	0.05	0.19	0.34	0.26	0.82
Double-Terrain	0.23	0.21	0.06	0.07	0.15	0.13	0.43
		Fr < 1.05		1.05 ≤ Fr ≤ 1.20		Fr > 1.20	

1800 UTC 27 November 2016. Table 6.4 contains results from the Froude number analysis for d02 the regional domain.

The d02 Froude number results for the 27 November 2016 case study continued the pattern of large Froude number values for the no-terrain simulation. However, the half-terrain simulation featured favorable Froude number values during the cold-air damming. Even elevation heights of half the actual elevation would impede surface flow under the regional conditions evaluated for this case study. The actual-terrain simulation resolved favorable Froude number for cold-air damming both before and during the cold-air damming time steps. Opposite of the no-terrain simulation is the double-terrain simulation in which Froude number values were favorable throughout the case study for impeded surface flow.

For d03, the no-terrain simulation remained consistent with large values of Froude number in which surface flow would continue unimpeded. The half-terrain simulation for

this domain was limited to only 1 time step (1800 UTC on 27 November 2016) in which flow was unimpeded. Every other time step resolved favorable values of Froude number meaning the surface flow would be impeded around half values of actual terrain height. The actual-terrain simulation observed significant results in all the cold-air damming event time steps contained Froude number values that would impede surface flow or somewhat impeded surface flow. The double-terrain simulation again featured low values of Froude number resulting in impeded surface flow.

Results of Froude number numerical analysis favored a surface flow weak enough to contain trapped cold air up against the elevation of the Ozark Plateau especially during the critical time steps of the cold-air damming event evaluated in this WRF modeling exercise.

CHAPTER 7. CONCLUSIONS

7.1 Summary

An icing event in eastern Arkansas in the early spring of 2014 led to motorists along Interstates 44 and 55 in the region becoming stranded overnight when roads and highways in the area became impassable due to hazardous icy conditions. Local law enforcement and the Arkansas National Guard were mobilized to assist stranded motorists and evacuate those in need when the situation warranted. This occurred, however, when no precipitation was observed to be falling in the region. An initial investigation of conditions during this impactful icing event led to a hypothesis that cold-air damming caused by the topography of the Ozark Plateau was to blame for the treacherous travel conditions.

This investigation of a potential cold-air damming event became the first phase of a larger research study on Ozark Plateau induced cold-air damming events. This initial phase was an observational study on meteorological conditions during the period of this icing event to determine if cold-air damming was occurring and if so, what conditions were present to create this event. The study found that the consistent presence of an anticyclone to the north and northeast of the region of interest in eastern Arkansas was necessary in providing 10-m wind flow that would support cold-air damming in the region. This easterly surface flow was terrain-orthogonal which helped to push and trap the cold, dense air within the flood plain up against the elevation increase of the escarpment of the Plateau to the west resulting in a sustained cold-air damming event for the region. A variety of resources were utilized to determine cold-air damming and examine its intensity during the event. Resources included synoptic-scale surface

pressure maps, 10-m wind and relative humidity charts, observed sounding data and modeled sounding output, as well as observed point-location meteorograms. Finally, the Froude number was utilized to conduct a numerical analysis on the strength of the surface flow to overcome terrain obstacles in the path of the flow. This analysis led to the observation of conditions and characteristics of a prolonged, impactful cold-air damming event in the region during the 04 March 2014 case.

The initial phase of research led to the second phase which addressed the question of if the Ozark Plateau could create a cold-air damming event, how often does this phenomenon occur and how intense are these cold-air damming events? METAR reports from 6 ASOS stations located between southeastern Missouri, eastern and central Arkansas, and eastern Tennessee was analyzed over a 5-year period between 01 January 2016 and 31 December 2020 excluding the months of May through September. This METAR reports were examined to contain specific present weather conditions including freezing rain (FZRA), freezing fog (FZFG), freezing drizzle (FZDZ), and mist (BR).

The study found 34 instances of these present weather conditions at 6 locations during the 5-year period. A set of characteristics was established using evidence from the initial March 2014 case study to identify cold-air damming events among the 34 case studies. These characteristics are listed and explained in Chapter 3, Section 3.2.2. In total, 9 characteristics were used to identify cold-air damming. The first 6 were to determine if the case study was a cold-air damming event and the final 3 to determine if the cold-air damming event was an impactful cold-air damming event. Of the 34 potential cold-air damming case studies, only 6 satisfied the 6 characteristics established to identify cold-air damming. Of the 6 case studies that did satisfy those conditions only 4 of those 6

cases of cold-air damming satisfied the characteristics and conditions to determine an impactful cold-air damming event.

The final phase of research shifted from an observational approach to a numerical modeling approach. The WRF model was utilized to study the effect of terrain height on cold-air damming events. This approach was important specifically for the Ozark Plateau due to its lower elevation heights compared to the main regions where cold-air damming can be found: the southern Appalachians and the Rocky Mountains. For this analysis, phase 2 cases of Ozark Plateau induced cold-air damming were analyzed. The initial 04 March 2014 case and a case from the 5-year study, 27 November 2016, became the focus for this numerical modeling analysis.

The WRF model was used to simulate these events when the terrain is manipulated. In total, 42 simulations were performed altering terrain by multiplying it by values of 1.0, 0.0001, and values between 0.1 and 2.0. Using a 3-domain approach (outlined in Chapter 3, Section 3.3.1) the WRF model simulated these events using a fine spatial resolution. 2-m temperature fields, 10-m wind fields, and 10-m wind streamline fields were analyzed comparatively between the actual-terrain (terrain*1.0) simulation and the various manipulated terrain simulations to understand how the events were altered when terrain is either diminished or exaggerated. Analysis showed that 2-m temperature fields and 10-m wind fields, both in direction and velocity, were influenced by increasing elevation height (including the actual-terrain simulation).

The Froude number was again employed in this numerical modeling approach to understand the strength of 10-m wind flow (or lack thereof) needed to overcome different terrain elevation heights. The Froude number was calculated singularly for both the

regional (d02) domain and the innermost (d03) domain for each time step of each case study. These values were then compared to gain understanding of what terrain values were needed to sufficiently impede 10-m wind flow during these cold-air damming events. Froude number calculations from the d02 (regional) domain were treated as a qualitative check on the Froude number values of the innermost (d03) domain with its finer spatial resolution. Results were understood (discussed previously in Sections 6.4.1 and 6.4.2 of Chapter 6) in that some of the cases did not require large elevation height values to impeded flow where others did.

7.2 Synthesis

This study set out to determine if cold-air damming could occur in a location in which it had not been previously identified. This was a novel concept in that previously cold-air damming events had only been associated with the southern Appalachians and the Front Range of the Rocky Mountains. This study was the first to identify a cold-air damming event associated with the region associated with the Ozark Plateau. In doing so, the research found synoptic and mesoscale atmospheric characteristics that were similar when cold-air damming was perceived to be occurring. These characteristics became necessary conditions for this region to support a cold-air damming event. Parent anticyclone placement and the subsequent terrain-orthogonal wind directional component found in its southern flank occurring over the region of interest was needed for these events to take place and maintain strength over time. It is understood that an anticyclone to the north-northeast of the region of interest is not required to have terrain-orthogonal 10-m wind flow in the region of interest. It is inferred, however, that such placement of

an anticyclone can aid in not only the presence of a cold-air damming event in the region, but also maintain the event's atmospheric conditions and longevity. This was especially true along the southeastern edge of the Plateau which is located just west of the flat elevation of the large Mississippi River flood plain covering much of the region of interest.

Vertical profiling for these events must contain a terrain-orthogonal directional component in the vertical wind profile at and near the surface as well as a temperature inversion in the lower levels of the profile. The inversion is needed to help trap the surface layer of cold, dense air up against the elevation of the Ozark Plateau. For impactful cases of cold-air damming the stable surface layer below the inversion must be moist with the temperature and dewpoint temperature profiles being within 5°C of each other.

The Froude number analysis was crucial in understanding a 10-m wind flow that would be impeded by a terrain feature such as the escarpment of the Ozark Plateau. The utility of the Froude number was realized in all 3 phases of research and resulted in perhaps the most compelling evidence for identifying cold-air damming in the Ozarks region. Combined with the chart analysis of the initial phase regarding the 04 March 2014 and how it compared to previous studies mentioned earlier, observations of conditions present strongly suggest that cold-air damming can be achieved in the region of the Ozark Plateau.

Cold-air damming that does occur in the Ozarks region should be found in the presence of very specific atmospheric conditions to maintain a prolonged life cycle and impact the region. These conditions are favorable anticyclone placement, a terrain-

orthogonal 10-m wind directional component, at or below-freezing 2-m temperatures, sufficient surface moisture, low-level cloud cover, and favorable Froude number calculations. Combined with results from the WRF modeling phase of research, **what set the initial case apart from other cases was the role and impact of the snowpack in, and just to the northeast of the region of interest. The intensity and impact of this March 2014 case was unmatched by any of cold-air damming cases found in the 5-year study. It was this very specific setup that led to this initial case being as impactful as was reported.** Though the results of the second phase of research only yielded 6 of 34 potential cases becoming a cold-air damming event, this results in an average of slightly more than 1 cold-air damming event per year given the 5-year period of analysis. The applied science question then becomes what does this mean for future cold-air damming events? What are the weather forecasting implications of this study?

The forecasting question is organic in nature: what conditions of the atmosphere would signal the potential for an impactful cold-air damming event to occur? The presence of a terrain-orthogonal 10-m wind is critical for a cold-air damming event to exist and, therefore, the 10-m directional wind component forecast becomes the focal point when initially looking for potential impactful cold-air damming events. Figure 7.2, a cold-air damming forecast checklist, reinforces the importance of the 10-m wind forecast as the first 3 required characteristics are centered on 10-m wind speed and direction. Once the 10-m wind terrain-orthogonal component has been identified to be favorable, low-level wind speeds then need to be examined in much the same way one would identify wind speeds favorable for fog. One of the observed conditions found in METAR reports for both the initial case study of the first research phase and the cases

found to be cold-air damming events in the second phase of research was freezing fog (FZFG). It was established based on observations in Chapter 3, Section 3.1.2 that a threshold of 5-kt 10-m winds was the maximum speed found in which a cold-air damming could exist in the region of interest for the Ozark Plateau. Therefore, the forecaster needs to identify calm to 5-kt wind speeds on both surface charts and model sounding output in the region of interest in which cold-air damming could occur. This range of wind speeds is sufficient for the region of interest associated with the Ozark Plateau; however, the wind speed range will be determined by the height of the cold-air damming obstacle in question. To determine the wind speed range for potential cold-air damming events the Froude number calculation is a resource that can be used to find these speed values. Outlined in Chapter 3, Section 3.2, and reiterated in Chapter 6, Section 6.4, the Froude number was used in this study as a ratio of momentum (kinetic energy) to obstacle height when evaluating the strength of the 10-m wind field to flow over the Ozark Plateau. Using this version of the Froude number calculation the forecaster can use model output and a height value representing maximum obstacle height to evaluate 10-m wind speed and its ability to flow over the terrain obstacle in question. To reiterate, Froude number values less than 1.05 would signal an impeded surface flow. Froude number values greater than 1.20 represent a surface flow that is unimpeded by the obstacle and therefore would not create a cold-air damming event. For Froude number values between 1.05 and 1.20 the surface flow is somewhat impeded in that the surface flow could not flow over the highest elevation height values of the obstacle but may be able to flow over or around lower elevations in the region of interest.

Due to this possibility, values of Froude number calculations up to 1.20 are regarded as favorable when forecasting for potential cold-air damming events.

Once the forecaster has satisfied 10-m wind conditions favorable for a cold-air damming event, impactful 2-m temperature and surface moisture become the criteria of focus. For impactful cold-air damming, 2-m temperature was required to be at or below freezing during the observed times of cold-air damming events. This requirement remains for the forecaster when evaluating potential impactful cold-air damming events. The 2-m temperature must reside at or below freezing (32°F or 0°C depending on temperature scale) for an impactful cold-air damming event to take place. If 2-m temperature rises above the freezing threshold during the event, the event is no longer considered impactful, or the event may be coming to an end. Regarding surface moisture, the research used the conventional 5°C dewpoint depression difference between 2-m temperature and 2-m dewpoint temperature to evaluate whether sufficient surface moisture was in place. The same exercise can be employed by the forecaster when evaluating if sufficient surface moisture is in place for potential cold-air damming events. In cases where the dewpoint depression is 5°C or less surface moisture is said to be sufficient to support an impactful cold-air damming event. For cases in which the dewpoint depression is greater than 5°C the cold-air damming event is regarded as not impactful. Regarding the forecasting checklist (Figure 7.2) if the 10-m wind, 2-m temperature, and surface moisture characteristics are found than an impactful cold-air damming event in the region of interest should be considered likely. At this point the focus should shift to examining the longevity of the potential cold-air damming event.

Figure 7.1 - A map of favorable anticyclone placement in reference to the region associated with the Ozark Plateau prone to cold-air damming events. The yellow box represents the region in which cold-air damming associated with the Ozark Plateau occurs. The red circle indicates the area of the United States in which an anticyclone can be found to be favorable for cold-air damming to occur in the region highlighted by the yellow box.

A more traditional answer to this forecasting question would be to look synoptically for favorable anticyclone placement, however, it is understood that a favorable terrain-orthogonal 10-m wind can exist without the presence of a parent anticyclone. Despite this understanding, it is prudent to analyze synoptic charts for favorable anticyclone placement and associated 10-m flow for favorable 10-m terrain-orthogonal winds. In cases in which this occurs, the cold-air damming event has potential to be more impactful in that the event will be longer lasting if the anticyclone maintains a favorable position to promote terrain-orthogonal winds.

Figure 7.1 depicts the region of the United States where an anticyclone can be found to be favorable for helping to create and maintain cold-air damming events in the alluvial plain of the Mississippi River just east of the southeastern flank of the Ozark Plateau.

Beyond 10-m winds, surface moisture, and 2-m temperatures, the forecaster needs to address cloud cover and the potential for other atmospheric phenomena impacting the region of interest when there exists potential for a cold-air damming event. Sustained cloud cover over the region of interest can help to prolong the potential cold-air damming event by mitigating the effects of daytime heating and supporting the presence of sufficient surface moisture. In the event of surface-layer clouds, such as fog, the cloud cover may enhance hazardous ground conditions through riming processes during impactful cold-air damming events. Ample surface moisture should signal low-level clouds, but model products can also be employed to evaluate the presence of clouds during the cold-air damming event. One of the characteristics of the initial case study from the first phase of research that made that event a novel cold-air damming event was the lack of radar reflectivity over the region of interest while the event was impacting the area. While radar reflectivity (or lack thereof) was omitted from the checklist created to help identify potential cold-air damming events, it is important for the forecaster to understand how precipitation growth processes evolve before, during, and after a potential cold-air damming event. Simulated radar reflectivity is a model product that can be utilized to understand if a more organized precipitation developing event may impact the region of interest when a potential cold-air damming event is possible. Organized radar reflectivity may signal the encroachment of another weather system and conditions for a favorable cold-air damming event would need to be re-evaluated.

COLD-AIR DAMMING FORECASTING CHECKLIST

Required Cold-Air Damming Characteristics

- ☐ Presence of terrain-orthogonal surface winds during the potential cold-air damming event
- ☐ Forecasted surface winds are 5 kts or less during the potential cold-air damming event
- ☐ Froude number calculations are less than 1.20 supporting impedance of surface flow

*If surface wind characteristics are not found, no further evaluation is needed

Impactful Cold-Air Damming Characteristics

- ☐ Forecasted 2-m temperatures during the potential cold-air damming event are at or below freezing
- ☐ Forecasted surface layer dewpoint depressions are 5°C or less during the cold-air damming event supporting sufficient surface moisture

Long-Lasting Cold-Air Damming Characteristics

- ☐ Presence of a parent anticyclone in a favorable position to support terrain-orthogonal surface winds
- ☐ Temperature inversion present in model sounding output just above surface during potential cold-air damming event
- ☐ Presence of cloud cover during the potential cold-air damming event

Figure 7.2 – A checklist that can be utilized by forecasters to evaluate the potential for cold-air damming to occur. The checklist is broken down into 3 segments: required characteristics, impact characteristics, and long-lasting characteristics.

Broken down into 3 segments, the cold-air damming checklist (Figure 7.2) is designed to help the forecaster identify potential cold-air damming events in any region where a juxtaposition of higher elevation adjacent to flatter elevation exists. The alluvial flood plain of the Mississippi River located in southeastern Missouri and eastern Arkansas serves as the template for this checklist though it is intended to be configured to any region with similar characteristics. Configurations may include adjusting the terrain-orthogonal 10-m wind directional range as well as establishing the region for favorable parent anticyclone placement. The first portion of the checklist focuses on orientation and speed of 10-m winds. These 3 characteristics need to be satisfied for a cold-air damming event to be possible. Once those conditions are satisfied the forecaster can move into the impactful and long-lasting characteristics. Beyond the required conditions the more characteristics that are satisfied the more likely an impactful, long-lasting cold-air damming event becomes. The forecaster should determine the duration and extent of the event and inform partners as needed.

REFERENCES

Adamski, J.C., Petersen, J.C., Freiwald, D.A., and Davis, J.V., 1995: Environmental and Hydrologic Setting of the Ozark Plateaus Study Unit, Arkansas, Kansas, Missouri, and Oklahoma. U.S. Geological Survey, Water-Resources Investigations Report 94-4022.

American Meteorological Society, 2016: Damming, Glossary of Meteorology, https://glossary.ametsoc.org/wiki/Damming.

American Meteorological Society, 2014. Froude Number, Glossary of Meteorology, https://glossary.ametsoc.org/wiki/Froude_number.

American Meteorological Society, 2022. Virtual Potential Temperature, Glossary of Meteorology, https://glossary.ametsoc.org/wiki/Virtual_potential_temperature.

Bailey, C.M., Hartfield, G., Lackmann, G.M., Keeter, K.K., and Sharp, S., 2003: An Objective Climatology, Classification Scheme, and Assessment of Sensible Weather Impacts for Appalachian Cold-Air Damming. *Wea. Forecasting.*, **18**, 641-661.

Baker, D.G., 1971: A Study of High Pressure Ridges to the East of the Appalachian Mountains. Ph.D. dissertation, Dept. of Meteorology, Massachusetts Institute of Technology, 127 pp.

Bell, G.D. and Bosart, L.F., 1988: Appalachian Cold-Air Damming. *Mon. Wea. Rev.*, **116**, 137-161.

Bosart, L.F., Pagnotti, V., and Lettau, B., 1973: Climatological Aspects of Eastern United States Back-Door Cold Front Passages. *Mon. Wea. Rev.,* **101**, 627-635.

Carr, J.A., 1951: The East Coast “Backdoor” Front of May 16-20, 1951. *Mon. Wea. Rev.,* **79**, 100-105.

Changnon, S.A., 2003: Characteristics of Ice Storms in the United States. *J. Appl. Meteor. Climatol.*, **42**, 630-639.

Colquhoun, J.R., Shepherd, D.J., Coulman, C.E., Smith, R.K., and McInnes, K, 1985: The Southerly Burster of South Eastern Australia: An Orographically Forced Cold Front. *Mon. Wea. Rev.*, **113**, 2090-2107.

Day, C. and Roberts, J. 2014: Idled Wheels Choke Icy Interstates. Accessed June 21, 2022; published 05 March 2014, https://www.arkansasonline.com/news/2014/mar/05/idled-wheels-choke-icy-interstates-20140305/.

Dunn, L., 1987: Cold Air Damming by the Front Range of the Colorado Rockies and its Relationship to Locally Heavy Snows. *Wea. Forecasting*., **2**, 177-189.

Forbes, G.S., Anthes, R.A., and Thomson, D.W., 1987: Synoptic and Mesoscale Aspects of an Appalachian Ice Storm Associated with Cold-Air Damming. *Mon. Wea. Rev.*, **115**, 564-591.

Fritsch, J.M., Kapolka, J., and Hirschberg, P.A., 1992: The Effects of Subcloud-Layer Diabatic Processes on Cold-Air Damming. *J. Atmos. Sci.*, **49**, 49-70.

Hong, S.Y., and Lim, J.O., 2006: The WRF Single-Moment 6-Class Microphysics Scheme (WSM6). *J. Korean Meteor. Soc*., **42**, 129-151.

Iacono, M.J., Delamere, J.S., Mlawer, E.J., Shephard, M.W., Clough, S.A., and Collins, W.D., 2008: Radiative Forcing by Long-Lived Greenhouse Gases: Calculations with the AER Radiative Transfer Models. *J. Geophys. Res.*, **113**, D13103.

Janjic, Z.I., 1994: The Step-Mountain Eta Coordinate Model: Further Developments of the Convection, Viscous Sublayer, and Turbulence Closure Schemes. *Mon. Wea. Rev.*, **122**, 927-945.

Janjic, Z.I., 1996: The Surface Layer in the NCEP Eta Model. *Eleventh conference on numerical weather prediction, Norfolk, Virginia, 19-23 1996. Amer. Meteor. Soc., Boston, MA*, pp. 354-355.

Janjic, Z.I., 2002: Nonsingular Implementation of the Mellor-Yamada Level 2.5 Scheme in the NCEP Meso Model. *NCEP Office Note No. 437*, 61 pp.

Keeter, K.K., Businger, S., Lee, L.G., and Waldstreicher, J.S., 1995: Winter Weather Forecasting Throughout the Eastern United States. Part III: The Effects of Topography and the Variability of Winter Weather in the Carolinas and Virginia. *Wea. Forecasting.*, **10**, 42-60.

Lesnick, G., 2014: Beebe critical of highway response to winter storm. Accessed 21 June 2022; published 05 March 2014, https://arkansasonline.newsbank.com/.

Liu, Y., Geerts, B., Miller, M., Daum, P., and McGraw, R., 2008: Threshold radar reflectivity for drizzling clouds. *Geophys. Res. Lett.*, **35**, L03807, doi:10.1029/2007GL031201.

Mesinger, F., 1993: Forecasting Upper Tropospheric Turbulence Within the Framework of the Mellor-Yamada 2.5 Closure. *Res. Activ. in Atmos. and Ocean. Mod., WMO, Geneva, CAS/JSC WGNE*, **Rep. No. 18**, 4.28-4.29.

Monin, A.S., and Obukhov, A.M., 1954: Basic Laws of Turbulent Mixing in the Surface Layer of the Atmosphere. *Contrib. Geophys. Inst. Acad. Sci. USSR* **151**: 163-187 (in Russian).

Rackley, J.A. and Knox, J.A., 2016: A Climatology of Southern Appalachian Cold-Air Damming. *Wea. Forecasting.*, **31**, 419-432.

Richwein, B.A., 1980: The Damming Effect of the Southern Appalachians. *National Wea. Digest.*, **5**, 2-12.

Skamarock, W. C., Klemp, J. B., Dudhia, J., Gill, D. O., Liu, Z., Berner, J., … Huang, X. -yu. (2021). A Description of the Advanced Research WRF Model Version 4.3 (No. NCAR/TN-556+STR). doi:10.5065/1dfh-6p97

Stauffer, D.R. and Warner, T.T., 1987: A Numerical Study of Appalachian Cold-Air Damming and Coastal Frontogenesis. *Mon. Wea. Rev.*, **115**, 799-821.

Stull, R.B. 1995. Meteorology Today for Scientists and Engineers. 385 pp.

Tewari, M., Chen, F., Wang, W., Dudhia, J., LeMone, M.A., Mitchell, K., Ek. M., Gayno, G., Wegiel, J., and Cuenca, R.H., 2004: Implementation and Verification of the Unified NOAH Land Surface Model in the WRF Model. *20th conference on weather analysis and forecasting /16th conference on numerical weather prediction*, pp. 11-15.

Tiedtke, M., 1989: A Comprehensive Mass Flux Scheme for Cumulus Parameterization in Large-Scale Models. *Mon. Wea. Rev.*, **117**, 1779-1800.

Xu, Q., 1990: A Theoretical Study of Cold Air Damming. *J. Atmos. Sci.*, **47**, 2969-2985.

Zhang, C., Wang, Y., and Hamiton, K., 2011: Improved Representation of Boundary Layer Clouds over the Southeast Pacific in ARW-WRF Using a Modified Tiedtke Cumulus Parameterization Scheme. *Mon. Wea. Rev.*, **139**, 3489-3513.

VITA

Jonathon Thomas Bongard began his atmospheric career at Saint Louis University in the fall of 2001. While attending classes at SLU Jonathon had the opportunity to study forecasting under Professor Ben Abell who made a profound impact on Jonathon. While he did not graduate from SLU, he learned a great deal there about meteorology that would influence his choice to return to academia years later in Columbia, Missouri.

Jonathon returned to school in 2014 achieving an Associates Degree at Moberly Area Community College. It was the following year though, when Jonathon enrolled at the University of Missouri as an Atmospheric Science undergraduate. It was then that after being the only student old enough to get Dr. Patrick Market's 80's movie references they became fast friends. Dr. Market helped reinvigorate Jonathon's passion for forecasting and built upon the foundation laid by Ben Abell years earlier in St. Louis. Jonathon took this passion and began helping with research forecasting for grad students in the MU program. This translated to an opportunity to attend grad school himself after earning his bachelor's degree in 2017.

Jonathon's graduate career at the University of Missouri was a busy one. Outside of research responsibilities, Jonathon took part in teaching atmospheric science courses, launching weather balloons, setting up and analyzing data from a micro rain-radar (MRR). Jonathon also worked as the Lead Meteorologist for Fair Saint Louis in which he helped Fair leadership with weather decision support keeping fairgoers safe. Jonathon earned his master's degree in 2019 under his advisor Dr. Neil Fox. MU's School of Natural Resources kept paying Jonathon, so he kept showing up and was able to research and complete a doctoral degree under his mentor and friend Dr. Patrick Market in 2023. These experiences helped Jonathon secure employment with the National Weather Service (NWS) in Elko County, Nevada. Working for the NWS has been a lifelong dream of Jonathon's and his passion for weather forecasting will pay off as Jonathon begins his new career. Jonathon looks forward to settling down with his fiancée Whitney and his stepdaughter Greenlee in northeastern Nevada.